THE ELECTRODEPOSITION OF COMPOSITIONALLY MODULATED MULTILAYER COATINGS FOR ENHANCED CORROSION RESISTANCE

by

G. CHAWA

BSc. (DAMASCUS)

A Thesis Submitted in Fulfilment of The Regulations for The Award of The Degree of

Master of Philosophy
at Loughborough University of Technology

January 1996

Supervisor: Dr. G.D. Wilcox

Institute of Polymer Technology and Materials Engineering

9644 6317

To   **my mother**

To   **my wife**

To   **my daughter Rahaf**

And to

      my son Loai

Acknowledgements

SYNOPSIS

The concept of electrodeposited multilayer coatings has been examined using both a dual and single bath process route. The effectiveness of an electrodeposition coating technique was initially investigated on the copper-nickel system. Compositionally modulated metallic coatings (CMMC's) were formed by the alternate electrodeposition of copper and nickel. Individual layer thicknesses were varied from 10 nm to 2μm by close control of the plating current density with a computer assisted pulse plating facility.

Following successful deposition of CMMC's using the copper-nickel system, investigations were concentrated on the zinc-nickel system on steel substrates again both dual and single bath techniques were utilised , the former to produce CMMC's of alternate zinc and nickel as well as layered structures of either zinc or nickel with a commercial zinc-nickel alloy. A single bath technique was used to produce compositionally modulated alloy multilayer coatings (CMAMC's) consisting of alternate layers of two compositions of zinc-nickel alloy .

Conventional salt spray and more rapid electrochemical corrosion tests were carried out to asses the effectiveness of the layered coatings, as well as scanning electron microscopy and despersive x-ray analysis to study the morphological and compositional changes in the coating structures.

Results indicate the improvements of corrosion rersistance of many of layered structures over similar (in thickness) conventional electrodeposited zinc coatings.
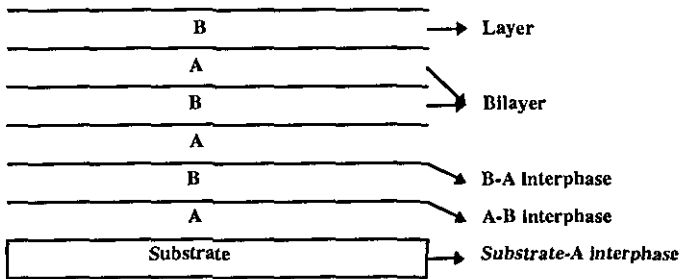
Abreviations and Terminology

Abreviations	
LCZ	Low-cyanide Zinc
NCZ	Non-cyanide Zinc
RCE	Rotating Cylinder Electrode
RDE	Rotating Disc Electrode
SCE	Saturated Calomel Electrode
SHE	Standard Hydrogen Electrode
SEM	Scanning Electron Microscopy/Microscope
TEM	Transmission Electron Microscopy/Microscope
EDAX	Energy Dispersive X-ray Analysis
nm	Nanometer
μm	Micron
CAPP	Computer Assissted Pulsed Plating
NSST	Neutral Salt Spray Test
CVD	Chemical Vapour Deposition
PVD	Physical Vapour Deposition
CMM	Compositionally Modulated Multilayer
CMMM	Compositionally Modulated Metal Multilayer
CMAM	Compositionally Modulated Alloy Multilayer
DBT	Dual Bath Technique
SBT	Single Bath Technique
I_{corr}	Corrosion Current
E_{corr}	Corrosion Potential
M1/M2 CMM	A deposit of individual layers of M1 and M2 commencing a layer of M1 adjacent to the substrate

Terminology (see below)	
Layer	One homogenous single-layer in the coating
Bilayer	Consists of two different layers, which are repeated through the coating
Wavelength	The thickness of a bilayer
Coating	The multilayered CMM coating ranging from the substrate to the surface
Substrate-A interphase	The interphase between the substrate and the first layer
A-B interphase	The interphase between the first type of layer and the second type of layer counted from the substrate
B-A interphase	The interphase between the second type of layer and the first type of layer counted from the substrate

B → Layer

A

B → Bilayer

A

B → B-A Interphase

A → A-B Interphase

Substrate → Substrate-A Interphase

Figures

(1) Cathode current efficiency of various zinc baths

(2) Corrosion resistance performance of 9 microns thick zinc deposits in salt spray test

(3) The effect of nickel content in Zn-Ni alloy on resistance to corrosion

(4) Schematic representation for CMMM and CMAM coating systems

(5) Schematic diagram for a soft x-ray reflector

(6) Schematic presentation of the experimental set-up used for electrodeposition of CMM coatings by the dual bath technique

(7) Schematic representation of dual bath electrodeposition automated apparatus

(8) Schematic representation of pulsed current regimes

(9) Types of rotating electrodes

(10) Cumulative number of publications versus year of publications

(11) Unit cells of the three most important lattices

(12) Schematic presentation for the types of cubic lattices

(13) The relationship between Knoop hardness and the {111} content of copper foil

(14) The relationship between the structure of electrodeposits to operating conditions of the electrodepositing solution

(15) A plot of ultimate tensile strength vs. copper layer thickness for 90 % nickel, 10% Cu electrodeposited layered composites

(16) A plot of wear rates as a function of load for copper, nickel and Cu/Ni multilayers

(17) Superimposed Pourbaix diagram of copper and nickel

(18) Dual bath electrodeposition cell set-up

(19) Dual bath electrodeposition sequence for M1/M2 multilayers

(20) Rotating cylinder electrode cell

(21) Schematic representation of single bath experimental set-up

(22) Cathodic polarisation cell set-up

(23) Potentiodynamic polarisation cell set-up

(24) SEM micrographs of the layered structure of Cu/Ni CMMM coatings

(25) A micrograph of a smeared microlayered structure of Cu/Ni CMMM coating

Tables

(25) Porosity of different types of deposited coatings

(26) Bath composition and operation conditions for the dual bath Zn/Ni CMMM electrodeposition

(27) Cathode current efficiencies for different types of coatings on different substrates

(28) Morphological characteristics for Ni/Zn CMMM coatings

(29) Morphological characteristics for Zn/Ni CMMM coatings

(30) Electrochemical corrosion data for the layered coatings studied

(31) The corrosion behaviour of different types of layered coatings

(32) Bath composition and plating conditions for single bath electrodeposition of Cu/Ni CMAM coatings

(33-46) Characteristics of electrodeposited Zn/Ni alloys on a steel substrate at 2.55-169.9 A/dm^2 and various rotation speeds

(47) Corrosion data for different types of Zn-Ni alloy coatings

(48) Corrosion performance in NSST for different types of Zn and Ni alloy coatings.

(49) Corrosion data and their operating conditions for different types of Zn/Ni multilayer alloy coatings and comparison with single Zn-Ni alloy layers

(50) EDAX analysis of outer surface and multilayer cross-section compositions for Zn/Ni CMAM coatings

(51) The current density and potential values for Zn-2%Ni and Zn-13%Ni alloy single layer coatings and 2, 4, 8 and 12 layer Zn-2%Ni/Zn-13%Ni and Zn-13%Ni/Zn-2%Ni CMAM coatings at different potentiodynamic regions

Chapter One

Introduction

Electrogalvanised zinc alloy coatings, such as Zn-Ni, Zn-Co, and Zn-Fe have been marketed successfully for the protection of steel strip and small components and are well established as effective sacrificial coatings for ferrous surfaces. Their ability to confer improved corrosion protection over conventional electrodeposited zinc coatings in salt environments is widely reported in the literature (21,91).

Compositionally modulated multilayer coatings have been recognised for certain systems, as possessing enhanced physical and electrical properties and have been successfully deposited electrochemically for alloys including Cu/Ni, Ni/P etc. The application of this type of system for corrosion protection has not been widely addressed. However, the concept of compositionally modulated or layered coatings is not a new phenomenon in surface coating technology. Layering of electrodeposited coatings has been used widely with decorative chromium where a three component system is utilised (Cr, Ni, Cu).

The electrodeposition of repetitive multilayered structure for improved surface properties is relatively new and is receiving keen interest from a number of research groups world-wide. These materials basically consist of alternating repeated layers. The majority of investigations have centred around the electrodeposited copper/nickel system(44). Electrodeposition technique for these types of multilayers have centred around two systems namely the dual bath technique (DBT) and the single bath technique (SBT). In general, researchers have been divided between the two techniques, both having their advantages and disadvantages.

The inherent properties which can be offered by the so-called compositionally modulated multilayers and the growing demands for a materials that have excellent wear and corrosion properties to increase the service life of steel products, have been encouragement's needed to look at this new field of application and to apply it to a zinc alloy system.

The investigations reported in this work have centred around DBT and SBT, broadly using zinc and nickel as the system of interest.

The simplicity offered by Cu/Ni compositionally modulated multilayer system in terms of bath chemistry and operating process make it a good model to use to gain a better understanding of the techniques used in compositionally modulated multilayer production and the electrochemical principals behind them.

The main experimental investigations were centred around the Cu/Ni and Zn/Ni multilayer systems.

1- Cu/Ni structures were electrodeposited by means of dual and single bath techniques by using two different CMM production processes (DBT and SBT). It was necessary to to become aware of the production sequences as well as the problems encountered with them.

Initial studies on the copper/nickel system were carried out using copper and nickel solutions suggested by Haseeb et al. (44) followed by the investigations of copper/nickel single bath system in order to establish a good understanding of the high speed electrodeposition processes used by this technique and to produce multilayered coatings at a nanometer level.

When this had been accomplished, the main experimental investigations of the electrodeposition of zinc/nickel CMMM and CMAM coatings were carried out to

produce multilayered coatings of different types by the two aforementioned techniques and then to study the performance and electrochemical corrosion behaviour of these multilayered coatings by using different techniques, and to be able then to compare them with the performance and electrochemical corrosion behaviour of single layer coatings.

Layered coatings of zinc, nickel and zinc-nickel alloy deposited by the DBT produced large increases in corrosion resistance over similar thickness single layer coatings.

An acid sulfate Zn-Ni alloy system was then investigated to see if it could be utilised to produce layered structures of different alloy compositions, a full analysis of the effects of electrodeposition variables on alloy compositions allowed electrodepositing conditions to be recognised which would produce the conditions necessary for a repetitive structure made up of two alloy compositions.

This SBT has been successfully utilised to produce such structures, which, in general, produce coatings of different corrosion resistance.

Chapter 2   LITERATURE REVIEW

2-1 Sacrificial Coatings

Sacrificial coatings are used primarily for protection of metal substrates, often iron and steel (they are some times called anodic coatings which means that electrochemically they are anodic to the substrate).

The whole process aims to protect the substrate anodically by means of a galvanic cell set up between the substrate " e.g. steel " and the coating metal. The coating metal behaves anodically to the substrate and corrodes preferentially, the sacrificial coating will still protect at coating pores provided the pores are not too large. Zinc and cadmium are two major metals which behave in this manner with steel.

2-1-1 Zinc plating

Zinc electrodeposition on steel is not a new technology, the process has been used for decades on household appliances and other materials. Furthermore the Japanese have electrogalvanized their auto body steel for a decade or more (1). The electrodeposition of zinc dates back to 1915 - 1920 (1) when both the acid and cyanide baths were in their early stages of development. The importance of zinc plating has not diminished in recent times because of the economy of deposition and the excellent corrosion resistant provided by zinc coatings.

From its electronegative potential of -0.76 V vs. SHE, it might be expected that zinc could not be electrodeposited from an aqueous solution, but in fact the high over potential of hydrogen on most substrates does permit such deposition (2).

Zinc electroplating in general can be divided in to three major categories:

1- Alkaline cyanide

2- Alkaline non-cyanide / low-cyanide

3- Acid

Each of these categories may be further subdivided; the cyanide into conventional and so-called medium cyanide, and the acid into sulfate, chloride and fluoborate.

2-1-1-1 Zinc cyanide baths

The cyanide baths were first selected for general purpose plating because of their excellent throwing power. The environmental and safety considerations for cyanide and the development of addition agents to improve the throwing power of acid zinc solution resulted in their rapid rise in popularity over cyanide baths (3).

The composition of zinc cyanide solution; plating conditions and their uses are shown in table (1).

Table (1) Cyanide Zinc Baths

Type	High Cyanide Bright Zinc	Medium Cyanide Bright Zinc	Low Cyanide Bright Zinc
Major Uses	Bright protective coatings on fasteners and other steel components	Bright protective coatings on fasteners and other steel components	Bright protective coatings on fasteners and other steel components
Typical Composition	Zinc oxide　　　45　g/l Sodium cyanide　100　g/l Sodium hydroxide　35　g/l Poly sulphide　　　1　g/l (as brightener)	Zinc oxide　　　20　g/l Sodium cyanide　30　g/l Sodium hydroxide　60 g/l Poly sulphide　　1 g/l (as brightener)	Zinc oxide　　　10 g/l Sodium cyanide　15 g/l Sodium hydroxide 75 g/l Poly sulphide　　1 g/l (as brightener)
Operating Conditions Temperature ($^{\circ}$C)	20 to 35	18 to 30	15 to 40
Current density (A dm^{-2})	1 to 2.5	1 to 3	1 to 2.5
Cathode Current efficiency (%)	75 to 90	-	-
pH	Highly alkaline	Highly alkaline	Highly alkaline
Anodes	99.99 % Zinc lead free	99.99 % Zinc lead free	99.99 % Zinc lead free
Agitation	not usual	not usual	not usual
Deposition rate per micron	1.1min at 4 A dm^{-2}	2 min at 2 A dm^{-2}	4.5 min at 1 A dm^{-2}
Safety considerations	Toxic	Toxic	Toxic

From ref. (3)

Anode efficiency in zinc baths is usually higher than cathode efficiency due to zinc dissolution by chemical action.

The cyanide concentration depends on the operating conditions and the concentration of other constituents, therefore the NaOH / Zn ratio plays an important rule in cyanide bath chemistry.

Additives are generally added to cyanide baths to improve surface brightness, they are usually organic compounds such as polyvinyl alcohols, polyvinyl acetates and aromatic aldehydes.

The importance of hydroxide ions in cyanide - zinc baths can be summarised as follows (1):

1- They are the main charge carrying species.

2- They aid anode corrosion.

3-They act as a throwing power efficiency regulators.

Agitation also has benefits, it permits some increase in operating current density and gives a good thermal distribution all over the bath.

2-1-1-2 Low-cyanide Alkaline Bath / Non-cyanide alkaline bath

The need for reducing the cost of waste - control without affecting bath properties has led to the development of new low and non-cyanide baths. Table (2) shows the composition of a dilute alkaline bath which has similar operating conditions to those of the cyanide bath with one exception - it is more difficulty to control.

Constituent	Concentration (g/l)
Zinc	7- 20
Total NaCN	7-50
Total NaOH	75 -100
Na_2CO_3	20 -100
Ratio NaCN/Zn	1- 2.5

Table (2) Dilute Cyanide Bath. From ref. (3)

6

The use of such a dilute bath has not been successful since the waste - control problem is not solved completely despite decreasing the heavy metal and cyanide contents in the waste water.

In the late 1960 's and through the 70's more anti-pollution laws have been introduced in West Germany, Switzerland and Great Britain which have given rise to a truly non-cyanide process.

A small amount of cyanide has been added to non-cyanide alkaline (zincate) baths resulting in the so-called low cyanide or LCZ baths, a typical formulation and operating conditions are shown in table (3) .

The development of organic addition agents has led to the formation of alkaline cyanide-free baths (NCZ). Boto (4) has listed additives suitable for alkaline non-cyanide baths, these include mixtures of aromatic and hetrocyclic polyethylene glycol (as levelling agent), triethanolamine, furfural, lignin sulphonate and gelatine.

Type	Low- cyanide Bright Alkaline Zinc	Non-cyanide Bright Alkaline Zinc
Major uses	Bright protective coatings on fasteners and other components	Cyanide free alternative to conventional zinc plating solution
Typical composition	Zinc oxide 10 g/l NaCN 15 g/l Poly-sulphide 1 g/l	Zinc oxide 10 g/l NaOH 80 g/l Brighteners
Plating Conditions Temperature (°C) Cathode Current efficiency (%) pH Anodes Agitation Deposition rate per micron Safety considerations	25-30 Highly Alkaline 99.99 % Zinc free lead Not usual 4.5 min at 1 A dm^{-2} Toxic	20-35 Highly Alkaline 99.99 % Zinc free lead Not usual 3.2 min at 2 A dm^{-2} Toxic

Table (3) LCZ and NCZ Bright Alkaline Zinc Baths. From ref. (2)

2-1-1-3 Acid zinc baths

Acid zinc electrolyte systems have seen rapid changes in the past two decades. Acid zinc baths have several formulations based primarily on either sulfate or chloride. Until the late 1960's most uses of acid baths were restricted to high speed production and purely for protective purposes . For application such as continuous steel wire and strip plating, acid zinc baths are suitable because of the high potential plating speed and low operating costs requirements , whilst the poor throwing power and lack of fully bright deposits which are the main disadvantages of acid zinc baths are not serious problems in such applications.

The search for cyanide-free zinc baths resulted in the mid-1960's in the so-called neutral chloride bath which, with appropriate additives, is capable of producing bright deposits and is competitive with alkaline baths for general plating.

Acid zinc baths have several advantages over the cyanide baths, they are mainly used for the plating of cast and malleable irons and also case hardened steel; also they are more suitable for electroplating high tensile steels which are susceptible to hydrogen embrittlement.

Zinc sulfate baths are the most widely used acid baths, other baths are formulated with chloride and fluoroborate; perchlorate and sulfamate but are little used.

The addition of chlorides and sulfates of sodium, ammonium and aluminium increase the electrolyte conductivity; free acid also serves this purpose .

Addition agents are required for the production of bright smooth deposits, most common are dextrin, liquorice, glucose and gelatine (2). Typical acid zinc baths are shown in table (4) as well as their operating conditions.

Table (5) shows the advantages and disadvantages of the three basic zinc bath formulations and table (6) shows the deposit properties of the various types of zinc baths.

Type	Bright Acid Zinc	Acid Zinc Sulfate
Major Uses	Alternatives to cyanide - containing solutions suitable for the plating of cast iron , malleable iron , high tensile steels .Throwing power is not as good as cyanide baths .	Matt zinc plating suitable for cast and malleable iron for wire and strip plating .
Typical Composition	Zinc Chloride 100 g/l Ammonium 180g/l Chloride Addition Agent Brightener Additive	Zinc Sulfate 350 g/l Aluminium Sulfate 25 g/l Sodium Chloride 25 g/l Boric Acid 20 g/l Dextrin or other Additives
Operating Conditions Temperature Current Density Cathode Current Efficiency pH Anodes Tank Rate of Deposition per micron	 18-30 °C 1 to 5 A/dm^2 100% 4.5- 6 99.99% Zinc Rubber or Plastic Lined 1.25 min at 3 A / dm^2	 15-40 °C 1 to 10 A/dm^2 100% 3.5- 4.5 99.99% Zinc High Temperature Plastics 0.8 min at 5 A / dm^2

Table (4). Acid Zinc Baths. From ref. (3)

Type	Efficiency %	Distribution	Ductility	Brightness	Pitting	Environ-mental
Cyanide Zinc						
High Cyanide	65-80	Very good	good	Fair	Non	Poor
MediumCyanide	65-75	Good	Good	Fair	Non	Fair
Low Cyanide	60-70	Fair	Fair	Fair	Non	Fair-good
Alkaline Zinc						
Non-Cyanide	60-75	Fair-good	Fair	Fair	Non	Good
High Concentration	65-80	Fair	Fair	Poor-Fair	Non	Fair
Acid Zinc						
Ammonuim	93-97	Poor	Poor	Good	Yes	Fair
Ammonium /Potassium	95-98	Poor	Poor	Verygood	Yes	Fair-good
Potassium	95-98	Poor	Poor	Verygood	Yes	Good

Table (6) Zinc deposit properties. Adapted from ref. (1-3)

Type	Advantages	Disadvantages
Bright Cyanide Zinc Baths	- Availability of a vast amount of technology on the cyanide bath. - Development of protective and decorative finishes at low cost. Good throwing and Covering Power. - Ease of Electrolyte Control. - Versatility of Application. - Availability of Waste Disposal Methods.	- Toxicity. - Poor bath conductivity. - Lower efficiency. - Lack of levelling characteristics - Hydrogen embrittlement.
Alkaline Non-Cyanide Baths	- The basic chemical make - up costs and operating costs of this bath are lower than that of any other solution. - The bath may be employed in steel tanks. - The zincate bath is the least toxic of all the commonly employed electrolytes. - The zincate bath exibits excellent throwing power. .	- The bath has very limited operational latitude when compared to other systems. - Zincate deposit are infact more brittle than deposits from other zinc electrolytes.
Bright Acid Zinc Baths	- They are relatively cheap to make-up and maintain. - They can be operated in a wide range of compositions without affecting the deposit. - They are relativly non-toxic. Very high cathod current efficiencies. - Levelling ability. - High conductivity.	- Poor throwing and covering power. - Attack of anodes at lower pH values. - Highly corrosive electrolyte. - More critical cleaning and degreasing required prior to plating. - *Lack of fully bright deposit. (*) This property has greatly improved with the use of proper additives.

Table (5) Advantages and disadvantages of basic zinc bath formulations.

Adapted from ref. (1-2-5).

A comparison of cathode current efficiencies for various zinc baths as a function of current density are illustrated in figure (1).

2-1-1-4 Corrosion Resistance of Electrodeposited Zinc Coatings

As stated earlier in section 2-1-1; the main application of zinc electroplating processes is for protection purposes. Corrosion resistance can be evaluated by many means :

1- Salt spray test

2- Outdoor exposure test

3- Humidity test

4- Electrochemical tests .
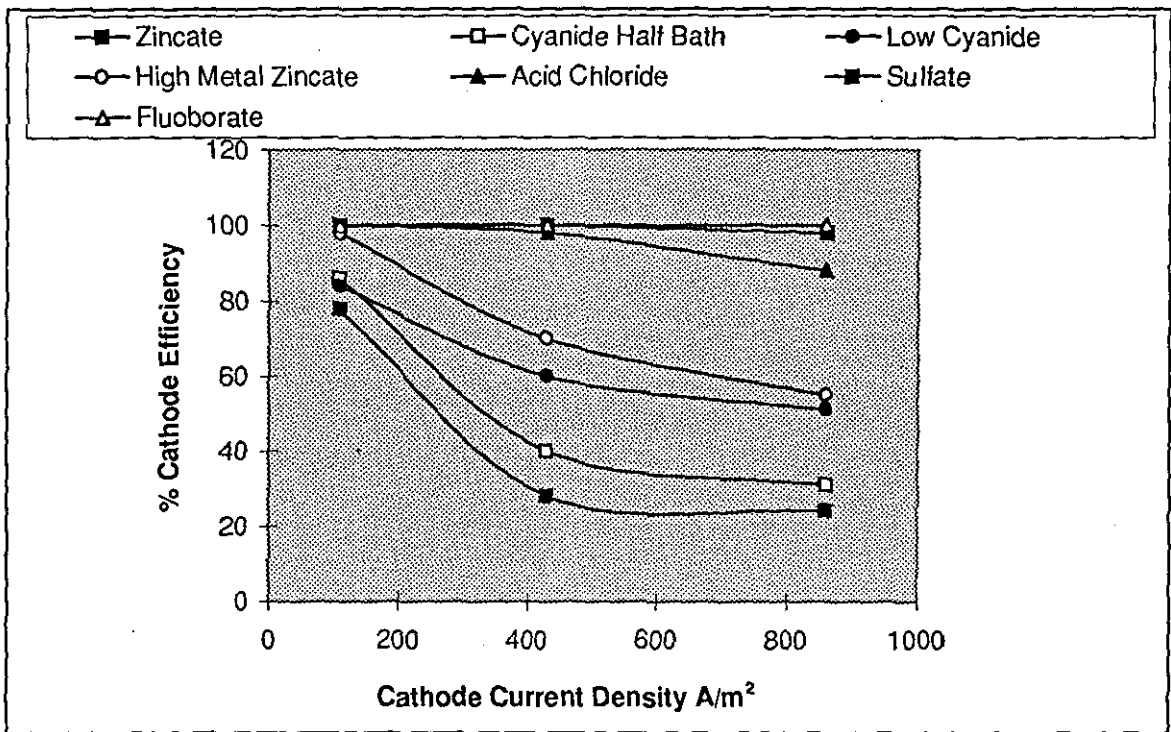
Figure (1). Cathode current efficiency of various zinc baths (From ref. (5))

The corrosion resistance capability of zinc deposit depends upon:

1- Zinc thickness

2- Porrosity and structure of the deposit (grain size and orientation)

Several electrodeposited zinc coating systems have been investegated. Figure (2) shows the corrosion resistance performance of 9 microns thick zinc deposits after salt spray testing (6).

The zinc baths in question were:

1- Ammonium chloride bright zinc

2- Ammonium free-chloride bright zinc

3- Neutral matt zinc

4- Cyanide bright zinc

5- Cyanide matt zinc

6- Zincate bright zinc.
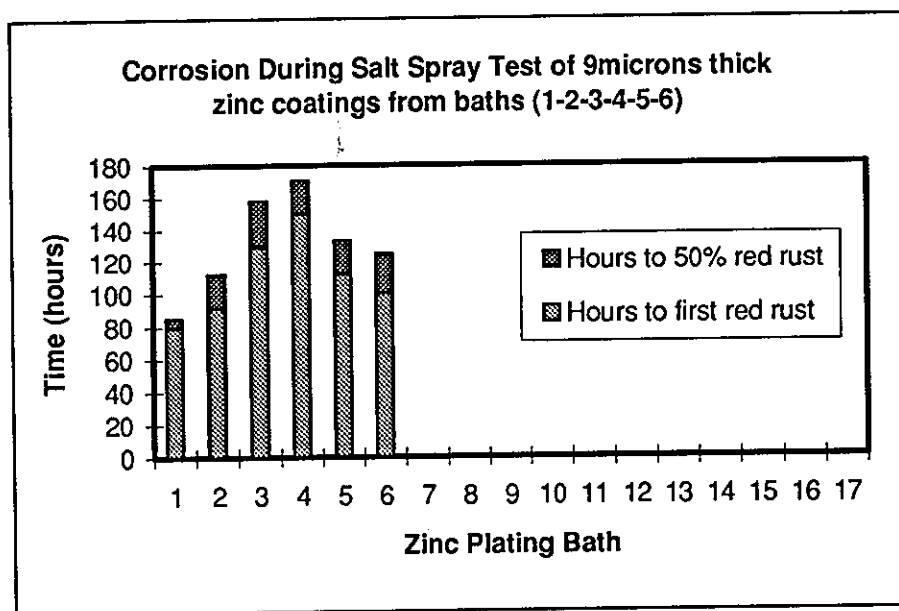
Figure (2). From ref. (6)

2-1-2 Cadmium plating

Unlike zinc, cadmium and its compounds are highly toxic; their effects are similar to those of mercury and arsenic (2). Cadmium plate must never used on parts that will come in to contact with foods or beverages. Moreover, because of its high price and toxicity, cadmium is used as a protective electroplate only in those circumstances in which zinc is not equally satisfactory or where special properties are required. Cadmium is more easily soldered than zinc; it does not form bulky corrosion products that interfere with the functioning of moving parts; it is easily deposited on cast and malleable iron and therefore is often used as a strike before zinc plating on these materials; unlike zinc it is resistant to alkalis; and it is somewhat superior to zinc in corrosion protection in naval specifications. The high price and occasional shortages of cadmium have tended to discourage its use, and the popularity of cadmium plating is decreasing.

Cadmium is almost always plated from the cyanide bath. As with all cyanide processes, waste-control problems have made researchers look for other alternatives, leading to the development of fluoborate, sulfate and chloride solutions not containing cyanide. But these baths have not had a success comparable to that of the cyanide baths.

Table (7) shows the composition and operating conditions of typical cyanide-cadmium solutions.

2-1-2-1 Acid Cadmium Baths

Cadmium, like zinc, when plated from cyanide baths, can cause hydrogen embrittlement of the substrate; when embrittlment becomes a serious problem, acid baths, especially fluoborate, have some advantages. More recently the waste-control problems associated with cyanide solutions have renewed interest in the acid solutions. A fluoborate bath has the composition shown in table (8).

13

Composition and operating conditions	Rack plating	Barrel Plating
Cadmium oxide, g/l	25-35	17-23
Cadmium metal, g/l	22-31	15-20
Sodium hydroxide, g/l	15-22	10-14.5
Sodium cyanide, g/l	75-90	90-100
Addition agents, g/l	0.1-15	0.1-15
Cathode current density, A/m^2	150-400	-
Anode current density, A/m^2	200	-
Temperature, °C	20-30	-

Table (7). Cyanide cadmium baths. From ref (2).

Composition and operating conditions	Range
Cadmium Fluoborate, g/l	150-300
Ammonium fluoborate, g/l	60-120
Boric acid, g/l	20-30
pH	1-4
Licorice, g/l	1-2
Temperature, °C	10-40
Current density, A/m^2	100-600

Table (8). Cadmium fluoborate bath. From ref. (2)

2-2 Zinc-based Alloys

Research and developments of zinc alloys has been one of the major topics of the late 1980's and 1990's. Zinc-based alloy coatings were investigated because of continuing corrosion problems of normal zinc plated steel substrates due to the high chemical reactivity of pure zinc coatings. A possible solution for this problem was to alloy zinc electroplate by anomalous co-deposition with less reactive metals to give binary alloys (7). Anomalous co-deposition allows low percentage's of more noble transition metals such as iron-group metals to be co-deposited with zinc from a mixed solutions during

14

electroplating because of over potential barrier effect caused by hydroxide films. Hence, the alloying lowers the chemical reactivity of zinc coatings and improve their corrosion resistance(8).

A variety of metals can be co-deposited with zinc, Krohn and Bohn (9) have published a chart showing all the alloys that have been reported as being deposited up to the 1970's.

Zinc alloy coatings are now being applied to a wide range of steel components due to their excellent corrosion resistance, good weldability, paintability and mechanical properties.

2-2-1 Zinc-nickel alloy electrodeposited coatings

The electrodeposition of zinc-nickel alloys was first reported in 1905 and commercially developed in the early 1940's under the trade name coronizing (10). But the actual commercial adoption of zinc-nickel alloys took place in Japan in the 1980's (11). There are two types of zinc-nickel plating systems which can be considered:

1- Acid-type bath.

2- Alkaline-type (non cyanide) bath.

2-2-1-1 Acid-type baths

Acidic electrolytes usually contain certain buffering agents, such as boric acid or acetic acid, to stabilise the pH during plating. Some electrolytes also contain a brightener, such as strontium sulfate (12), a levelling agent such as phenolic derivative, LA aromatic carboxylate to refine grain size (13) and a stress reliever, such as organic nitrogen or sulphur containing compounds.

Three major baths can be found (see below). Table (9) shows the types used in electrodeposited Zn/Ni alloy.

1- Sulfate bath

Zinc-nickel alloy containing 10-13% nickel is applied to steel coils using insoluble anodes and an electrolyte containing zinc and nickel sulfate (14).

2- Chloride bath

Matsuda (15) has described the use of a chloride-based solution and soluble anodes to electrodeposit zinc-nickel alloys. Anodes can be ingot, bars, plates, or baskets containing zinc or nickel pellets.

Komoda et al (14) claimed that the mode of alloy deposition, by addition of sufficient potassium chloride, can be changed from anomalous deposition to equilibrium deposition (Zn to Ni ratio in alloy deposition = Zn to Ni ratio in solution).

3- Sulfate-chloride bath

Killian et al (16) used a mixed sulfate-based solution which contained ammonium chloride so that soluble anodes may be utilised, these are titanium baskets containing nickel or zinc pieces. The nickel content in the alloy was 11.5 ± 2 %.

The use of a similar solution has been described to deposit a 15% nickel alloy, said to be resistant to whisker formation in electrical equipment during long-term storage, in contrast to coating with zinc, cadmium, or tin (17).

2-2-1-2 Alkaline-type baths

The electrolyte consists of zinc oxide and a nickel salt (sulfate, chloride) as the major source of zinc and nickel ions. The electrolyte in these cases contains also either sodium or potassium hydroxide (19). Despite some advantages of the alkaline processes over acid baths (such as the corrosive nature of the latter), alkaline baths deposit coatings containing less nickel, and also have the associated effluent problem with the use of ammonium ions (as a complexing agent in the electrolyte).

2-2-1-3 Structure and physical properties of zinc-nickel alloy electrodeposits

The structure of zinc-nickel electrodeposits varies according to the nickel content in the alloy electrodeposits, with 10-17% nickel they have a single gamma phase coating which is a mixture of intermetallic compounds of $NiZn_5$-Ni_5Zn_{21}.....etc (20). Electrodeposits containing less than 10% nickel are a mixture of gamma and eta phases, while, higher contents than 17% give a mixture of gamma and alpha phases (21).

It is reported (22) that a deposit which has a mixture of gamma and alpha phases tends to have a high tensile stress and brittleness. It is also found that at 5-15% nickel the

deposits exhibit reasonably ductile characteristics and have a slightly compressive stress, and furthermore give sacrificial protection to steel.

2-2-1-4 Corrosion resistance of Zn-Ni alloys

The corrosion resistance of Zn-Ni alloys has been extensively studied; it has been generally found the best improvement in the corrosion resistance offered by zinc is when it is alloyed with 11-14% of nickel (figure (3)). It was stated that zinc-nickel alloys provide 5-6 times higher resistance to corrosion than does electrodeposited zinc. Although, there are slight variation in results between researchers.
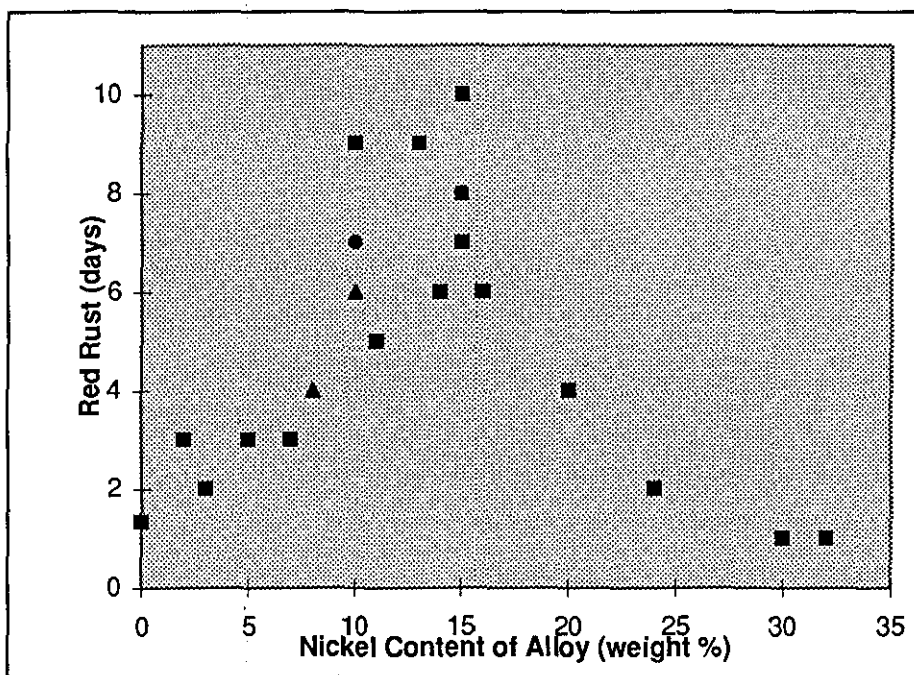
Figure (3) The effect of nickel content in Zn-Ni alloy coatings on resistance to corrosion. From ref. (21)

2-2-2 Zinc-iron alloy coatings

Zinc-iron electrodeposition processes are based on two major baths; sulfate and chloride.

The sulfate based bath contains sulfates of zinc and iron and sodium together with organic substances including sodium acetate and citric acid. Table (10) shows the sulfate formulations for electrodeposited Zn/Fe alloy.

Adaniya (22) claimed that an addition of ammonium sulfate improves the quality of the deposit and widens the plating range. Whilst, the potassium chloride improves anode corrosion.

The major problem with zinc-iron alloy plating is control of electrolyte, mainly because of formation of ferric hydroxide (the hydroxide incorporated in the coating, resulting in poor adhesion). Geduld (1) stated that the addition of citric acid prevents precipitation of ferric hydroxide by complexing ferric iron in the bath.

Zn/Ni Alloys Electrolytes	g/l	Operating Conditions
$ZnSO_4.7H_2O$	260	Nickel strike bath prior to alloy
$NiCl_2.6H_2O$	240	plating
CH_3COOH	3%v/v	50 °C, pH 1.5-3.5, C.D 32 A/dm^2
$ZnCl_2$	104.1	50 °C, pH 4.5, C.D 50 A/dm^2
$NiCl_2.6H_2O$	113.5	
CH_3COOH	2.2% v/v	
$ZnCl_2$	50	Zn and/or Ni anodes , 40 °C, pH
$NiCl_2.6H_2O$	15-100	4.5, C.D 3 A/dm^2
NaCl	200	
NH_4Cl	30	
Brightener, Stress Reliever and Wetting Agent		
$ZnCl_2$	83.3	25-30 °C, pH 5.5,
KCl	210	C.D 1-.4 A/dm^2
H_3BO_3	25	
$NiCl_2.6H_2O$	1-40	
$ZnCl_2$	135	25-60 °C, pH 4.8
$NiCl_2.6Cl_2$	142	C.D 3.12 A/dm^2
H_3BO_3	30	
NaCl	156	
Brightener and Leveling Agent		
Zinc	6-12	Zinc or steel anodes, continuous
NaOH	100-120	filtration, cathode C.D 1- 4.5
Nickel	0.7-1.5	A/dm^2, 21-32 °C
Zinc/Nickel	6-7:1	

Table (9). Types of electrodeposited Zn/Ni alloy electroplating baths
   From ref. (18)

Zinc-iron alloy coatings of 15-25% iron are claimed (22) to exhibit good weldability and corrosion resistance and be used mainly for automotive applications.

Zn/Fe Alloy Electrolyte	g/l	Operating Conditions
$ZnSO_4.7H_2O$	500	40 °C, pH = 3,
$FeSO_4.7H_2O$		C.D = 50 A/dm²
Na_2SO_4	30	
$CH_3COONa.3H_2O$	20	
$C_6H_8O_7$	5	
$ZnSO_4.7H_2O$	9	50 °C, pH 1.7,
$FeSO_4.7H_2O$	250	C.D = 20 A/dm²
Ammonuim sulfate	100	
Citric acid	0.5	
KCl	10	
Teepol W.A	0.4 ml/l	

Table (10). The sulfate types of electrodeposited Zn-Fe alloy electroplating baths. From ref. (18)

2-2-3 Zinc-cobalt alloy coatings

The electrodeposition of Zn-Co alloy coatings can be carried out by acid or alkaline baths. The source of zinc in the electrolytes is either zinc oxide or other zinc salts (chloride). Tables (11) and (12) show the three typical electrolytes and their operating conditions.

Abibsi and Dennis (23) reported that zinc-cobalt alloy coatings with 1% cobalt from an acid bath give corrosion properties similar to that of zinc-nickel alloys. Sard (24) stated that 0.6-0.8% cobalt in zinc-cobalt alloy coatings give a 50-100% increase in corrosion resistance over conventional zinc.

Alkaline cyanide free systems that are less widely used, give a smooth and bright finish with alloy deposit contents of 4% cobalt (24).

19

Zn/Co Alloy Acid Electrolytes	g/l	Operating Conditions
ZnCl$_2$	83.3	30, 35 & 40 °C, pH 5.5
KCl	210	CD 1-4 A/dm^2
H$_3$BO$_3$	25	
CoCl$_2$.6H$_2$O	1-25	
ZnO	10	10-50 °C,
NaOH	117.3	C.D 0.5-10 A/dm^2
CoSO$_4$.7H$_2$O	33.7	
Tetren	0.06	
Additives		

Table (11) Acid types of electrodeposited Zn-Co alloy electroplating baths From ref. (18)

Zn/Co Alloy (Alkaline) Electrolyte	g/l	Operating Conditions
ZnCl$_2$	78	20-32 °C, pH 5-5.5,
NaCl	200	C.D 50 A/dm^2
H$_3$BO$_3$	20	
Co^{++}	1-4	
Additives		

Table (12) Alkaline type of electrodeposited Zn-Co alloy electroplating bath From ref. (18)

2-2-4 Zinc-manganese alloy coatings

The electrolytes used in zinc-manganese alloys are usually based on citrate-sulfate (see table (13)) or fluoborate baths. The citrate-sulfate system suffers from drawbacks which include low cathode current efficiency, and bath instability. The bath instability may be due to the oxidation of divalent manganese ions to the trivalent state and subsequent reaction with the citrate to form an Mn low solubility complex. To overcome this problem, Sagiyama et al (25) added metal pieces to the electrolyte which were used to oxidise manganese to Mn^{++} ions. A typical formulation of a citrate-sulfate system is; 70 g/l zinc sulfate, manganese sulfate 50 g/l, Trisoduim citrate 200

g/l at 30-50 °C, pH=3, and current density 1.5-4 A/dm^2, adding sodium thiosulphonate is said to enhance the cathode current efficiency.

A fluoborate system has been used to improve the cathode current efficiency up to 80% but the toxicity of fluoborate might be a problem (11).

Zn/Mn Alloy Electrolytes	g/l	Operating Conditions
ZnSO$_4$.7H$_2$O	70	30-50 °C, pH 3,
MnSO$_4$.H$_2$O	50	C.D 1.5-4 A/dm^2
Na$_3$C$_6$H$_5$O$_7$.2H$_2$O	200	
ZnSO$_4$.7H$_2$O	68.9	50-60 °C, pH 3-6
MnSO$_4$.H$_2$O	30.3	C.D up to 50 A/dm^2
Na$_3$C$_6$H$_5$O$_7$.2H$_2$O	47.6	
Na thiosulphonate	0.1-0.15	

Table (13) Sulfate-based Zn-Mn alloy electroplating baths
From ref. (18)

The excellent corrosion resistance of zinc-manganese alloy electrodeposits is widely reported, it has been found that an alloy composition of 50-65% manganese gives the best corrosion resistance to conventional salt spray testing. The formation of gamma-Mn$_2$O$_3$ on the alloy surface is said to be responsible for the level of corrosion resistance(11).

Zinc-nickel, zinc-iron, and zinc-cobalt alloys are the most commonly used zinc alloy systems, whilst Zn-Mn alloy coatings give a promising corrosion resistance results but are not used commercially; others like zinc-tin alloys which are used for their superior solderability and low toxicity in electronic applications and zinc-10% chromium alloys which are said to give superior corrosion resistance over conventional zinc plate (21) have little commercial usage.

2-2-5 Findings

- According to various reported papers, the zinc/nickel alloy system seems to give the best corrosion resistance (in certain environments) with respect to the other main zinc alloy systems. Table (14) shows a comparison of the corrosion performance of yellow and black chromated zinc and zinc alloys in a salt spray test.

Comparative corrosion performance results of yellow chromated zinc and zinc alloy			
		WCP[1]	RR[2]
Neutral Salt Spray	Heated[3]	Zn<Zn/Fe<Zn/Co<Zn/Ni	Zn<Zn/Fe<Zn/Co<Zn/Ni
Neutral Salt Spray	Not Heated	Zn<Zn/Co<Zn/Ni<Zn/Fe	Zn<Zn/Fe<Zn/Co<Zn/Ni
Comparative corrosion performance results of black chromated zinc and zinc alloy			
		WCP[1]	RR[2]
Neutral Salt Spray	Heated[3]	Zn<Zn/Ni<Zn/Fe<Zn/Co	Zn<Zn/Fe<Zn/Co<Zn/Ni
Neutral Salt Spray	Not Heated	Zn<Zn/Ni<Zn/Co<Zn/Fe	Zn<Zn/Fe<Zn/Co<Zn/Ni
(1)- Resistance to White Corrosion Product			
(2)- Resistance to Red Rust			
(3)- Prior to corrosion testing, the test panels were heated for 1 hr at 120 °C			

Table (14) Comparison of Corrosion Performance for Basic zinc Alloy Systems. From ref. (18)

2-3 Compositionally Modulated Multilayer (CMM) Coatings

2-3-1 Introduction

The search for new classes of materials that have unique properties not obtainable in normal materials is a major aim of many current researchers. One of these classes of new materials, which has attracted considerable interest in recent years, is called either Compositionally Modulated Metal Multilayer (CMMM) or Compositionally

Modulated Alloy Multilayer (CMAM) coating. These materials consist, basically, of very thin repetitive layers (ranging from a few nanometers to a few microns) of two different materials (these could be in the form of pure metals or alloys). Figure (4) shows a schematic representation of these two forms, (in order to differentiate between a stack of pure metal layers and a stack of alloy layers it is proposed to call the first one a CMMM (compositionally modulated metal multilayer) coatings and the second CMAM (compositionally modulated alloy multilayer) coatings.
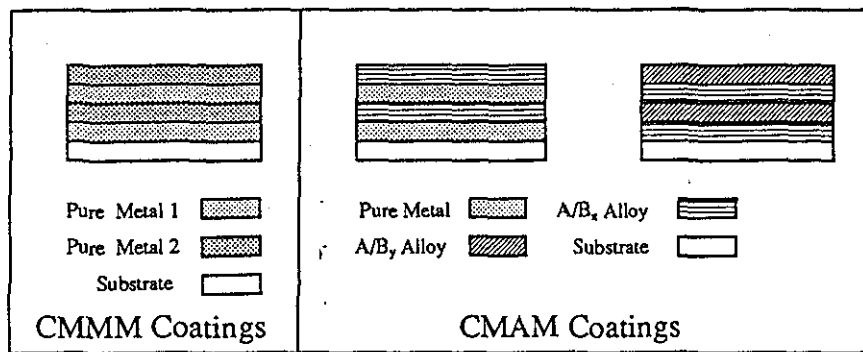
Figure (4) Schematic representation of CMMM and CMAM coatings

The concept of "modulation" results from a variation of deposit structure and deposition, occurring systematically or regularly by controlling a deposition parameter (e.g. current, agitation, potential, temperature etc.) or varying bath composition (26). The initial requirements for a deposition process for such materials are as follows (27):

1- The process has to be able to produce multilayers at an atomic level.

2- The layers produced have to be of a definable purity.

3- The process must produce well defined and regular thin layers and interfaces .

4- Planar growth processes should predominate which means the process has to be capable of producing a highly smooth surface.

5- Low temperature deposition process, to produce an abrupt interface (high temperature processes could produce inter-diffusion particularly with very thin layers (e.g. there is no diffusion in Cu on Pt system and thus the interface is abrupt).

6- The structure has to be reproducible.

The reason for depositing very thin layers of different materials stacked sequentially is to obtain special property effects (28) e.g. :

2-3-1-1 Thin film effect

The deposition of thin films on an atomic scale has allowed new structures to be made for semiconductors applications (29). The film effect was caused by a thin film of one metal sandwiched by thick films of the other (26); and can be observed by an increase of wear resistance, tensile strength and by an important improvement of many mechanical , electrical and optical properties.

2-3-1-2 Interface effect

In order to achieve a perfect coherent superlattice (A pure three dimensional arrangment of atoms) which gives a rise to a new structure with enhanced properties, sharp interfaces between layers should be present.

2-3-1-3 Coupling effect

An effect which is due to inherent property differences between adjacent layers. Interesting properties of magnetic multilayers are associated with the coupling effect between the magnetic moments of different layers, one of the multilayered structures that exhibits interesting properties, arising from anti ferromagnetic inter layer coupling, is the Fe/Cr/Fe system (30).

2-3-1-4 Periodic effect

This effect can be easily observed by the soft x-ray mirrors which consist of a strictly regular alternating arrangement of heavy materials (W, Mo, Ni) and light materials (C, Si) figure (5).
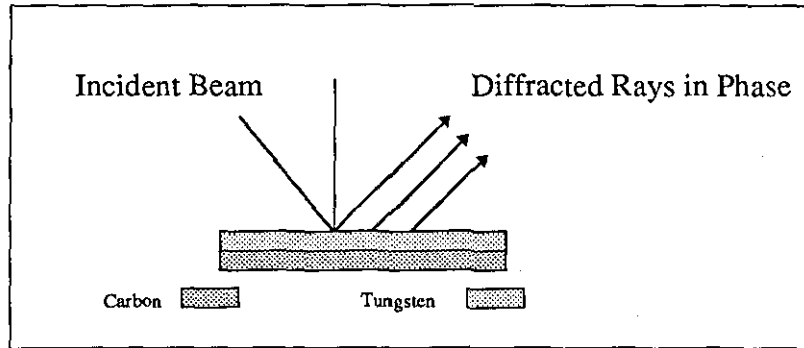
Figure (5) Schematic diagram for soft x-ray reflector

Figure (5) shows a schematic diagram for a soft x-ray reflector. The reflectivity of such a system can be increased by a factor of 10^3 with regard to bulk materials due to an increasing of the diffracted rays (31). The main applications of these mirrors are in the biological, microelectronics and x-ray instrumentation fields.

2-3-2 CMM's properties

As a result of the above effects multilayers can behave as new materials with remarkable properties not obtainable in "normal" metals and alloys; these properties include:

2-3-2-1 Super modulus property

The super modulus effect can be understood as being a result of interfacial stresses characteristic of interface boundaries as found in multilayered thin films (32). For systems based on a face centred cubic (fcc) structure, such as the Cu/Ni system, a repeat bilayer thickness of about 1.5 to 2 nm gives an enhancement of 100% or more to elastic properties (33); such behaviour has been termed "the super modulus effect".

2-3-2-2 Superconductivity

It has been shown that a special crystalline structure with alternating metals (copper, barium) and rare earth (yttrium) oxides has a superconductivity behaviour at liquid nitrogen temperature (34). The advantages of such structures are; no electrical loss, high speed possibilities and high sensitivity to the magnetic field.

The fields of application of these kinds of structures are in microelectronics and in electrical engineering (alternators, transformers).

2-3-2-3 Magnetic property

Many experiments have been carried out in the magnetic domain especially on bulk materials for magnetic head or recording media (35). New magnetic properties have been observed using superlattices and many researchers observed an enhancement of magneto resistance or a change of magnetisation direction for ultra thin layers (35). Cobalt has been particularly studied and it has been shown, down to 1.2 nm for one or a few nanolayers, cobalt sandwiched in crystallised gold gives interesting magnetic properties.

2-3-2-4 Optical property

As mentioned earlier, the reflectivity of a regular alternating arrangement of specific heavy and light materials can be increased 1000 times with respect to bulk materials (31).

2-3-2-5 Mechanical properties

Tungsten and copper-tungsten alloy multilayers exhibit a hardness levels significantly higher than the commercial sintered material (36), also Hilliard et al. (33) have shown that the biaxial modulus of the modulated structures Au/Ni, Cu/Pd, Cu/Ni and Ag/Pd increases by several hundred percent over their bulk materials.

Multilayers of hard material coatings have been employed for cemented carbide for cutting tools due to the increased wear resistance imparted by this kind of multilayer; the two important multilayers for such an application appear to be TiC / Ti (CN) / NiN and TiC / Al_2O_3 / TiN.

Other interesting mechanical, magnetic and electrical properties as well as an improvement of corrosion resistance imparted by electrodeposited CMM coatings will be discussed later in detail.

2-3-3 CMM coating techniques

Deposition of compositionally modulated multilayers has been carried out by three different techniques (the third technique is the process of interest in this investigation).

2-3-3-1 Physical vapour deposition (PVD)

The term physical vapour deposition covers three major techniques, evaporation - sputtering - and ion plating (37).

PVD technology has been developed very rapidly in recent years enabling deposition of a wide range of inorganic materials metals, alloys, compounds or their mixtures as well as some organic materials. The deposition take place inside a vacuum chamber which contains the vapour source and the substrate. A modulation of structure, properties and deposition rate of the coating is possible since the use of different atmospheres (inert / reactive gas) or of different heating methods of the vapour source (induction / electron beam) or magnitude of the electrical voltage of the substrate is possible.

Deposition takes place according to:

1- Synthesis of the materials to be deposited (transition from a condensed phase (liquid or solid) to the vapour phase.

2- Transport of the vapour between the source and substrate.

3- Condensation of vapours (and gases) followed by film nucleation and growth. Table (15) summarises the general advantages and disadvantages of the three different deposition techniques.

2-3-3-2 Chemical vapour deposition (CVD)

Chemical vapour deposition (CVD) is a process in which nucleation and deposit growth on the substrate occur as a result of a stable solid reaction taking place in an environment where a vapour phase chemical dissociation or chemical reaction occurs (38).

CVD uses a variety of energy sources such as heat , plasma, ultra violet light etc. to enable the reaction to take place over a wide range of pressures and temperatures. Some of the well-known processes are:

1- The Mond Process:

$$Ni(CO)_4 \rightarrow Ni + 4CO$$

2- The Arkel Process:

$$TiI_4 \rightarrow Ti + 2I_2$$
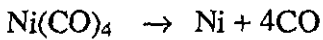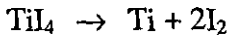
3- The Kroll Process:

$$TiCl_4 + 2\,Mg \rightarrow Ti + 2\,MgCl_2$$
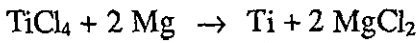
This technique has also been used to form free-standing, simple and complex shaped articles from metals which are not very amenable to fabrication e.g. tungsten :

$$WF_6 + 3H_2 \rightarrow W + 6\,HF$$
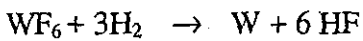
2-3-3-3 Electrodeposition Technique

1- Introduction

Compositionally modulated alloys have been produced for many years by electrochemical synthesis (38). This technique which has the inherent advantages of low cost, of the possibility to produce large scale fabrications, of operating at room temperature and producing CMMM coatings as well as CMAM coatings on a wide range of shapes and of substrate sizes at a relatively high deposition rate. The electrodeposition technique also suffers from some disadvantages such as poor throwing power, possible hydrogen embrittlement (especially with steel substrates) and difficulties in producing ultra thin layers. However, the use of specific plating processes (high speed electrodeposition, anodic preparation of substrates, etc.), suitable plating conditions and additives (such as stress relievers) has overcome some of these disadvantages. Multilayers produced by electrodeposition have several forms and have been applied to substrates (e.g. steel) to improve their properties for many years; these forms are (26):

1- Organic / metal multilayer coatings (e.g.)

Paint
Phosphate layer
Zinc
Steel
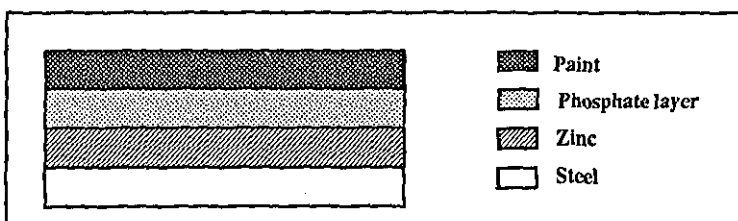
The zinc layer provides sacrificial protection in case the paint degrades or is damaged; the paint provides primary protection as well as a decorative role.

2- Metal / metal coating system (e.g.)

Cr (0.2-2 μ m)
Ni (5-30 μ m)
Cu
Steel
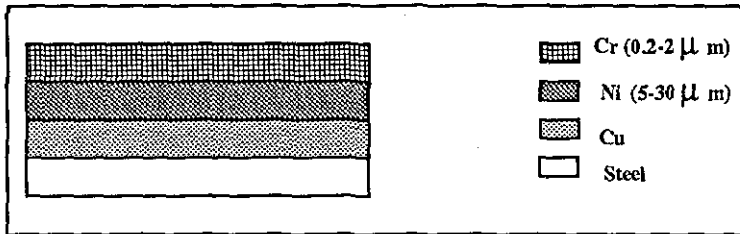
The hard chromium layer provides wear resistance and a decorative finish to the substrate, while the nickel under layer acts as a noble metal protection barrier.

Furthermore, an alloy of 80% nickel-20% chromium was produced by depositing alternate layers of nickel (18.8 μ m) and chromium (6.2 μ m) and then heat treated for 4 hours at 1000 ^{0}C. This treatment completely diffused the nickel and chromium, developing a homogeneous alloy which resisted air oxidation at elevated temperatures more effectively than nickel or chromium alone (39).

Layered coatings up to 25 microns in thickness are being applied to helical washers used out doors. A bottom layer of 2.5 microns of tin with a top coat of 5 microns of zinc was tested against both 7.5 microns of zinc and 7.5 microns of cadmium, the tin-zinc layered coating was superior to the zinc coating and equivalent to the cadmium coating (40).

3- Alloy/alloy coating system (e.g.)

A multilayered coating consists of a zinc alloy and a top of an iron-phosphorous alloy (41), the iron-phosphorous improves the over all corrosion resistance.

Dhar and Ooij (42) deposited a dual-layer alloy coating system with optimal defomability and adhesion characteristics which consisted of a Zn-1% Co first layer on steel followed by a Ni-28% Zn second layer.

The under layer was designed to provide galvanic protection against the pitting corrosion of steel, the top layer was incorporated to improve the surface adhesion of

the coated object. They claimed that the dual layer coating offers excellent corrosion protection (42).

These forms of macrolayered coating systems which are generally applied for corrosion protection purposes differ from microlayered systems which provide a distinctive enhancement of physical and mechanical properties as stated before.

Moreover, the electrodeposition technique can be an attractive alternative for the production of these types of multilayers because of its low investment cost (e.g. no vacuum required). The electrolytic deposition rates can easily reach 10 nm per second and clearly there is the possibility of plating large scale surfaces in suitably sized process tanks. Most electroplating solutions can be operated close to room temperature which minimises the danger of inter-layer diffusion during deposition (a potential problem with higher temperature processes).

Despite the above advantages offered by this technique, it can suffer from certain disadvantages such as poor throwing power, hydrogen embrittlment of the substrates (especially steel) and difficulties in achieving very thin layered structures due to the time required for the re-distribution of ions in the diffusion layer at the cathode surface (43). Moreover, with the use of proper cleaning and plating processes and additives the technique could overcome some of these disadvantages (table (14)).

The electrodeposition of multilayers can be broadly carried out by two methods:

2- Dual Bath Technique (D.B.T)

In the dual bath electrodeposition technique, the substrate is transferred repeatedly between two separate electrolytes. Agitation by means of aeration or mechanical stirring can be used to enhance deposit properties. Figure (6) illustrates a simple schematic presentation of the experimental set-up used for the electrodeposition of CMM's by the dual bath technique.

The dual bath process, by definition, requires the substrate to be rinsed between each transfer. This is vital to prevent cross-contamination of the solutions (44).

30

Table (15) Advantages and disadvantages of three different production techniques of CMM coatings.

Technique	Advantages	Disadvantages
Physical Vapour Deposition (PVD)	- Versatile. - Thin and thick films are possible. - Several variations in technique. - Highly smooth coating surface finish. - No toxic pollutants or effluents are produced. - Very fined-grained coatings. - Low deposition temperature . - Very high purity of the deposits .	- Expensive and sophisticated technology. - Not suitable for mass production .- Coating/substrate adhesion can be problematical. - Poor throwing power.
Chemical Vapour Deposition (CVD)	- Good throwing power. - Relatively low capital investment costs. - Non-electrically conducting substrates can be coated. - Coating/substrate adhesion very good. - Complete and uniform coating of complex shapes. - Different components can be coated at the same time. - Suited for the mass production of small items.	- Relatively long coating and overall process times. - Some limitation on the size of components to be coated. - The high deposition temperature required limits the types of substrates which can be coated.
Electrodeposition Technique	- Low investment cost. - The possibility to plate large scale surfaces. - Can be operated at room temperature. - High deposition rate. - Suitable for mass production	- Poor throwing power. - Possible hydrogen embrittlment. - Difficulties encountered in producing ultra thin layers.

The simplicity of the dual bath technique in terms of solution chemistry and control as well as the capability of this technique to produce alternate layers of pure metals and the possibility to deposit a wide range of metals are the main advantages that characterise this technique. Unfortunately, this technique also suffers from certain drawbacks which make it unpopular despite its conceptual simplicity (43). These drawbacks include the possibility of forming an oxide layer on the specimen surface during each transfer from one bath to the other. It can also be technically difficult to automate the process and there are potential difficulties in scaling it up for mass production (45).
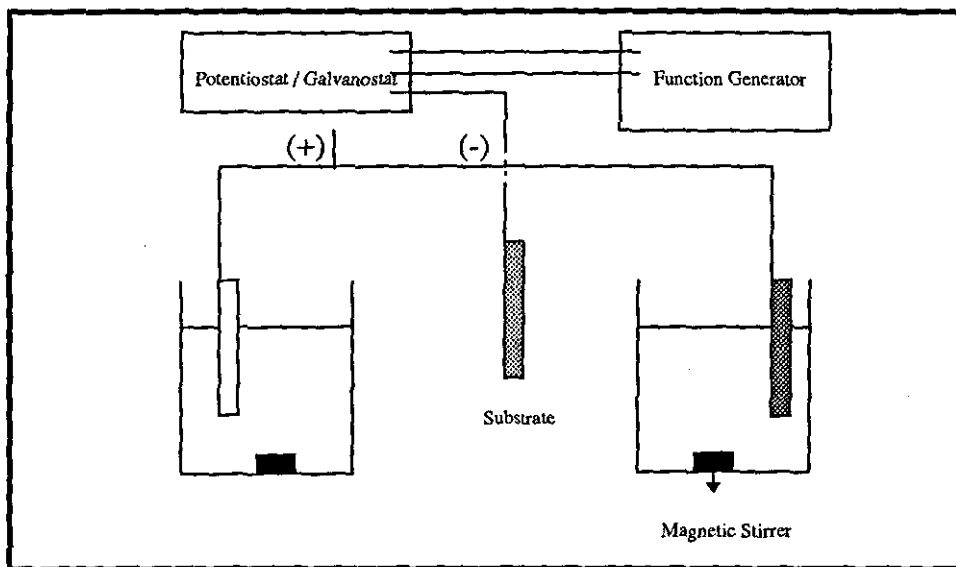
Figure (6) Schematic presentation of the experimental set-up used for the electrodeposition of CMM's by the dual bath technique.

Nevertheless, Roos et al (46) have made a successful attempt to build up an automated dual bath electrodeposition system consisting of a rotating wheel (which the substrate is mounted on) and solutions which are pumped through two wedge-shaped nozzles, which allow the electrolyte flow to impinge on the substrate. The cleaning of the substrate is achieved through two steps by a combination of hot and cold distilled water jets or a nitrogen jet and a rubber wiper (figure (7)).

The substrate rotation speed, the flow rate of solutions through the nozzles and other plating conditions can be adjusted before and also during the plating sequence.

This automated system has been used to produce homogeneous and multilayered films of Ni, Cu, Co and NiP$_x$ over a wide range of compositions with crystalline and amorphous microstructures.
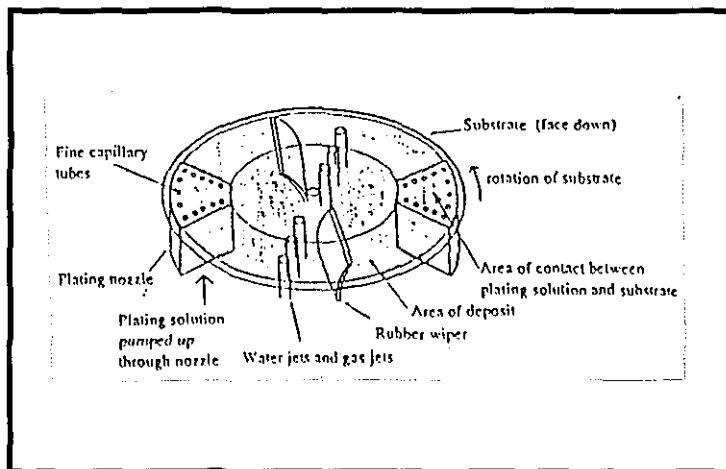
Figure (7), Schematic presentation of dual
bath electrodeposition apparatus used by Roos et al (46).

3- Single bath technique (S.B.T)

The single bath technique, which consists of a single electrolyte containing two
different metal ions, is usually based on a pulsed plating process. There are several
conditions which have to be satisfied for the deposition of a layered structure from a
single bath (43,64) these can be summarised as:

1- The two constituents which build up the layered structure must have different
deposition potentials and different cathodic reversible potentials, so that the more
electropositive one (or more noble-metal [1]) can be deposited for a desired length of
time with out the deposition of the more electronegative (less noble -metal [2]).

2- The concentration of metal [1] must be sufficiently low enabling the less noble metal
to be deposited at a high cathodic potential.

3- The redissolution of the metal [2] by anodic process when the potential is returned
to its original value must be sufficiently slow, so the layer of the metal [2] remains
relatively intact until it is covered by a new layer of metal [1].

The major advantages of the single bath technique are that the substrate remains in the
electrolyte (unlike the dual bath technique). Hence the risk of bath contamination, as

33

well as the risk of forming an oxide layer on the cathode surface, is eliminated. However, the single bath technique suffers from some drawbacks such as the difficulties of depositing a high purity layered structure which means that the single bath technique is only really capable of producing CMAM coatings.

These electrochemical requirements restrict this technique to specific metals systems and also necessitate the use of sophisticated control equipment. Furthermore, the process which produces compositionally modulated systems has to be reproducible, controllable and capable of producing multilayers with desired properties.

Consequently, it is necessary to select the appropriate control equipment that can facilitate the electrodeposition parameters and maintain them at fixed values.

Whilst some deposition parameters can easily be controlled and do not need sophisticated equipment such as temperature, pH and concentration. The pulsed current and agitation which play a vital part in the production of this type of deposit, need more sophisticated equipment and have to be closely controlled and maintained to achieve the desired results.

3-1 Pulsed current electrodeposition

Plating with a modulated (pulsed) current has been employed for many years (47). However, the effect of pulsed current on various aspects of metal deposition has been broadly investigated and it has been stated (48) that certain benefits can be obtained by the use of pulsed current. Popov et al (48) claimed that a maximum deposition rate can be achieved and increased by several order of magnitude and that power saving can be realised by the use of pulsed current. The major advantages of pulsed plating can be summarised as follows:

1- A more fine grained deposition can be obtained. This is because higher current densities can be used during pulsed plating which leads to an increase in adatom concentration on the cathode surface, resulting in an increased nucleation rate and therefore a finer grained structure(49).

Furthermore, Krivstov (50) observed that plating with pulsed current permitted the use of higher applied currents and it was still possible to obtain smoother deposition of copper and zinc.

2- The use of higher current density pulses can produce deposits with reduced porosity as a result of a dense grain structure and improved surface coverage (51).

3- Soft and crack free deposits of chromium can be obtained (52).

4- The current efficiency can be increased and hence the plating rate, with the use of pulse current (for rhenium and iron electrodeposition) (53). Ozerov et al (54) claimed that the rate of deposition could be increased by reducing the pulse duration. Conversely, Puippe et al (55) observed a decrease in plating rate in both gold-cobalt and copper electrodeposition.

5- High purity with low electrical resistance deposits (56). The possible reason behind it is due to the desorption of adsorbed particles from the cathode (54).

6- Enhancement of mechanical properties such as tensile strength e.g. for nickel deposits (56), ductility e.g. gold-cobalt alloy plating (57) and ductility, hardness and elongation e.g. copper deposits (58).

The pulse plating process which has been applied to produce multilayers by the single bath technique has four possible regimes (59):

1- Single current pulse regime

In this regime, metal [1] is first deposited due to the imposed cathodic current until its ions are depleted in the cathode diffusion layer and the rate of its deposition becomes limited by ionic diffusion from the bulk solution and hence concentration polarisation occurs and results in co-deposition of metal [2].

The concentration of the ions of metal [1] must be sufficiently small so that concentration polarisation due to slow diffusion leads to the transition to the deposition potential of metal [2] within the duration of the pulse leaving enough time for the deposition of the second layer.

However, the single-current pulse regime has limitations due to difficulties encountered in achieving a desirable layer thickness as well as difficulties in controlling the amount of metal [1] contained in the electrodeposited layer of metal [2] hence the amount of the former metal is proportional to the ratio between its diffusion limiting current and the total applied current.

2- Dual-current pulse regime (59)

The dual current pulse regime was developed due to the limitations of the single current pulse regime. The process has four parameters which can be set independently I_{M1}, T_{M1}, I_{M2}, T_{M2}, the current pulse I_{M1} which is low, is first applied to deposit only a layer of metal [1] at a specific time T_{M1}, the value of I_{M1} is determined by the hydrodynamic condition of the solution. After a desired thickness of pure metal [1] has been achieved, the current is increased to a level I_{M2} leading to the deposition of metal [2] which must be sufficiently higher than the diffusion limiting current of ions of the metal [1] I_{M1}. The process is repeated after a time sufficient to obtain the desired thickness of metal [2].

3- Triple-current pulse regime

Lashmore et al (60) were the first to introduce the so-called triple- current pulse technique. In addition to the high current I_{M2} and low current pulse I_{M1} used in a dual-current pulse regime they introduced a short zero current pulse just after the high current pulse. This was found to sharpen the transition substantially. Using this technique Lashmore et al were able to obtain good quality multilayers. Hosokawa (61) claimed that a smoother uniform deposition can be obtained by application of dual current pulse with an adequate anodic current pulse in a low current pulse period.

4- Quadruple-current pulse regime

A four-current pulse regime has been adopted during the present experimental work. The quadruple-current pulse regime consists of four phases "figure (8)":

1- Phase one represents a current below the diffusion limiting current of metal [1] which allow for the deposition of metal [1] without the risk of depositing metal [2].

2- The second phase represents a small current [phase 2] $\langle\langle$ [phase 1] which is far below the diffusion limiting current of ions of metal [1] and also much lower than the phase 1 current. The second phase is applied for a specific small period.

The benefit of the second phase is in permitting the solution to " recover " from phase one. The ions of metal [1] and even metal [2] are redistributed in the electrolyte and this makes it possible to deposit a relatively pure metal [2] during the third phase. This will occur because there is no concentration polarisation due to metal [1] . Moreover,

phase two gives the possibility of changing the hydrodynamic conditions of the solution between phases 1 and 3.

The usefulness of applying a small current in phase 2 instead of zero current is to prevent oxidation reactions from taking place on the cathode surface.

3- Phase three involves applying a significant current to electrodeposit substantially ions of metal [2]. This phase three current is considerably higher than the diffusion limiting current of ions of metal [1] and hence reduces the metal [1] content of this electrodeposited layer to a minimum.

4- As phase two.

This regime has been used successfully in later investigation of Cu/Ni and Zn/Ni systems.
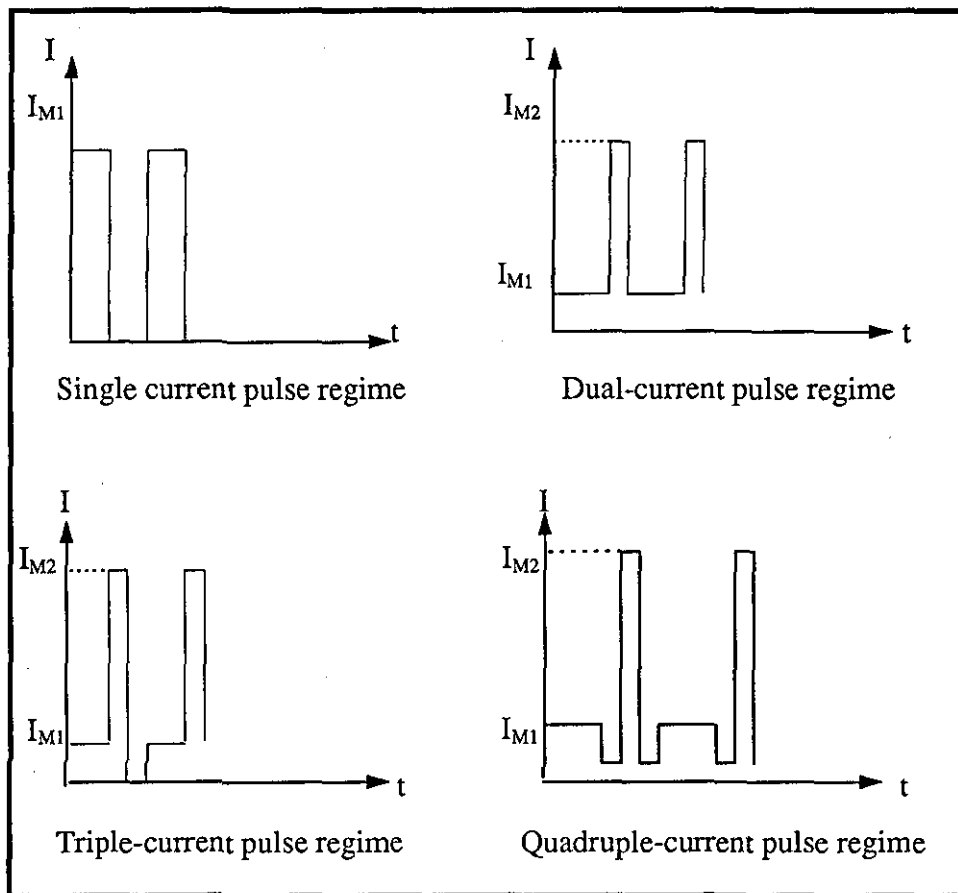
Figure (8). Schematic representation for pulsed current regims

3-2 Agitation

Agitation is usually applied to improve deposit properties such as uniformity, reduce porosity and increase homogeneity and it is generally carried out by means of air bubbling, mechanical stirring or electrode movement. The latter form of agitation is the only one capable of producing reproducible and controllable agitation and hence has definite advantages over the rest.

Electrode movement can be divided into two categories:

- Reciprocal movement.

- Rotational movement.

The latter is widely used as a means of simulating agitation process for high speed electrodeposition.

The beneficial effects of rotating the electrode on the structure of electrodeposited metals are evident and may be attributed to the change in the constitution of the cathode film, and can be listed as follows:

1- Reduction of whiskers formation (growth perpendicular to the surface) which leads to the production of a smoother surface.

2- Removal of bubbles on the cathode surface which if not removed could lead to porosity in the coating.

3- Reduction of crystal size due to the reduction of crystal growth rate.

3-3 Types of rotating electrodes

1- Rotating disc electrode (RDE)

The rotating disc electrode consists of a metal disc embodied in the tip of a cylindrical body made of an insulating material. This is connected to a cylindrical shaft which is driven by an electric motor with adjustable speed. The disc is contacted through an internal connector in the shaft and a brush contact (or mercury reservoir), figure (9). The rotation of the electrode causes a pump effect in the process cell and electrolyte flows towards the disc. This flow is laminar over a relative wide range of rotation speeds.

2- Rotating cylinder electrode (RCE)

The rotating cylinder electrode consists of a cylindrical electrode fixed to a rotating shaft . Unlike the rotating disc electrode, turbulent flow occurs readily at relatively low rotation speeds. With appropriate cell design the current distribution over the electrode surface is uniform and the rate of electrodeposition can be enhanced 5-20 times (62).
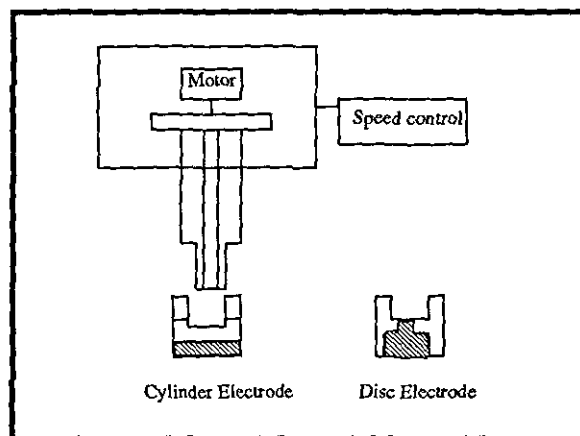
Figure (9). Schematic diagram of rotating electrodes

3- Rotating ring disc electrode (RRDE)

The rotating ring disc electrode is basically a RDE with a second ring shaped electrode mounted concentrically at a very small distance from the disc, where the disc and ring are electrically contacted separately (64).

4- Historical development of electrodeposited CMM coatings

The reported work on the electrodeposition of multilayers can be devided into two main periods. An early period which goes back to 1921 and ends in 1967. Since then no reported work has been published until recently when increasing interest in the electrodeposition technique of producing multilayers has occurred due to its advantages over conventional methods such as CVD and PVD. Hence, it can be said that the second period started in 1981 with growing interest until now.

Figure (10) shows cumulative number of publications versus year of publications (43).

4-1 Historical development in dual-bath CMM coatings

The first ever reported attempts to produce CMM coatings dates back to 1921 when Blum (38) produced a Cu/Ni and Cu/Ag layered structures by depositing alternate layers from two electrolytes by manually transferring the substrate in a repetitive mode, the thinnest layers produced were in the neighbourhood of 25μ m. The layered structure showed enhancement of the tensile strength of copper/nickel multilayers compared to either copper or nickel alone. Blum attributed the effect to grain strengthening due to the fact that the grain size of the coating was very small as initially deposited but grew as the coating thickened.
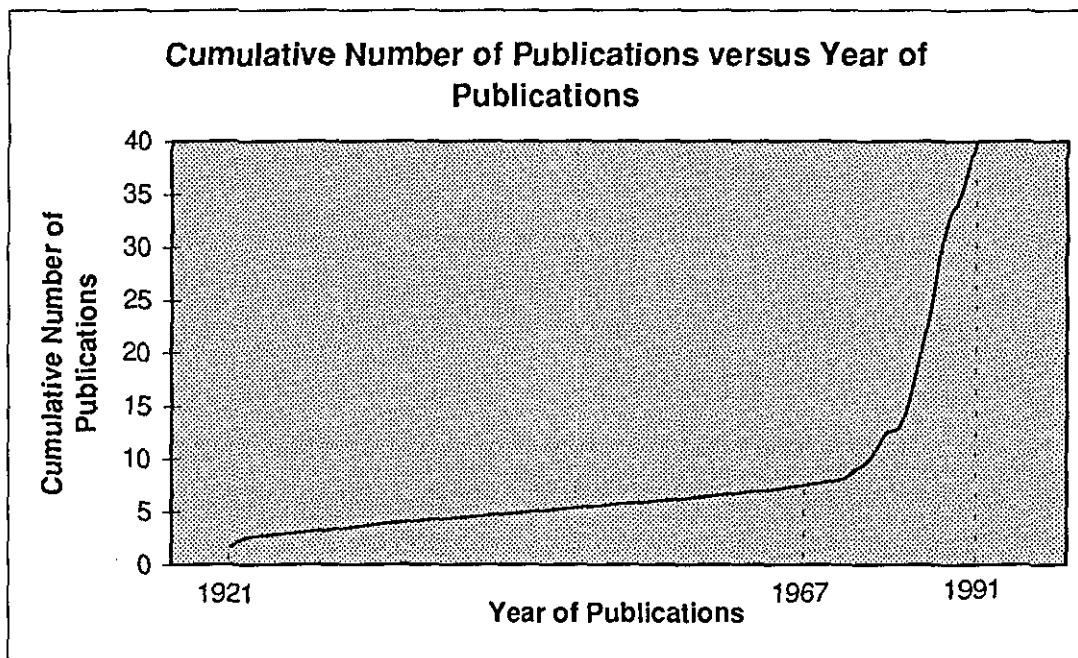
Figure (10) From ref. (44)

A second attempt was carried out by Koeppe (63) and Deubner (64) in 1931 to produce a Cd/Ag multilayer coatings as an x-ray mirrors with a dual bath technique but both attempts were unsuccessful.

Recently, in 1981 Odgen (65) used the dual bath technique to produce Cu/Ni multilayer coatings. However, Odgen did not provide the details of the technique used. Later on, Barral et al (66) used this technique to produce compositionally modulated films of Ni/Zn, The deposition was carried out at a constant potential using a rotating

disc electrode. Several hundred nanometer thick layers were produced using this manual transfer technique.

In 1993, Roos et al (67) made an important enrichment to the dual bath technique by building up an automated dual bath electrodeposition apparatus, and depositing several kinds of multilayered films of NiP_x/NiP_y, Cu/Ni and Co/NiP_x, (table (16)). They were made with a range of repeat thicknesses. They claimed that the produced Ni/NiP_x and NiP_x/NiP_y multilayers produced had the highest quality, with repeat thicknesses as low as 1.9 nm.

Component	Nickel Solutions		Nickel Phosphorous Solutions			Copper Solution	Cobalt Solution
	Sulfate	Sulfamate	A	B	C	Sulfate	Sulfate
$NiSO_4.6H_2O$	195	-	154	169	171	-	-
$NiCl_2.6H_2O$	174	30	46	50.7	50.5	-	-
$NiCO_3.xH_2O$	-	-	26	16.9	16	-	-
H_3BO_3	40	30	-	-	-	-	30
$Ni(SO_3NH_2)_2.4H_2O$	-	230	-	-	-	-	-
HNO_3	-	-	30	5	2.6	-	-
H_3PO_4 ml/l	-	-	35	35	35	-	-
$CuSO_4. 5H_2O$	-	-	-	-	-	200	-
H_2SO_4	-	-	-	-	-	60	-
$CoSO_4.. 7H_2O$	-	-	-	-	-	-	200
$CoCl_2. 6H_2O$	-	-	-	-	1.5	-	30
pH	3.5	3.5	1.5	1.5		0.5	35
Temp. °C	45	50	68	68	68	37	40

Table (16) Compositions of plating solutions, g/l - From ref. (67)

Furthermore, Haseeb et al (44) stated that down to the smallest sublayer thickness (3.4nm), Cu/Ni multilayers can be achieved by the dual bath technique with distinct and continuous layers using copper sulfate and nickel sulfamate based solutions.

4-2 Historical development in single bath CMAM coatings

The first reported work on the single bath technique was made by Brenner in his Ph.D. dissertation (68), he stated that it was possible to electrodeposit a multilayer alloy from a single electrolyte containing salts of two metals, and he produced copper-bismuth alloys with alternating layers of different compositions. They were obtained by automatic switching of the current density between two widely separated values, he

was able to achieve layer spacing in the 100 nm range. The deposit was cross sectioned and etched to form a small diffraction grating.

Twenty one years later, Koehler (69) was the first to point out that laminated structures of certain dissimilar materials assembled according to specific criteria should display enhanced mechanical properties.

In 1983, Cohen et al (70) reported that it is possible to produce a Ag/Pd CMAM structure from a concentrated chloride bath (table (17)).

Constituent	
LiCl	500 g/l
AgCl	12 g/l
PdCl$_2$	3 g/l
HCl	20 ml
H$_2$O	1000 ml
Operating Conditions	
Temperature	85 + 0.5 °C
Agitation	moderate stirring ring (about 10 cm / sec)

Table (17). Chloride-based Ag/Pd CMAM electroplating bath

They showed that the CMAM structure of the Ag/Pd alloy coating with a layer thickness below 50 nm is feasible with lower average current densities and bath concentrations and may exhibit certain desirable properties in electrical contact applications such as reduction of electrical resistivity, increasing corrosion resistance, minimise cost and minimisation of the formation of a tarnish film. The layered structure produced composed of relatively thick layers of an alloy rich in Ag, alternating with thin layers rich in Pd.

Tench et al (71) found a sharp increase in tensile strength in the copper/nickel system when copper layers become thinner than 0.4 microns, later on they described a new method for preparing multilayered alloys by periodically interrupting electrodeposition of the less noble metal.

Visibly smooth, nodule free Cu/Ag alloys of controlled composition have been prepared using a cyanide bath containing 60 g/l copper cyanide, 102 g/l potassium cyanide, 15 g/l potassium carbonate, 15 g/l potassium sodium tartarate and 34 mg/l silver cyanide. The temperature was maintained at 60°C, the deposition was performed on a rotating cylinder electrode at 750 rpm.

In 1986, Lashmore et al (60) reported that production of alternating thin copper and nickel or cobalt multilayer structures with layer thickness ranging from 2 to 200nm. Both potentiostatic and galvanostatic electrodeposition were investigated. Consequently, they claimed that the potentiostatic technique allows the production of sharp interfaces between bilayers but does not permit accurate control over thickness. A coherent structure over a range of layers of a Cu/Ni CMAM has been maintained. The electrolytes used consisted of nickel or cobalt sulfamate solution (90 g/l Ni or Co) , copper sulfate (0.75 g/l Cu) , and 30 g/l boric acid , the pH of the solution was maintained between 3 and 3.5 at room temperature.

In 1987, Yahalom et al (72) reported a method which allows layers of Cu/Ni multilayer structure as thin as 0.8 nm to be produced The method consists of : 1) sulfate baths instead of sulfamate baths 2) using a triple galvanostatic pulse consisting of nickel pulse, an anodic pulse, and a copper pulse 3) electropolishing the substrate .

Rosset et al (73) produced a bright smooth deposit of Ni/Mn CMAM coatings utilize an electrolyte based on chlorides and sulfate salts; the most noble metal Ni was at a very dilute level in the electrolyte compared to the less noble Mn, a ratio ranging from 1/16 to 1/100 has been suggested. The morphology of the Ni/Mn CMAM coatings relies on the dissolution of the Mn layer ocurred when switching to deposit the more noble Ni layer.

In 1988, Ruff et al (74) claimed that there seem to be some improvement in the lubricated wear resistance, a decrease in the friction coefficient and in the voltage drop across sliding contacts when the layers of copper and nickel are less than 100 nm thick.

Furthermore, Despic et al (75) have used a dual rotation speed process which consists of a pulse trains of copper and nickel each of which is applied at different rotation speeds 5000-500 rpm respectively. Later on in 1991 Despic (59) has investigated two different multilayer systems; 1) Cu/Pb deposited from 0.01M copper acetate and 0.1M lead acetate in 1M fluoboric acid (HBF$_4$) 2) Cu/Ni deposited from 0.02M copper sulfate and 2M nickel sulfate in 0.5M sodium citrate . Well defined layers of pure Cu and Ni containing

some copper were produced using a dual-current pulse train . They claimed that the Cu/Pb multilayer system produced is unsuitable for laminar deposition because all the Pb is dissolved during the copper cycle before another lead pulse is applied.

In 1988, Celis et al (76) demonstrated the feasibility of pulsed electrodeposition in a single bath for Cu/Ni-Cu and Ni/Ni-P systems. The electrolyte which was used to produce Cu/Ni-Cu consisted of ; 0.2 N $CuSO_4.5H_2O$, 0.2 N $NiCl_2.6H_2O$, 0.2 N $C_6H_8O_7$ and 0.2 N H_3BO_3 with NH_3 as a pH regulator. The bath was operated at room temperature at pH = 6. The second electrolyte that was used to produce Ni/Ni-P consisted of ; 150 g/l $NiSO_4.6H_2O$, 50 g/l $NiCl_2.6H_2O$, 40 g/l H_3PO_3 and 30 g/l H_3PO_4, the bath was operated at 65 °C .

In 1992, Despic et al (59) stated that the micro hardness of laminar deposits of Cu/Ni multilayer coatings decreases with the increase of layer thickness. The deposition was carried out from an electrolyte containing 2M $NiSO_4.7H_2O$, 0.02M $CuSO_4.H_2O$, 0.5M $C_6H_5Na_3O_7.2H_2O$ applying a dual current pulse .

In the work of Hosokawa et al (61) the deposition of three types of alloys has been investigated Cu/Ni, Ag/Sn and Pb/Zn. The composition of these baths to obtain structure modulated films are:

1) 0.05 mol/l $CuSO_4$, 0.5 mol/l $NiSO_4$, 1 mol/l Na_2SO_4 at pH=3;

2) 0.0025 mol/l $KAg(CN)_2$, 0.025 mol/l $Sn_2P_2O_7$, 1.4 mol/l $K_4P_2O_7$ at pH=10.3;

3) 0.05 mol/l $Pb(BF_4)_2$, 0.5 mol/l $Zn(BF_4)_2$, 0.1 mol/l HBF_4 at pH=1-2. All experiment were carried out at 25-30 °C. Smooth layered structures could be obtained effectively in all kinds of alloys investigated especially in the Pb/Zn alloy system by applying an adequate anodic current pulses within the low current pulse period.

Kalantary et al (77) claimed that the compositionally modulated alloy of Zn/Ni produced better corrosion resistance than a single alloy layer deposit. Furthermore, they stated that the higher the number of repeated layers the better the corrosion resistance of the total coating system. They used an acidic based electrolyte containing 35 g/l zinc as zinc sulfate, 35 g/l nickel as nickel sulfate, and 80 g/l sodium sulfate. The electrolyte was operated at pH=2 and at room temperature.

5- Structure of electrodeposited multilayers

5-1 Introduction

The properties of all materials are determined by their structure, even minor differences often deeply affect the properties of electrodeposited metals (82). The three most important crystal lattices usually found commonly in electroplated metals are:

1- Face centred cubic (FCC)

2- Body centred cubic (BCC)

3- Hexagonal close packed (HCP)

All are shown in figure (11).

Body-centered cubic   Face-centered cubic
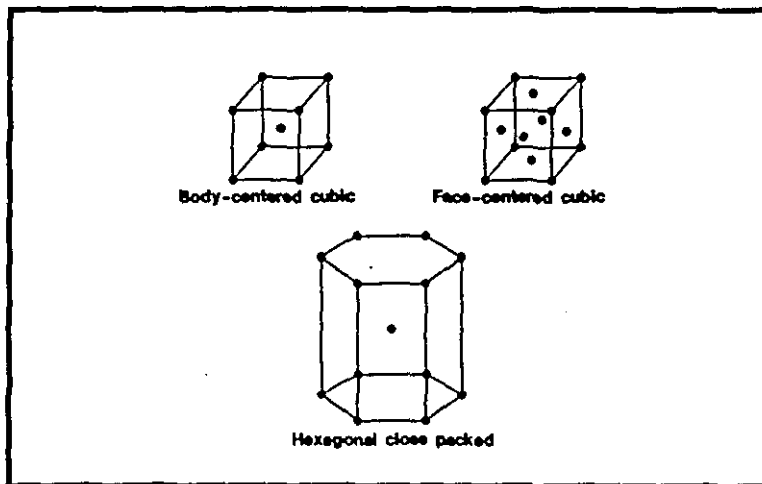
Hexagonal close packed

Figure (11) Unit cells of the three most important lattices.

However, it is often more convenient to specify grain structures encountered with electrodeposited metals, these are : 1) Columnar 2) Fibrous 3) Fine grained and 4) Banded.

Columnar structures usually exhibit lower strength and hardness than the other structures but high ductility. Fibrous structures have an intermediate properties between columnar and fine-grained deposits, whilst fine grained structures exhibit higher electrical resistivity due to the presence of co-deposited foreign material (nucleating agents), these structures

45

usually have relatively high strength and are brittle (78). Laminar (or banded) structures exhibit high strength and hardness but low ductility.

Furthermore, the texture (preferred orientation of grains) of electrodeposited coatings can noticeably affect a variety of functional properties of materials such as formability, corrosion behaviour, magnetic properties, wear resistance and porosity. The most important crystal plane structures are {100},{110},{111} and are shown for cubic lattices in figure (12).

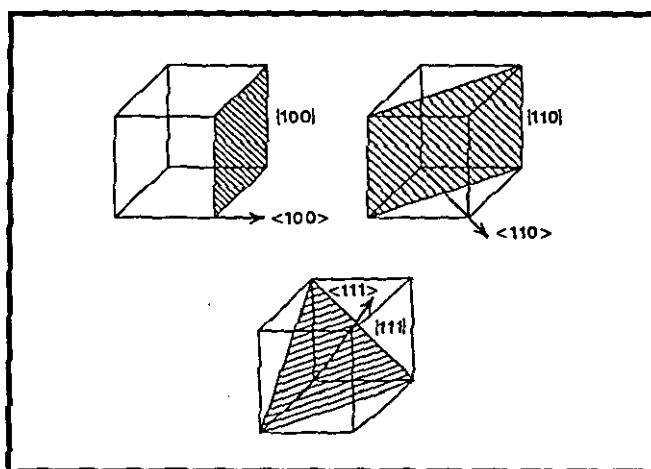Figure (12). {100},{110},{111}crystal plane structures

These effects can be seen in the corrosion behaviour of zinc alloy coatings which are affected by texture in terms that the layer can act either sacrificially or as a protective corrosion barrier. Zinc grains with a near {0001} basal orientation have much lower corrosion currents in sodium hydroxide solution than those of other orientations; the corrosion data in 0.5 N sodium hydroxide solution for polycrystal and oriented crystal specimens are shown in table (18).

Exposed crystal plane	Corrosion current $\mu A /cm^2$	Calculated corrosion rate μ / year
{0001}	81	4.8
{1010}	127	7.5
{1120}	261	15.3
Polycrystal	160	9.4

Table (18). Corrosion data in 0.5 N sodium hydroxide solution for polycrystal and oriented crystal specimens. From ref. (79)

Moreover, zinc grains with {0002} orientations parallel to the sheet surface provided better adherence than those of other orientations. Figure (13) illustrates the relationship between knoophardness and the {111} content of copper foil adapted from ref. (80).
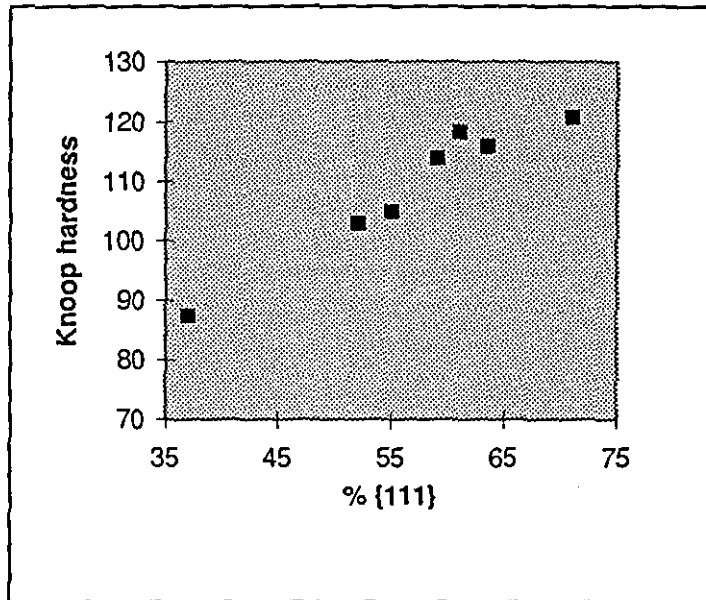

Figure (13) The releationship between
Knoop hardness and the {111} content of copper foil
From ref. (80)

The magnetic properties of cobalt / phosphorous thin films is also affected by texture orientation, the films with minimum preferred orientation exhibit maximum coercivity values (81).

The structures of electrodeposited multilayers are varied and depend upon the metals used in electrodeposition, the source of the metals (acidic or alkaline electrolytes), the other constituents of the electrolytes, substrate surface preparation , type of substrate, multilayer production technique and operating conditions. Figure (14) illustrates the relationship between the structure of electrodeposits to operating conditions of the electrodepositing solution (82).
In general, the structure of electrodeposited multilayers is far more complicated than that of normal metal or alloy coatings, this is due to the interfaces present between layers, the different layer interactions, layer thicknesses and layer coherency (43).
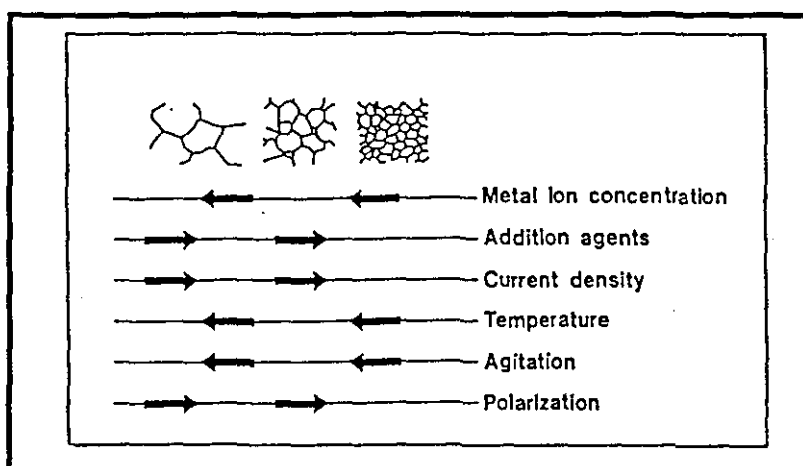
47

Figure (14): Relationship of structure of electrodeposits to operating conditions of solutions. From ref. (82).

Several researchers (67, 71, 83) have investigated the microstructures of layered coatings especially Cu/Ni multilayer systems using different techniques such as scanning electron microscopy (SEM), transmission electron microscopy (TEM), auger electron microscopy (AES), x-ray diffraction and energy dispersive spectroscopy (EDAX). Different Cu/Ni structures have been produced, Celis et al (76) claimed that a layer thickness of 100 nm grows with a predominantly {220} fibrous structure, for a 5 nm layer the growth occurs in a uniform columnar fashion. X-ray diffractometer studies showed that the electrodeposited Cu/Ni CMAM coatings display a mixed {100}, {111},{110} or {200} textures (83). Table (19) shows a survey of thicknesses and structures of different multilayer systems produced by several researchers.

6- Properties of electrodeposited multilayers

6-1 Tensile strength

The most research work on the tensile strength of CMM coatings has been carried out on the Cu/Ni multilayer system. Blum (38) was the first to point out the enhancement in tensile strength of Cu/Ni multilayers. Tench and White (71) claimed a sharp increase in tensile strength of Cu/Ni multilayers when the copper layer thickness fell below 400 nm,

they found that the tensile strength of a layer copper thickness of 10 nm was about 1300 MPa, and was three times the strength of pure nickel.

Published Paper Authors	System	Production Technique	Thickness (nm)	Structure
Bennett (83)	Cu/Ni	S.B.T	1 to 6	{111} texture
Wouters (84)	NiP/Sn	D.B.T	500 to 100	Straight uniform structure
Blum (38)	Cu/Ni	D.B.T	25	Very small grain structure
Blum (38)	Cu/Ag	D.B.T	25	-
Barral (66)	Ni/Zn	D.B.T	20 to 100	-
Roos (46)	NiP_x/NiP_y	D.B.T	1.9	High quality deposits
Haseeb (44)	Cu/Ni	D.B.T	3.5	Distinct and continuous sublayers
Brenner (68)	Cu/Bi	S.B.T	100	-
Cohen (70)	Ag/Pd	S.B.T	5	-
Tench (71)	Cu/Ag	S.B.T	-	Smooth, nodule free
Lashmore (60)	Cu/Ni Cu/Co	S.B.T	2 to 300	Coherent structure, {111}, {100} grain textures
Rosset (73)	Ni/Mn	S.B.T	-	Bright and smooth deposits
Lashmore (60)	Cu/Fe	S.B.T	-	High quality deposits
Roos (46)	Co/NiP_x	D.B.T	10-20 nm	irregular multilayers, uneven interfaces

Table (19). Survey of thicknesses and structures of different multilayer systems.

A maximum reported value for the tensile strength of Cu/Ni electrodeposited multilayers occurred at 20 nm thickness for which the copper and nickel layers were 2 and 18 nm thick respectively (71), this value is 70% higher than the maximum tensile strength achieved by physical vapour deposited Cu/Ni CMAM coatings which were found at a layer thickness of 2 nm (figure (15)).

6-2 Wear resistance

Wear studies for compositionally modulated multilayers have been carried out by a number of researchers. Cohen (70) reported in 1987 that the electrodeposited multilayer system of Ag/Pb has better antifriction performance than the more conventional sputter deposited carbon, also a smooth wear track was observed on the Ag/Pb electrodeposited

CMAM coatings where as a rough and grooved wear track was detected on the sputter deposited carbon.
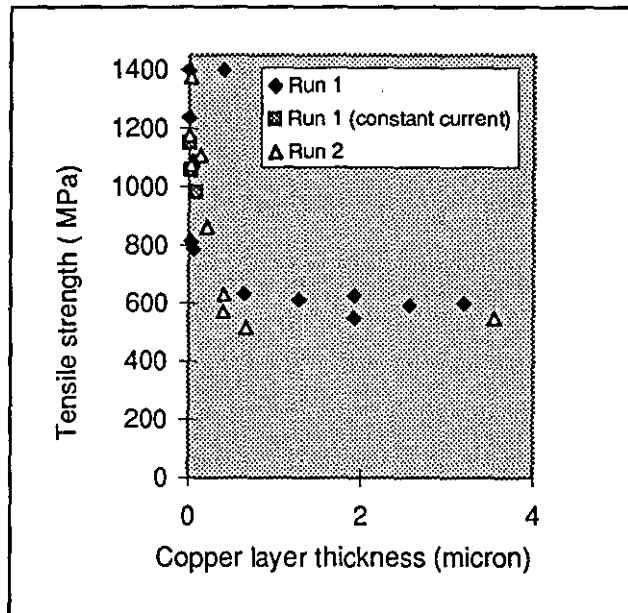

Figure (15). Plot of Ultimate Tensile Strength vs. Copper Layer Thickness for 90% Ni,10% Cu electrodeposited layered composites. From ref. (71)

Ruff et al (74) reported that the wear rate in an unlubricated test of two layer thicknesses (10 and 100 nm) Cu/Ni multilayers was found to be lower than of either copper and nickel, also it was found that the 10 nm layer thickness had a lower wear rate than the 100 nm. In lubricated test condition, an improvement of wear resistance was also observed. Figure (16) shows that the copper coating exhibits the highest wear approximately twice that of the nickel deposit.

6-3 Magnetic properties

The magnetic properties of electrodeposited Cu/Ni (85) and Co/Cu (86) CMAM coatings were found to be similar to those which had been physical vapour deposited. It was found that there is an improvement in magnetic properties for both Ni and Co layers in electrodeposited Cu/Ni and Co/Cu CMA coatings respectively. The improvement in magnetic properties of Ni was found to be larger in thinner layers.
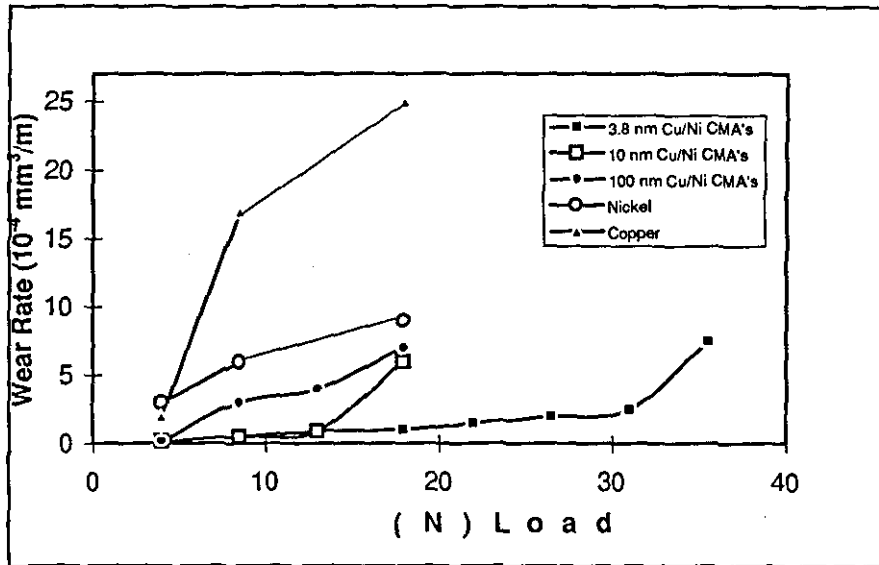
Figure (16). Wear rate as a function of load for copper, nickel and Cu/Ni multilayers.
From ref. (43)

Bennett et al (86) claimed that the electrodeposited Cu/Ni samples display strong
anisotropies in addition to the demagnetisation contributions. The results are qualitatively
similar to the evaporated samples. They related this effect to the Ni/Cu interface.

6-4 Electrical resistivity

The electrical resistivity of electrodeposited Cu/Ni multilayers(86) was found to be
strongly dependent on the thickness of the deposit. A maximum electrical resistivity
occurred at the same thickness, that is 20 nm (43) and then decreased with further
decrease in thickness.

6-5 Corrosion resistance

Wiel and Sheu (87) have studied the corrosion resistance of a number of chromium-based
multilayers with individual layer thickness of 250 nm. They found that an electrodeposit
of multilayered Cr/Mo with alternate layers richer and poorer in molybdenum had
improvements in corrosion resistance in sulphuric acid. Multilayered deposits with

51

alternate amorphous and crystalline chromium and also with various carbon contents showed improvement in corrosion resistance especially in hydrochloric acid.

Kalantary et al (77) stated that Zn/Ni CMAM coatings had better corrosion resistance when compared to single alloy Zn/Ni layer deposits.

2-4 CMM Systems of Interest

It is important to summarise the major reported work carried out by several researchers which is related to the author's present work. Two systems are of major interest; Cu/Ni and Zn/Ni compositionally modulated multilayer systems.

2-4-1 Copper/nickel CMM coating systems

The electrodeposition of Cu/Ni CMM coatings with a layer thicknesses ranging from a few microns to a nanometer scale or less with distinctive mechanical properties have been successfully produced by two electrodeposition techniques, namely dual and single bath:

2-4-1-1 Dual bath Cu/Ni electrodeposition technique

The deposition sequence of the Cu/Ni coating system by the dual bath technique is shown in figure (17). After immersing the prepared substrate, which can be copper or steel, in the nickel plating solution a constant current which can be either direct or pulse of a specified value and waveform is applied to deposit a nickel layer of a desired thickness. At the end of the nickel plating period, the substrate is taken out immediately, dipped and stirred in a beaker of deionized water. A second rinse in another beaker of deionized water is also necessary to remove any nickel plating solution which could be left on the substrate surface completely. After that, the substrate is rinsed in the copper plating solution. This procedure is used to ensure the removal of the water film from the substrate (and to replace it with a copper solution film) which if not removed could result in a porous non-epitaxial deposit (87). Wiel et al. (87) attributed this effect to the decomposition of water droplets clinging to the substrate when the current / voltage is applied in the copper plating solution. The substrate is transferred then to the copper plating bath and a copper layer of desired

thickness is then deposited. Typically, the transfer and rinsing operation together take about 10 seconds (44). The same procedure is then carried out to deposit a second Ni layer after rinsing the substrate in the dual rinse baths and immersing it in a nickel solution.

The electrodeposition of copper and nickel layers are carried out in several kinds of electrolyte. Table (20) shows the compositions of these baths and their operating conditions as well as crystal textures produced.

Findings

1- The electrodeposited Cu/Ni multilayers produced by the dual bath technique and several researchers consist of continuous and distinct copper and nickel layers.

2- Cu/Ni multilayers produced by the DBT grow epitaxially with a columnar structure with a fine grain structure.

Component	Nickel solutions sulfate g/l	Nickel solutions sulfamate g/l		Copper solutions sulfate g/l	
		1	2	1	2
$NiSO_4.6H_2O$	195	-	-	-	-
$NiCl_2.6H_2O$	174	30		-	-
$Ni(NH_2SO_3)_2.4H_2O$	-	230	400	-	-
$CuSO_4.5H_2O$	-	-	-	90	200
H_3BO_3	40	30	30	-	-
H_2SO_4	-	-	-	200	60
pH (^0C)	3.5	3.5	3.5-4	-	0.5
Temperature	45	50	30+1	30+1	37
Current density mA / cm^2	-	20		5-50	-
Crystal texture	{111} fcc	{200}fcc		{110},{100}, {220} fcc	

Table (20). Composition of plating solution and available operating conditions for Cu/Ni multilayers.

3- Existence of facets which are found in copper layers is dependent on the copper layer thickness.

4- The growth of Cu/Ni multilayers occurs in a similar fashion to the SBT in spite of the interrupted deposition, substrate transfer and intermediate rinsing between consecutive layer deposition cycles.

5- The texture of Cu/Ni CMM's is found to be dependent on the electrolyte used, type of substrate and individual layer thickness. However, the texture of Cu/Ni CMM's, in general, has the planes {220}fcc for copper and {111} fcc for nickel.

6- The periodic exposure of the fresh metal surface to the atmosphere did not disrupt continuous growth of the crystals (46) this comment is agreed with Haseeb et al.(43) when they claimed that no detrimental surface reaction or oxidation during substrate transfer affected the regularity of the electrodeposition process.

2-4-1-2 Single bath Cu/Ni electrodeposition technique

Nickel and copper can be alternately deposited from a single electrolyte. The superimposed Pourbaix diagram of copper and nickel, (figure (17)) shows two distinct regions that are due to the potential difference between the two standard redox potentials which is equal to 600 mV (SHE). At potentials in region 1 only copper will be deposited, if the potential is increased and stepped to region 2 both copper and nickel will be deposited. The copper limiting current depends on concentration thus, if the concentration of copper in the electrolyte is low, the deposits in region 2 will consist essentially of nickel. The nickel deposit, however, will contain a small amount of copper but the ratio of copper to nickel in region 2 can be determined arbitrarily either by altering the nickel deposition potential or by changing the composition ratio in the electrolyte. The copper limiting current, however, is very sensitive to the hydrodynamic condition around the cathode surface and can be increased rapidly by stirring the electrolyte with a RCE, RDE, or by ultrasonic means.

Therefore, the more noble metal, copper, is first to be deposited at a low cathodic potential. The copper layer can be deposited for a desired period of time without the deposition of nickel and if the concentration of copper is kept sufficiently low the nickel layer will be deposited at a high cathodic potential with only a low copper content.

Compositionally modulated alloy multilayer coatings of Cu/Ni have been prepared galvanostatically and potentiostatically, and different kinds of wave forms have been applied (dual and triple pulse regimes). The dual pulse regime has been used by most researchers.
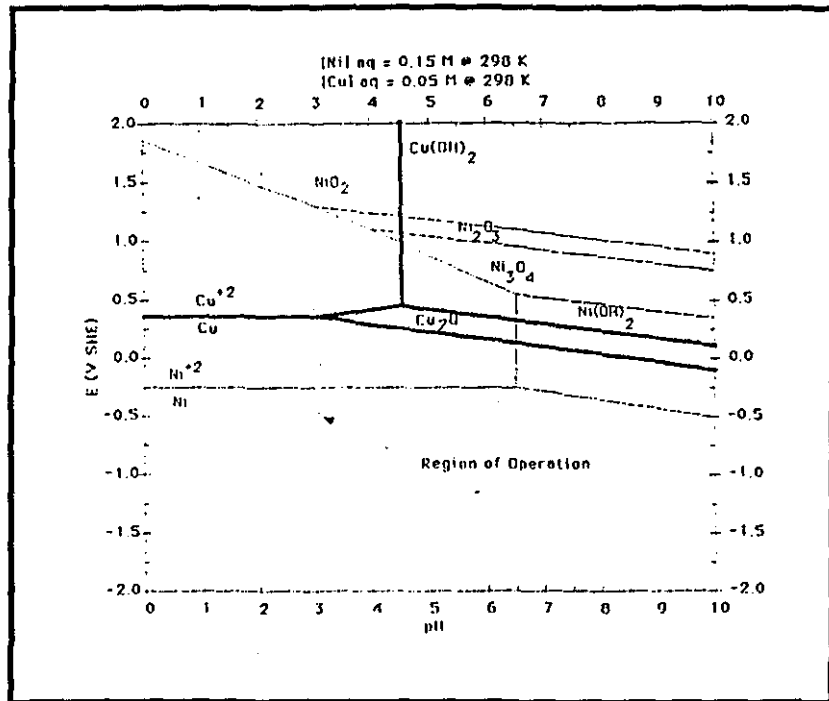
Figure (17). Superimposed Pourbaix diagram of copper and nickel

Whilst, the triple pulse regime was first applied by Lashmore et al (60), they claimed that the short zero current pulse which was applied directly after the high current pulse to give sharp and good quality multilayers. An anodic, short, low current pulse has been applied by Hosokawa (61) which he claims gives a smoother uniform multilayer deposit.

The electrodeposition of Cu/Ni CMAM coatings have been performed using different types of electrolytes. Table (21) shows the composition of these electrolytes and their available operating conditions.

<u>Findings</u>

1- The potentiostatic technique allows the production of sharp interfaces but does not permit accurate control over thickness (60).

Composition and Operating Conditions	Bath 1	Bath 2	Bath 3	Bath 4	Bath 5
Composition					
Nickel Sulfamate	330 g/l	-	90 g/l (Ni^{++})	-	72g/l (Ni^{++})
Nickel Sulfate	-	2 mol/l (Ni^{++})	-	0.5mol/l (Ni^{++})	-
Nickel Chloride	45 g/l	-	-	-	-
Copper Sulfate	150ppm (Cu^{++})	0.02mol/l (Cu^{++})	0.75g/l (Cu^{++})	0.05mol/l (Cu^{++})	0.64g/l
Sodium Sulfate	-	-	-	1mol/l	-
Sodium Citrate	-	0.5mol/l	-	-	-
Boric Acid	35 g/l	-	-	-	37-45g/l
Operating Conditions					
pH	-	-	3-3.5	3	3.8
Temperature(°C)	-	-	Ambient	25-30	50+1
Crystal Texture	{111} fcc Ni,{220} fcc Cu	-	-	-	-
Thickness (nm)	1.4,1.6,2,6,9				3.55microns to 10nm

Table (21). Composition of plating solution and available operating conditions for SBT Cu/Ni multilayer coatings.

2- Sharp interfaces between adjacent layers has been obtained and all the layers growth epitaxially upon each others in a columnar fashions in most cases.

3- At higher concentration of copper ions (0.8-0.1 mol/l) in the solution, the resolution between the two layers becomes poor and the deposit roughens.

4- The copper deposit grows with a three different plane textures, this is due to the influence of substrate surface, the electrolyte composition and layer thickness. These textures are {110}fcc, {100}fcc, {220}fcc.

5- The nickel deposit grows with predominantly {111} fcc texture.

2-4-2 Zn-Ni compositionally modulated multilayer coating systems

Reported work on Zn-Ni CMM coatings appears to be very small and, only two references have been found. The first work concerned the deposition of a stack of repetitive pure layers of zinc and nickel by the dual bath technique without giving any indication of the beneficial effect of this type of coating (66). The second concerned the deposition of Zn/Ni compositionally modulated alloy multilayer coatings from a single bath by controlling the mass transfer and applied cathodic pulse current which lead to significant differences in Zn/Ni layer compositions (77).

The second work investigated the enhancement of corrosion resistance which can be achieved by Zn/Ni layered coatings; whilst, the first work only concerned the deposition of pure repetitive layers of zinc and nickel.

2-4-2-1 Dual bath elctrodeposition of Zn/Ni CMMM coatings

Baral and Maxmovitch (66) produced compositionally modulated films of Zn and Ni by depositing repetitive pure layers with about 20 to 500 nm layer thicknesses by alternating the substrate between two separate solutions.

The deposition was carried out at constant potential, the plating solutions consisting of nickel and zinc electrolytes. Table (22) shows the composition and operating conditions of both plating baths.

Composition	Nickel Bath	Zinc Bath
Nickel sulfate	300 g/l	-
Zinc sulfate	-	280 g/l
Boric acid	40 g/l	-
Ammonium sulfate	-	30 g/l
pH	5	6-7
Current density	15-25 mA/cm^2	15-25 mA/cm^2

Table (22) The Composition and Operating Conditions of Zinc and Nickel Plating Baths used by Baral and Maxmovitch (66).

The deposition was carried out by utilising a rotating disc electrode (RDE) at 1000 rpm to obtain well defined hydrodynamic conditions at a potential -1.4 V vs.SCE for both nickel and zinc plating on an area of 0.2 cm^2. This method allowed the production

of alternate layers of pure metal (16 to 22 layers of zinc and nickel) with a regular thickness.

2-4-2-2 Single Bath Electrodeposition of Zn/Ni CMAM Coatings

Unlike the copper/nickel CMAM coating system, the modulated alloy multilayers of Zn/Ni do not behave in the same electrochemical deposition manner. From the standard electrode potential of nickel (-0.25V vs.SHE) and zinc (-0.76V vs. SHE) one can expect that in a single electrolyte which contains the two components, Ni as a more noble metal will deposit first at a low cathodic potential before the deposition of the less noble metal Zn. In fact, this theoretical consideration does not occur. this is due to so-called anomalous deposition which means that the less noble metal is likely to deposit first due to the formation of zinc hydroxide on the cathode surface. Therefore, it may be difficult to deposit a layered structure of pure metals of zinc and nickel from a single bath.

Kalantary et al (77) claimed that it is possible to deposit a repetitive layers of zinc-nickel alloys each layer containing a specific nickel content by careful control of the electroplating conditions such as current density and electrode movement. Furthermore, they stated that an enhancement of corrosion resistance in Zn/Ni CMAM coatings over single alloy layer deposits can be achieved, and the higher the number of repeated multilayers the better the corrosion resistance of the total coating system.

The electrodeposition was carried out from an electrolyte having 35 g/l zinc as zinc sulfate, 35 g/l nickel as nickel sulfate and 80 g/l sodium sulfate at 23°C, the electrolyte pH was 2. The electroplating of Zn/Ni CMAM coatings was acheived using a rotating cylinder electrode by variation of the rotation speeds (0, 50, 100, 500, 1000, 1500 rpm) and the current density (0.5, 1, 10, 50, 100, 130 A/dm^2).

They observed that at low current densities $\leq$ 10 A/dm^2 the alloy composition is almost the same with changing rotation speed. Whilst, at higher current densities $\geq$ 50 A/dm^2 the composition changes significantly with change in rotation speed. The maximum nickel content in the deposit was achieved at 50 rpm and then decreases with increase in rotation speed.

Chapter 3

Experimental Procedures

3-1 Introduction

The electrochemical evaluations and assessments of the different types of coatings were carried out utilising different techniques and test methods. Table (23) shows the major tests that have been used in evaluating the deposition behaviour and assessing the coating quality.

Tests used in evaluating the deposition behaviour	Tests used in assessing deposit quality
1- Hull cell test [1]. 2- Cathodic polarisation behaviour. 3- Cathodic current efficiency measurement.	1- Adhesion test. 2- Porosity test. 3- Scanning electron microscopy, and optical microscopy. 4- Auger electron spectroscopy (AES), secondary ion mass spectroscopy (SIMS), and tranmission electron microscopy (TEM).[2] 5- Corrosion tests[3] : 5-1 Salt spray test. 5-2 Electrochemical test.

(1)- This test was applied only in the investigation of Zn/Ni CMMM coating systems.
(2)- These tests were applied only in the investigation of Cu/Ni CMAM coating systems.
(3)- This test was applied only for the Zn/Ni CMM coating systems.

Table (23). Tests used in the investigations of CMM coating systems.

Two different electrodeposition techniques have been used to produce the different types of multilayers, they are dual and single bath techniques.

The dual bath technique has been used to make multilayers from Cu/Ni, Zn/Ni, Zn/Zn-Ni alloy, and Ni/Zn-Ni alloy adopting the same plating procedure proposed by Haseeb et al

(44) for the dual bath electrodeposition of Cu/Ni CMMM coatings. The single bath technique was employed using the general principals reported by several researchers (75, 60).

The coatings produced were examined to evaluate the coating quality. Adhesion and porosity were examined with simple mechanical and chemical tests respectively. The corrosion resistances were examined using conventional salt spray and electrochemical corrosion tests.

The multilayer structure and surface morphology were studied using scanning electron microscopy (SEM) and the compositions of the films were determined with an energy dispersive x-ray spectrometer (EDAX) coupled to the SEM.

3-2 Experimental procedures for the dual bath electrodeposition of Cu/Ni and Zn/Ni CMM coating systems

3-2-1 The deposition sequence and cell set-up

The discussion of the dual bath electrodeposition procedure will apply to all multilayer systems produced by this technique. Hence, in this discussion M1 and M2 could be Cu, Ni, Zn, or Zn-Ni alloy. The dual bath electrodeposition of such coatings was carried out under galvanostatic conditions using a direct current system.

The M1 and M2 baths were two litre glass beakers containing appropriate metal anodes. The plating baths were placed in a water bath to enable the plating temperature to be controlled to ± 1°C. The coatings were deposited on 0.5 mm thick mirror-like pre-finished Hull cell (copper / mild steel) coupons (102×76 mm). The anode and cathode were immersed in the electrolyte and connected consecutively to a potentiostat (galvanostatic mode) which was used to vary the current levels which were measured with a digital multimeter. Figure (18) shows a diagram of the dual bath electrodeposition cell set-up.

60
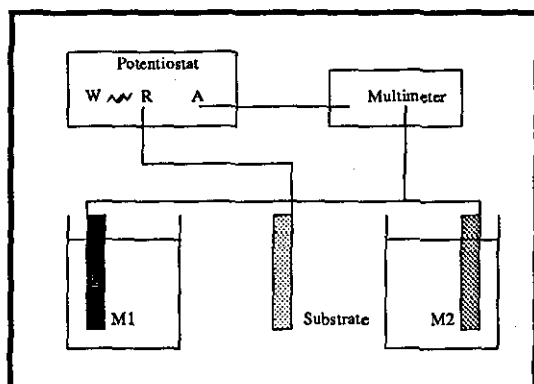
Figure (18). Dual bath electrodeposition cell set-up.

The electrodeposition was carried out by electrodepositing the required thickness of coating consequentively from each bath. After the M1 layer was deposited, the panel was removed from the bath, rinsed in a dual step process with deionised water, followed by immersion in the M2 electrolyte. The electrodeposition of the M2 layer was then carried out. The same sequence was carried out after the electrodeposition of the M2 layer which involved rinsing in the dual step process (deionised water followed by M1 electrolyte) and the electrodeposition of another M1 layer of metal. Figure (19) shows the sequence that was used in the electrodeposition of M1/M2 multilayers.

3-2-2 Galvanostatic deposition of multilayer coatings from dual baths

3-2-2-1 Bath Preparation

All the baths indicated in table (24) were prepared from general purpose reagents (or higher purity) dissolved in deionised water.

3-2-2-2 Cathode Preparation

All cathode material (i.e. copper and mild steel) consisted of masked panels consisting of a one-sided active area of 10 cm x 8 cm. Both types of panel were initially degreased in alkaline solution containing 40 g/l Na_2CO_3 and 5 g/l NaOH for 5 minutes at 60°C. They were then rinsed in tap water prior to etching. The copper panels were etched in 50% (v/v) S.G 1.42 HNO_3 and the mild steel panels in 50% (v/v) S.G 1.18 HCl. Both types of panel were subsequently rinsed in tap water, deionised water and finally acetone before drying in a hot air stream. The copper panels were activated in 10% (v/v) S.G 1.84 H_2SO_4 prior to use.
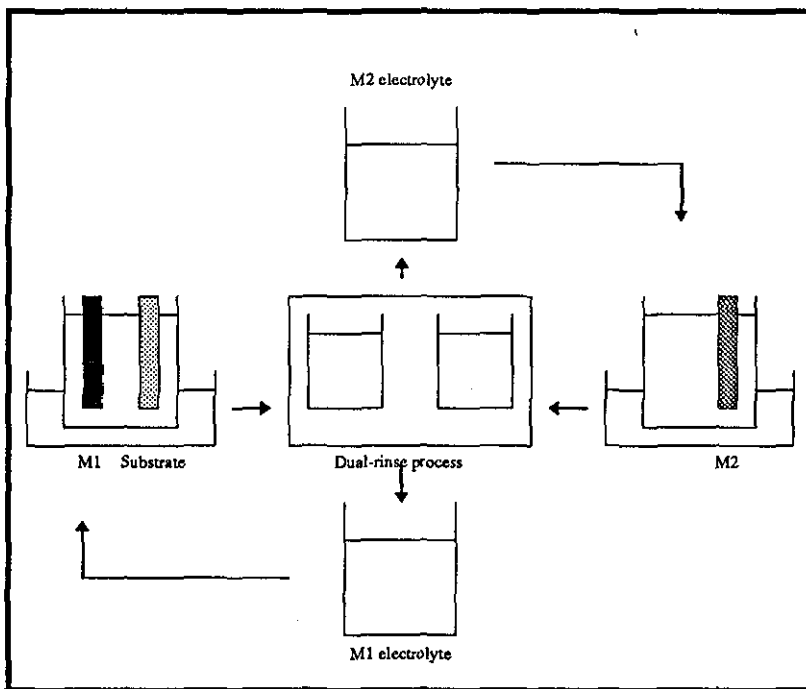
Figure (19). Dual bath electrodeposition sequence for M1/M2 multilayers

3-3 Experimental procedures for the single bath electrodeposition of Cu/Ni and Zn/Ni CMAM coating systems

High speed electrdeposition techniques have been used to produce several types of Cu/Ni and Zn/Ni CMAM coatings. Electrodeposit compositions were varied by changing current density and electrode rotation speed with the different electrolytes specially formulated for electrodeposition applications.

3-3-1 The deposition sequence and cell set-up

The discussion of the single bath electrodeposition procedure applies to all Cu/Ni and Zn/Ni compositionally modulated alloy multilayer coating systems produced by this technique. The single bath electrodeposition of such coatings was carried out under galvanostatic conditions using a pulse current system with two different pulse regimes and was used to plate Cu/Ni from different formulated single baths, and Zn/Ni from a sulfate based bath. Both electrolyte compositions and plating conditions are given in table (24).

The Zn/Ni single layer alloy and Cu/Ni, Zn/Ni CMA layered coatings have been produced under galvanostatic conditions using a modulated direct current system and adopting high speed electrodeposition facilities which consisted of:

3-3-1-1 Rotating Cylinder Electrode (RCE)

A rotating cylinder electrode (RCE) rig, which consisted of a drive motor (180PM04 DC model), rated at 180V DC, 1.2 A with a speed range of 10-2000 rpm, a tachogenerator MP56 DC allowing the speed range to be controlled to within 0.1%. Silver-graphite brushes were used to transfer the applied current to the speed controlled rotating electrode. Figure (20) shows a simple schematic of the RCE cell.
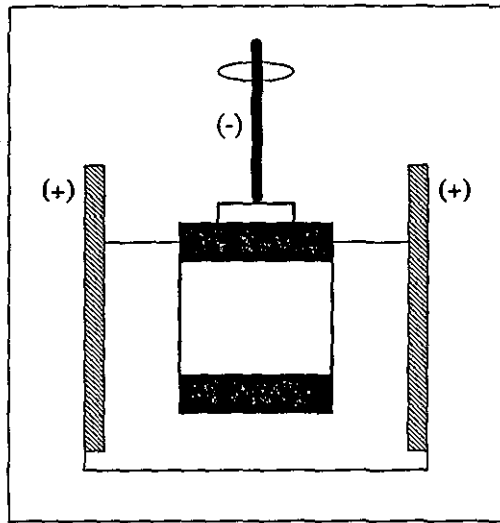
Figure (20). RCE cell

3-3-1-2 Computer assisted pulse plating unit (CAPP)

In conjunction with the RCE apparatus, a 25V/20A Axel Akermann CAPP unit with associated software and controlling PC was used. The current and voltage outputs were monitored with a digital multimeter.

An over-all experimental set-up is shown in figure (21)

1- Process cell 2- RCE 3- Silver-graphite brushes 4- Anodes 5- CAPP
6- Current measurement 7- Voltage measurement 8- Current / Voltage modulation measurement
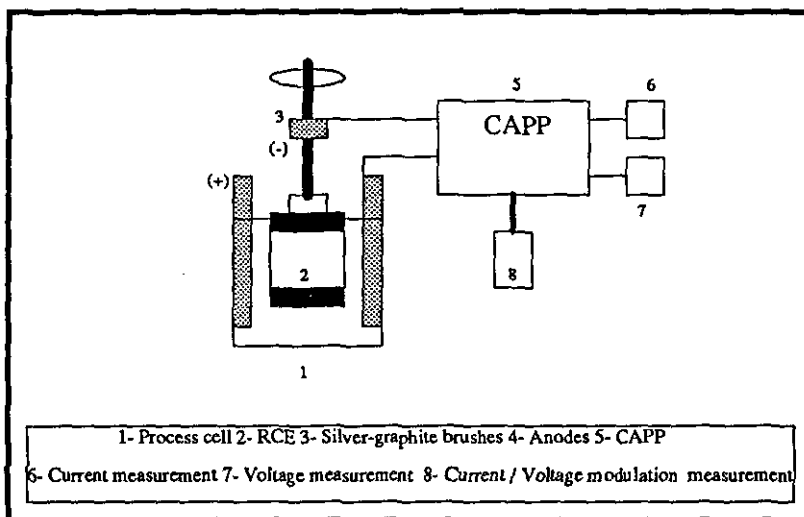
Figure (21). Schematic representation of single bath experimental set-up

3-3-1-3 Cathode preparation

Electrodeposits were formed on tubular copper and steel cylinders and 50 micron copper foils (Goodfellow Metals 99.5%), the copper cylinders had a radius of 3 cm and an external surface area of 66 cm^2, whilst the steel cylinders had a radius of 2.5 cm and an external area of 19.6 cm^2, these were attached to a rotating cylinder electrode holder. The holder was insulated on its outer surfaces to prevent electrodeposition on all surfaces except the test specimens.

Prior to electrodeposition the copper substrates were degreased in alkaline solution consisting of 40 g/l Na$_2$CO$_3$ and 5 g/l NaOH, for 5 minutes at 60°C, rinsed in deionised water, electropolished in 775 ml/l H$_3$PO$_4$ + 225 ml/l propylene glycol for 1 minute, rinsed in deionised water, and then activated in 10% (v/v) S.G 1.84 H$_2$SO$_4$. Whilst, the steel substrates were degreased in alkaline solution consisting of 40 g/l Na$_2$CO$_3$ and 5 g/l NaOH, for 5 minutes at 60°C, rinsed, pickled in 50% (v/v) S.G 1.18 HCl, rinsed with deionised water and then acetone, and finally dried in a hot air stream.

3-4 Test methods

3-4-1 Cathodic polarisation test method

Prior to the cathodic polarisation tests commencing, the electrode was masked with PTFE tape until a surface area of 9 cm^2 was in contact with the solution. It was then mounted in a holder and placed in the processing solution which contained an auxiliary electrode (copper or mild steel anode), reference electrode "Saturated calomel electrode" (SCE). The rest potential was measured using a digital multimeter (Thander type TM 355) and the ministat precision-potentiostat (H.B. Thompson) was switched to run and the sweep unit (Rayliegh Leigh Instruments Ltd. MP 120) activated.

A plot of the cathodic polarisation curve was obtained by connecting an X-Y recorder between the output and auxiliary sockets of the potentiostat and the outputs of the sweep unit. The system used in this test is shown in figure (22). All potentiodynamic polarisation

scans were made at a constant sweep rate of 200 mV/min, all potentials were measured with respect to a saturated calomel reference electrode (SCE).
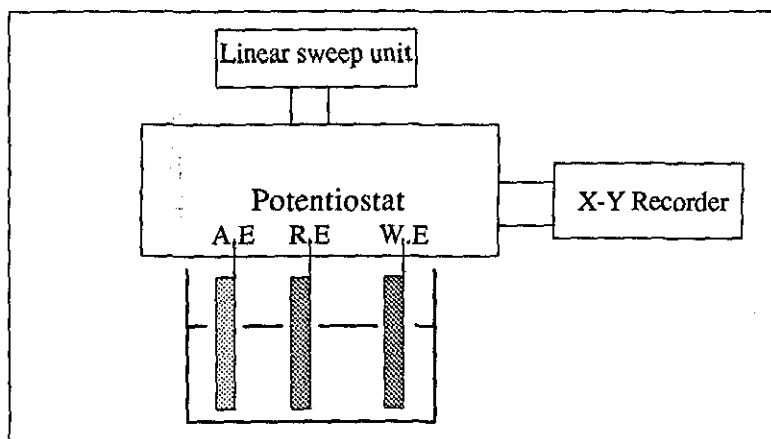
Figure (22). Cathodic polarisation cell set-up

3-4-2 Hull cell test method

The Hull cell test was used for testing the suitability (in terms of visual quality) of several zinc and nickel electroplating solutions over a wide range of current densities. An anode was fitted at the rectangular end of the box and a cathode plate (10 cm) wide was placed along the sloping side.

The solution to be tested was preheated to operating temperature before it was transferred to the Hull cell. The anode (zinc or nickel) and the cathode (mild steel or zinc plated steel) were connected to a power supply capable of producing a range of 1 to 3 A. In most cases 2 and 3 A were used. Before the test the mild steel panels were pre-treated as mentioned earlier in Section (3-2-2-2).

3-4-3 Cathode current efficiency measurements

In electrodeposition, cathode current efficiency is important for both efficient electrodeposition of metals and alloys and for economical reasons. It is a measure of the effective utilisation of electrical energy in terms of the actual percentage of applied current being used in electrodeposition of metals and alloys.

66

The pre-weighed plated sample was rinsed with de-ionised water after plating and then dried under hot water. The plated sample was weighed again and cathode current efficiency (C.C.E) was calculated.

C.C.E = (actual weight gain ÷ theoretical weight gain) x 100%

3-4-4 Porosity test method

A ferroxyl test was used to evaluate the porosity of nickel and zinc plated steel samples. The test solutions consisted of potassium ferricyanide (50 g/l of $K_3Fe(CN)_6$) as an indicator and sodium chloride (0.2 g/l) with 10 g/l of sodium sulfate as the corroding agent. Agar (10 g/l) was added to prevent spread of the blue spots. Filter papers were moistened with a solution containing only 20 g/l sodium chloride and 10 g/l agar and were stored dry. Immediately before the test, the dried papers were moistened with deionised water, pressed firmly for about 2 minutes on the plated steel and then removed and dipped into the ferricyanide solution. Blue colour spots indicated areas where the iron was exposed (88).

3-4-5 Adhesion test method

The adhesion test method was carried out using an adhesive tape (Hi-Tek Product Ltd.). A strip of adhesive tape was placed in contact with the coated panels, pressed firmly with a finger nail to eliminate air bubbles and to ensure good adhesion between the coated surface and the tape. After about 10 seconds, the tape was lifted quickly from one edge manually by a steady pulling force applied at about a 90° angle to the coated surface plane. The tape was then inspected for any trace of metal coating. If no trace of the coating was noted on the tape, this suggested good adhesion between the substrate and the coating.

3-4-6 Microsectioning for optical and SEM observations

The most direct method of investigating the thickness, the distribution, and the structure of single and layered coatings was by the micro examination of metallographic cross-

sections. Extensive micrographic work has been carried out in order to examine the microstructure of the electroplated multilayers.

The coated test pieces were examined to determine the principal areas of interests, the specimens were cut with a low speed diamond saw into small pieces. One piece of each specimen was positioned in a suitable simple mould and encapsulated with a two pack cold setting epoxy system which enabled the resin to be cured quickly at room temperature. When the curing/hardening of the resin was completed, the encapsulated specimen was ground by means of abrasive materials to a suitable standard (1200 grit silicon carbide paper) and polished with a diamond paste to a 1 micron level. The polished specimen was then examined under an optical microscope to evaluate the quality of the polished surface since the presence of very fine scratches will not aid the observation of multilayer structures.

Prior to scanning electron microscopy, the specimen was etched in a suitable etching solution which etched one kind of the combined layers selectively, this emphasised the contrast between adjacent layers. Etching also served to remove traces of coating metal that may have been smeared over hard or adjacent layers during polishing.

3-4-7 Neutral salt spray test method (NSST)

A set of three samples of each type of Zn/Ni CMM coatings was tested in a neutral salt spray employing a humidified 5% sodium chloride (A.R Grade) spray at 35°C in accordance with ASTMB117. This test was undertaken in an effort to measure the corrosion resistance of the Zn/Ni CMM coatings. The corrosion resistance of these samples was then compared to single layer coatings.

3-4-8 Electrochemical corrosion measurements

Two equipment systems have been used in this evaluation:

The first was used for the evaluation of zinc/nickel coatings produced by the dual bath technique. The electrochemical corrosion measurements were made utilising the potentiodynamic polarisation technique in order to characterise the corrosion behaviour of

Zn/Ni CMM coatings and to measure the corrosion potential, corrosion current and polarisation resistance. The corrosion data obtained was then compared to single layer coatings of Zn, Ni and Zn-Ni alloy and an attempt was made to draw comparisons with the salt spray test results. The equipment consisted of a AMEL 553 potentiostat, a Thompson DRG16 ramp generator and Quicklog data acquisition software. All potentiodynamic polarisation scans were measured with respect to a saturated calomel electrode (SCE) as a reference, with a pure lead counter electrode.

Both cathodic and anodic polarisation scans were performed in an quiescent 3.5% sodium chloride solution at pH = 5.8 and room temperature (23°C), after an initial delay of 15 minutes for sample equilibrium, the open circuit potential (E_{corr}) was recorded. A constant scan rate of 60 mV/min was used in all such experiments. Figure (23) shows the system used in this test. The resulting current was plotted on a logarithmic scale and the corrosion current, I_{corr} obtained by extrapolating the linear portion of the curve back to the corrosion potential E_{corr}.
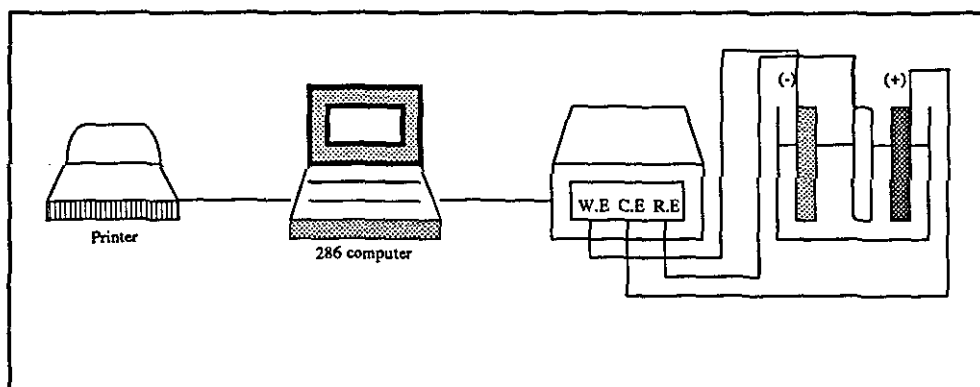
Figure (23). Potentiodynamic polarisation cell set-up.

The second method was used in the evaluation of Zn/Ni CMAM coatings produced by the single bath technique. An ACM Instruments Auto Tafel corrosion measurement system was used, the E_{corr} and the corrosion current density I_{corr} were determined for each type of coating. Linear polarisation resistance (LPR) was measured by polarising the sample to

$\pm$ 20 mV at constant scans rate of 6 mV/min to study the corrosion behaviour of Zn-Ni alloy coatings. This type of measurement was not generally applicable for the layered coatings because the polarisation between $\pm$ 20 mV will only give corrosion data for the outer surface after short immersion times.

The Tafel plots were analysed and the values of E_{corr} and I_{corr} were extracted using a software routine provided with the computerised corrosion measurement system.

Chapter 4

EXPERIMENTAL RESULTS AND DISCUSSIONS

4-1 The dual bath investigations

Introduction

The dual bath electrodeposition investigations can be divided into two main sections:

4-1-1 The dual bath electrodeposition investigations of the copper/nickel

4-1-2 The dual bath electrodeposition investigations of the zinc/nickel CMM coating systems.

The dual bath electrodeposition of such coatings was used to plate nickel from the selected sulfamate based bath, copper from a sulfate based bath, zinc from the selected sulfate based bath, and zinc-nickel alloy from a Lea Ronal proprietary zinc-nickel plating bath (ZINNI). Bath compositions and plating conditions are given in table (24). The table includes other baths which were investigated for their suitability.

4-1-1 The dual bath electrodeposition investigations of the copper/nickel CMMM coating system

4-1-1-1 Introduction

Initial studies on the copper/nickel system were carried out using copper and nickel solutions suggested by Haseeb et al (44). Table (24) shows the composition and operating conditions of these two baths.

Composition and operating conditions	Cu/Ni CMMM coatings		Zn/Ni CMM coatings						
	Copper Bath g/l	Nickel bath g/l	Zinc bath (1) g/l	Zinc bath (2) g/l	Zinc bath (3) g/l	Zinc bath (4) g/l	Nickel bath (1) g/l	Nickel bath (2) g/l	Zn-Ni alloy (ZINNI) g/l
Copper sulfate	90	-	-	-	-	-	-	-	-
Nickel sulfamate	-	400	-	-	-	-	300-400	-	-
Zinc sulfate	-	-	375	350	180	350	-	-	$30(Zn^{++})$
Nickel sulfate	-	-	-	-	-	-	-	300	$30(Ni^{++})$
Nickel chloride (or Sodium chloride)	-	-	-	-	-	-	-	44-56 (22-28)	-
Sulfuric acid	200	-	-	-	-	-	-	-	-
Boric acid	-	30	-	-	-	20	25-30	28-41	-
Sodium sulfate	-	-	70	-	-	-	-	-	-
Magnesium sulfate	-	-	60	-	-	-	-	-	-
Ammonium sulfate	-	-	-	30	-	-	-	-	-
Sodium acetate	-	-	-	-	45	-	-	-	-
Aluminium sulfate	-	-	-	-	-	25	-	-	-
Ammonium ion	-	-	-	-	-	-	-	-	100-110
Lea Ronal proprietary additives	-	-	-	-	-	-	-	-	3 types
Total chloride	-	-	-	-	-	-	-	-	277
Sodium chloride	-	-	-	-	-	25	-	-	-
pH	2	3.5	3-4	3-4.5	3-4.5	3.5-4.5	3-4	3-4.5	5.8
Temperature (°C)	30	30	55-65	40-55	30-50	25	35	30	40
Current density / A dm^{-2}	2	2	25-40	10-60	10-30	2-10	2	4.3	2,5,10
Agitation	No	No	Mech.	Mech.	Mech.	Mech.	Mech.	Mech.	Moderate aeration
Anode	Cu	Ni	Zn	Zn	Zn	Zn	Ni	Ni	Zn

Table (24). Bath compositions and plating conditions

These solutions were used to produce a number of layered structures with bilayer thicknesses of approximately 1-8 microns.

4-1-1-2 Cathode current efficiency measurments

In order to measure the cathode current efficiencies of copper and nickel, measurements were carried out on different types of substrates since the cathode current efficiency could be different according to the substrate type. The resultant cathode current efficiencies were as follows:

Copper on copper foil substrate   99%

Copper on copper plated substrate   99%

Copper on nickel plated substrate	97%
Nickel on nickel plated substrate	95%
Nickel on copper plated substrate	94%
Nickel on copper foil substrate	92%

The results show differences in cathode current efficiencies, these differences could be probably attributed to hydrogen evolution on the cathode surface. Hence, from the cathode current efficiency values, it could be said that under certain conditions some of the electrons supplied to the cathode surface react with hydrogen ions to form hydrogen gas $(2H^+ + 2e^- \rightarrow H_2)$. In nickel plating over a copper foil substrate, about 8% of the total electrons reacted with hydrogen ions where as about 2% of the total electrons in copper plating reacted with hydrogen ions. Therefore, the plating efficiency of nickel deposition on copper was only about 92%.

4-1-1-3 Scanning electron microscope (SEM) observations

The observation of microsectional layered structures has been carried out by SEM. The Cu/Ni coatings produced were, in general, smooth, pore-free, and had good adhesion properties. Figure (24) shows typical SEM micrographs of the layered structure of Cu/Ni CMMM coatings produced. The lower side of the micrographs is the substrate side, the dark bands represent the etched copper layers, whilst, the bright ones are the less etched nickel layers.

It could be seen from the above micrographs that a smooth and adjacent layered structure with sharp interfaces can be produce (in most cases) using the dual bath technique with relatively equal layer thicknesses, also the possible oxidation of the surface which might take place during transformation of the substrate between baths does not affect the layer continuity at the interfaces between layers.

Initial results showed in some cases, a difficulty to observe clear inter layer structure due to smeared copper over the adjacent nickel layers which has occurred during polishing.

| Cu/Ni CMMM micrograph of (10) layers the thickness of each layer is /5/ microns. | Cu/Ni CMMM micrograph of 20 layers the thickness of each layer is /1/ micron. |
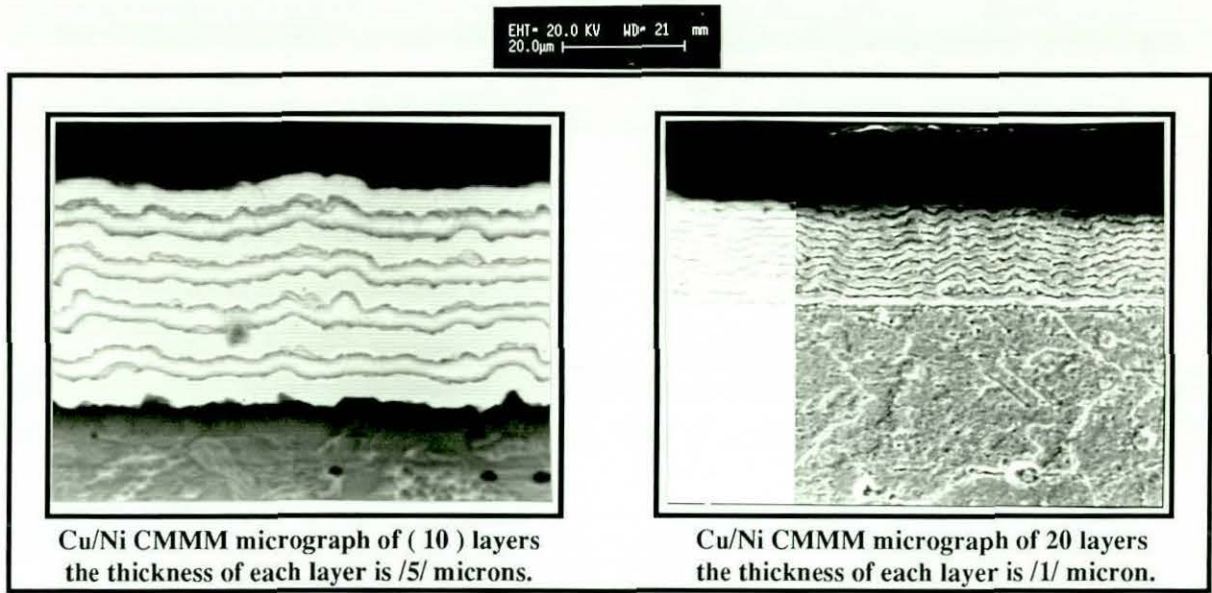
Figure (24). SEM micrographs of the layered structure of Cu/Ni CMMM coatings.

Figure (25) shows a micrograph of this unclear microlayered structure of a Cu/Ni CMMM coating.
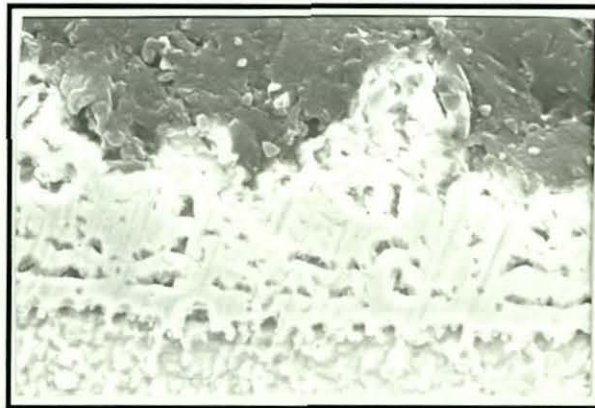
Figure (25). A micrograph of a smeared microlayered structure Cu/Ni CMMM coating

In order to produce the greatest possible inter-layer clarity, three different etching solutions were investigated:

1- 10 g/l potassium chromate, 40 ml/l sulfuric acid, 1 drop of hydrochloric acid (100ml)

2- 10g ammonium persulfate, 100 ml water.

3- 5g ferric Chloride, 50 ml hydrochloric Acid, 100 ml water.

They were applied separately to the polished Cu/Ni samples. Figure (26) shows the effect of different etching solutions on the clarity and the contrast of the micrographs produced by SEM.

SEM micograph of etched 10 layer Cu/Ni CMMM coating using sol. (1).

SEM micrograph of etched 10 layer Cu/Ni CMMM coating using sol. (2).

SEM micograph of etched 10 layer Cu/Ni CMMM coating using sol. (3).
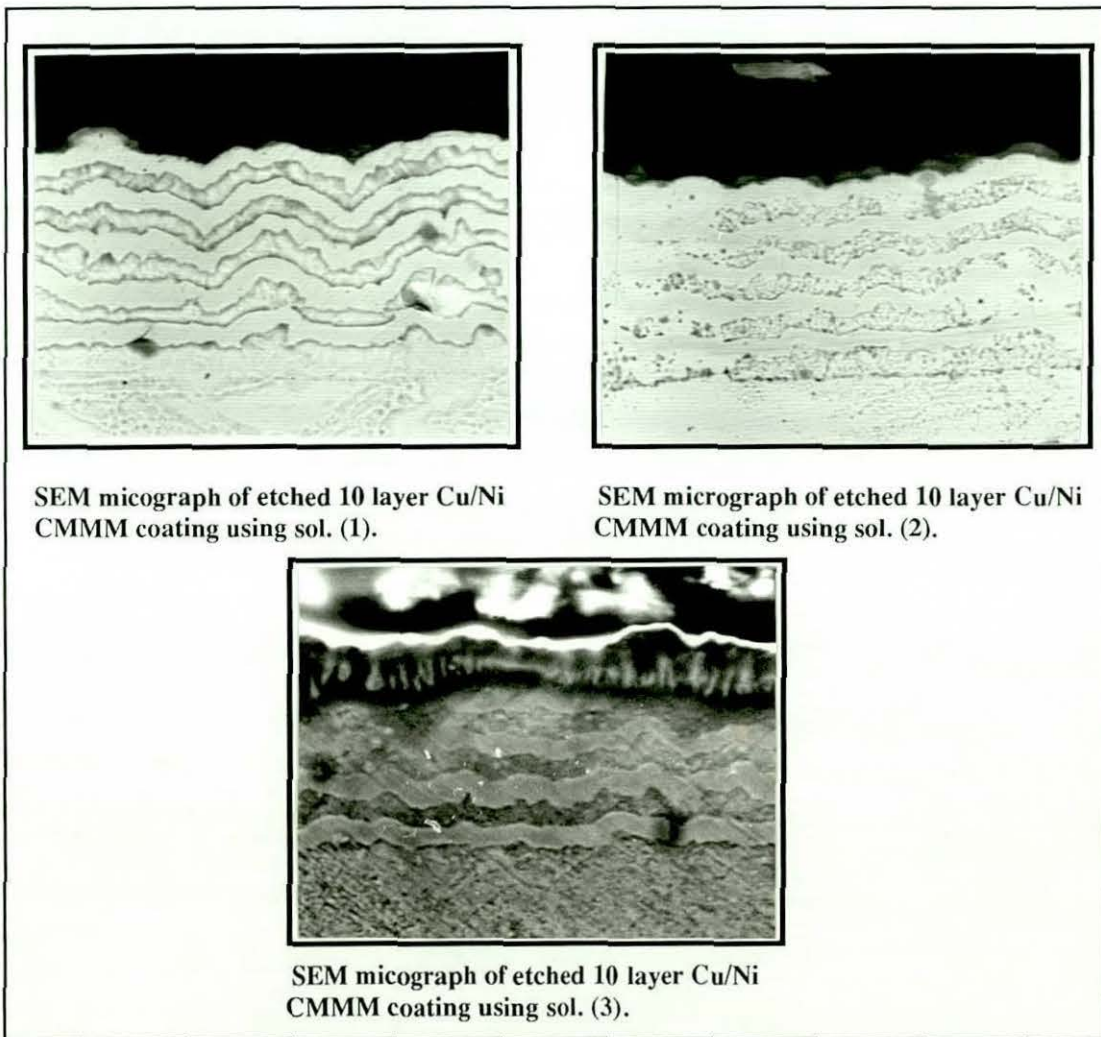
Figure (26). The effect of different etching solutions on the clarity and the contrast of the micrographs produce by SEM.

Figure (26) indicates that the solutions (2) and (3) affect both metals and produce less inter-layer clarity and etching solution (1) was considered to produce the greatest inter-layer clarity.

4-1-1-4 Effect of agitation

The plating was carried out using two different hydrodynamic conditions in order to investigate the effect of agitation on the quality of the deposited layers.

1- Mechanical agitation (stirrer paddle)

2- No agitation

Figures (27) and (28) show the effect of agitation on the smoothness of the layered structures. Figure (27) represents a layered structure produced under quite high mechanical agitation, whilst, figure (28) represents a layered structure produced in quiescent conditions. This effect on the smoothness of the layered structure could be attributed to highly disturbed copper and nickel ions in the diffusion layer around the cathode, which led to a variation in the ion concentration around the cathode surface and hence, promoting roughness on the deposited layer.
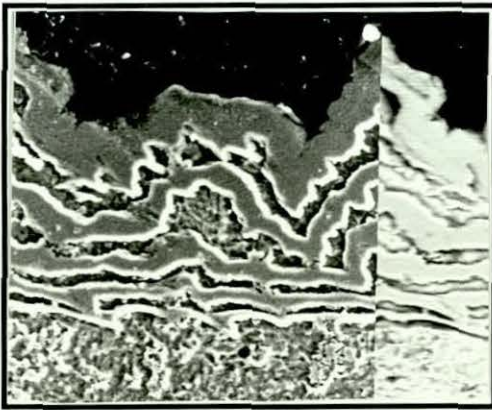
Fig. (27). SEM micrograph of Cu/Ni CMMM coating produced using quite high agitation
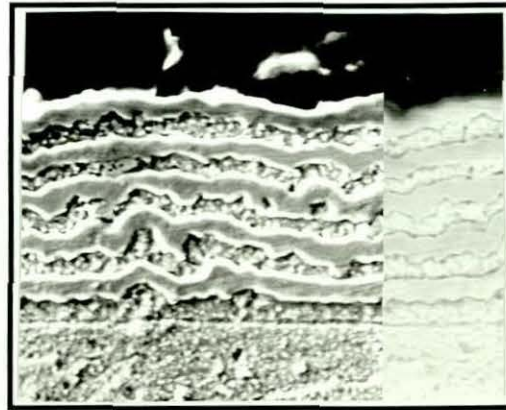
Fig. (28).SEM micrograph of Cu/Ni CMMM coating produced using quiescent conditions

4-1-2 The dual bath investigations of the zinc/nickel CMM coating system

Introduction
Initial investigations were carried out to select the appropriate zinc and nickel electrolytes which could be used in the production of Zn/Ni CMM coatings. The problems encountered in the electroplating of the nickel layer over the zinc plate had to be solved initially in order to produce the Zn/Ni CMM coatings.

4-1-2-1 Galvanostatic electrodeposition investigations of zinc coatings
The initial investigations were carried out by cathodic potential/current curves followed by a Hull cell test.

4-1-2-1-1 Cathodic polarisation studies
Figure (29) show the cathodic polarisation behaviour of four different types of zinc baths, the cathodic polarisation behaviour of these baths seem to be similar with no significant differences.

4-1-2-1-2 Hull cell studies
The Hull cell test was used to determine the suitable plating current density which the bath could be operated at over the widest range of current densities without plating defects (e.g. burnt or powdery deposits). Figure (30) shows a schematic representation of zinc electrodeposition onto the steel substrate Hull cell panels carried out in the four different types of zinc baths. The effect of cathodic current density on the quality of the zinc deposits produced at a Hull cell current of 2 A have been studied. The panels show the effect of current density on the quality of zinc deposit and also show that electrolyte (4) has a better coating quality over a wide range of current densities. This might be attributed to the presence of boric acid as a buffering agent and aluminium sulfate which enhance the conductivity of the zinc electrolyte.

Electrolyte (4) was selected mainly due to the Hull cell results and also since it can be operated at room temperature. The operating conditions of the selected electrolyte were; current density 45-50 mA/cm^2, pH 3.5, at 25 °C.

Cathodic Polarisation Curves for the Different Types of Zinc Baths mentioned in table (24). (Sweep Rate 200 mV/min, Sample area 4 cm^2, R.P. 1200 mV vs. SCE in all cases)
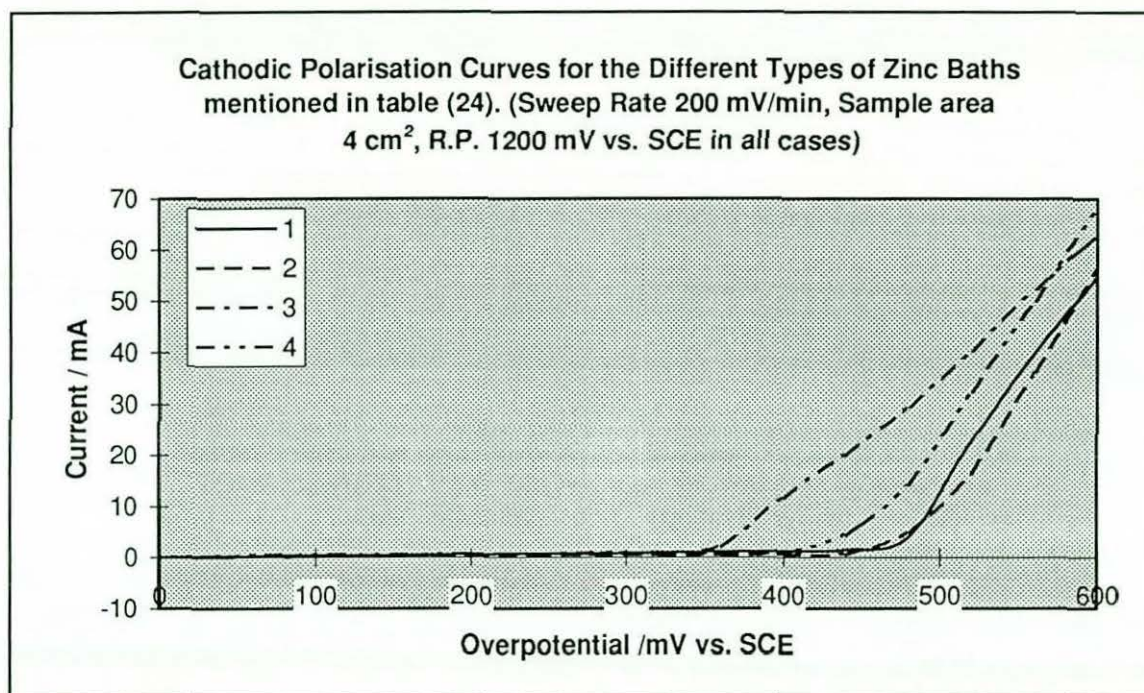
Figure (29)

4-1-2-1-3 SEM observation

The surface morphology of an 8 microns thick zinc deposit is shown in figure (31). It indicates that the zinc crystallites are predominantly hexagonal platelet shaped. The presence of grains with a specific hexagonal geometry in the deposit results from a layered texture which is made by a repeated sandwiched-like epitaxial growth of hexagonal platelet shaped zinc crystals (89).

(A) Burned, (B) Porous, (C) Semi-bright Grey, (D) Spotted, (E) Dark Grey, (F) No Deposit, (G) Crystalline, ▨ Pale, (I) Pitted, (J) Powdery.
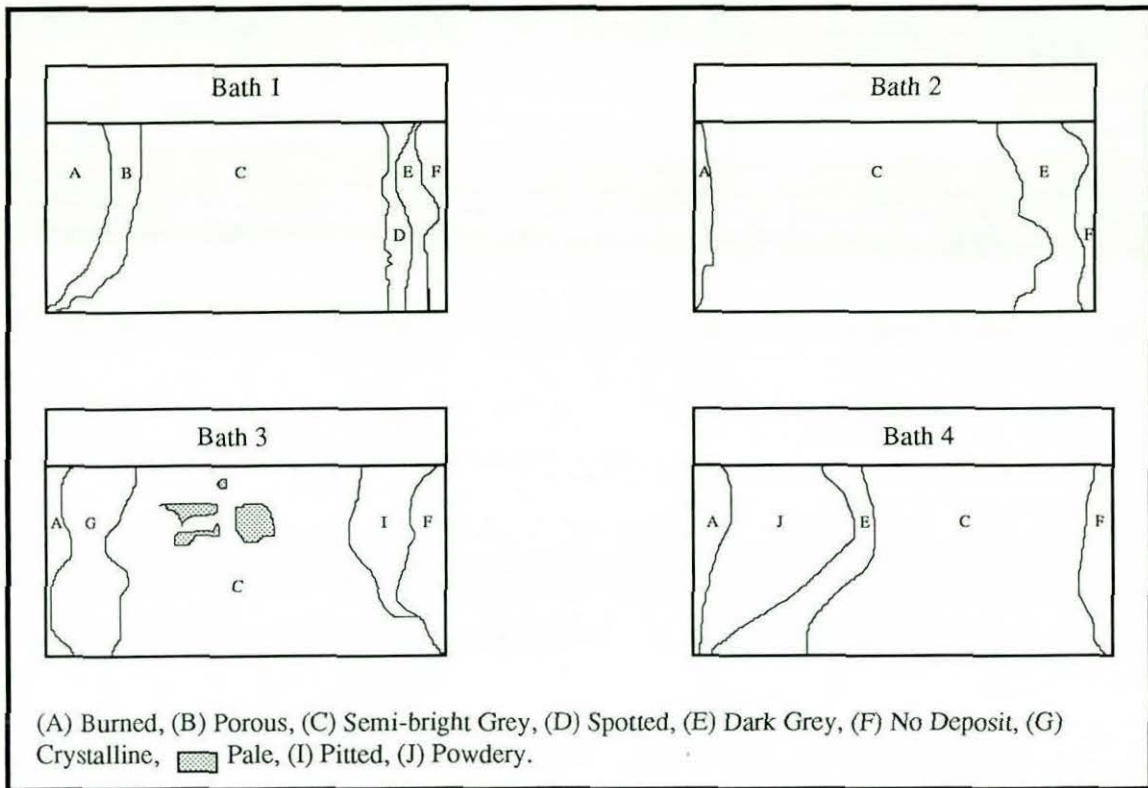
Figure (30) Hull cell panels for the four different zinc baths investigated. The test was carried out at a Hull cell current of 2A.

Figure (31). Surface morphology of an 8 micron thick zinc deposit

4-1-2-2 Galvanostatic electrodeposition investigations of the nickel coating

Two nickel baths were examined using the cathodic polarisation and Hull cell tests.

4-1-2-2-1 Cathodic polarisation studies

Figure (32) shows the cathodic polarisation behaviour of two different types of nickel baths, at two hydrodynamic conditions.

Cathodic polarisation studies showed quite similar results for nickel sulfamate and nickel sulfate based baths. Both baths had a similar low current regime (100 to 300 mV overpotential) and then the curves started to rise with increasing applied potential, mostly at the similar potential values.

Cathodic Polarisation Curves for Two Types of Nickel Bath
(Sweep Rate 200 mV / min, Sample Area 4 cm², R.P - 900 mV vs. SCE)

— Sulfate Solution with Agitation   — — — Sulfate Solution without Agitation
····· Sulfamate Solution with Agitation   — · · — Sulfamate Solution without Agitation
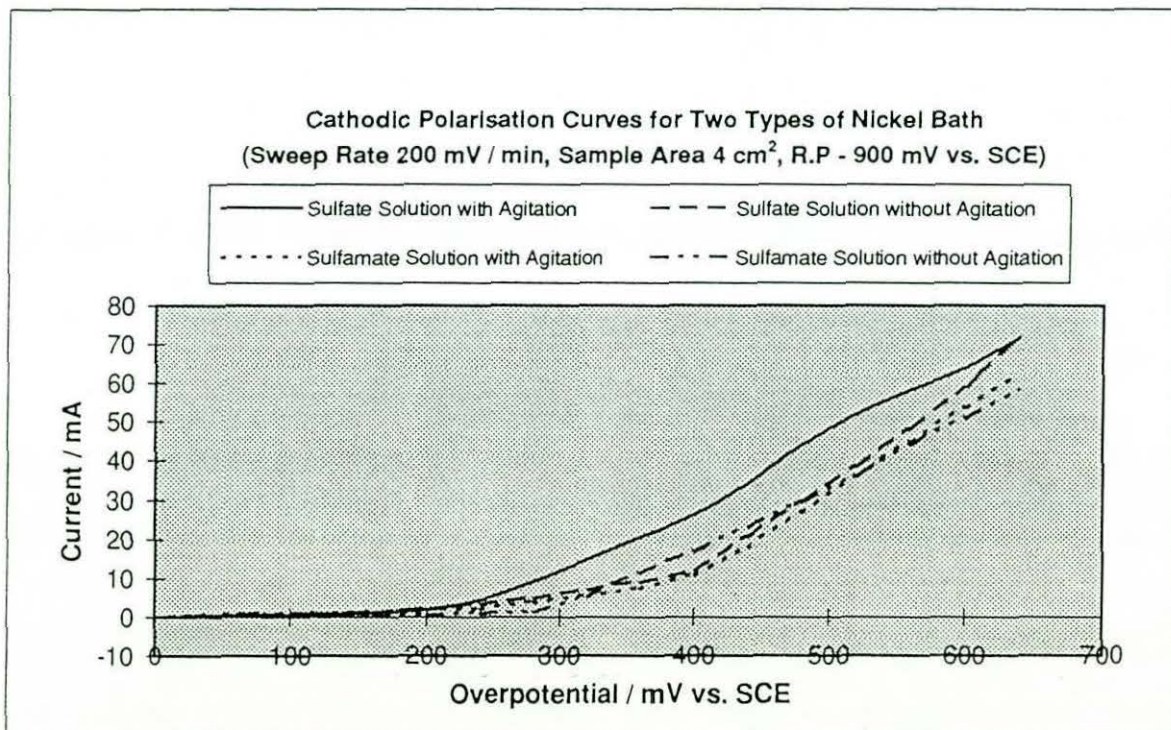
Figure (32)

4-1-2-2-2 Hull cell studies

Figure (33) shows a schematic of Hull cell panels for sulfate and sulfamate based nickel baths.

(A) Burned, (B) Bright, (C) No Deposit
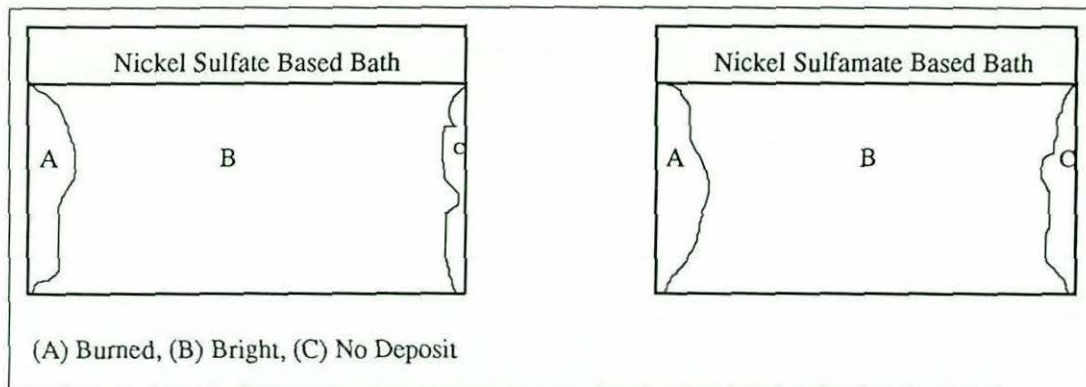
Figure (33) Hull cell panels for the two nickel baths. The test was carried out at a Hull cell current of 2A.

Hull cell test panels showed that both electrolytes produced good quality deposits over a wide range of current densities.

4-1-2-2-3 SEM observation

The surface morphology of an 8 micron thick nickel deposit is shown in Figure (34). It indicates that the surface morphology of this single nickel layer seems to have very fine nodular crystals with very clear, small crystal boundaries.

Figure (34). SEM micrograph of an 8 microns thick nickel deposit.

4-1-2-3 Galvanostatic electrodeposition investigations of nickel coatings on zinc plated steel

Initial trials showed major problems in depositing nickel on zinc plated steel. Further investigations have been carried out on nickel solutions to enable the nickel to be deposited on zinc.

The study of electrodeposition behaviour was carried out using Hull cell and SEM tests and cathode current efficiency measurements, the nickel deposition has been carried out using several plating conditions, by varying the current density, pH, and the level and position of agitation. The quality of the deposits was tested by adhesion and porosity tests.

4-1-2-3-1 Hull cell studies

This test was applied on two different nickel solutions in order to select the appropriate solution that gave good quality deposits over the widest range of current densities. Hull cell test panel schematics are shown in figure (35). It can be observed that current density has a strong effect on the quality of the nickel deposit on zinc. Also, Hull cell trials suggested that the nickel sulfamate based bath produced better coverage on zinc - an important requisite for this type of layered coating and that the current densities at which nickel on zinc electrodeposition can occur has a larger operating window with the nickel

82

sulfamate based bath. On the basis of the Hull cell test results and because the nickel sulfamate based electrolyte produces deposits with the lower internal stress(which would prove advantageous in terms of coating integrity, particularly in aggressive environments), the nickel sulfamate based bath was selected to be used for further investigation. It was found that with the use of nickel sulfamate based bath, the current density which gave the best quality nickel deposits was 76 mA/cm^2.
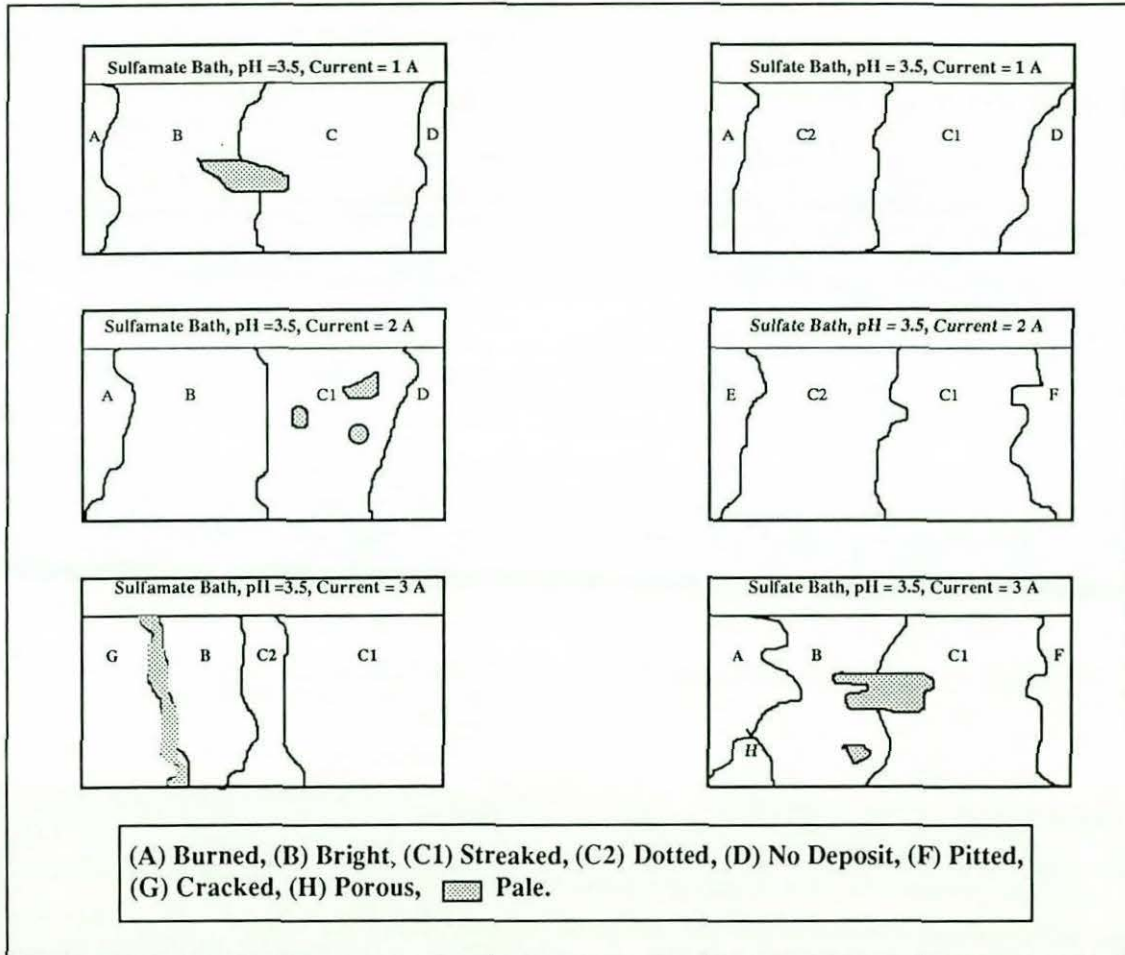
Figure (35). The Effect of current density on the quality of nickel deposit on zinc plated steel substrate, using Hull cell tests.

It was observed at lower current densities ($\leq$ 50 mA/cm^2) the deposit became very streaky indicating that perhaps the zinc coating was being attacked leaving a brown lined deposit. Figure (36) shows the microstructure of the nickel deposit on the zinc deposited at a current density of 40 mA/cm^2. There appears to be evidence of cratering on the deposit

surface which suggests hydrogen bubbles could well have been present on the surface during deposition.
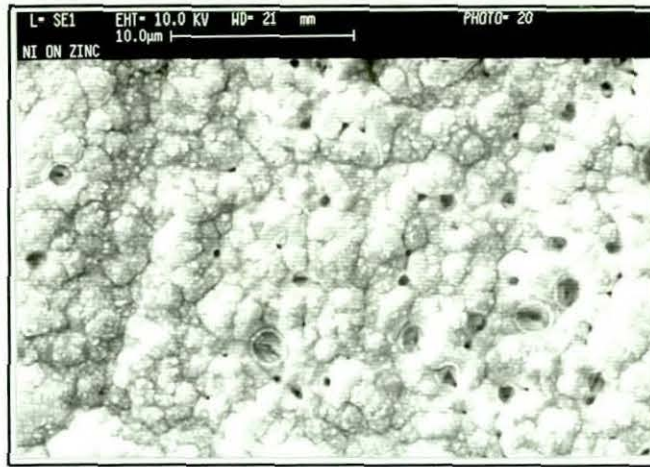
Figure (36). Evidence of hydrogen bubbles having been present on the nickel deposited onto zinc.

4-1-2-3-2 Effect of pH

The pH value of the nickel sulfamate based electrolyte had a strong effect on the quality of the nickel deposit on the zinc. A series of pH values of 3.5, 4.5 and 5 were examined. Figure (37) shows the surface morphology of 2 microns of nickel deposited over zinc plated steel at pH $\approx$ 3, pH=4.5, and pH=5. The micrographs indicate that at pH=5 the deposit appears to have a cracked structure. In order to investigate the reason for this effect, further investigations were carried out to measure the pH value of the solution near to the cathode surface. It was found that the pH increased by a value of 1 to 1.5 due to the hydrogen evolution. This means that when the pH of the bulk solution was 5, the approximate pH around the cathode surface was 6 to 6.5 and this could lead to the formation of colloidal nickel hydroxide $Ni(OH)_2$ on the growth sites which inhibits the process of nucleation and grain growth.

The surface morphology of the nickel deposited at pH = 3 was found to have better more compact structure. The samples produced at pH= 3,4.5,5 were tested in order to evaluate the adhesion properties of nickel deposit. It was found that the deposit produced at pH=3 had a good adhesion properties, whilst the deposits produced at pH= 4.5 and 5 had bad

84

adhesion properties. This effect was also believed to be due to the formation of the colloidal nickel hydroxide on the cathode surface.

Surface morphology of 2 microns of nickel deposited over zinc plated steel at pH=3

Surface morphology of 2 microns of nickel deposited over zinc plated steel at pH=4.5

Surface morphology of 2 microns of nickel deposited over zinc plated steel at pH=5
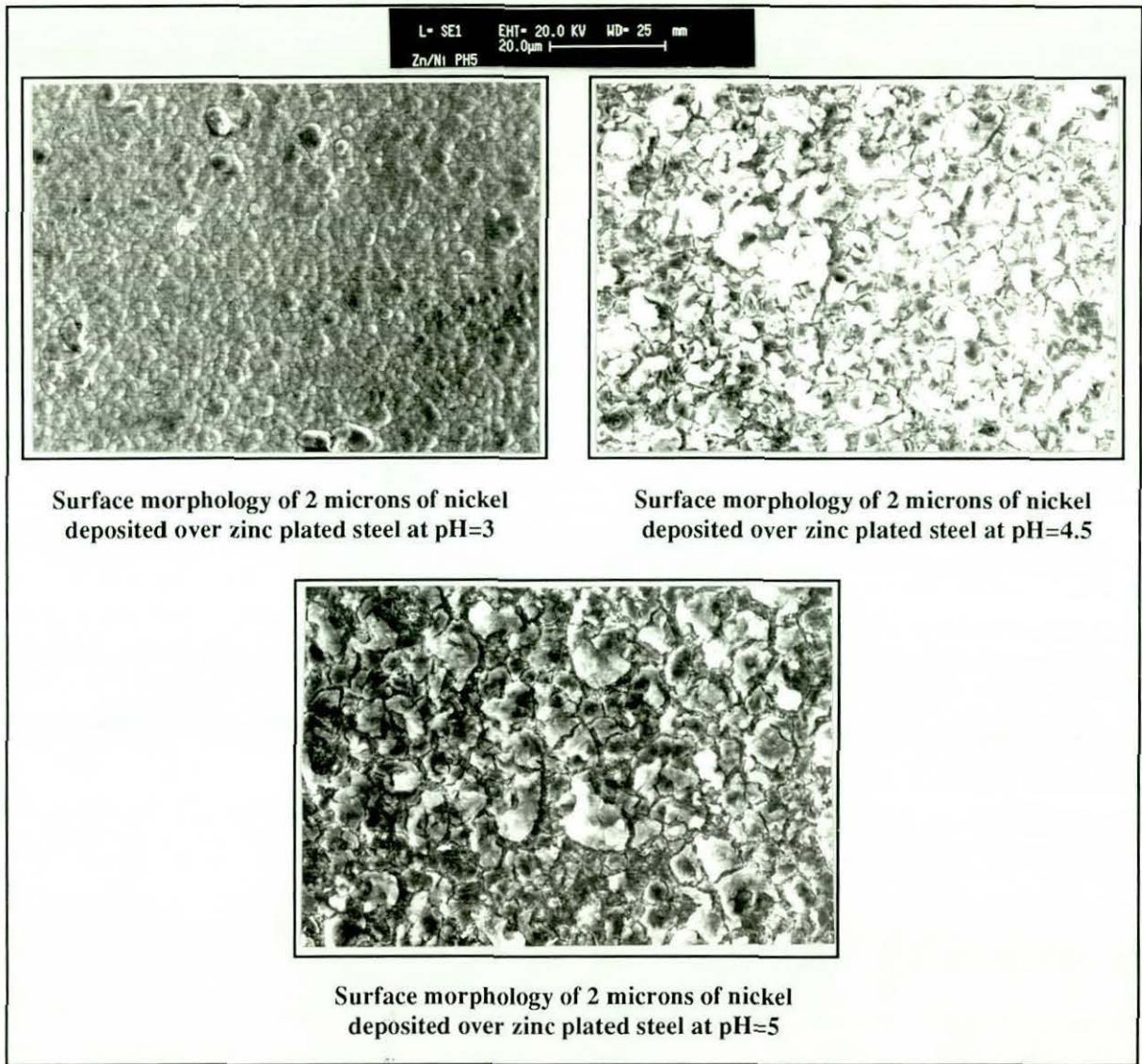
Figure (37). The surface morphology of 2 microns of nickel deposited over zinc plated steel at pH = 3, pH=4.5, and pH=5.

4-1-2-3-3 Effect of agitation

It was found that it is important to lower the hydrogen occlusion taking place on the cathode surface as soon as possible. Thus it was decided to concentrate the agitation below the cathode to improve the overall deposit quality.

According to the aforementioned results in order to achieve an acceptable zinc/nickel layered coating the following points needed to be observed:

1) The current had to be raised gradually to its optimum plating level to avoid poor deposition.

2) Agitation had to be concentrated below the cathode for uniform deposition.

3) The current density required to electrodeposit nickel onto zinc needs to be maintained at a high level to minimise zinc dissolution during the initial stages of film formation. This results in a slightly inferior cathode current efficiency for this part of the coating cycle.

In order to prove the effectiveness of the proposed operating conditions in the success of depositing nickel over zinc plate, successive layers of zinc and nickel were deposited at different operating conditions by utilising the proposed operating conditions first (see above) and then changing the operating conditions by lowering the current density (to 30 and 40 A/cm^2) and changing the location of mechanical stirrer to the centre. Figure (38) shows a micrograph of a 6 layers Zn/Ni CMMM coating, the first two layers were deposited at the proposed operating conditions and the next four layers were deposited at lower current densities and with a different mechanical stirrer locations. Figure (38) indicates that it is necessary to combined all the proposed points (see above) to achieve a good covering of nickel on zinc. On the other hand, by changing the proposed operating conditions the dissolution of zinc will take place according to displacement reaction with nickel ions ($Zn + Ni^{++} \rightarrow Zn^{++} + Ni$).

Figure (38) Optical micrograph of a 6 layers Zn/Ni CMMM
coating made at different operating conditions (500X magnification)

-

4-1-2-3-4 Porosity investigations

A series of different electrodeposited layered coatings were examined in order to evaluate

the porosity of the deposits which in turn would have a marked influence upon the

protective quality of the coatings. Table (25) shows that a nickel deposit of 2 microns had

a porosity value of 20%, whilst the nickel deposit at 1 micron had a porosity value of 25%

of the total tested surface area. The possible cause of this effect is due to co-deposited

hydrogen in the coating which will lead to highly stressed nickel deposits. The other kinds

of coatings have not showed any trace of porosity, using the test method outlined earlier

(Section 3-4-4).

Type of coatings	Thickness (μ)	Porosity (%)
Zinc	1	0
Zinc	2	0
Nickel	1	25
Nickel	2	20
Zn/Ni	2 (Bilayer thickness)	0
Ni/Zn	2 (Bilayer thickness)	0
Zn-Ni alloy	1	0
Zn-Ni alloy	2	0

Table (25). Porosity of different types of coatings.

4-1-2-4 Galvanostatic electrodeposition investigations of zinc-nickel alloy coatings

The electrodeposition of Zn-Ni alloys was carried out using a Lea Ronal proprietary zinc-nickel (ZINNI) plating process. The ZINNI process has been designed to produce highly corrosion resistant alloy coating of approximately 90% zinc and 10% nickel content. The ZINNI plating solution and operating conditions are shown in table (24).

The zinc-nickel alloy coating was deposited on mirror polished mild steel panels over a range of current densities (2, 5, 10 A/dm^2) with a nominal coating thicknesses of 8 microns.

4-1-2-4-1 SEM observation and EDAX measurements

Three different samples were prepared at a range of current densities of 2, 5 and 10 A/dm^2 in order to study the surface morphology and to measure the deposit composition.

Figures (39), (40), (41) show surface morphology of these deposits. It can be seen that at a current density of 2 A/dm^2 the deposit has big feather-like nodular crystals, as the current density increased to 5 A/dm^2 the crystals become smaller. Whilst, the structure of the Zn-Ni alloy deposited at 10 A/dm^2 has much finer feather-like crystals. This is believed to be due to the effect of high current density as well as the effect of the additives.

EDAX measurement showed that the composition varied with variation of current density as follows:

Zn-Ni at 2 A/dm^2 had 12 % Ni

Zn-Ni at 5 A/dm^2 had   9 % Ni

Zn-Ni at 10 A/dm^2 had 11% Ni
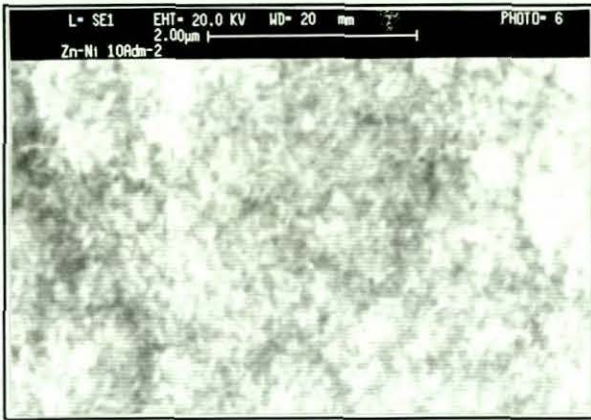
Fig. (39). Surface morphology of a Zn-Ni alloy coating electrodeposited at a current density of 2 A/dm^2
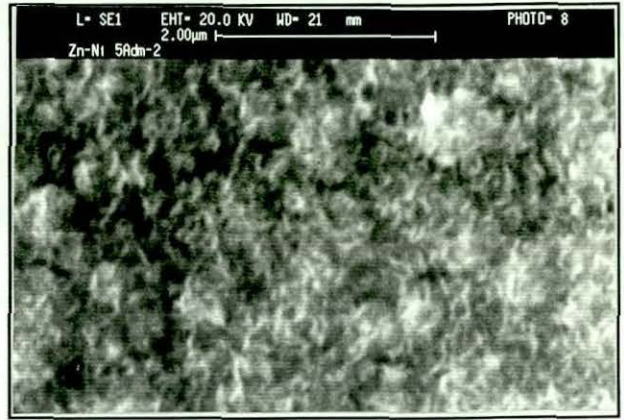
Fig. (40). Surface morphology of a Zn-Ni alloy coating electrodeposited at a current density of 5 A/dm^2
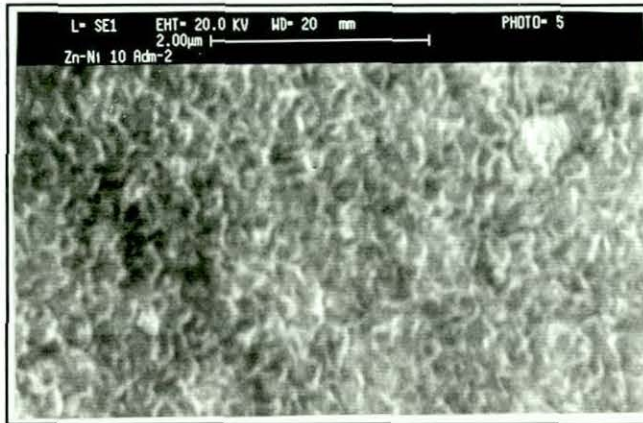
Figure (41). Surface morphology of a Zn-Ni alloy coating electrodeposited at a current density of 10 A/dm^2

4-1-2-5 Galvanostatic electrodeposition investigations of zinc/nickel CMM coatings

The electrodeposition of Zn/Ni CMM coatings was carried out using three different baths in order to produce different types of multilayers such as Zn/Ni CMMM coatings, Zn/Zn-Ni CMAM coatings, and Ni/Zn-Ni CMAM coatings.

89

4-1-2-5-1 Galvanostatic electrodeposition investigations of zinc/nickel CMMM coatings

Two different types of multilayers have been produced, Zn/Ni and Ni/Zn CMMM coatings. Figure (42) shows a schematic representation of these two types consisting of four layers.
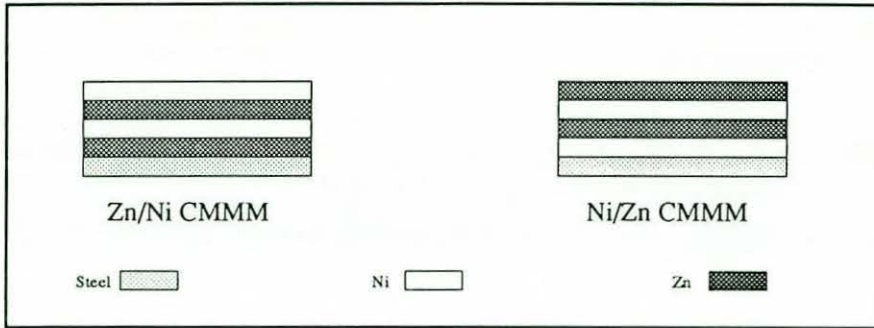
Figure (42). Schematic representation of Zn/Ni and Ni/Zn CMMM coatings

A series of layered structures was produced using the selected zinc and nickel baths and operating conditions. Table (26) shows the composition and operating conditions of the two baths.

Layered deposits were produced to an overall nominal thickness of 8 microns. These electrodeposits were then studied using SEM for the examination of the layered structure, outer surface morphology, and corrosion tested by simple neutral salt spray and anodic polarisation tests.

Table (26). Bath compositions and operating conditions

Compositions and operating conditions	Zinc bath	Nickel bath
Nickel sulfamate	-	300 g/l
Zinc sulfate	350 g/l	-
Boric acid	20 g/l	30 g/l
Aluminium sulfate	25 g/l	-
Sodium chloride	25 g/l	-
pH	4.5	3
Current density A/cm^2	45-50	76
Temperature	25	30
Agitation	Mechanical stirrer	Mechanical stirrer
Anode	Zinc	Nickel

4-1-2-5-2 Galvanostatic electrodeposition investigations of Zn/Zn-Ni and Ni/Zn-Ni CMAM coatings

Four different types of Zn/Zn-Ni and Ni/Zn-Ni CMAM coatings were produced.
Figure (43) shows a schematic representation of these four types, each containing four layers.

Initial trials showed that it was possible to deposit such layered coatings without significant problems using the selected zinc and nickel baths and ZINNI bath, and adopting the same plating procedure used with the Zn/Ni CMMM coatings.

Layered deposits were produced to an over all nominal thickness of 8 microns. These electrodeposits were then studied using SEM for the examination of the layered structure, outer surface morphology, and corrosion tested by simple neutral salt spray and anodic polarisation tests.
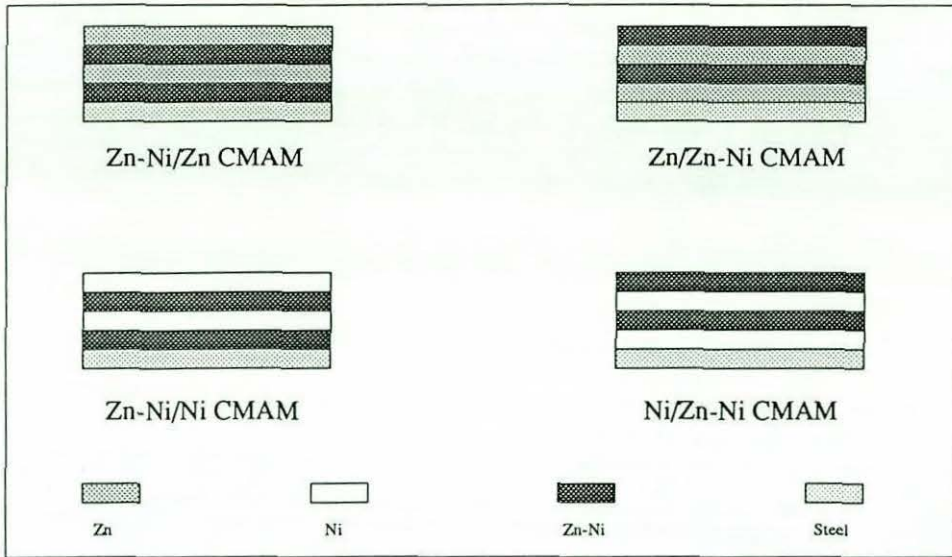
Figure (43). Schematic representation for four types of
Zn/Zn-Ni and Ni/Zn-Ni CMAM coatings

4-1-2-6 Cathode current efficiency measurements

Table (27) illustrates the cathode current efficiencies for the different types of coatings on
the different substrates.

Type of deposit	Substrate	C.C.E (%)
Nickel	Steel	92
Zinc	Steel	98
Zinc-nickel alloy	Steel	94
Zinc	Nickel plated substrate	95
Zinc	Zinc-nickel plated substrate	96
Nickel	Zinc plated substrate	85
Nickel	Zinc-nickel plated substrate	87
Zinc-nickel alloy	Zinc plated substrate	92
Zinc-nickel alloy	Nickel plated substrate	96

Table (27) Cathode current efficiencies for different types of coatings on
the different substrates.

The cathode current efficiency values indicate that the nickel deposit has the lowest cathode current efficiency especially on zinc plated steel which is accompanied by hydrogen evolution and leads to a relatively porous deposit.

4-1-2-7 SEM observation studies

A series of different layered electrodeposited structures have been studied using optical and scanning electron microscopes.

Prior to optical microscopy and SEM examination, the mounted samples were etched in 2% nital for varying periods in order to clarify the interfaces between the adjacent layers.

Tables (28) and (29) illustrate a series of layered structures made of 4 and 8 layers for Zn/Ni and Ni/Zn, also the tables contains an outer surface morphology of these types of layered coatings. Whilst figure (44) shows the outer surface morphology and the layered structure of Zn/Zn-Ni and Zn-Ni/Ni coatings.

4-1-2-7-1 Surface morphology studies

It can be seen that the outer surface morphology of 8 layers Ni/Zn CMMM

(8 microns) coating has a smaller acicular crystals size when compared to 8 microns zinc and nickel single layer coatings and the 4 layer Zn/Ni CMMM (8 microns) coating. This indicates that there is a strong relationship between crystal forms and individual layer thickness, and that the grain size of the deposit increases with the thickening of the electrodeposited layer. This illustrates that the rate at which the crystal grow is proportional to the layer thickness and hence to the plating time.

Also, it can observed that an outer layer zinc morphology for the 4 and 8 layer Ni/Zn CMMM coatings has a more compact and dense crystal structure than that of an 8 microns single layer zinc coating. This may suggest that the outer layer surface of the 8 and 4 layer Ni/Zn CMMM coatings have a more pore-free structure and hence, have a better corrosion performance.

On the other hand, the surface morphology of the 8 microns nickel single layer seems to have a very fine nodular crystal structure with very small crystal boundaries, whilst the

93
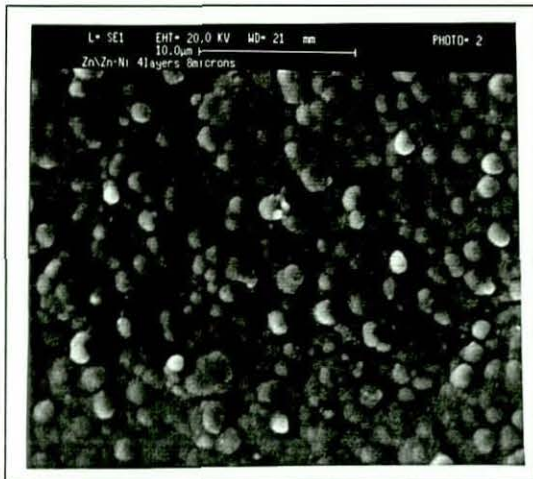
Outer surface morphology for 4 layer
Zn/Zn-Ni CMAM coating.
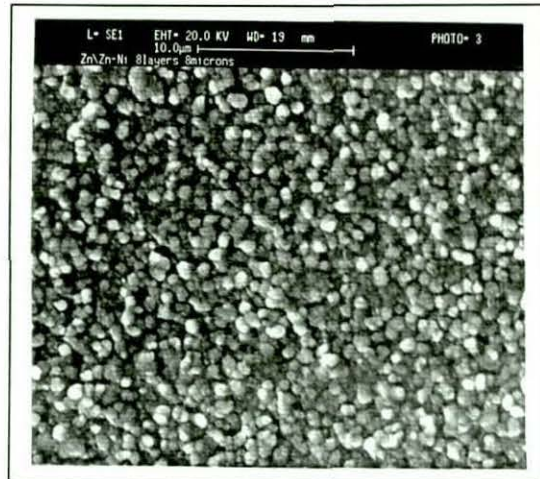
Outer surface morphology for 8 layer
Zn/Zn-Ni CMAM coating.
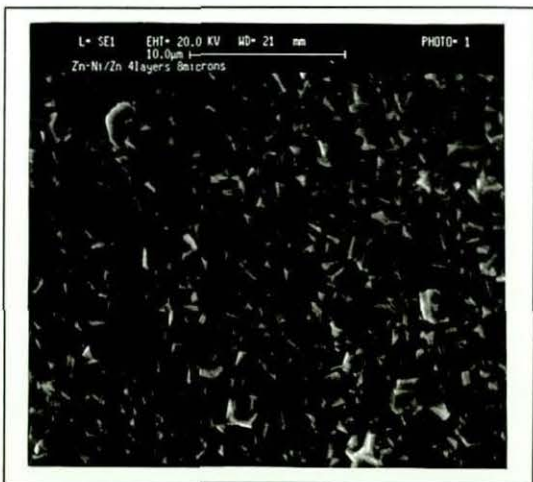
Outer surface morphology for 4 layer
Zn-Ni/Zn CMAM coating.
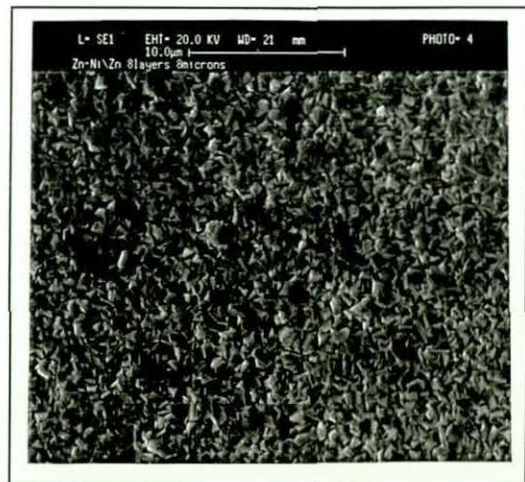
Outer surface morphology for 8 layer
Zn-Ni/Zn CMAM coating.

Figure (44). Morphological characteristics for different types of CMM coating

Table (28)

Morphological characteristics for Ni/Zn CMMM coatings
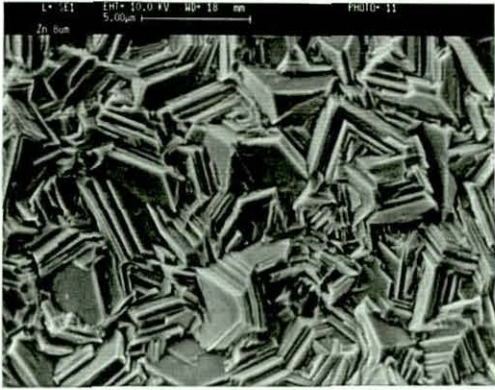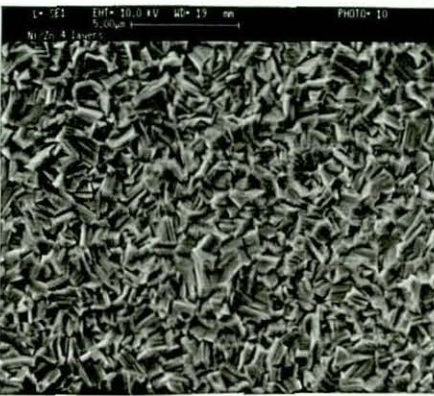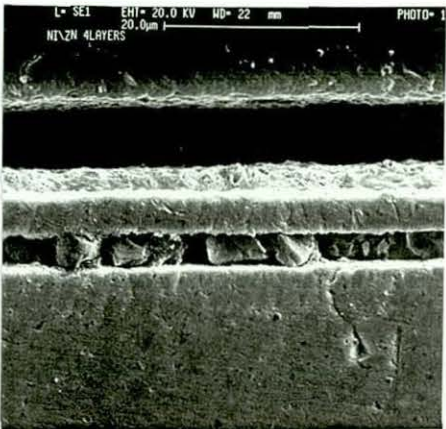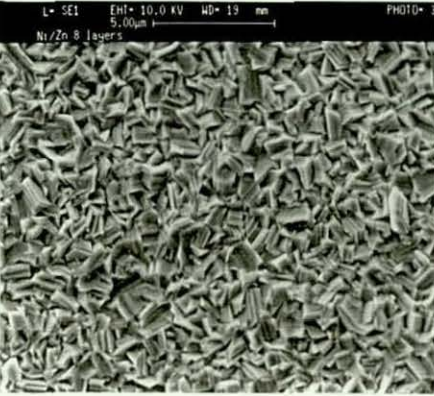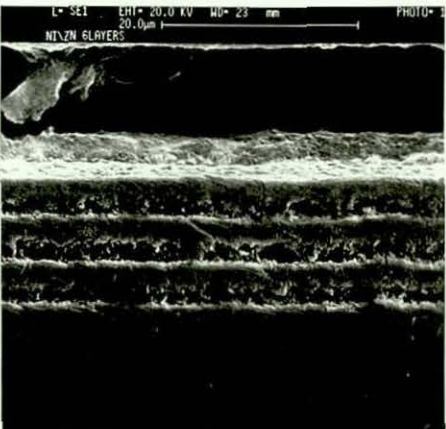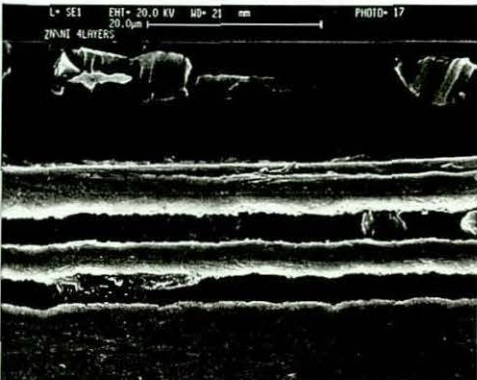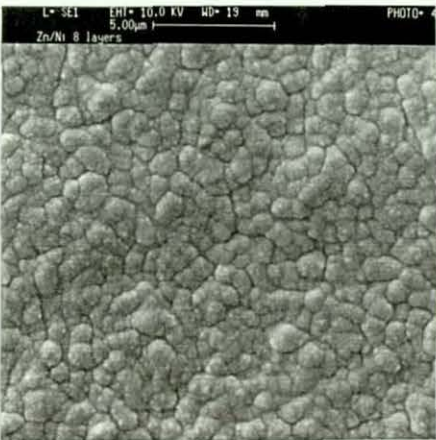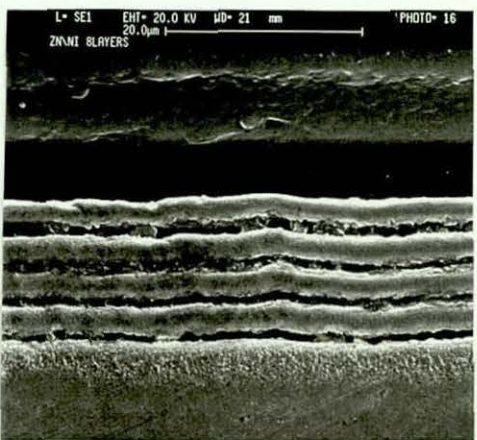
Type of CMMM coating	Number of layers	Outer surface morphology	
Zn	1		
		Outer surface morphology	Cross-sectional micrograph
Ni/Zn	4		
Ni/Zn	8		

Table (29)

Morphological characteristics for Zn/Ni CMMM coatings

Type of CMMM coating	Number of layers	Outer surface morphology	
Ni	1		
		Outer surface morphology	Cross-sectional micrograph
Zn/Ni	4		
Zn/Ni	8		

outer surface morphology of the 4 and 8 layer Zn/Ni CMMM coatings seems to have bigger nodular crystal sizes with very obvious grain boundaries which could suggest that the outer nickel layer of the Zn/Ni CMMM coatings has a quite high porosity. This is probably higher than the 8 microns nickel single layer, and hence the former would probably have worse barrier corrosion performance.

Figure (44) shows the outer surface morphology of 4 and 8 layer Zn/Zn-Ni CMAM coatings. It can be seen that the Zn-Ni alloy morphology is greatly affected by the occurrence of the zinc layer underneath as can be seen when comparing the surface morphology of the 8 microns zinc single layer and the 8 microns Zn-Ni alloy single layer. The shape of the crystals has been changed from feather-like large nodular crystals to rounded nodular crystals. Whilst, the outer layer morphology of 4 and 8 layers Zn-Ni /Zn suggest that the morphology of the zinc has not been appreciably changed when deposited onto a Zn-Ni alloy layer. These observations can be compared, to some extent, with the Zn/Ni CMMM coatings where the nickel layer was also affected by the zinc layer underneath but the reverse was less apparent.

4-1-2-7-2 Cross-sectional microscopy studies

Tables (28) and (29) illustrate the structures for 8 and 4 layer Zn/Ni and Ni/Zn CMMM coatings. These micrographs illustrate the layered nature of these electrodeposits with good individual layer contrast as a result of the etching techniques used. The nital etchant attacked the zinc layers most severely and has resulted in significant removal of zinc metal. The nickel layer seem less affected. The buried cubic crystals appeared in the micrographs inside the zinc layer are believed to be alumina (Al_2O_3) crystals left after polishing. The lower side of the micrographs is the steel substrate, the dark bands represent the etched zinc layer, whilst, the bright bands represent the nickel layer. It can be seen that the layered structure for 4 and 8 layer Zn/Ni CMMM coatings are more definable and the number of layers are more clear. On the other hand, the layer numbers for 4 and 8 layers Ni/Zn CMMM coatings seem to be undefinable, this is because the zinc outer layer is being etched back (the white bands appearing on the upper side of the micrographs represent the etched zinc layers). The first layer which is a nickel layer is also poor defined

due to the fact that the lightly etched nickel layers seem to have a similar contrast to steel substrate. Furthermore, it can be seen that the layered structure of the 8 layers Ni/Zn CMMM coating is not clear, this is because the zinc layers have not etched completely. Further etching was carried out on the 8 layer Ni/Zn CMMM mounted sample, figure (45) shows the nickel layer adjacent to the steel substrate which appeared as a light grey band and the zinc outer layer was removed almost completely.

It can be observed that, the layered structures of Zn-Ni/Ni and Ni/Zn-Ni CMAM coatings have similar layered structures to that of Zn/Ni and Ni/Zn respectively. It can also be seen from the layered structures for Zn/Zn-Ni and Zn-Ni/Zn that the bilayer structure which consists of two layers of Zn and Zn-Ni alloy also have the same layered structure as Ni/Zn CMMM coatings, this means that the both Zn-Ni alloy layer and Zn layer were etched by the Nital etching solution.
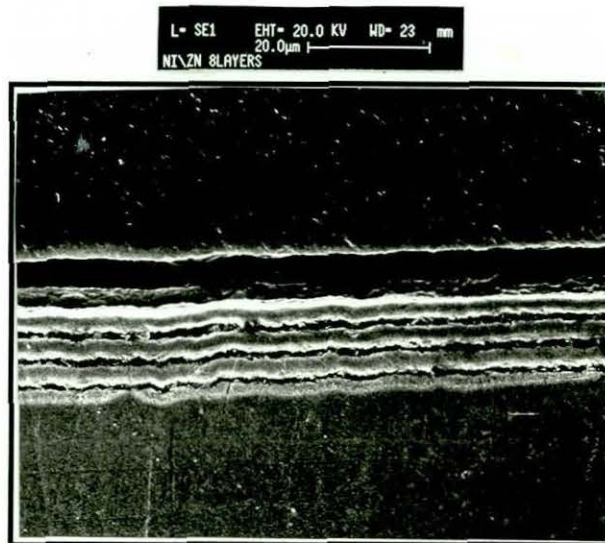
Figure (45). SEM micrograph for severely etched Ni/Zn CMMM coating

Figure (46A) shows a severely etched 8 layer Zn-Ni/Zn CMAM and 6 layer CMAM coating, it can be identified that upper layer, which is in this case zinc and Zn-Ni alloy respectively, have been etched back, this could be compared with the layered structure of Ni/Zn when the upper zinc layer has also been etched back.

95
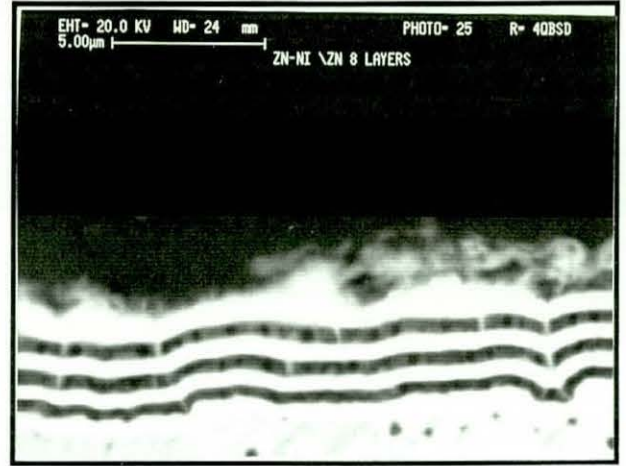
Figure (46A). SEM micrograph for severely etched 8 layer Zn-Ni/Zn and
6 layer Zn/Zn-Ni CMMM coatings

Figure (46B) shows a cross sectional micrograph of an 8 layer Zn-Ni/Ni CMAM coating. It can be seen that the layered structure is similar to that of the 8 layer Zn/Ni CMMM coating.
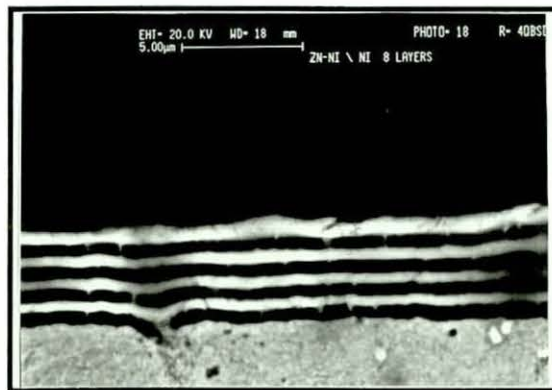
Figure (46B). SEM micrograph for 8 layer Zn-Ni/Ni CMAM coating

Figure (47) shows the EDAX measurement of the composition of the nickel upper layer of an 8 layer Zn/Ni CMMM coating. The graph indicates that the nickel upper layer has a small amount of zinc which could suggest that the nickel layer is quite porous or that the nickel layer has a small percentage of zinc present which is due to the contamination of the

nickel electrolyte with zinc ions which are dissolved in the electrolyte because of the displacement reaction that may take place between nickel and the zinc plated substrate during the early stages of the nickel electrodeposition.
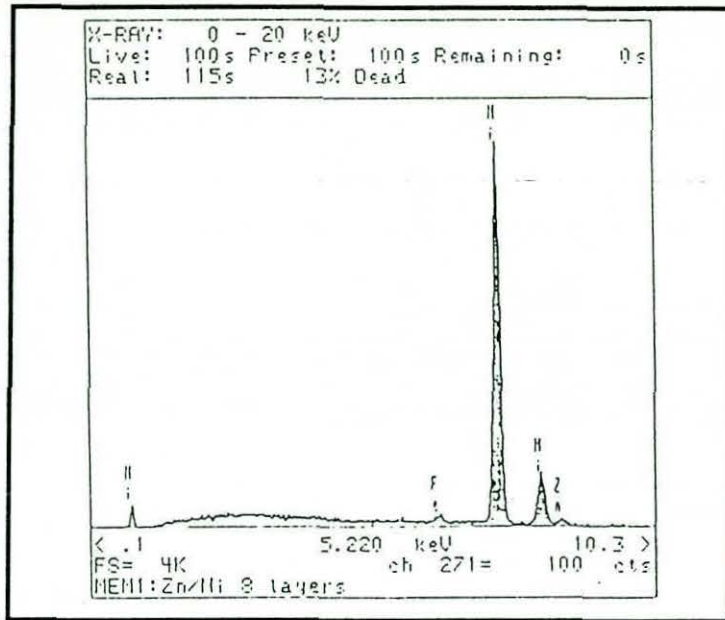
Figure (47) EDAX measurement of the purity of the nickel upper layer
of an 8 layer Zn/Ni CMMM coating

4-1-2-8 Electrochemical corrosion measurements of coated substrates

A series of layered structures of Zn/Ni, Ni/Zn, Zn/Zn-Ni, Zn-Ni/Ni, Zn-Ni/Zn, and Zn/Zn-Ni with overall nominal thicknesses of 8 microns were subjected to anodic polarisation tests in order to measure their corrosion behaviour and also to measure the corrosion potentials and corrosion currents of these types of coatings. The corrosion data was then compared to single layer coatings of Zn, Ni, and Zn-Ni alloy. The results of these qualitative corrosion studies are presented in table (31), which shows that the corrosion potential of Zn, Ni, and steel can be compared with the overall potentials for the other layered coating systems.

Two Zn/Ni systems (containing 4 and 8 layers) illustrate a mixed potential which has a relatively low (negative) value. Both systems have electrode potentials significantly lower

97

than the electrodeposited single nickel layer, suggesting that the upper surface layer, which is in this case nickel, is quite porous, the thicker the nickel coating the less the porosity (compare 4 layer structure with 8 layer structure). The porous nature of the nickel was confirmed as mentioned earlier using simple chemical porosity tests with steel as the substrate material.

The Ni/Zn layered electrodeposits produced more consistently low corrosion potentials being reasonably close to electrodeposited zinc. This would suggest that the zinc layers are relatively pore-free.

The corrosion potentials for 8 and 4 layer Zn-Ni/Ni CMAM coatings with respect to the corrosion potential for the nickel single layer, indicate that the nickel layers have a porous nature and also indicate that the porosity of the nickel layer of the 8 micron Zn-Ni/Ni CMAM coating is close to the porosity of the nickel layer of the 4 micron Zn-Ni/Ni CMAM coating. This could be attributed to the interaction of the nickel layer with the Zn-Ni sublayer.

The anodic polarisation behaviour of several multilayer systems has been studied in terms of the coating behaviour and their current response towards anodic potential changes.

The "S" type curve (see figure (56) for example) is repeated by many of the coatings containing zinc in the surface layer. Figure (49) illustrates an anodic polarisation curve for an 8 microns zinc single layer coating. It shows that the electrodeposited zinc produced a curve profile which suggests a system which corrodes rapidly initially (steeply rising current) and then forms, on the surface, a layer of corrosion products which may well consist of a stable film of $Zn(OH)_2$. Further increases in potential produce a fall in current until a sufficientely high a potential has been attained and the film begins to break down.

Figures (54) and (57) illustrate anodic polarisation curves for Zn/Ni multilayers which have a nickel layer on top and show no sign of passivation. Figure (54) which represent a 4 layer Zn/Ni CMMM coating shows a rapid increase in current density as the potential was increased.

Anodic Polarisation for Mild Steel in 3.5% NaCl Solution

Figure (48)

Anodic Polarisation Curve for 8 microns Zn Deposit in 3.5% NaCl Solution
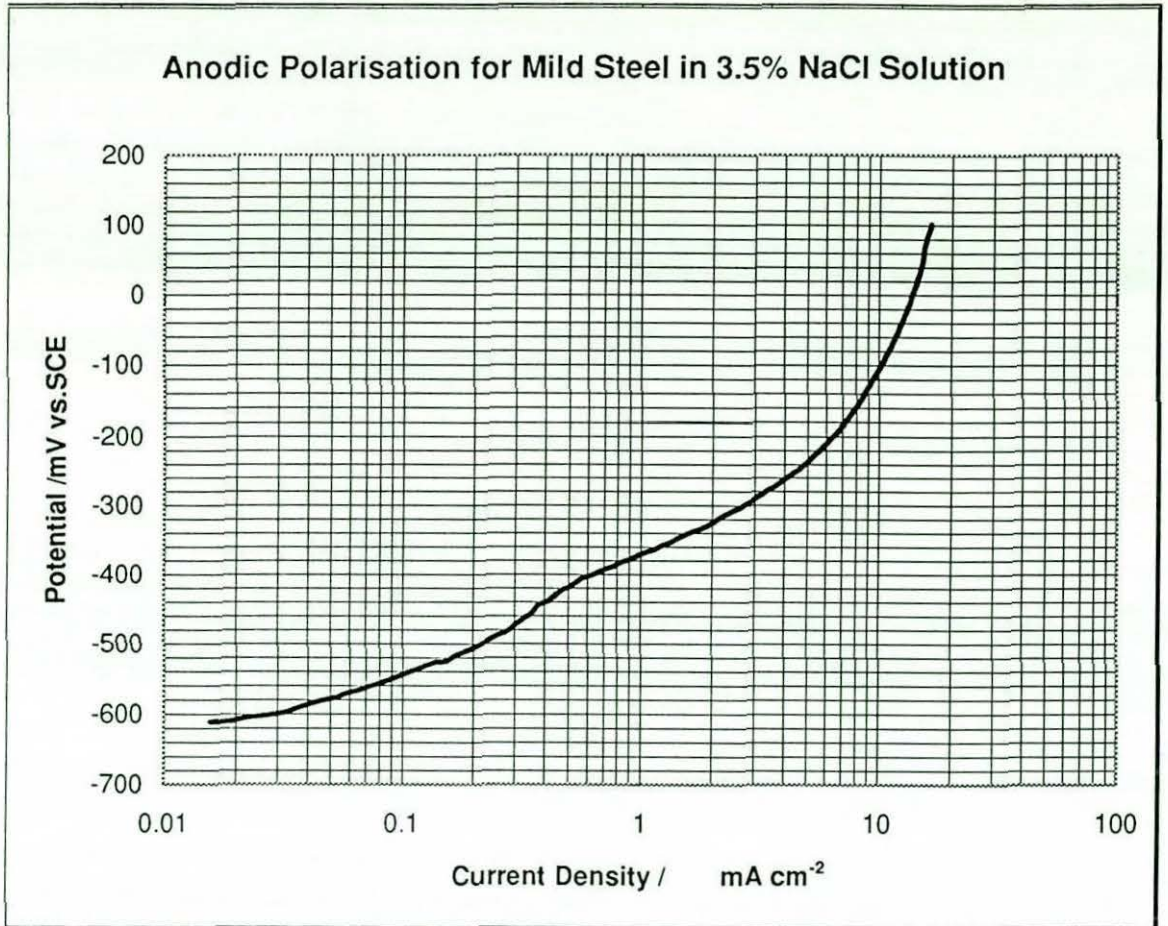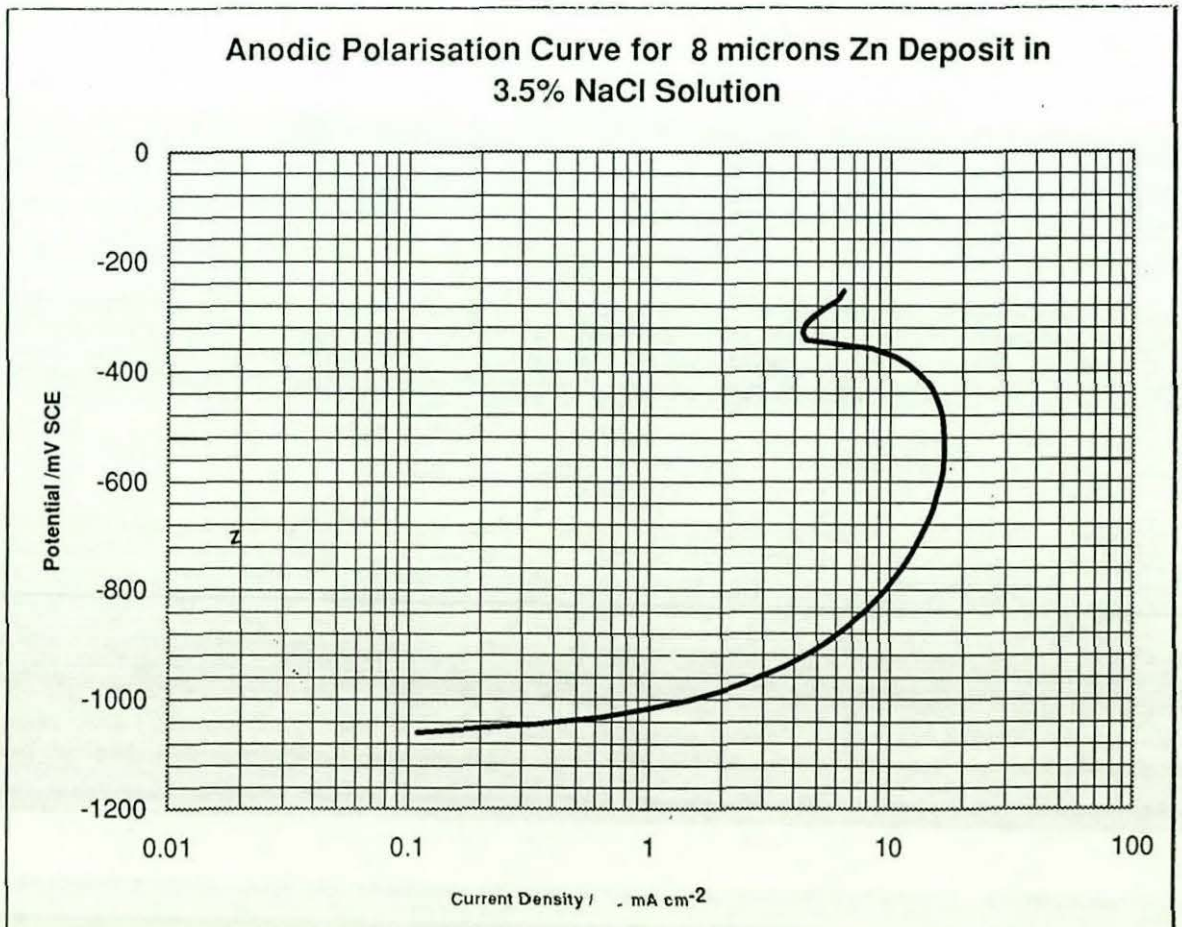
Figure (49)

Figure (50)   Anodic Polarisation of Nickel deposit in 3.5% NaCl Solution.
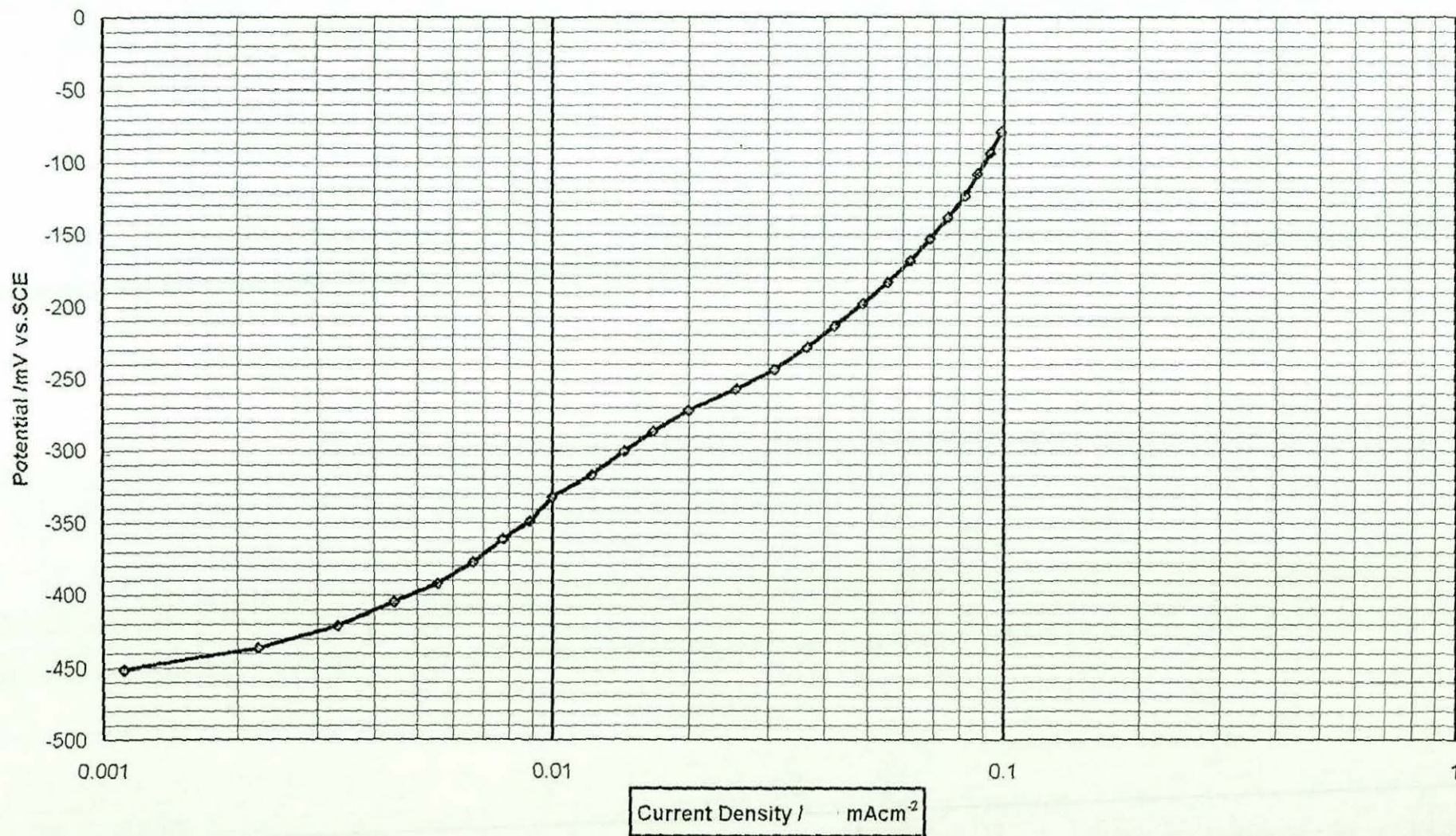
Anodic Polarisation Curve for 8 microns Zn-Ni Alloy at 2 A dm^{-2}
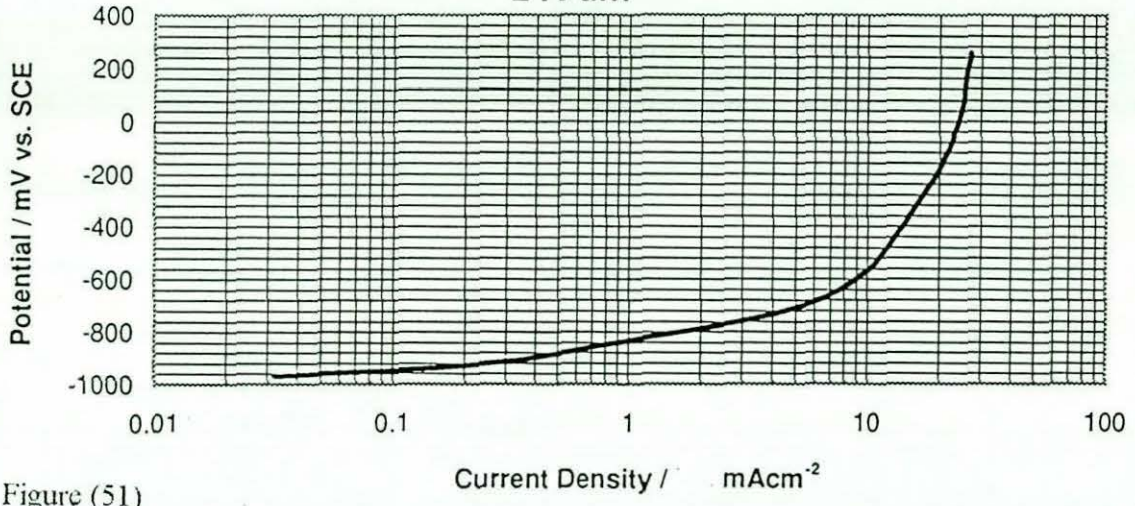
Figure (51)

Anodic Polarisation Curve for 8 microns Zn-Ni Alloy at 5 A dm^{-2}
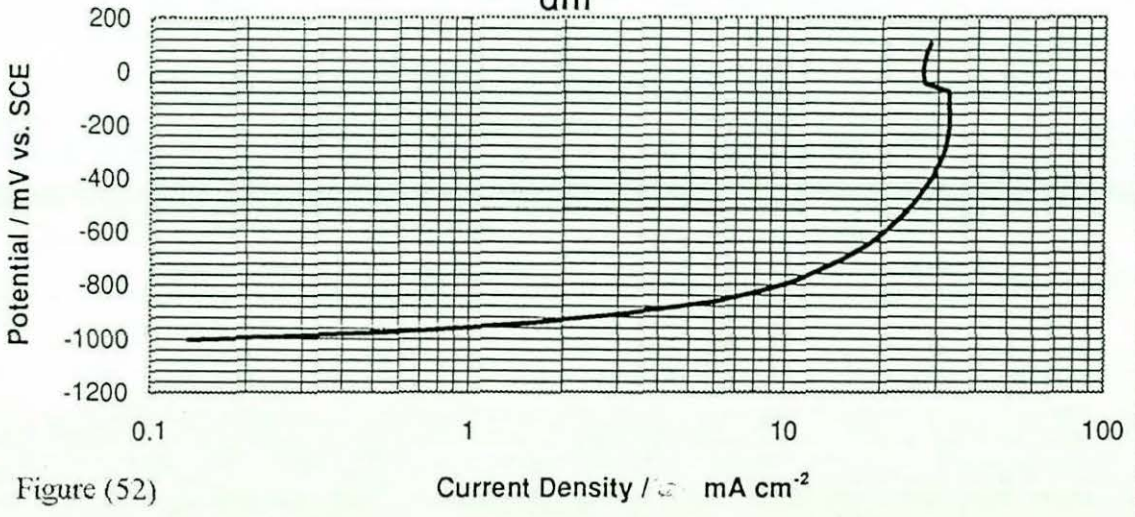
Figure (52)

Anodic Polarisation Curve for 8 microns Zn-Ni Alloy at 10 A dm^{-2}
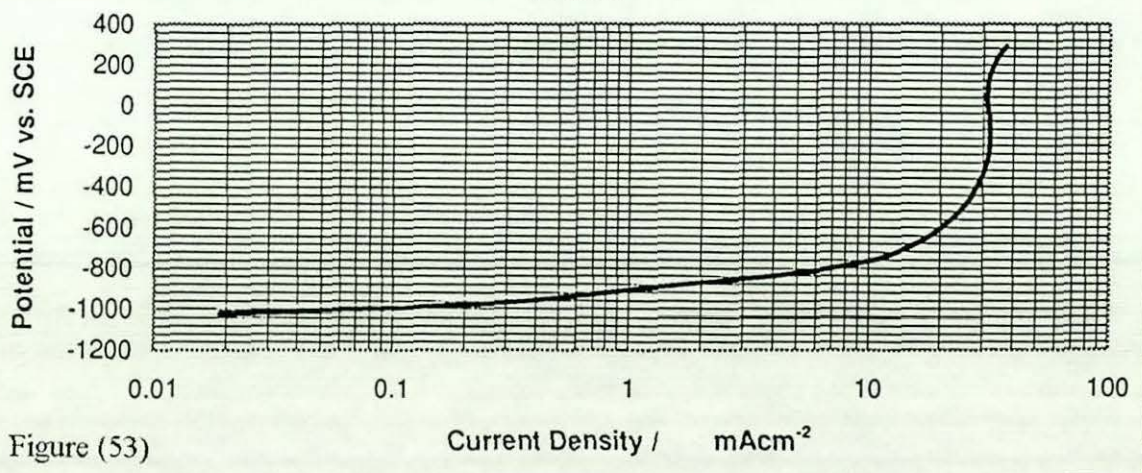
Figure (53)

Figure (54)   Anodic Polarisation of 4 Layers Zn/Ni CMA Coating in 3.5 % NaCl Solution
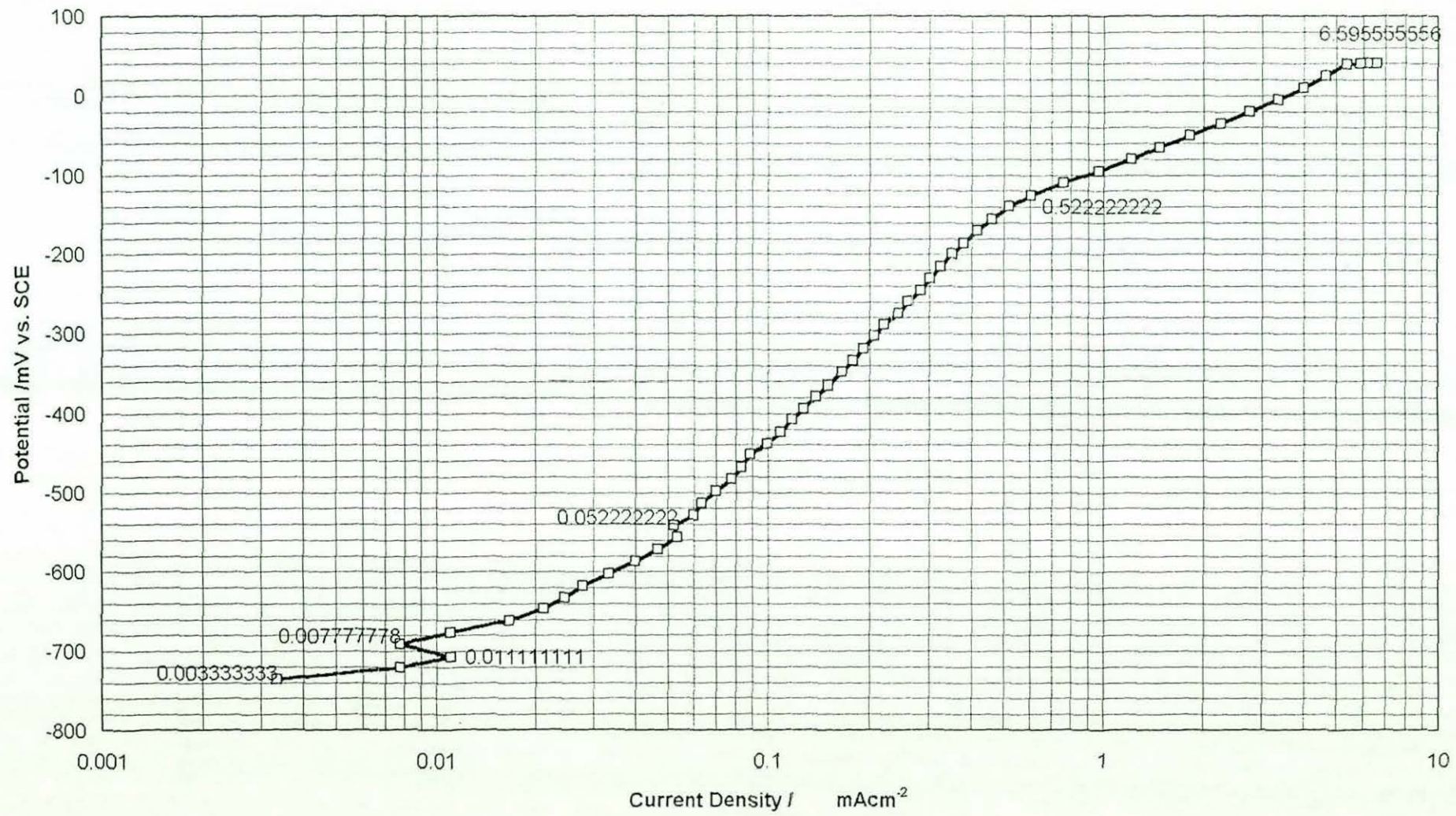
Figure (55)   Anodic Polarisation of 4 Layers Nickel/Zinc CMA Coating in 3.5 % NaCl Solution
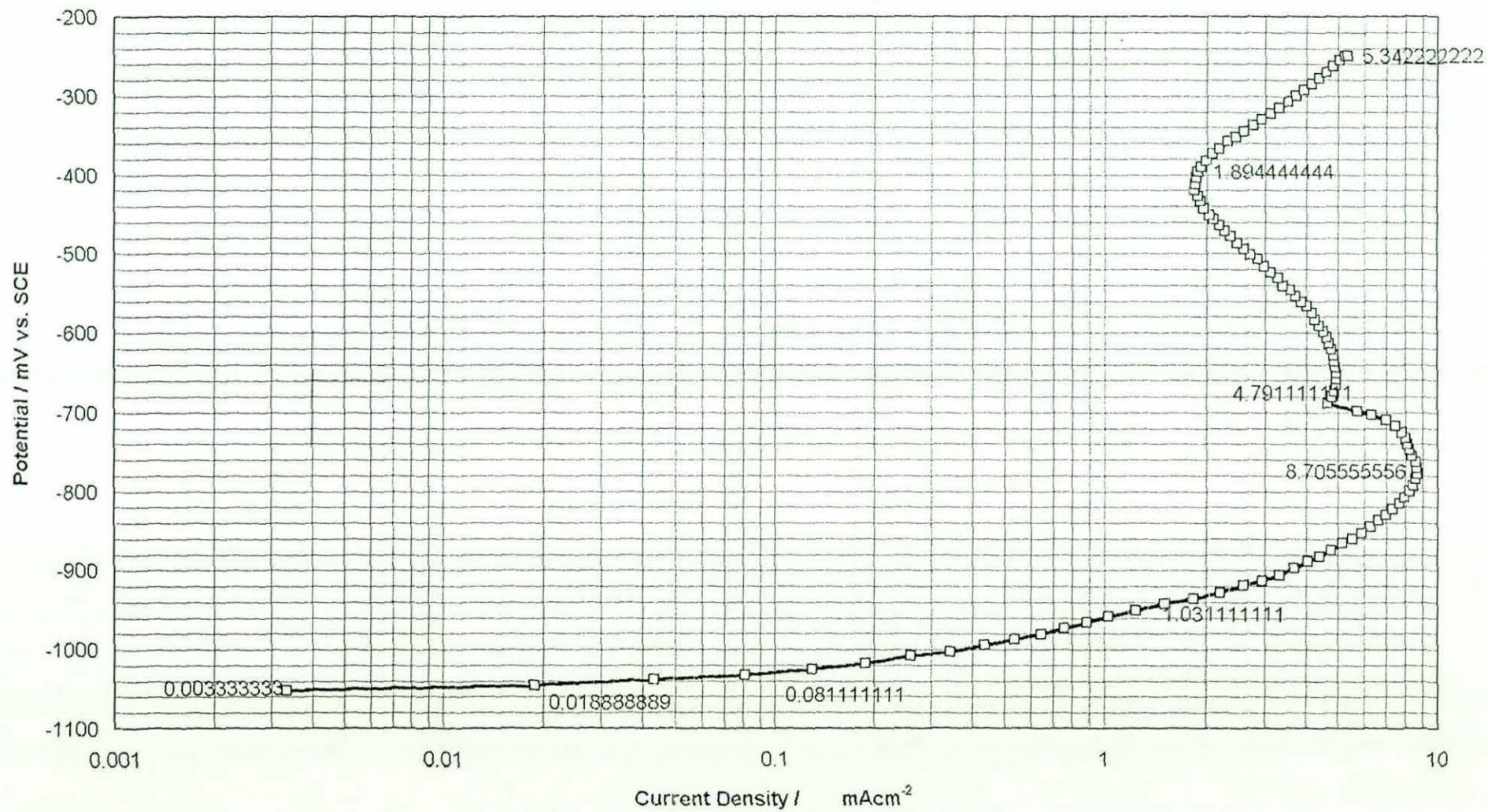
Anodic Polarisation Curve for 8 Layers Ni/Zn CMM Coating in 3.5% NaCl Solution
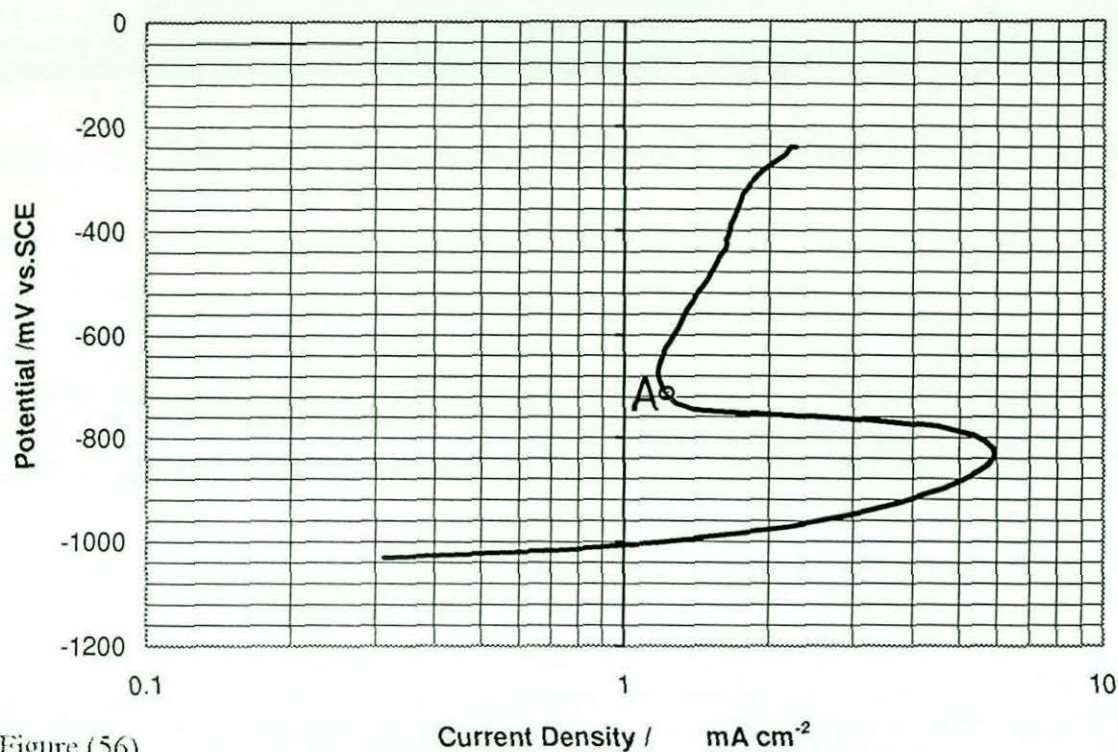
Figure (56)

Anodic Polarisation for 8 Layers Zn/Ni CMA Coating in 3.5% NaCl Solution
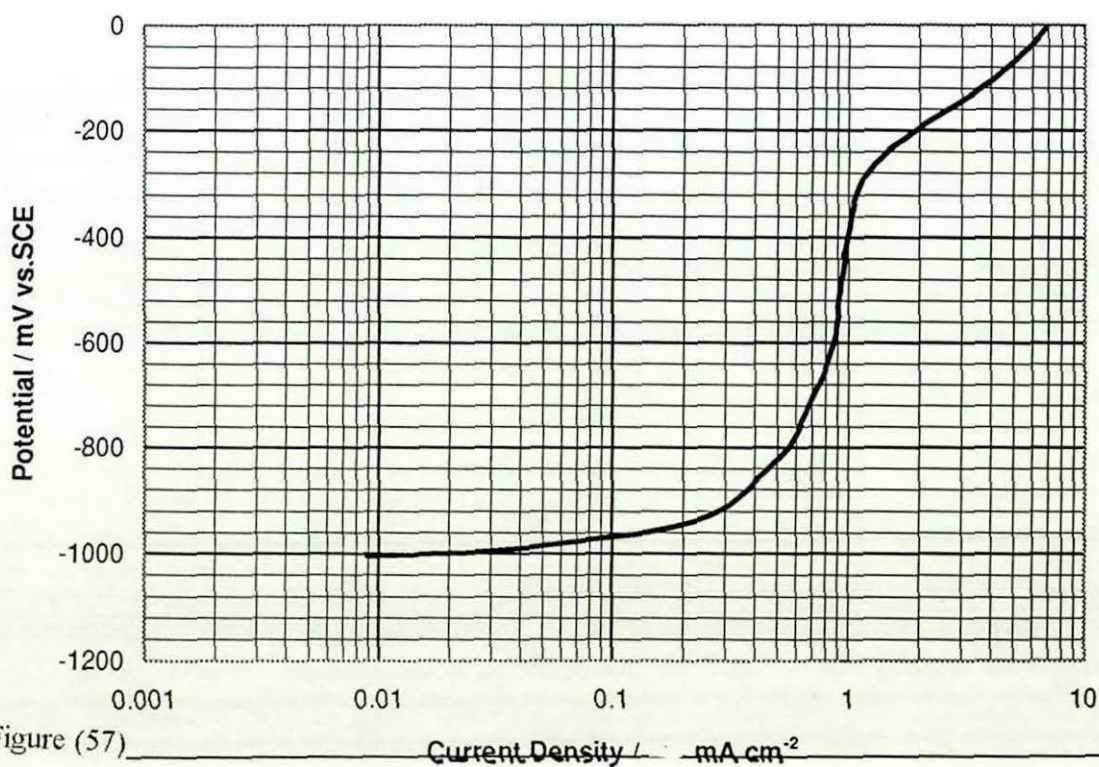
Figure (57)

Anodic Polarisation of 4 layers Zn / Zn-Ni CMA Coating in 3.5% NaCl Solution
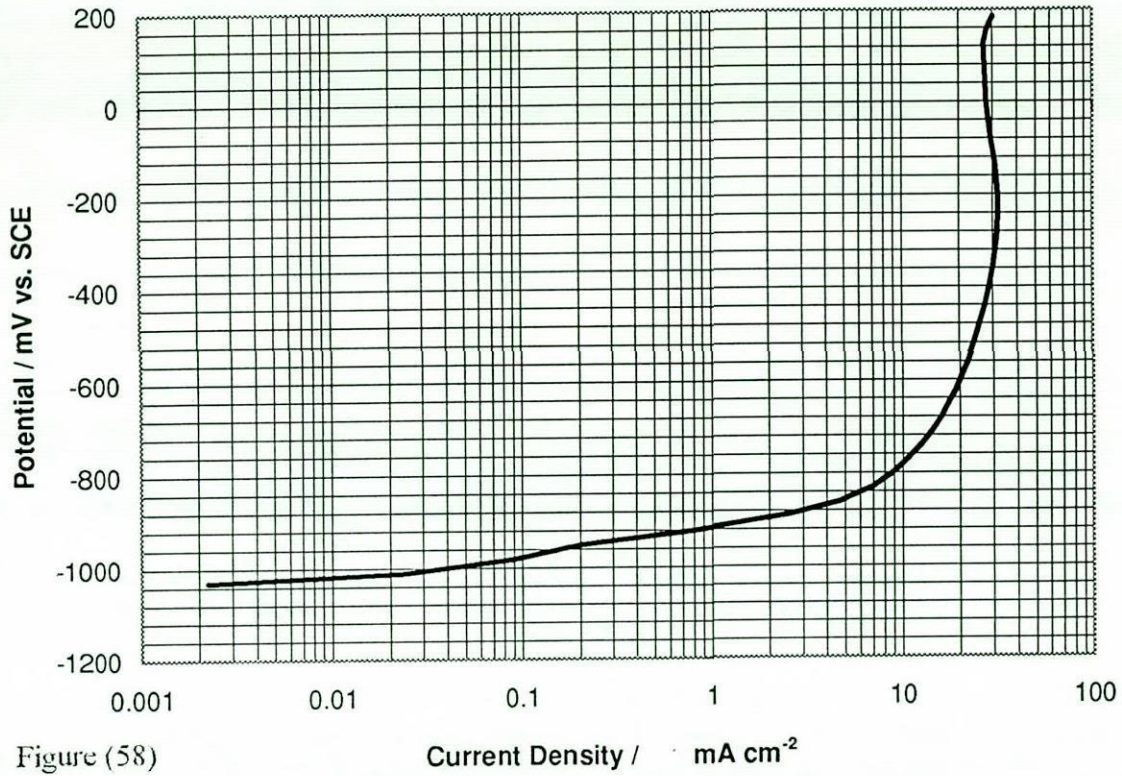
Figure (58)

Anodic Polarisation of 8 layers Zn / Zn-Ni CMA Coating in 3.5% NaCl Solution
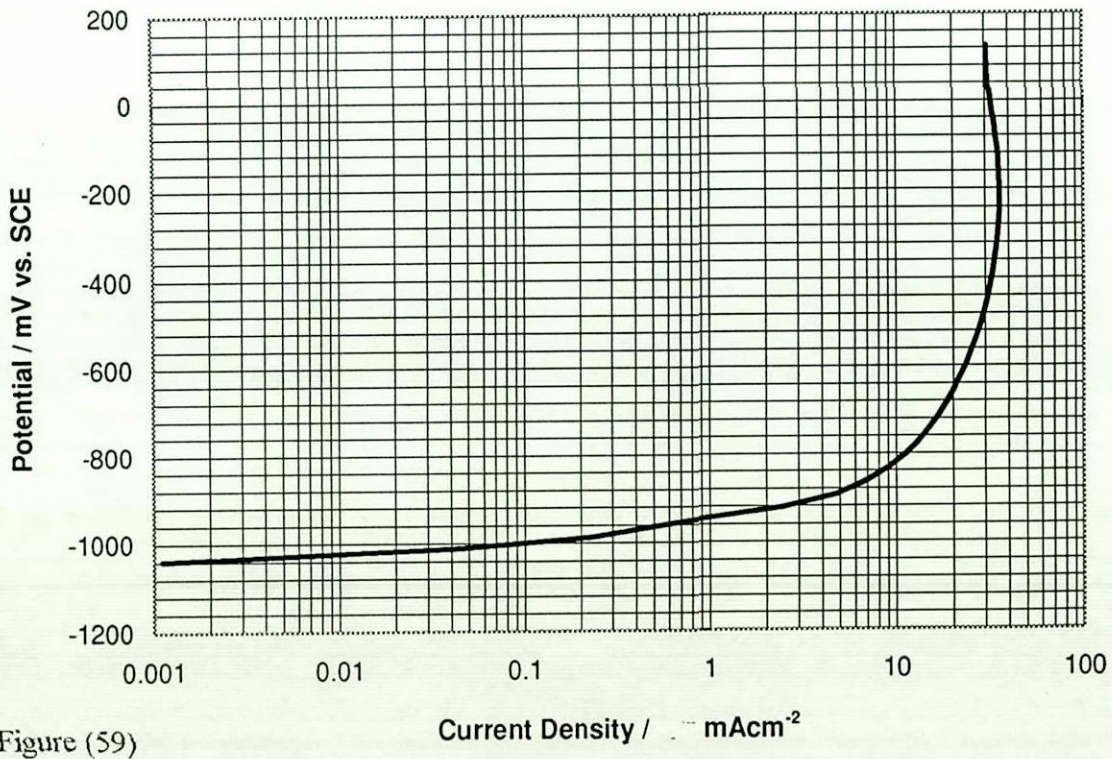
Figure (59)

Anodic Polarisation of 4 layers Zn-Ni / Zn CMA Coating in 3.5% NaCl Solution
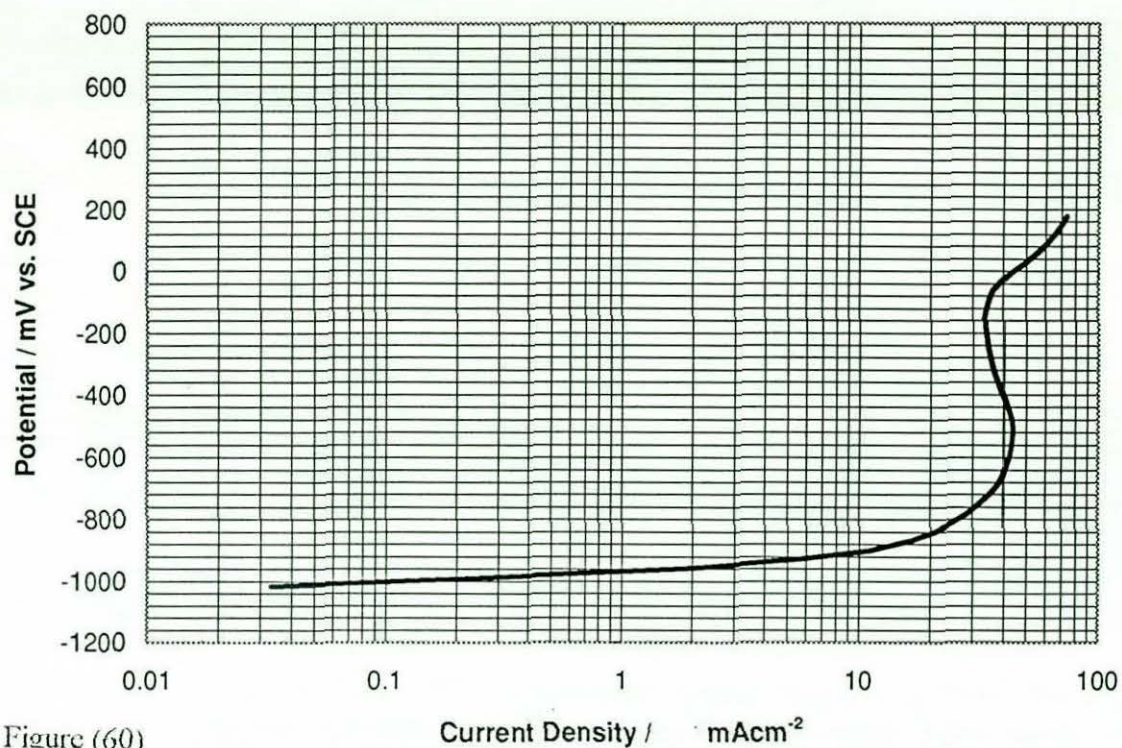
Figure (60)

Anodic Polarisation for 8 layers Zn-Ni / Zn CMA Coating in 3.5% NaCl Solution
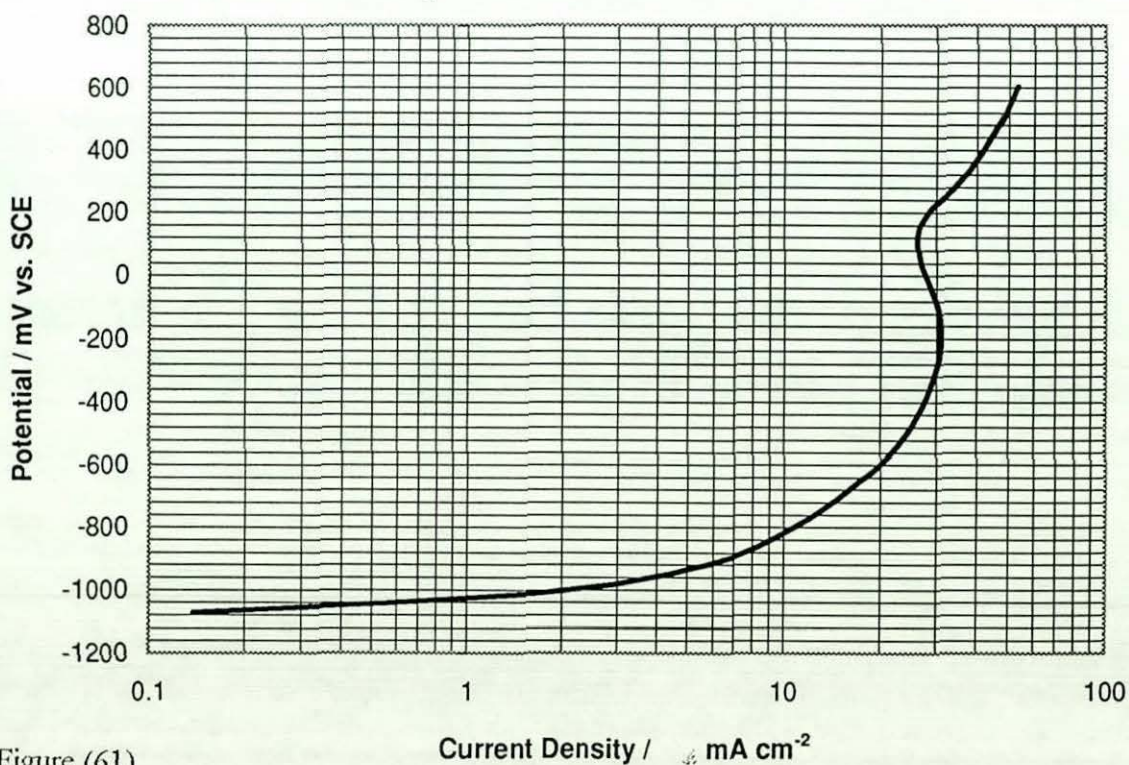
Figure (61)

Anodic Polarisation of 4 Layers Zn-Ni/Ni CMM Coating in 3.5% NaCl Solution
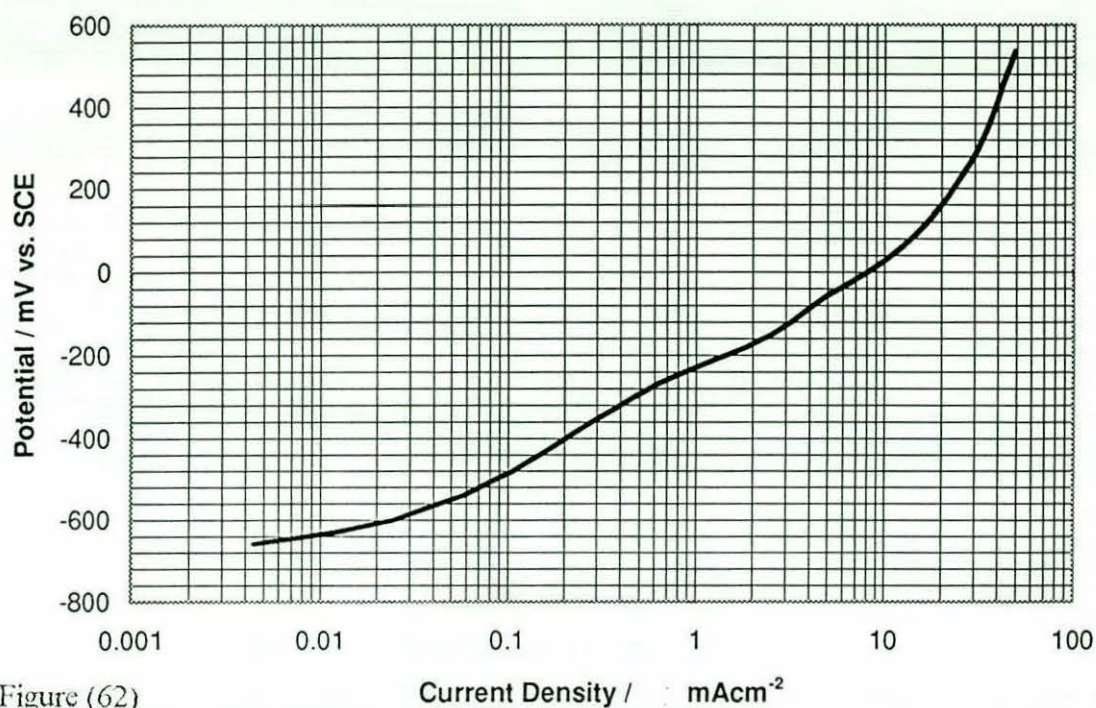
Figure (62)

Anodic Polarisation of 8 Layers Zn-Ni / Ni CMM Coating in 3.5% NaCl Solution
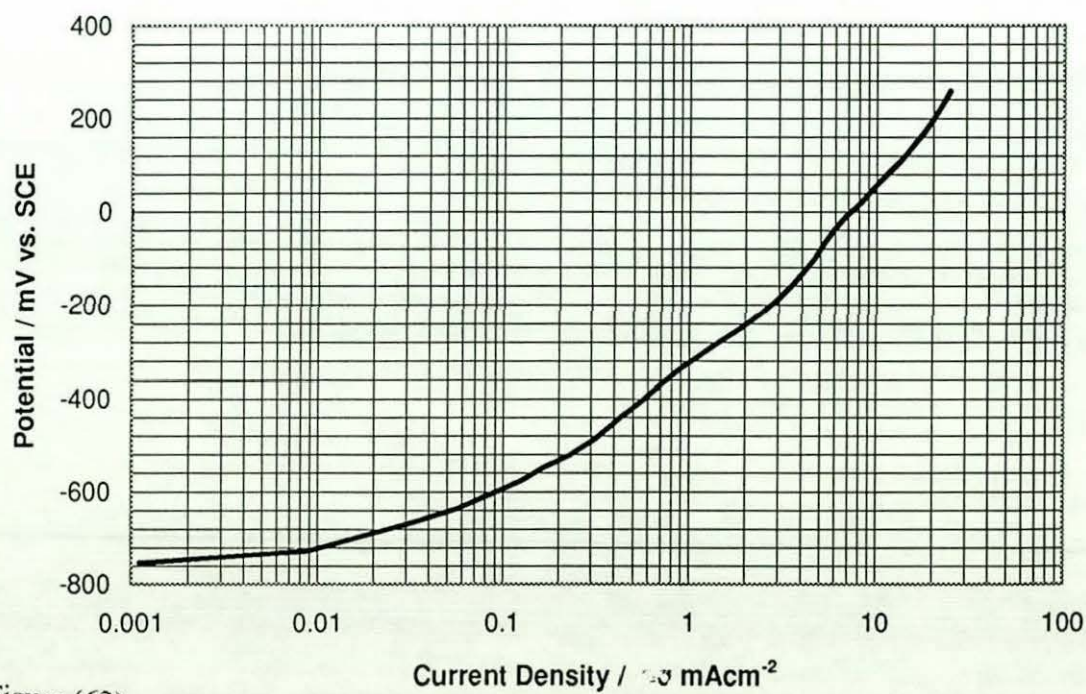
Figure (63)

Anodic Polarisation for 4 Layers Ni/Zn-Ni CMA Coating in 3.5% NaCl Solution
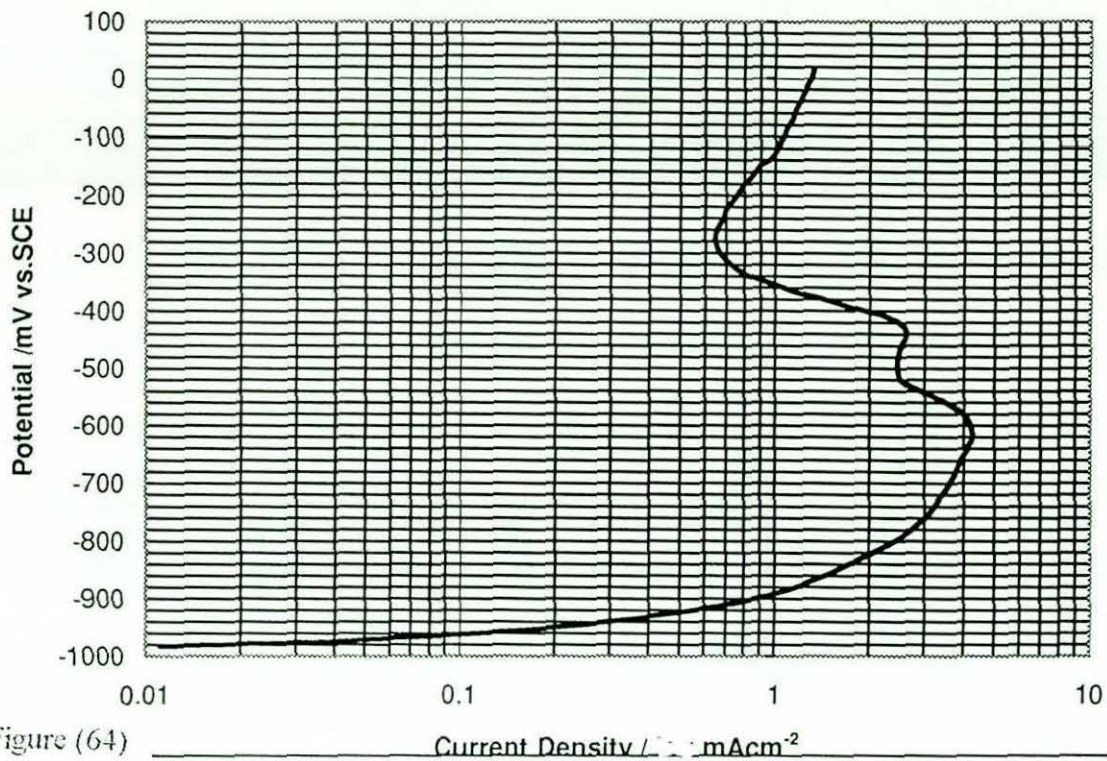
Figure (64)

Anodic Polarisation of 8 Layers Ni/Zn-Ni CMM Coating in 3.5 % NaCl Solution
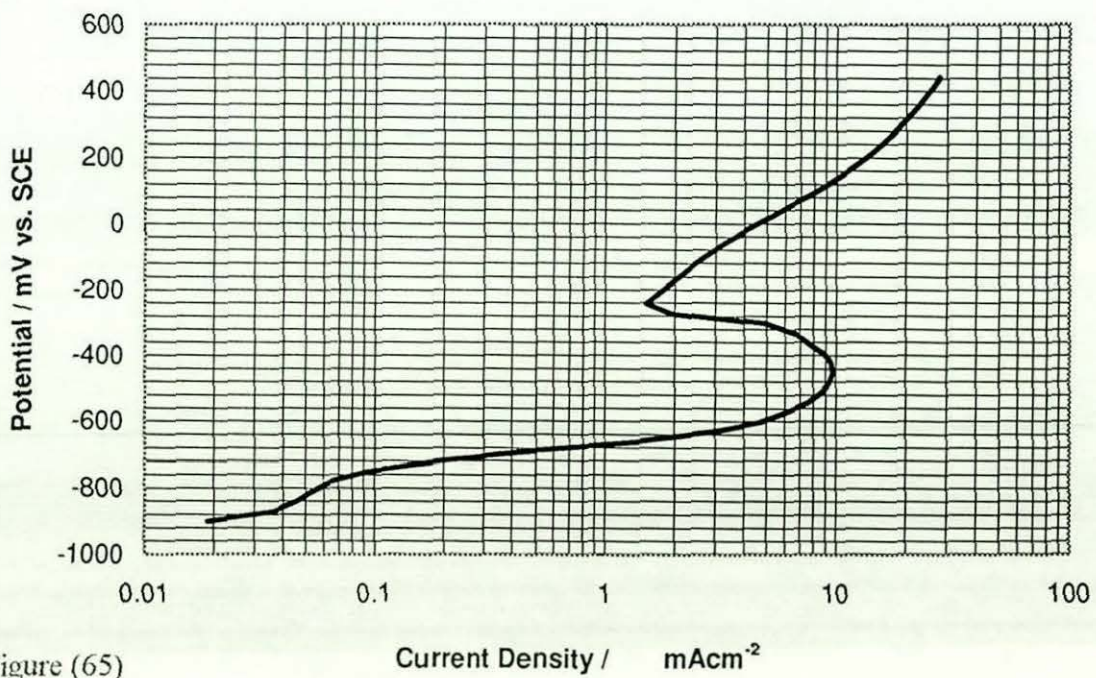
Figure (65)

The 8 layer Zn/Ni CMMM coating seems to behave quite differently from the 4 layer Zn/Ni CMMM coating. The same rapid increase of current density with an increase in potential occurs initially, a further increase in potential produces a limiting current until a sufficiently high potential has been attained and the corrosion product film begins to break down.

The difference in anodic behaviour of the 4 layer Zn/Ni and 8 layer Zn/Ni CMMM coatings suggest that 8 layer Zn/Ni CMMM coatings build up a thicker corrosion product film which led to the wider limiting current density region, this is due again to the porosity of the nickel layer on top of the coating, which is higher than the porosity of the nickel layer on top of the 4 layer Zn/Ni CMMM coating. Whilst the 4 layer Zn/Ni CMMM coating system has a quite similar anodic behaviour to the 8 microns single nickel layer. It does, however, have a greater increase in current density as the potential increases, this increase in current density is believed to be due to forming a very thin film of corrosion product which would promote a more sluggish increase in current density until this film is broken down due to the high applied potential.

The 4 and 8 layer Ni/Zn CMMM systems (figures (55) and (56)) exhibited interesting interactions between the upper (near surface) coating layers. Their "S" type curves were quite pronounced with marked reductions in current following the limiting current. It is thought that during the polarisation measurements as the coating dissolves, discrete areas of nickel will appear and for a wide range of potential be cathodic to the upper zinc-based coating layer. These cathodic sites could well produce appreciable surface pH rises, further stimulating the precipitation of surface corrosion products and resulting in a reduction in the anodic polarisation current. This type of cathodic-anodic interaction during anodic polarisation has been proposed by Dhar and Ooij (42) for electrodeposited zinc on a steel substrate.

Figures (58) and (59) illustrate curves for 4 and 8 layer Zn/Zn-Ni, and Zn-Ni/Zn CMMM systems, these too show evidence of an "S" shaped curve and could undergo similar reactions to Ni/Zn, although the potential difference between the two layer types will be less for Zn-Ni/Zn and Zn/Zn-Ni. The I_{corr} values for the 8 micron single nickel layer, 4 and 8 layer Zn/Ni CMMM coatings, 4 and 8 layers Zn-Ni/Ni CMMM coatings, prove the

porous nature of the nickel layers. With respect to the surface morphology of nickel single layer and 4 and 8 layer Zn-Ni/Ni CMAM coatings, it could be seen that the I_{corr} values have a strong relationship with the the activity of the deposited metal and hence the porosity in the nickel layer. This porosity leads to "uncovering" of the zinc or Zn-Ni alloy and hence the nickel layer became more active than the nickel single layer coating.

4-1-2-9 Neutral salt spray test studies

Table (31) summarises the corrosion behaviour of the 8 microns thick coatings on steel substrates. The time to the first appearance of red rust was measured as an indication of the protective abilities of the coatings and was the average time of three separate samples. The corrosion figures reported illustrate the improvements in times to red rust that can be achieved with the layered electrodeposits. A 4 layer Ni/Zn deposit produces significantely better corrosion protection than a single zinc layer of similar thickness. It is intreresting to note that if the layered structure is reversed (i.e. for Zn/Ni) the corrosion resistance is significantely diminshed. It was observed that after about 48 hours salt spray test, the nickel layer on top of Zn/Ni CMMM coatings tend to crack, whilst, the top layer on Ni/Zn CMMM coatings seemed to have a black surface after about 76 hours. It is believed to be due to some sort of dezincification process. The single layer Zn-Ni alloy electrodeposit gave a time to red rust of slightly less than both the Zn/Ni and Ni/Zn layered coatings. It is also interesting to note that for both Zn/Ni and Ni/Zn eight layers provided less corrosion resistance with respect to Zn/Ni and Ni/Zn four layers. These observations could be attributed to how porous the nickel layer was. Layering the Zn-Ni alloy with both Zn and Ni produced even greater increases in corrosion resistance. The optimum layer configuration(of those tested) appeared to be the four layer Zn-Ni/Zn which had a time to red rust value of 552 hours. Again for all the layered samples containing the Zn-Ni alloy, the lower the number of layers the greater the corrosion resistance.

Referring to the Zn-Ni/Zn and the Zn/Zn-Ni CMAM coating corrosion performance values, it can be observed that the Zn-Ni/Zn CMAM coatings perform much better than the Zn/Zn-Ni CMAM coatings. Again as with Zn/Ni and Ni/Zn coatings, the layered

100

Table (31) Corrosion Data for different Zn - Ni multilayer coatings (DBT) based on Zn , Ni , and Zn-Ni alloy of 8 microns thickness layers . Comparison with substrate steel , Zn , Ni and Zn-Ni Coatings are also shown .

Type of CMM Coating	Number of Layers	Ecorr mV cm^{-2} vs. SCE	I$_{corr}$ mA cm^{-2}	Hours to Red Rust
Zn	1	-1060	0.7	197
Ni	1	-450	0.002	71
Zn/Ni	4	-735	0.01	223
Zn/Ni	8	-1005	0.1	178
Ni/Zn	4	-1050	0.03	336
Ni/Zn	8	-1035	0.3	323
Zn-12%Ni	1	-996	0.2	313
Zn/Zn-Ni	4	-1030	0.04	329
Zn/Zn-Ni	8	-1040	0.04	287
Zn-Ni/Zn	4	-1020	0.3	551
Zn-Ni/Zn	8	-1080	0.9	518
Zn-Ni/Ni	4	-660	0.02	208
Zn-Ni/Ni	8	-670	0.01	181
Ni/Zn-Ni	4	-980	0.09	328
Ni/Zn-Ni	8	-900	0.03	276

structures with zinc on top perform better with respect to resistance to corrosion. This observation could be attributed to the noticeable change in the surface morphology of Zn-Ni alloy over zinc (see section 4-1-2-7-1).

The salt spray tests gave a good indication of the sacrificial corrosion protection capabilities of the coatings and thus it is difficult to compare their trends with the short-term electrochemiocal tests which give an indication of the coatings corrosion rates without exposing the substrate.

4-1-2-10 Measurements for the charge passed during anodic polarisation of 8 layer Ni/Zn CMMM coating

Further measurements were carried out to measure the potential/ current point where a 1 micron zinc layer has been removed completely from a layered coating. The measurements were carried out during the anodic polarisation of an 8 layer Ni/Zn CMMM system. The results suggest that at the end of fall back regime the whole 1 micron zinc layer was removed (see Appendix).

4-1-2-11 The suggested corrosion mechanism for Zn/Ni and Ni/Zn CMMM coating systems

The significant differences in the corrosion behaviour and performance of Zn/Ni and Ni/Zn CMMM coatings and similarly Zn-Ni/Ni and Ni/Zn-Ni CMAM coatings have been studied, and a possible mechanism is now suggested.

Figure (66) illustrates a schematic representation of the corrosion mechanism for the 4 layer Zn/Ni CMMM coating system, suggesting that the nickel layers are porous (as earlier experimental results confirmed).

At stage (1), the four layer coating system has a porous outer nickel layer (as coated). At stage (2), after a specific time, the voluminous corrosion products will emerge through the pores in the nickel top layer. At this stage because zinc is anodic (active) and nickel is cathodic, the porosity of the cathodic nickel electrodeposit on the zinc layer is critical.
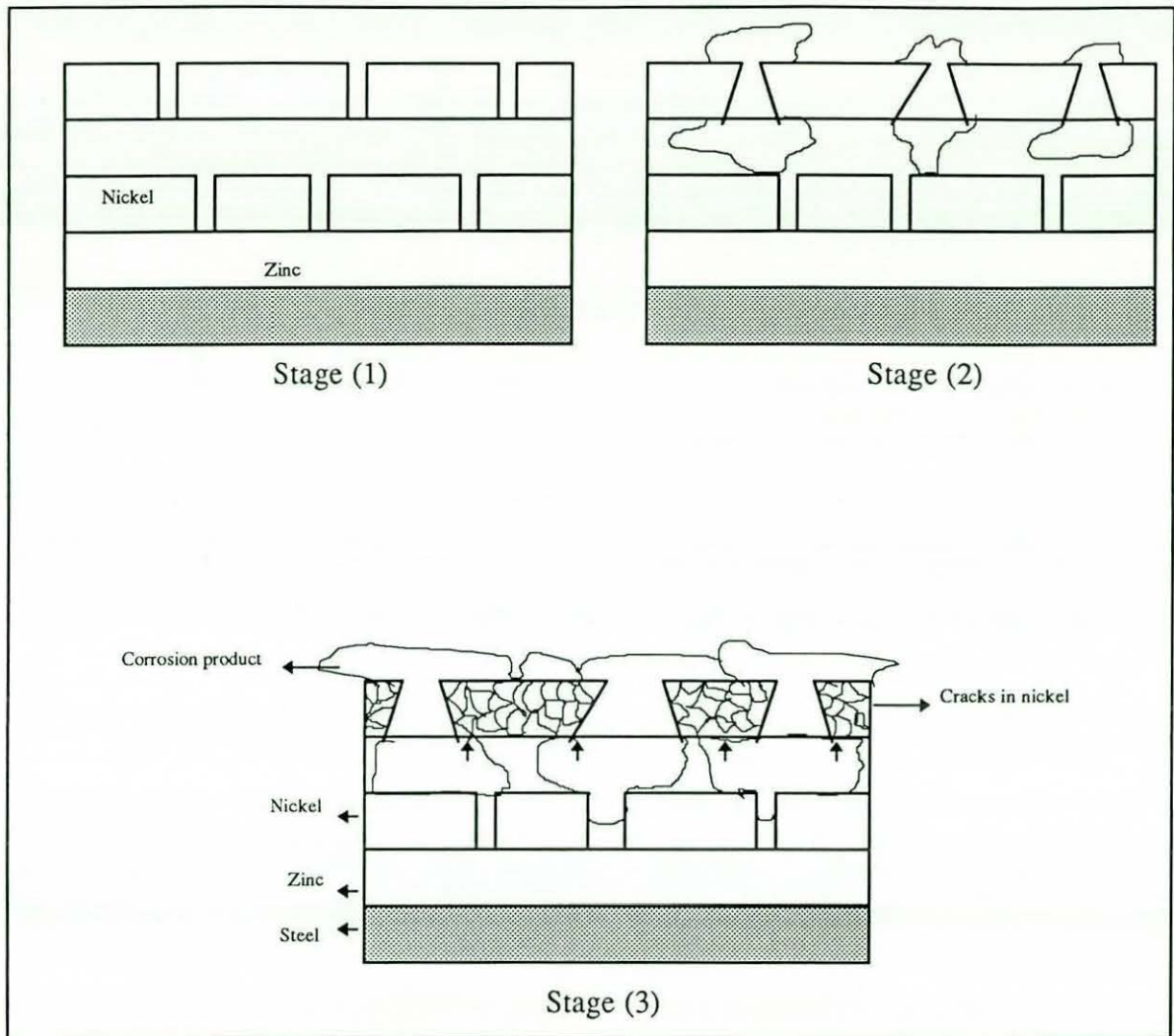
Figure (66) Possible corrosion mechanism of 4 layer Zn/Ni layered structure

The rate of corrosive attack that can occur on the zinc layer at any discontinuities (pores) in the nickel layer will be accelerated due to the presence of a relatively large cathodic area of electrodeposited nickel and the very small area of zinc exposed at the base of any pores in the coating. This can result in severe corrosion of the zinc layer underneath and consequent undercutting of the nickel layer.

Stage (3) represents a period where a large amount of voluminous corrosion product has been produced, promoting high pressure areas underneath the nickel layer which will push the nickel layer upwards and crack it. At the same time, the corrosion of the zinc layer

continues and extends to the zinc metal which is covering the pores in the second nickel layer leading to further severe corrosion of the next zinc layer.

The corrosion mechanism for the Ni/Zn CMMM coating system is different to that for the Zn/Ni CMMM coating. The top layer is now zinc and this plays an important part in the whole corrosion process indicating the situation even, when, after a specific time, the zinc layer is relatively corroded. The porous nickel layer with the zinc covering the pores will be covered with corrosion products and could possibly corrode preferentially to protect the nickel layer. This will lead to a faster zinc dissolution. However, the zinc layer on top is more likely to passivate after a specific time due to the formation of voluminous corrosion products such as $Zn(OH)_2$ and produce some kind of barrier film, and the whole layered system will then perform much better in resistance to corrosion. Figure (67) illustrates a schematic representation of the corrosion mechanism for the 4 layer Ni/Zn CMMM coating system, suggesting that the nickel layers are porous (as earlier experimental results confirmed).
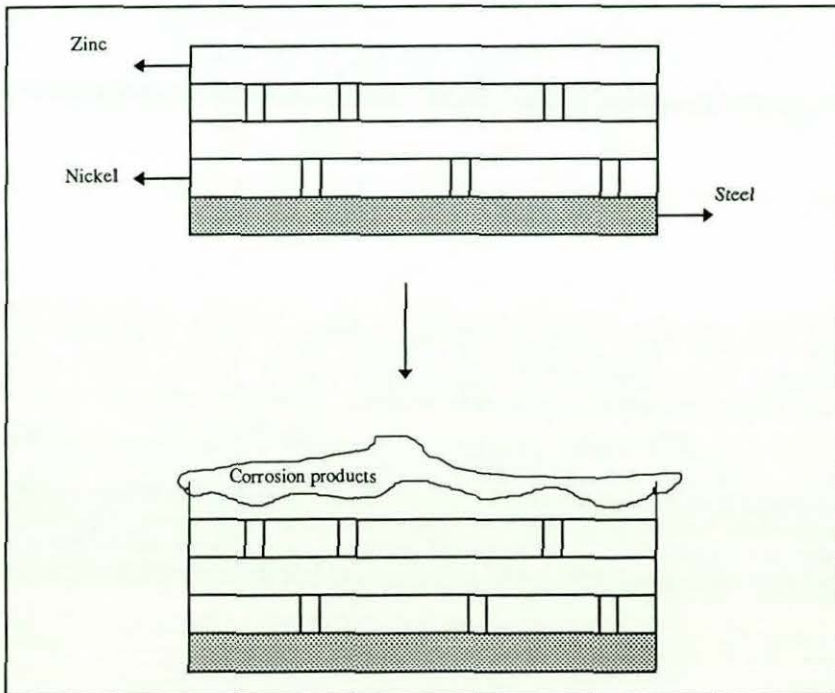
Figure (67)) Possible corrosion mechanism of 4 layer Ni/Zn layered structure

103

4-2 The Single Bath Investigations

Introduction

The single bath electrodeposition investigations could be divided into two main sections:

4-2-1 The single bath electrodeposition investigations of the copper/nickel

4-2-2 The single bath electrodeposition investigations of the Zn-Ni CMAM coatings.

4-2-1 The single bath investigations of the copper/nickel CMMM coating system

4-2-1-1 Introduction

Following initial investigation into a Cu/Ni CMMM dual bath system, further investigations were carried out on the Cu/Ni single bath system in order to establish a good understanding of the high speed electrodeposition processes used by this technique and to produce multilayered coating at a nanometre level.

As mentioned earlier, the production of these types of multilayers has been carried out under a pulsed current system with the use of a RCE.

Initially, two single bath formulations were examined as to their effectiveness at producing multilayer structures, the Despic (75) and the IMC baths which are shown in table (32).

4-2-1-2 Cathodic polarisation studies

Cathodic polarisation studies were undertaken to assess bath solutions, figures (68) and (69) show a series of curves at different rotation speeds from both baths respectively. It appears from analysis of the two figures that the IMC solution produced more definable mass transport limited plateaux at higher RCE rotating speeds. Also, the Despic solution was found to undergo large pH changes during electrodeposition and required constant pH adjustment. These findings thus suggested that the IMC solution was the better alternative to be utilised for the Cu/Ni CMAM single bath trials.

Constituent	Cu/Ni Despic bath	Cu/Ni IMC* bath
$CuSO_4.5H_2O$	1 g/l [Cu^{++}]	3.5 g/l
$NiSO_4.6H_2O$	100 g/l [Ni^{++}]	403 g/l
H_3BO_3	-	30 g/l
$Na_3C_6H_5O_7.2H_2O$	0.6 M	-
Copper current density	0.8 A/dm^2	1.7 mA/cm^2
Nickel current density	32 mA/cm^2	32 mA/cm^2
Agitation	RCE	500 rpm
Temperature	50	60
pH	3.5	3.5

(*) Bath suggested by the Institute for Microelectronics at the University Linkoping, Sweden

Table (32). Bath compositions and plating conditions for single bath electrodeposition of Cu/Ni CMM coatings

4-2-1-3 Effect of pulsed wave-form regimes

Two different pulse-current regimes have been examined in order to achieve a smooth linear layered structures, i.e. dual and quadruple pulsed-current regimes. Figures (70) and (71) show SEM micrographs of two Cu/Ni CMAM layered structures produced at the same optimum plating conditions utilising the aforementioned two pulsed regimes. The micrographs show that an "off time" (very small cathodic current applied) interposed between the current levels was effective to produce a smooth linear layered structure.

The duration of the very small cathodic current applied between the copper and nickel current pulses must be sufficiently long (5 sec) to allow complete relaxation of the diffusion layer which lead to better surface properties and minimised hydrogen occlusion which can have an adverse effect on coating properties.
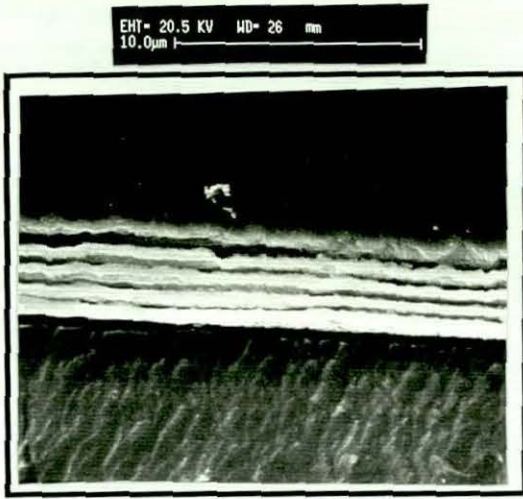
Figure (70) SEM micrograph of 10 layers Cu/Ni CMMM (500 nm each) coating produced by quadruple pulse-current regime
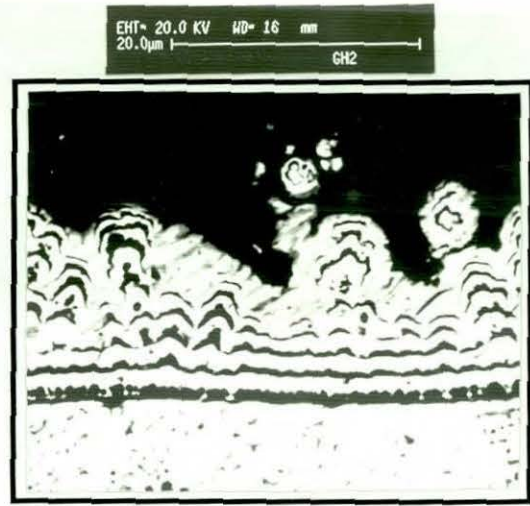
Figure (71) SEM micrograph of 10 layers (1μ each) Cu/Ni CMMM coating produced by a dual pulse current regime

Effect of the Rotation Speed of the Cathode on the Limiting Current of the Copper Deposition from the IMC Copper/Nickel Solution
(Sweep Rate 200 mV/min - R.P. -371 mV vs. SCE)
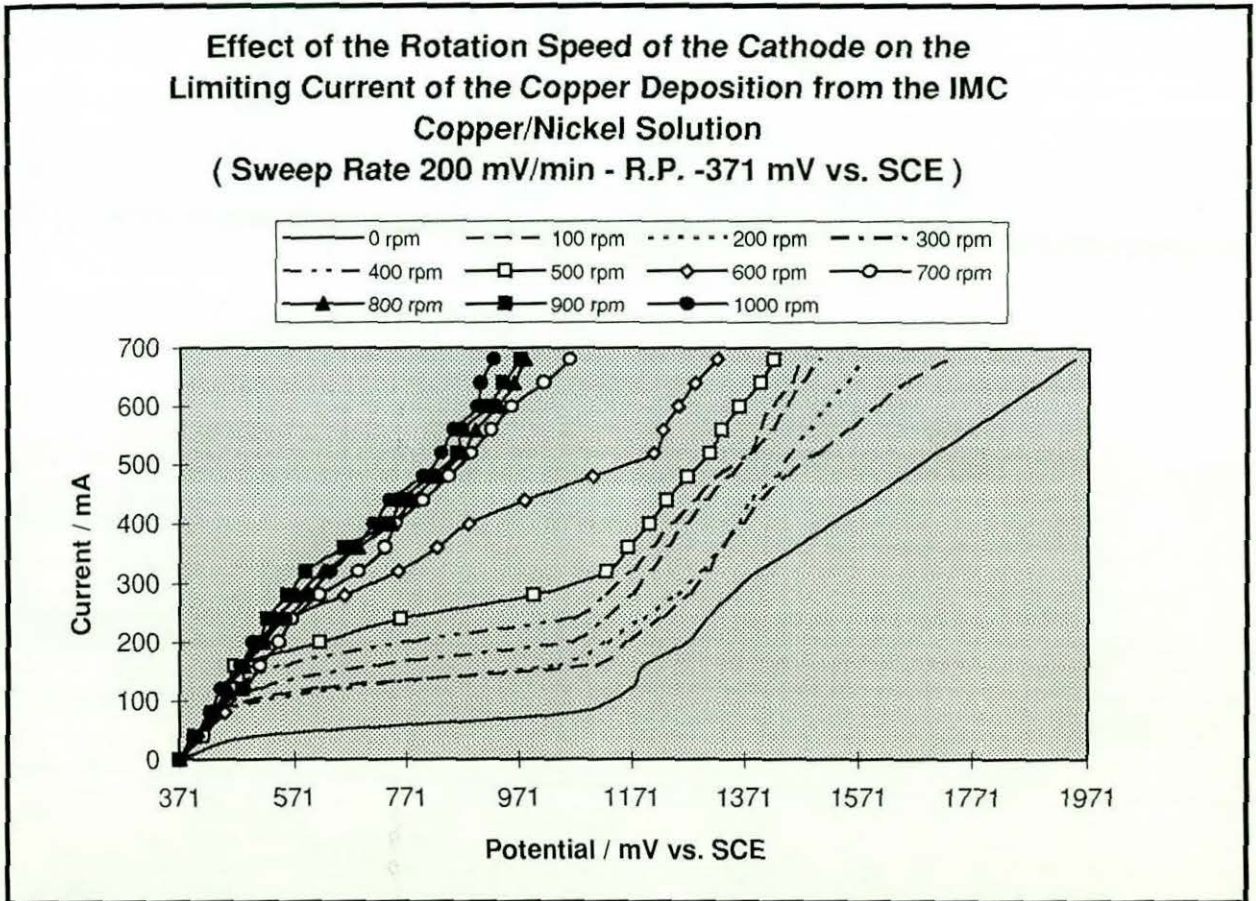
Figure (68)

4-2-1-4 Micro-sectional observations of Cu/Ni CMAM coatings

A series of layered structures of Cu/Ni CMAM coatings were examined using a variety of surface analytical techniques. Figures (72) and (73) show SEM micrographs of Cu/Ni CMAM coatings. It can be seen that a smooth, linear and adjacent layers can be achieved by this technique.
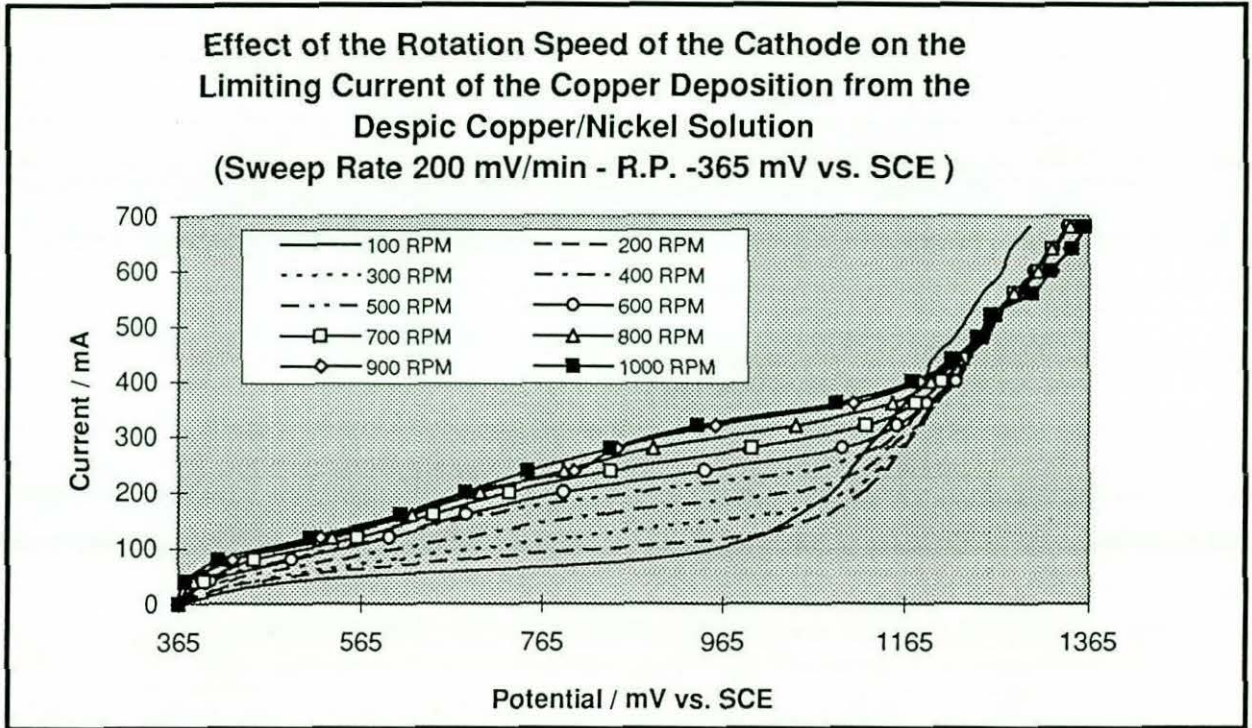
Figure (69)

Scanning electron microscopy proved problematic at bilayer thicknesses of less than approximately 50nm due to the approach of the limit of resolution. Coatings of bilayer thicknesses less than 50 nm required alternative techniques to prove the existence of a layered structure.

| Figure (72) | EHT= 20.0 KV WD= 19 mm
5.00µm | Figure (73) | EHT= 20.5 KV WD= 25 mm
2.00µm |
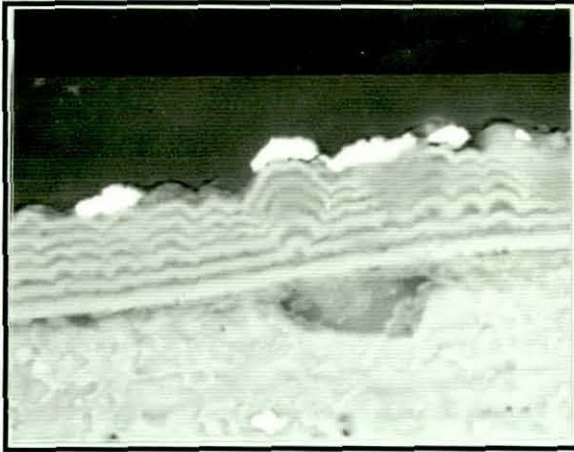
SEM micrograph of 12 layer (400 nm each) Cu/Ni CMAM coating.

SEM micrograph of 20 layer (40 nm each) Cu/Ni CMAM coating.

Initially auger electron spectroscopy (AES) and secondary ion mass spectroscopy (SIMS) were applied. However, both techniques failed to distinguish the periodic nature of the structure. This was thought to be as a result of the roughness of the substrate. Further samples have been prepared on very smooth copper foils, the samples were then examined by a TEM technique at the Institute of Microelectronics at the University of Linkoping in Sweden. Figure (74) shows the periodic nature of the structure of 25 nm Cu/30 nm Ni CMAM coating, the micrographs show a relatively smooth and adjacent layered structure with no signs of facets (local variations in the growth rate of copper) in the copper layers.

4-2-1-5 Nickel layer composition measurement

In order to measure the purity of the Ni layers with respect to copper , an EDAX coupled with an SEM was used.

Figure (75) shows that relatively pure nickel layers can be produced with only a very small trace amount of copper. Figure (75) proves that with the use of the quadruple pulse-current regime the possibility of significantly alloying the nickel layer with copper is very low.

Figure (74). TEM micrograph for 50 layer 25 nm Cu/30 nm Ni CMAM coating
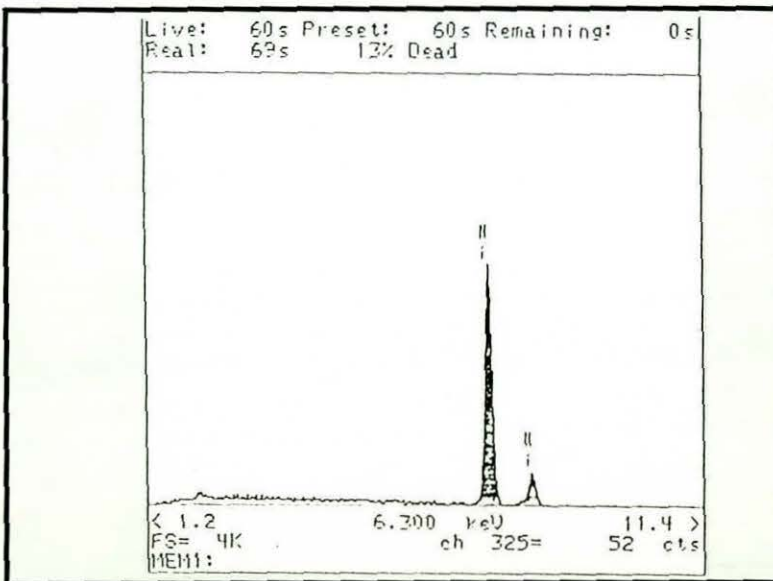
Figure (75). The composition of the electrodeposited nickel layer.

4-2-2 Single bath electrodeposition of single and multilayer zinc-nickel alloy coatings

4-2-2-1 Introduction

The investigation of single layer and multilayer coatings of the Zn-Ni alloy system by a single bath technique were carried out utilising a high speed Zn-Ni electroplating solution (77):

35 g/l Ni^{++} as $NiSO_4.6H_2O$

35 g/l Zn^{++} as $ZnSO_4.7H_2O$

80 g/l Na_2SO_4

pH 2 (adjusted with a dilute sulfuric acid)

Temperature 23°C

Electrodeposits were formed using both direct and pulsed current regimes. A series of single and layered structures were produce to an overall nominal thickness of 8 microns.

Initial investigations were carried out on the single layer coatings from this zinc-nickel alloy system in order to study the effect of current density and rotation speed on the electrodeposit composition, cathode current efficiency and deposit morphology and to evaluate their corrosion behaviour and performance. When this was been accomplished, the production of Zn/Ni CMAM coatings was then carried out utilising the appropriate plating conditions observed in the former investigations in order to build up repetitive layers of different compositions and then to be able to compare them with a single layer Zn-Ni alloy in terms of corrosion behaviour and performance.

4-2-2-2 Galvanostatic electrodeposition evaluation of single layer Zn-Ni alloy coatings

The Galvanostatic electrodeposition of single layer Zn-Ni alloy coatings were formed using a direct current system. The electroplating was carried out at RCE speeds of 0-2000 revolution per minute (rpm) and at current densities of 2.55-169.9 A/dm^2.

4-2-2-2-1 Effects of current density and rotation speed

4-2-2-2-1-1 Effect on deposit composition

The effect of current density on the nickel content at different rotation speeds in the Zn-Ni alloy electrodeposits was studied. Tables (33) to (46) and figures (76) to (93) show the effect of current density and rotation speed on the nickel content in the coatings. It was found that at a static condition, in the current density range of 2.55 to 35.7 A/dm^2, the amount of nickel in the deposit was found to be between 5-8%. It might be expected that more nickel would be present, particularly when taking into account zinc and nickel reduction potentials. The low nickel content could be due to "anomalous co-deposition" in which the activity of the nickel (the more noble metal) ions in the zinc electrolyte have been greatly decreased by a stable zinc complex formation, it is believed that zinc forms a hydroxide and behaves as a more noble metal than nickel or hydrogen. An increase in current density from 35.7 to 56.1 A/dm^2 resulted in an increase in nickel content to 11%. With further increase of current density from 56.1 to 96.9 A/dm^2, the nickel content was increased to 19%. At higher current densities from 135.9 to 159.9 A/dm^2, the nickel content reached a maximum value of 36% which is approximately three fold the nickel content deposited in the alloy at 56.1 A/dm^2 and seven fold that in the alloy the deposited at 2.55 A/dm^2. This is possibly due to the mechanism of alloy electrodeposition. Which, operating under static conditions at high current densities, the pH at the cathode surface increases considerably (perhaps as much as seven fold (90)), the zinc deposition then reaches its limiting current, and hence the concentration of zinc ions available at the cathode is decreased. Therefore, the amount of absorbed zinc hydroxide also decreases. This leads to an increase in the driving force for the deposition of hydrogen as well as nickel (77).

Unexpectedly, with further increase of current density to 169.9 A/dm^2 the nickel content dropped to about 29%.

By rotating the cylindrical cathode from 150 rpm to 2000 rpm in the zinc-nickel electrolyte, at low current densities, the nickel content in the deposit was found to drop in a close range from 7 to 4.5 at 2000 rpm. At higher current densities, the nickel content dropped significantly, at a current density of 96.9 A/dm^2 the nickel content had

dropped from 19% under static conditions to 4% at 2000 rpm. With further increase of current density to 135.9 and 152.9 A/dm^2, the nickel content dropped more significantly from about 36% at static conditions to about 5% at 2000 rpm. The main factor affecting the surface chemistry is the surface pH, it is possible that, when the electrode rotates at considerable speed and ionic species replenish the cathode diffusion layer, the pH at the cathode remains relatively low, this pH level could well be similar to the samples plated at low current densities. Such a pH level at the cathode surface and its effect on composition is the opposite to that which occurred at static conditions with high current densities. Whilst, at current densities higher than 152.9 A/dm^2, the amount of nickel dropped from about 29% to about 9%, which is rather unexpected. This might be due to the diffusion rate of nickel ions reaching its upper limit and further increase in current density will favour the deposition of zinc. Also, a high increase in current density causes the cathode potential to become more negative. This will favour electrodeposition of the less noble metal, hence, the nickel content was reduced.

As a general rule, the aforementioned trends could be explained by taking in to account the following principles:

1- The variation in composition of the deposit is due to the concentration changes at the cathode-solution interface(91).

2- The variation in composition of the deposit is due to the pH changes at the cathode-solution interface (91).

3- Nickel electrodeposition begins at a potential which is several tenths of a volt less noble than its equilibrium potential (91).

4- The deposition of nickel is easily further polarised when its deposition sites are occupied by adsorbed foreign substances like $Zn(OH)_2$, and in order to make the preferential deposition of zinc possible, the presence of an inhibitor for nickel deposition must be necessary. In the electrodeposition of Zn-Ni alloy, the zinc hydroxide formed by hydrolysis due to the pH rise at the cathode surface is regarded as such an inhibitor (91).

5- When the current density increases, the pH at the cathode surface rises due to the increased rate of hydrogen evolution which results in zinc hydroxide formation and subsequent adsorption on the cathode, which results in a further decrease in nickel

Table (33)

Characteristics of Electrodeposited Zn/Ni Alloys on a Substrate at 2.55 A dm^{-2} and Various Rotation Speeds

RPM	CATHODE CURRENT EFFICIENCY (%)	NICKEL CONTENT (%)	VISUAL APPEARANCE	SURFACE MORPHOLOGY
0	90.5	5.5	WHITE-GREY SPOTTED NON-UNIFORM DEPOSIT	
150	88.9	2.5	WHITE-GREY AT EDGES /DULL GREY AT THE CENTRE / NON-UNIFORM DEPOSIT	
350	88.5	3	WHITE-GREY AT EDGES /DULL GREY AT THE CENTRE / NON-UNIFORM DEPOSIT	
500	84.9	2	WHITE-GREY NON-UNIFORM DEPOSIT/ DULL AT THE CENTRE	
1000	79.1	1.5	SEMI-BRIGHT GREY UNIFORM DEPOSIT	
1500	76.3	1.5	SEMI-BRIGHT GREY UNIFORM DEPOSIT	
2000	69.7	2	BRIGHT WHITE-GREY UNIFORM DEPOSIT	

Table (34)

Characteristics of Electrodeposited Zn/Ni Alloys on a Steel Substrate at 5.1 A dm^{-2} and Various Rotation Speeds
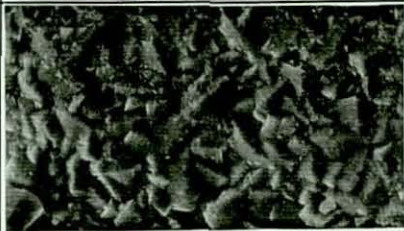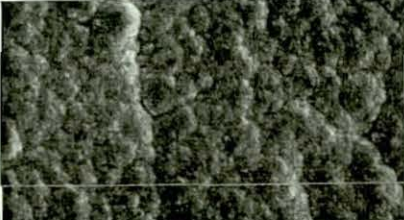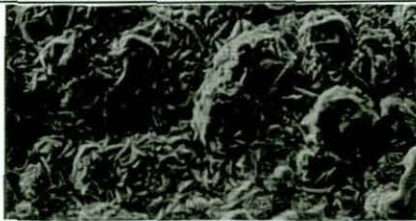
RPM	CATHODE CURRENT EFFICIENCY(%)	NICKEL CONTENT (%)	VISUAL APPEARANCE	SURFACE MORPHOLOGY
0	87.4	5	SEMI-BRIGHT WHITE-GREY STREAKY DEPOSIT	
150	83.3	2	BRIGHT WHITE-GREY UNIFORM DEPOSIT	
350	78.5	1.5	BRIGHT WHITE-GREY UNIFORM DEPOSIT	
500	81.9	1.5	BRIGHT WHITE-GREY UNIFORM DEPOSIT	
1000	77.4	2	BRIGHT WHITE-GREY UNIFORM DEPOSIT	
1500	79.4	2	BRIGHT WHITE-GREY UNIFORM DEPOSIT	
2000	76.3	1.5	BRIGHT WHITE-GREY UNIFORM DEPOSIT	

Table (35)

Characteristics of Electrodeposited Zn/Ni Alloys on a Steel Substrate at 15.3 A dm^{-2} and Various Rotation Speeds
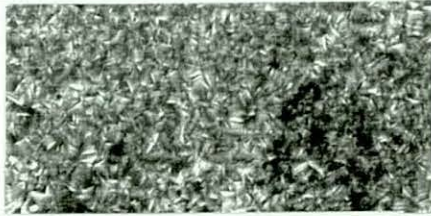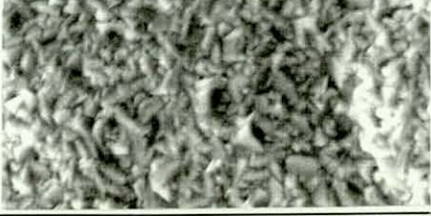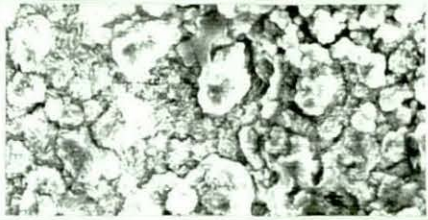
RPM	CATHODE CURRENT EFFICIENCY (%)	NICKEL CONTENT (%)	VISUAL APPEARANCE	SURFACE MORPHOLOGY
0	79.5	6.2	SEMI-BRIGHT WHITE-GREY UNIFORM DEPOSIT	
150	75.6	5	BRIGHT WHITE-GREY UNIFORM DEPOSIT	
350	74.5	4	BRIGHT WHITE-GREY UNIFORM DEPOSIT	
500	76.5	4.5	BRIGHT WHITE-GREY UNIFORM DEPOSIT	
1000	70.6	4	BRIGHT WHITE-GREY UNIFORM DEPOSIT	
1500	82.5	4.5	BRIGHT WHITE-GREY UNIFORM DEPOSIT	
2000	77.7	4.5	BRIGHT WHITE-GREY UNIFORM DEPOSIT	

Table (36)

Characteristics of Electrodeposited Zn/Ni Alloys on a Steel Substrate at 25.5 A dm^{-2} and Various Rotation Speeds
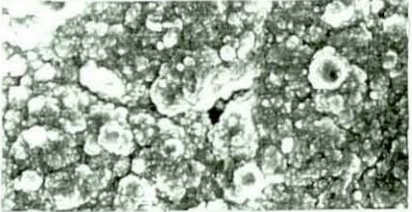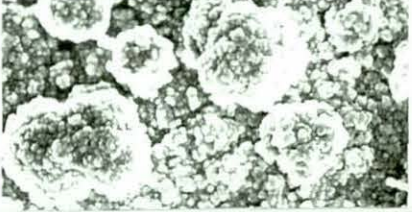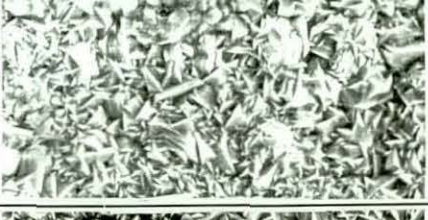
RPM	CATHODE CURRENT EFFICIENCY (%)	NICKEL CONTENT (%)	VISUAL APPEARANCE	SURFACE MORPHOLOGY
0	89.3	7	DARK GREY UNIFORM DEPOSIT / BURNED EDGES	
150	74.6	6.6	SEMI-BRIGHT DARK GREY UNIFORM DEPOSIT	
350	74.4	5	SEMI-BRIGHT WHITE-GREY UNIFORM DEPOSIT	
500	76.5	5	BRIGHT WHITE-GREY UNIFORM DEPOSIT	
1000	73.6	5.5	BRIGHT WHITE-GREY UNIFORM DEPOSIT	
1500	78.9	5.5	BRIGHT WHITE-GREY UNIFORM DEPOSIT	
2000	71.3	4.5	BRIGHT WHITE-GREY UNIFORM DEPOSIT	

Table (37)

Characteristics of Electrodeposited Zn/Ni Alloys on a Steel Substrate at 35.7 A dm^{-2} and Various Rotation Speeds

RPM	CATHODE CURRENT EFFICIENCY (%)	NICKEL CONTENT (%)	VISUAL APPEARANCE	SURFACE MORPHOLOGY
0	76.2	7.5	DULL DARK GREY DEPOSIT / BURNED EDGES	
150	66.4	5.8	BRIGHT WHITE-GREY UNIFORM DEPOSIT	
350	67.2	5	BRIGHT WHITE-GREY UNIFORM DEPOSIT	
500	69	6	SEMI-DULL GREY UNIFORM DEPOSIT	
1000	77.8	5	SEMI-BRIGHT WHITE-GREY UNIFORM DEPOSIT	
1500	70.4	5	BRIGHT WHITE-GREY UNIFORM DEPOSIT	
2000	73.4	5	SEMI-BRIGHT WHITE-GREY UNIFORM DEPOSIT	

Table (38)

Characteristics of Electrodeposited Zn/Ni Alloys on a Steel Substrate at 45.9 A dm^{-2} and Various Rotation Speeds
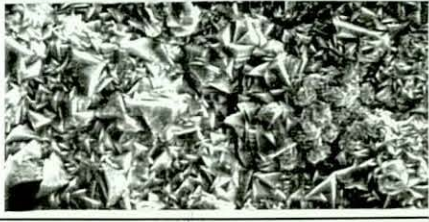
RPM	CATHODE CURRENT EFFICIENCY (%)	NICKEL CONTENT (%)	VISUAL APPEARANCE	SURFACE MORPHOLOGY
0	78.6	11.5	DULL WHITE -GREY UNIFORM DEPOSIT	
150	75.9	7.5	SPOTTED DARK GREY DEPOSIT/ BURNED EDGES	
350	66	6.5	SEMI-BRIGHT WHITE-GREY DEPOSIT	
500	66.7	5.5	SEMI-BRIGHT WHITE-GREY UNIFORM DEPOSIT	
1000	71.3	5	SEMI-BRIGHT WHITE-GREY UNIFORM DEPOSIT	
1500	68.5	5.5	SEMI-BRIGHT GREY UNIFORM DEPOSIT	
2000	68.5	5	SEMI-BRIGHT GREY UNIFORM DEPOSIT	

Table (39)

Characteristics of Electrodeposited Zn/Ni Alloys on a Steel Substrate at 56.1 A dm^{-2} and Various Rotation Speeds

RPM	CATHODE CURRENT EFFICIENCY (%)	NICKEL CONTENT (%)	VISUAL APPEARANCE	SURFACE MORPHOLOGY
0	74.3	11	MOTTLED DARK GREY DEPOSIT	
150	77	9.6	MOTTLED DARK GREY DEPOSIT	
350	65.4	5	DARK GREY DEPOSIT/ MOTTLED EDGES	
500	66	5.5	SEMI-BRIGHT WHITE- GREY UNIFORM DEPOSIT	
1000	64.2	5.5	DULL GREY UNIFORM DEPOSIT	
1500	68.8	5.5	DULL GREY UNIFORM DEPOSIT	
2000	65	4.5	SEMI-BRIGHT GREY UNIFORM DEPOSIT	

Table (40)

Characteristics of Electrodeposited Zn/Ni Alloys on a Steel Substrate at 66.3 A dm^{-2} and Various Rotation Speeds
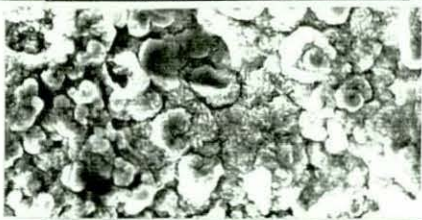
RPM	CATHODE CURRENT EFFICIENCY (%)	NICKEL CONTENT (%)	VISUAL APPEARANCE	SURFACE MORPHOLOGY
0	86.8	17	DARK GREY SPOTTED DEPOSIT	
150	83.9	13	SEMI-BRIGHT GREY SPOTTED DEPOSIT	
350	75.7	6.3	SEMI-BRIGHT GREY SPOTTED DEPOSIT	
500	68.2	6	DULL GREY UNIFORM DEPOSIT	
1000	67.9	6	SEMI-BRIGHT WHITE- GREY UNIFORM DEPOSIT	
1500	73.6	7	SEMI-BRIGHT WHITE-GREY UNIFORM DEPOSIT	
2000	67.8	4.5	SEMI-BRIGHT WHITE-GREY UNIFORM DEPOSIT	

Table (41)

Characteristics of Electrodeposited Zn/Ni Alloys on a Steel Substrate at 76.5 A dm^{-2} and Various Rotation Speeds

RPM	CATHODE CURRENT EFFICIENCY (%)	NICKEL CONTENT (%)	VISUAL APPEARANCE	SURFACE MORPHOLOGY
0	88.8	17.5	DARK GREY SPOTTED DEPOSIT / BURNED EDGES	
150	74.9	16	GREY SPOTTED DEPOSIT / BURNED EDGES	
350	67.9	10.7	GREY UNIFORM DEPOSIT	
500	73.6	6	SEMI-BRIGHT GREY UNIFORM DEPOSIT	
1000	68.9	5.5	SEMI-BRIGHT GREY UNIFORM DEPOSIT	
1500	72.6	6	GREY UNIFORM DEPOSIT	
2000	74	4.5	SEMI-BRIGHT GREY UNIFORM DEPOSIT	

Table (42)

Characteristics of Electrodeposited Zn/Ni Alloys on a Steel Substrate at 86.7 A dm^{-2} and Various Rotation Speeds

RPM	CATHODE CURRENT EFFICIENCY (%)	NICKEL CONTENT (%)	VISUAL APPEARANCE	SURFACE MORPHOLOGY
0	89.2	19	DULL DARK GREY DEPOSIT / BURNED EDGES	
150	76.4	12.8	DARK GREY DEPOSIT	
350	69.9	11	SEMI-BRIGHT GREY SPOTTED DEPOSIT	
500	70.7	7	SEMI-BRIGHT WHITE-GREY UNIFORM DEPOSIT	
1000	65.6	7	DULL GREY UNIFORM DEPOSIT	
1500	69.3	7	SEMI-BRIGHT GREY UNIFORM DEPOSIT	
2000	67.2	4	BRIGHT GREY UNIFORM DEPOSIT	

Table (43)

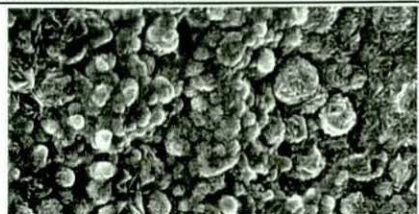## Characteristics of Electrodeposited Zn/Ni Alloys on a Steel Substrate at 96.9 A dm^{-2} and Various Rotation Speeds

RPM	CATHODE CURRENT EFFICIENCY (%)	NICKEL CONTENT (%)	VISUAL APPEARANCE	SURFACE MORPHOLOGY
0	91.7	19	DARK GREY SPOTTED DEPOSIT / BURNED EDGES	
150	77.4	15.6	DARK GREY SPOTTED DEPOSIT	
350	68.5	9.5	DARK GREY SPOTTED DEPOSIT	
500	67.6	8	GREY SPOTTED DEPOSIT	
1000	65.3	6.5	SEMI-BRIGHT WHITE-GREY UNIFORM DEPOSIT	
1500	66.9	5.5	SEMI-BRIGHT WHITE-GREY UNIFORM DEPOSIT	
2000	70.3	4	BRIGHT WHITE-GREY UNIFORM DEPOSIT	

Table (44)

Characteristics of Electrodeposited Zn/Ni Alloys on a Steel Substrate at 135.9 A dm^{-2} and Various Rotation Speeds

RPM	CATHODE CURRENT EFFICIENCY (%)	NICKEL CONTENT (%)	VISUAL APPEARANCE	SURFACE MORPHOLOGY
0	83	35.2	BURNED BLACK NON-UNIFORM DEPOSIT	
150	110	33.5	BURNED BLACK NON-UNIFORM DEPOSIT	
350	107	33.4	BURNED BLACK NON-UNIFORM DEPOSIT	
500	106	31.5	BURNED DARK GREY SPOTTED NON-UNIFORM DEPOSIT	
1000	86.6	15.3	SEMI-BRIGHT GREY UNIFORM DEPOSIT	
1500	74.5	5.8	SEMI-BRIGHT GREY UNIFORM DEPOSIT	
2000	78	4.5	BRIGHT WHITE-GREY UNIFORM DEPOSIT	

Table (45)

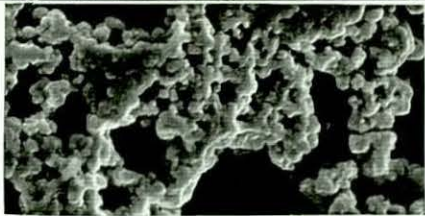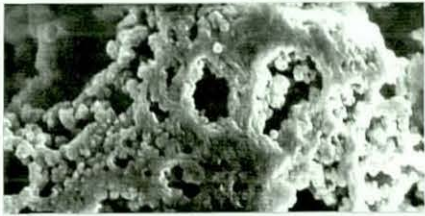**Characteristics of Electrodeposited Zn/Ni Alloys on a Steel Substrate at 152.9 A dm^{-2} and Various Rotation Speeds**
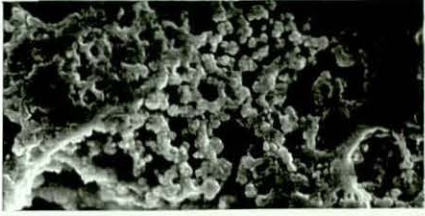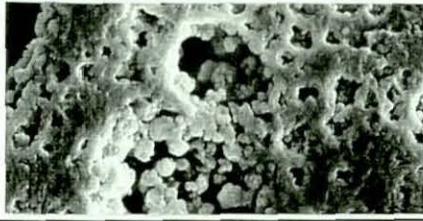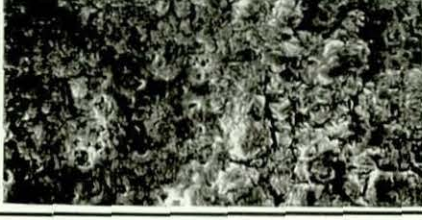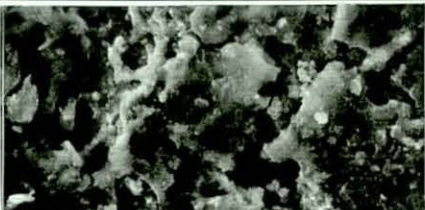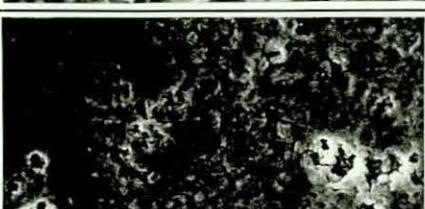
RPM	CATHODE CURRENT EFFICIENCY (%)	NICKEL CONTENT (%)	VISUAL APPEARANCE	SURFACE MORPHOLOGY
0	76	36.5	BURNED BLACK MOTTLED DEPOSIT	
150	115	33.3	BURNED BLACK MOTTLED DEPOSIT	
350	110.6	33.1	BURNED GREY MOTTLED DEPOSIT	
500	113	27.7	BURNED GREY MOTTLED DEPOSIT	
1000	98	15.9	SEMI-BRIGHT GREY STREAKY DEPOSIT	
1500	92.7	8.4	SEMI-BRIGHT GREY STREAKY UNIFORM DEPOSIT	
2000	98.5	7.5	SEMI-BRIGHT GREY UNIFORM DEPOSIT	

Table (46)

Characteristics of Electrodeposited Zn/Ni Alloys on a Steel Substrate at 169.9 A dm^{-2} and Various Rotation Speeds

RPM	CATHODE CURRENT EFFICIENCY (%)	NICKEL CONTENT (%)	VISUAL APPEARANCE	SURFACE MORPHOLOGY
0	11	29.3	DULL BLACK - GREY MOTTLED DEPOSIT	
150	22	29.5	DULL BLACK - GREY MOTTLED DEPOSIT	
350	71.3	31.7	BLACK - GREY MOTTLED DEPOSIT	
500	103	29.1	BLACK - GREY MOTTLED DEPOSIT	
1000	112	17	GREY DEPOSIT	
1500	111	11.9	SEMI-BRIGHT WHITE - GREY UNIFORM DEPOSIT	
2000	115	9.6	SEMI-BRIGHT WHITE - GREY UNIFORM DEPOSIT	

The Effect of Current Density on the Nickel Content of Zn-Ni Alloys at Different Rotation Speeds
Figure (76)
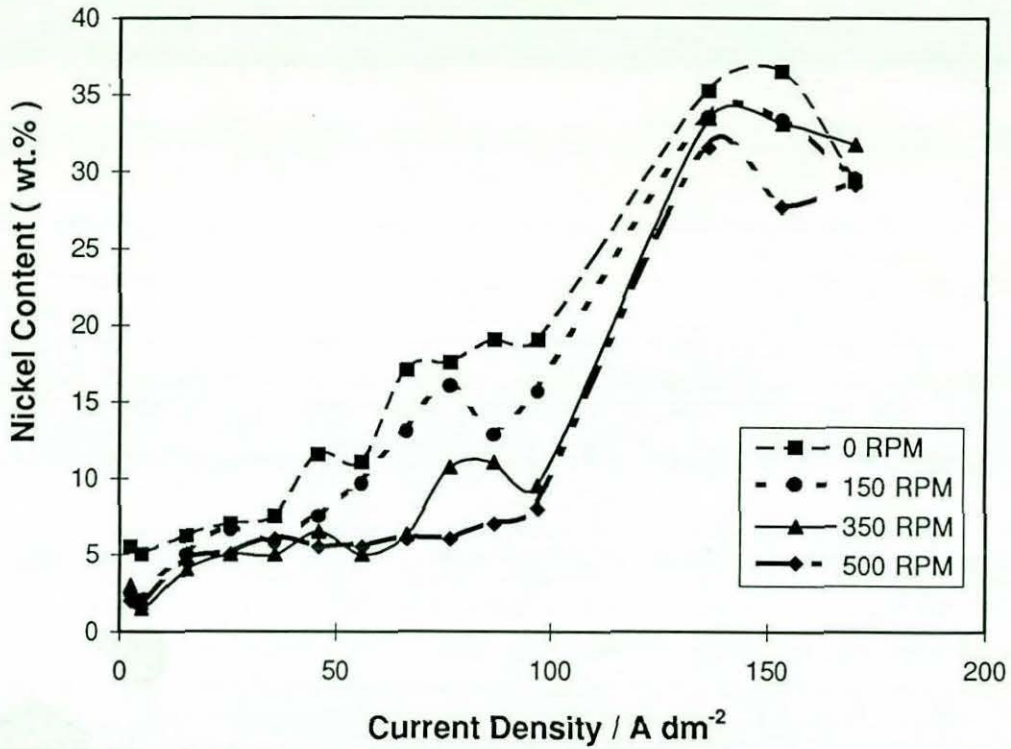
The Effect of Current Density on the Nickel Content of Zn-Ni Alloys at Different Rotation Speeds
Figure (77)
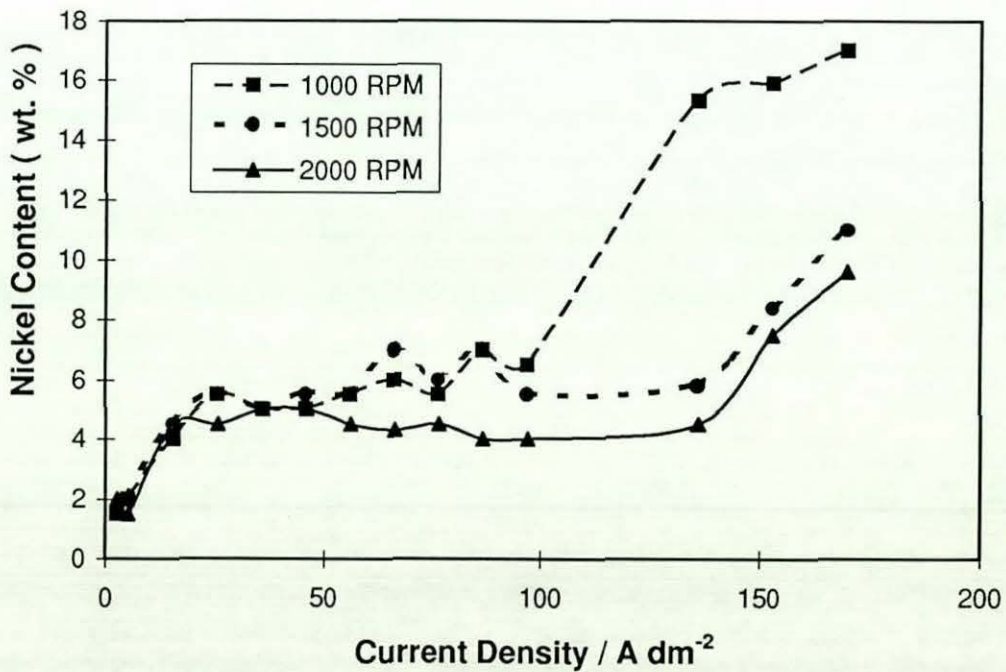
The Effect of Current Density on the Cathode
Current Efficiency of Zn-Ni Alloys
at Different Rotation Speeds
Figure (78)
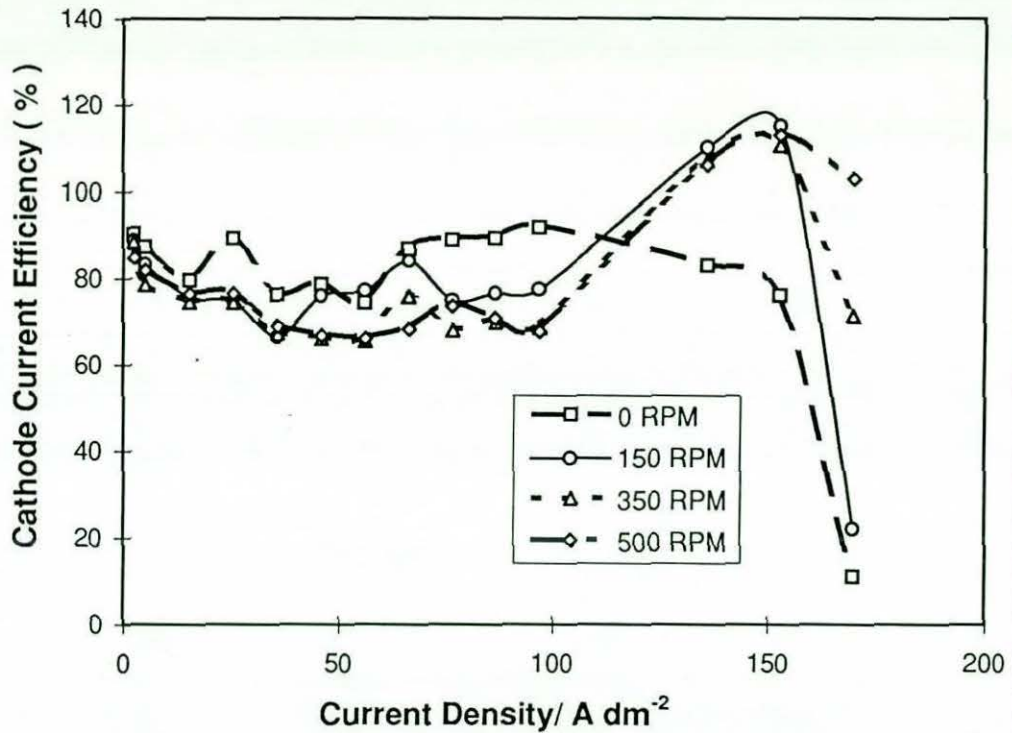
The Effect of Current Density on the Cathode
Current Efficiency of Zn-Ni Alloys
at Different Rotation Speeds
Figure (79)
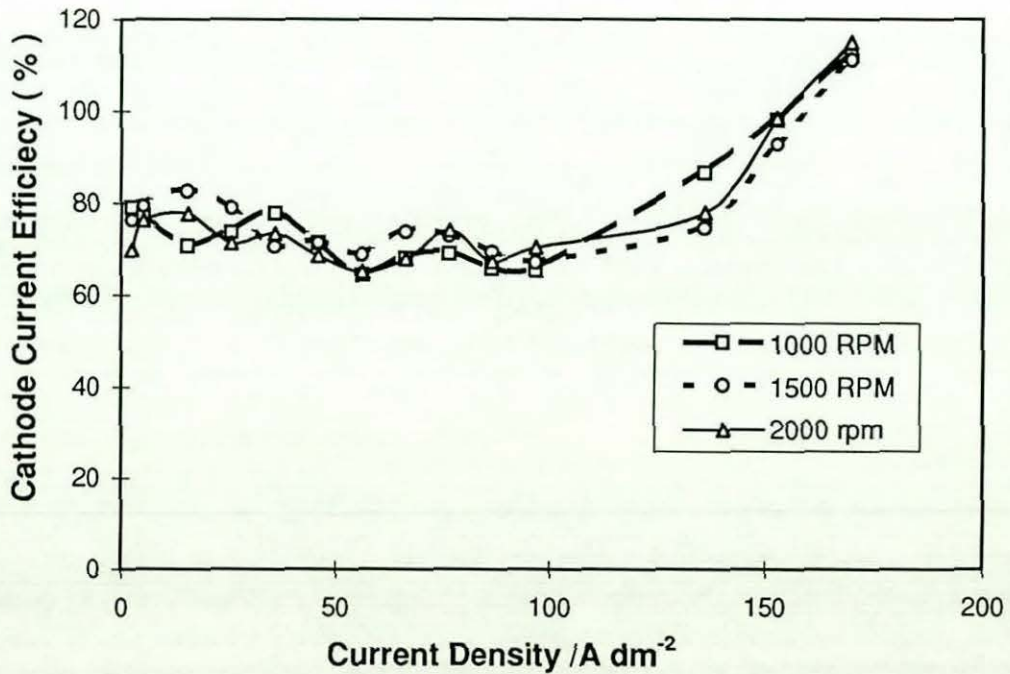
The Effect of Rotation Speed on The Nickel Content and Cathode Current Efficiency of Zn-Ni Alloys at 2.55 A dm⁻²
Figure (80)
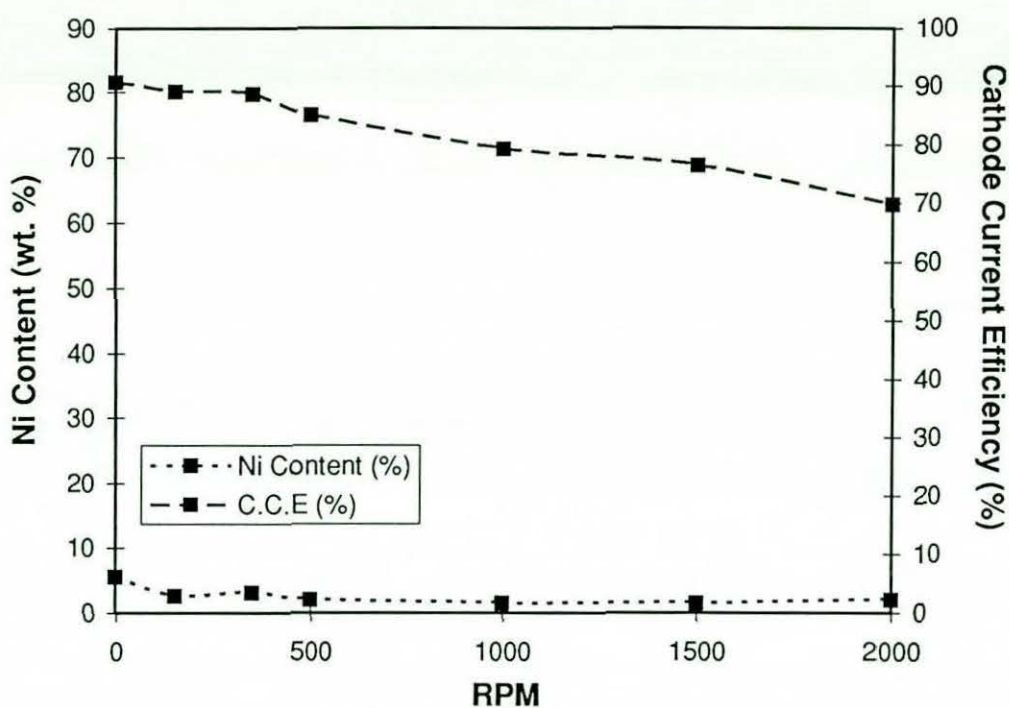
The Effect of Rotation Speed on The Nickel Content and Cathode Current Efficiency of Zn-Ni Alloys at 5.1 A dm⁻²
Figure (81)
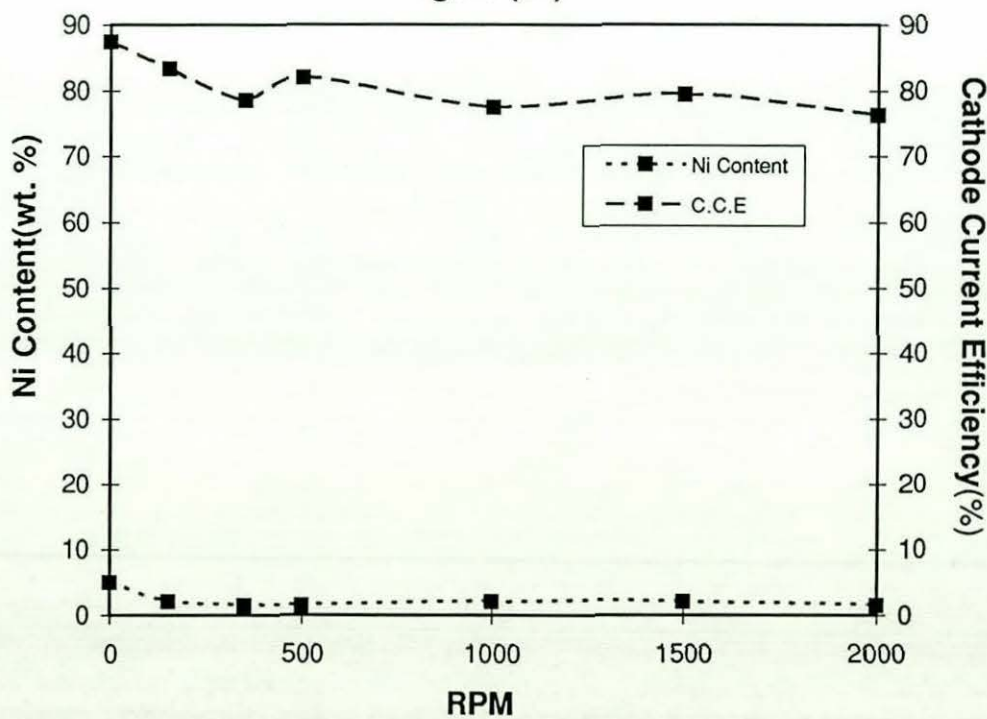
The Effect of Rotation Speed on The Nickel
Content and Cathode Current Efficiency of
Zn-Ni Alloys at 15.3 A dm^{-2}
Figure (82)
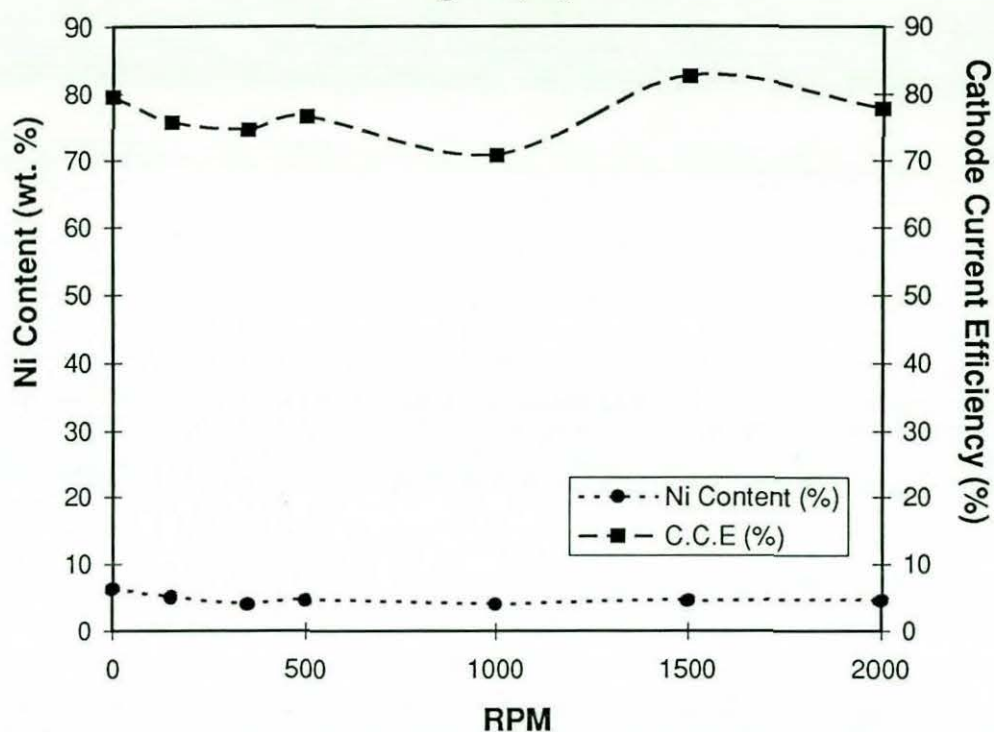
The Effect of Rotation Speed on The Nickel Content
and Cathode Current Efficiency of
Zn-Ni Alloys at 25.5 A dm^{-2}
Figure (83)
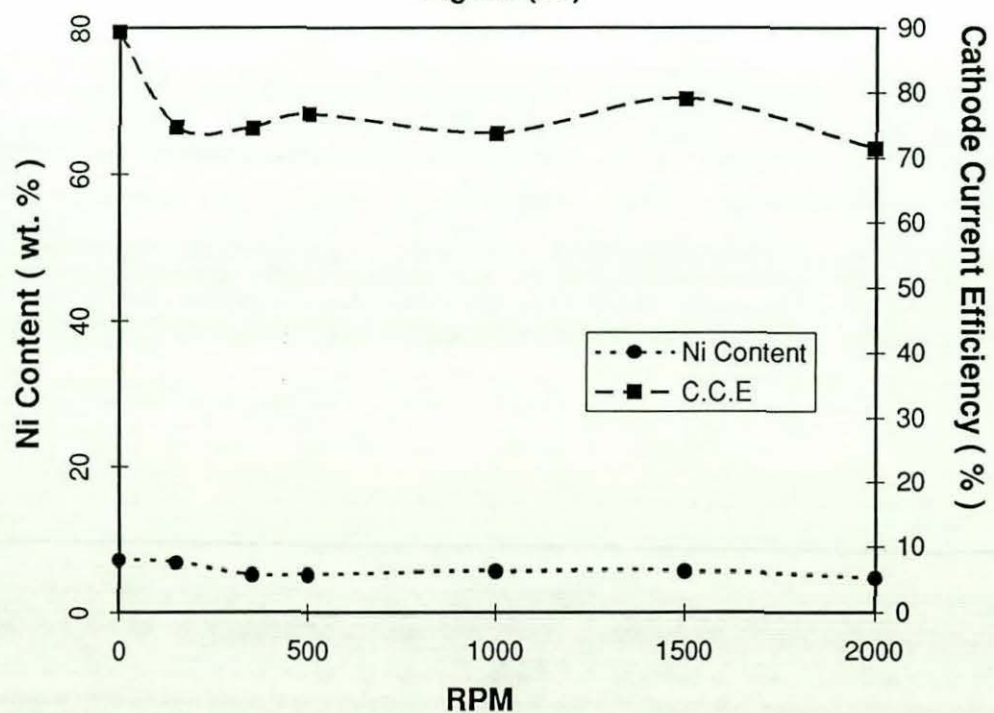
The Effect of Rotation Speed on The Nickel Content and Cathode Current Efficiency of Zn-Ni Alloys at 35.7 A dm^{-2}
Figure (84)
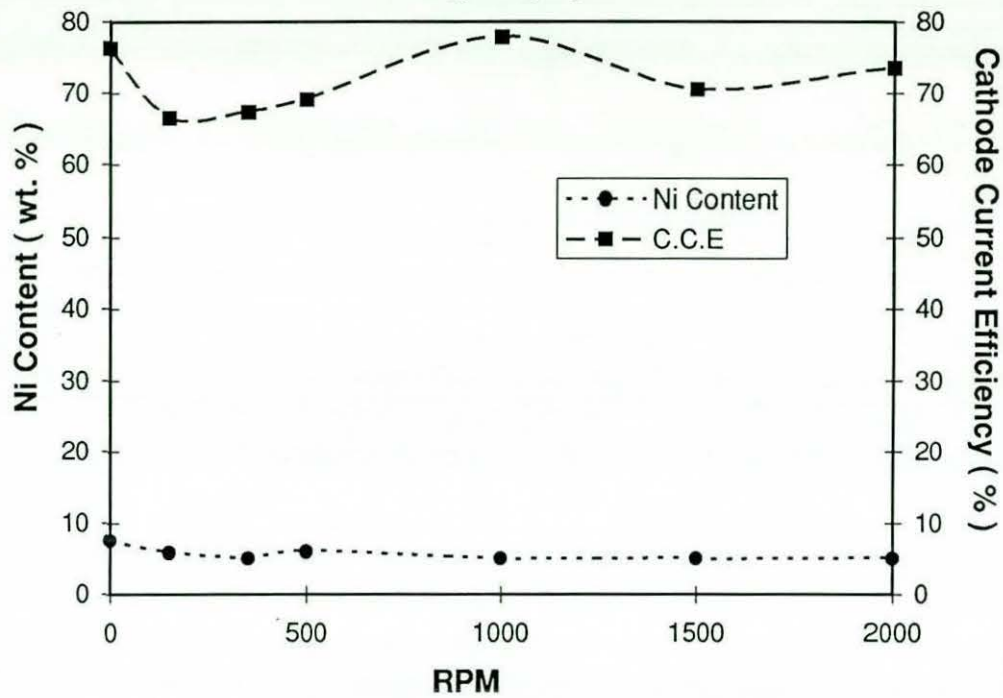
The Effect of Rotation Speed on The Nickel Content and Cathode Current Efficiency of Zn-Ni Alloys at 45.9 A dm^{-2}
Figure (85)
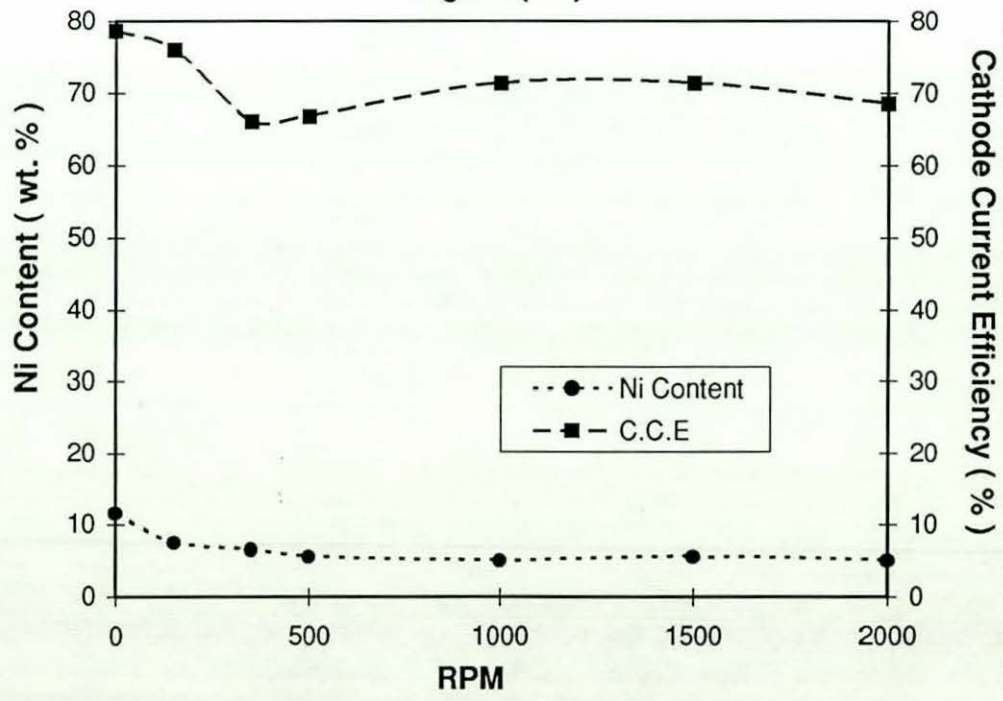
The Effect of Rotation Speed on The Nickel Content and Cathode Current Efficiency of Zn-Ni Alloys at 56.1 A dm^{-2}
Figure (86)
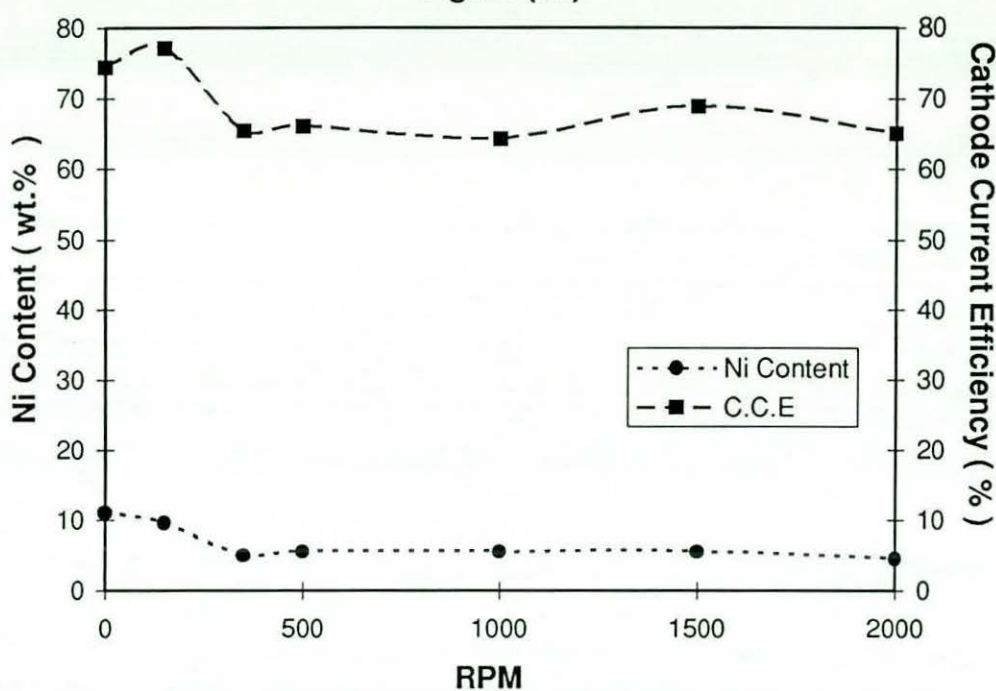
The Effect of Rotation Speed on The Nickel Content and Cathode Current Efficiency of Zn-Ni Alloys at 66.3 A dm^{-2}
Figure (87)
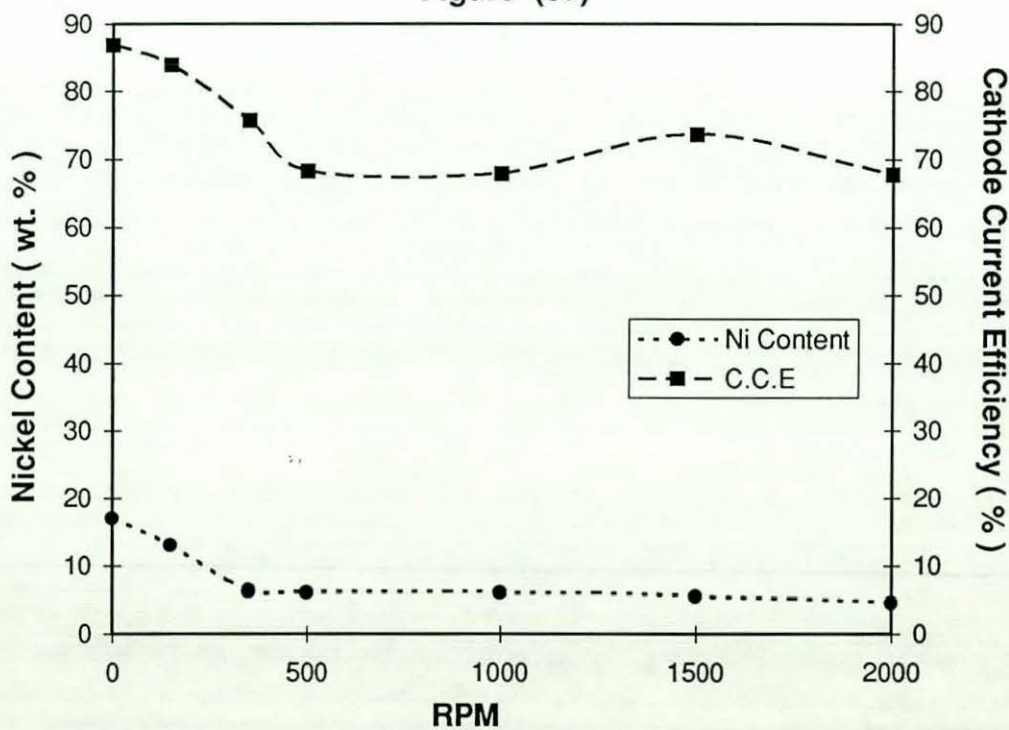
The Effect of Rotation Speed on The Nickel Content
and Cathode Current Efficiency
of Zn-Ni Alloys at 76.5 A dm^{-2}
Figure (88)
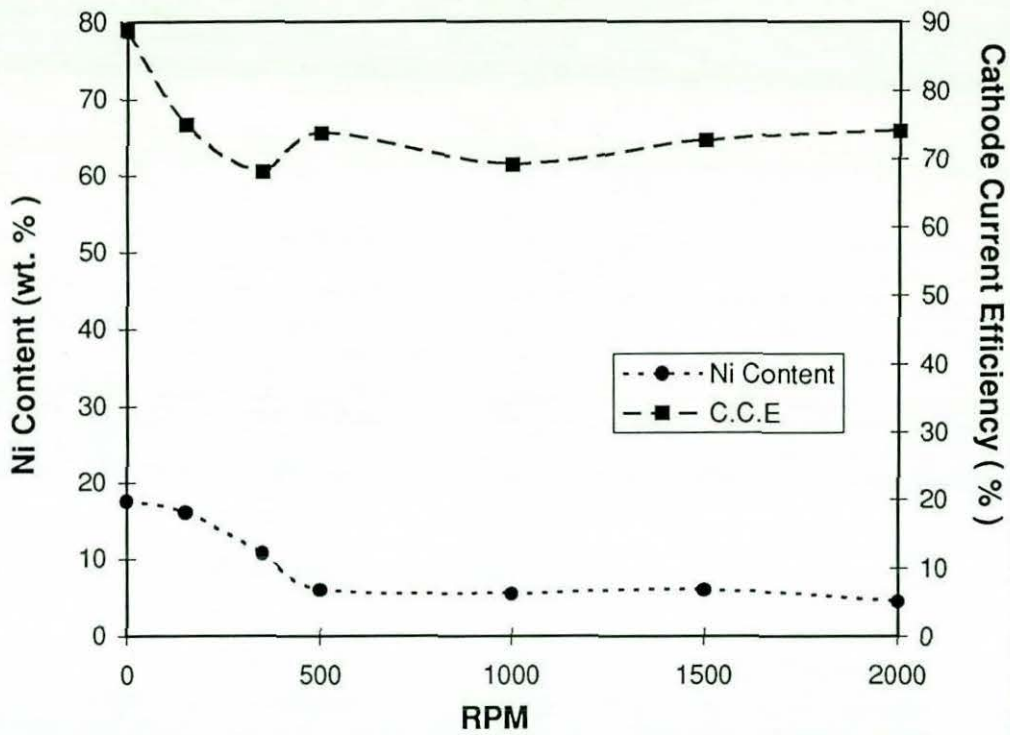
The Effect of Rotation Speed on The Nickel Content
and Cathode Current Efficiency
of Zn-Ni Alloys at 86.7 A dm^{-2}
Figure (89)
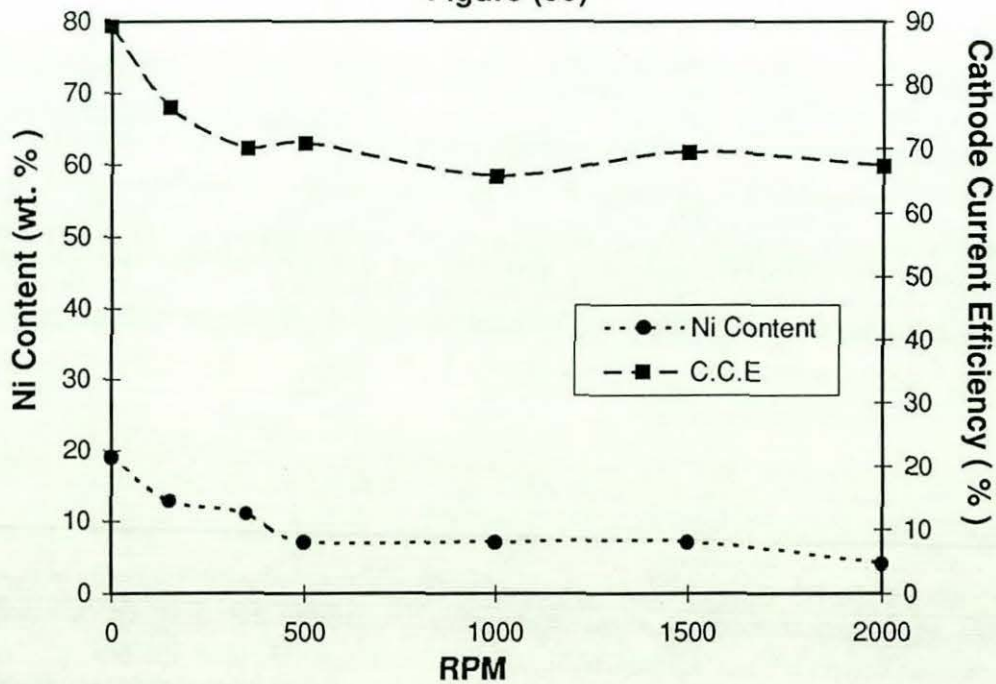
The Effect of Rotation Speed on The Nickel Content and Cathode Current Efficiency of Zn-Ni Alloys at 96.9 A dm⁻² — Figure (90)
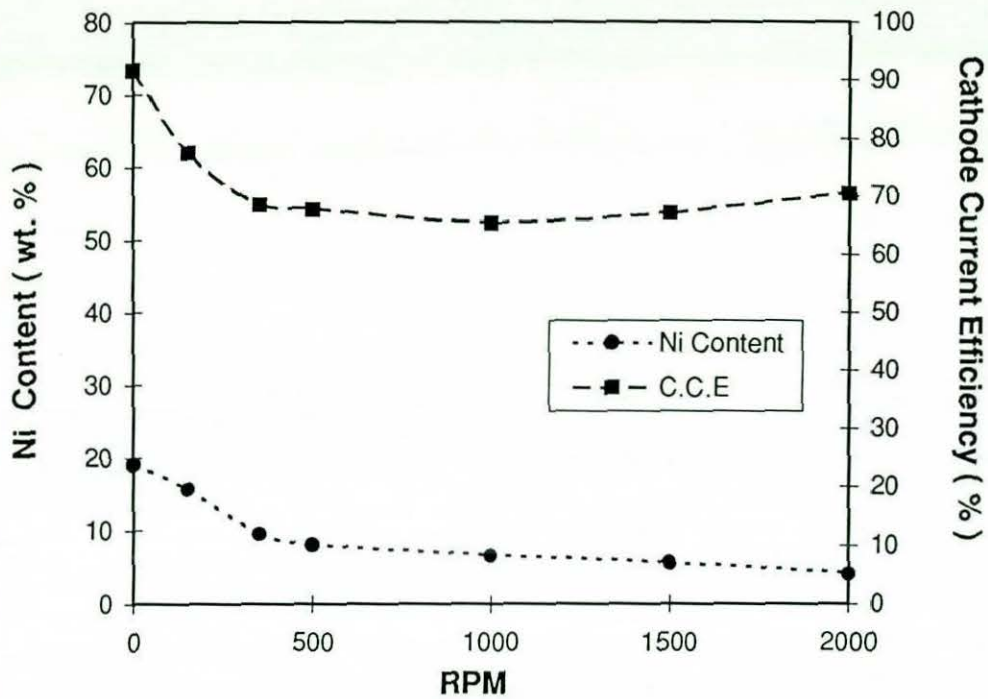
The Effect of Rotation Speed on The Nickel Contentand Cathode Current Efficiency of Zn-Ni at 135.9 A dm⁻² — Figure (91)
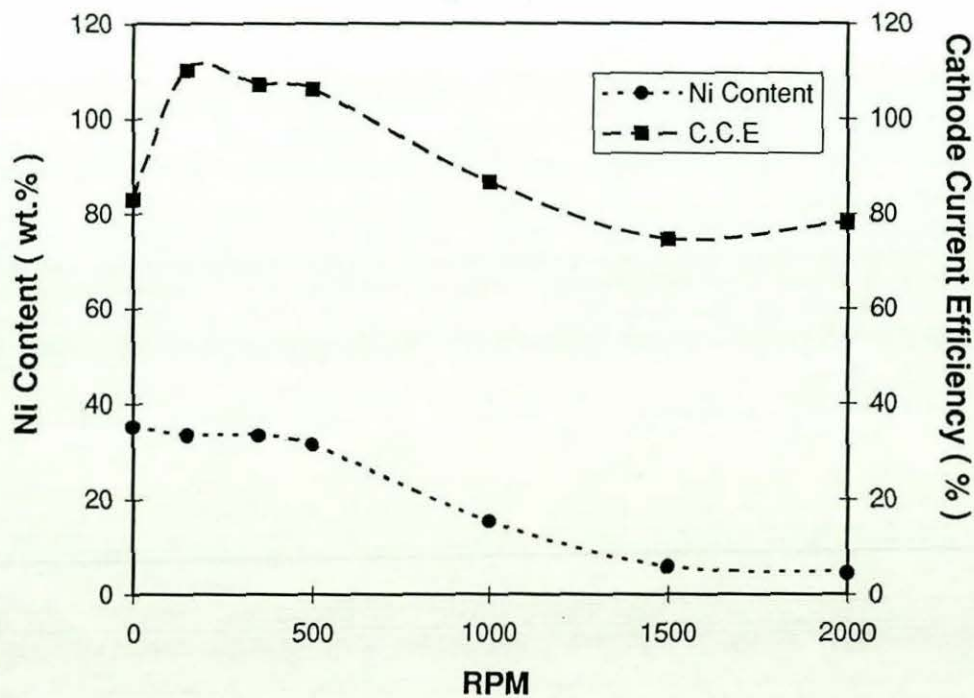
The Effect of Rotation Speed on The Nickel Content
and Cathode Current Efficiency
of Zn-Ni Alloys at 152.9 A dm^{-2}
Figure (92)
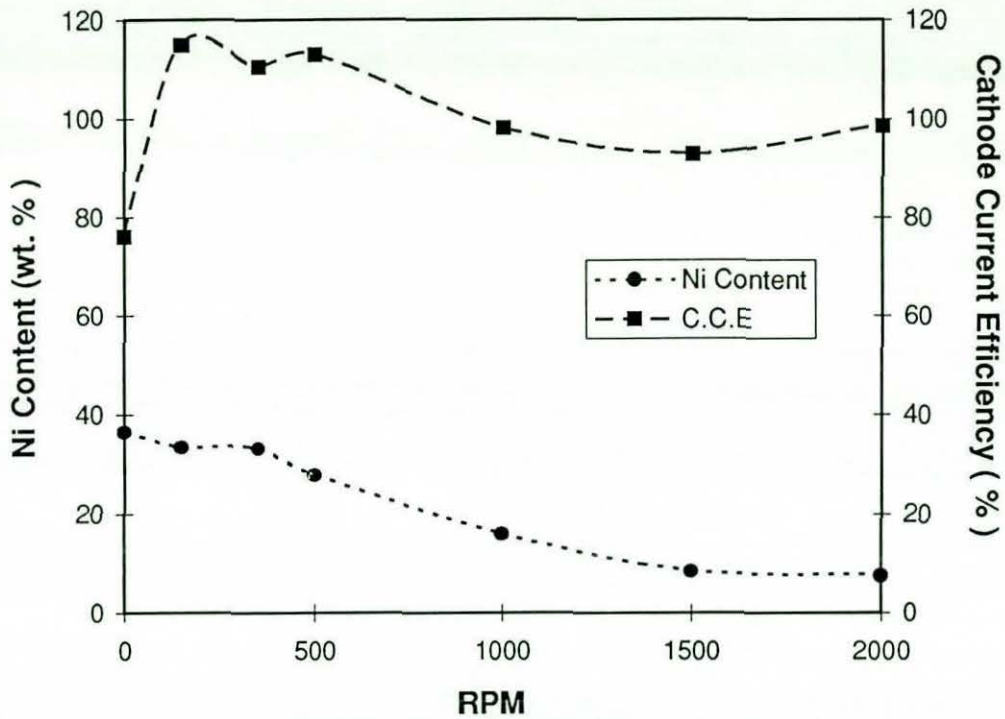
The Effect of Rotation Speed on The Nickel Content
and Cathode Current Efficiency
of Zn-Ni Alloys at 169.9 A dm^{-2}
Figure (93)
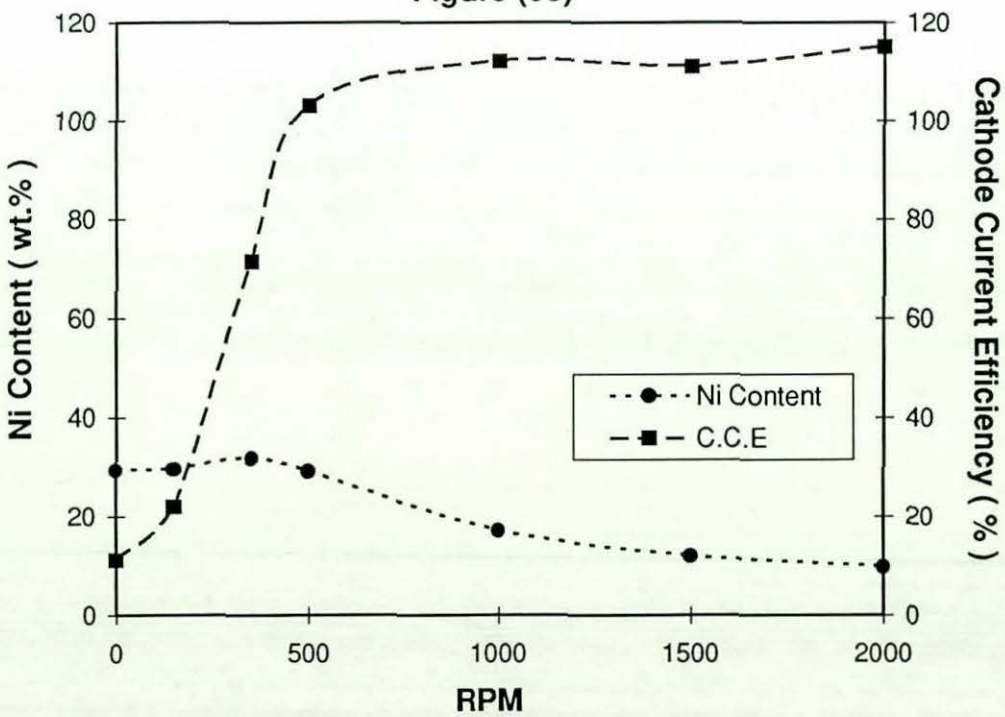
content. With further increase in current density, the nickel content increases. This is probably due to the fact that the nickel electrodeposits under charge transfer control.

6- The decrease in thickness of the cathode diffusion layer due to rotation of the cathode reduces the size of the diffusion layer and also brings the metal ratio of the bulk solution closer to the cathode surface. This favours an increased rate of deposition of zinc which is already depositing preferentially. This is due to the fact that the zinc has mass transfer control properties.

4-2-2-2-1-2 Effect on cathode current efficiency

The effect of current density on the cathode current efficiency in the Zn-Ni alloy electrodeposits at different rotation speeds was studied. From tables (33) to (46) and figures (76) to (93) it can be found that at static conditions, in the current density range of 2.55 A/dm^2 to 56.1 A/dm^2, the cathode current efficiency dropped from 90% to about 75%, and then increased to 86% with a further increase in current density to 66.3 A/dm^2. At current densities higher than 66.3 A/dm^2, the cathode current efficiency increased to 92% (at a current density of 96.9 A/dm^2) and then dropped at higher current densities of 135.9A/dm^2, 152.9 A/dm^2 and 169.9 A/dm^2 to 83%, 76% and 11% respectively.

By rotating the cylindrical cathode from 150 rpm to 2000 rpm, the cathode current efficiency was found to fluctuate. However, as a general trend, in the range of current densities of 2.55A/dm^2 to 96.9 A/dm^2, the cathode current efficiency decreased with an increase in rotation speed to a maximum value of 65%. At higher current densities of 135.9 A/dm^2 and 152.9 A/dm^2, the cathode current efficiency was increased to a maximum value of 115% at 150 rpm and then dropped to a value of 78% and 98% respectively at 2000 rpm. At current densities higher than 152.9 A/dm^2, the cathode current efficiency was increased significantly from 11% to 71.3% at 350 rpm. Another significant increase in cathode current efficiency was observed at 500 rpm from 71.3% to 103%. At higher rotation speeds of 1000 to 2000 rpm, the cathode current efficiency was increased to 111% and 115% respectively.

One main reason which could cause a fall in cathode current efficiency is hydrogen evolution. When the amount of hydrogen evolution increased less current will be used for metallic electrodeposition. It can be seen there is an increase in cathode current

efficiency as rotation speeds decrease. This is because of the depolarisation of the hydrogen evolution reaction occurs as rotation speed increased during electrodeposition. It was also observed that hydrogen evolution (gas bubbling was seen) increased with a further increasing of rotation speed, this results in more hydrogen evolving and a decrease in cathode current efficiency with faster rotation speed.

Generally, it was observed that the cathode current efficiencies were reduced at currents employed higher than 5.1 A/dm^2. The cathode current efficiencies were then increased with increase in nickel content. This increase in cathode current efficiency with respect to nickel content could be suggest that there was a change in cathode current efficiency of deposition of each metal or to experimental error.

4-2-2-2-1-3 Effect on visual appearance

The visual appearance of Zn-Ni alloy electrodeposits was affected by both current density and electrode rotation speed { tables (33) to (46)}. At a current density of 2.55 A/dm^2, the deposit was dull grey in the cathode rotation speed range of 0 to 500 rpm. However, as the speed increased from 1000 to 2000 rpm, the deposit was semi-bright to bright respectively. At higher current densities of 5.1 to 15.3 A/dm^2, the deposit was semi-bright white grey at the static condition, as the cathode rotation speed increased from 150 to 2000 rpm, the deposit was seem to become bright white grey.

At current densities higher than 15.3 A/dm^2 in the range of 25.5 to 96.9 A/dm^2, the deposit was dark grey in general at the static condition, as the cathode rotation speed increased from 150 to 500 rpm and from 1000 to 2000, the deposits were varied from semi-bright dark grey to semi-bright white grey and from bright dark grey to bright white grey. With further increase in current density to 135.9, 152.9, and 169.9 A/dm^2, the deposit was burnt and black over a wide range of rotation speeds (0 to 500 rpm) and then turned to be semi-bright to bright white grey at higher rotation speeds of 1000 to 2000 rpm. As a general trend, it could be said that in the range of 2.55 to 96.9 A/dm^2, at lower rotation speeds, the deposits were coarse and dark grey. Whilst, at higher rotation speeds, the deposit was smooth semi-bright white grey. At higher current densities, the deposit seem to be powdery and burned at low rotation speeds, and smooth semi-bright to bright at high rotation speeds.

It was observed that at high current densities with low rotation speeds, the deposit became powdery, this could be due to that, as the current density increased, the pH at the cathode surface rises due to the increased rate of hydrogen evolution which results in zinc hydroxide formation and subsequent adsorption on the cathode. This caused the deposit is become powdery and fall away from the cathode. This also contributed to the decrease in the cathode current efficiency for alloy deposition.

It was also observed that by changing cathode rotation speed, it was possible to control smoothness and uniformity of the deposit and also directly affect the brightness of the deposit.

4-2-2-2-1-4 Effect on surface morphology

The surface morphology of Zn-Ni alloy deposited samples are shown in tables (33) to (46). Both current density and cathode rotation speed have a controlling factor on surface morphology of Zn-Ni alloy electrodeposits. At a current density of 2.55 A/dm^2, the structure was found to be acicular with a little evidence of nucleation of granular crystals, as the rotation speed increased from 0 to 2000, the morphology of the deposits became predominantly acicular ranging from fine to coarse crystals.

At a current density of 5.1 A/dm^2, the morphology of the deposits appeared to be coarse acicular crystals at the static condition, at 150 rpm the structure was very fine clustered crystals with interlocking porosity. At higher cathode rotation speeds of 350 to 2000 rpm, the structure was nodular with crystals ranging from fine to coarse.

At a current density of 15.3 A/dm^2, the structure had acicular crystals ranging from coarse 3-D acicular crystals at 0 and 500 rpm, fine acicular crystals at 150, 350 and 1000 rpm, and at 1500, 2000 rpm, 3-D acicular crystals shapes with a nucleation of nodular crystals beginning to occur.

At a current density of 25.5 A/dm^2, the structures ranged from fine nodular crystals at 0 rpm, cauliflower-like structures at 150, 350 and 500 rpm (with bigger crystals at 500 rpm), fine nodular crystals at 1000 rpm, and coarse nodular crystals at 1500 and 2000 rpm.

At 35.7 A/dm^2, the structure ranged from a nucleation of acicular crystals on the 3-D nodular crystals at 0 rpm, large 3-D nodular crystals at 150 rpm with a nucleation of acicular crystals on them and also interlocking porosity, acicular crystals with a little

difference in size at 350 and 500 rpm, a nucleation of 3-D acicular crystals over large 3-D nodular crystal at 1000 rpm, a slight nucleation of nodular crystals over a coarse 3-D acicular crystals at 1500 and 2000 rpm.

At a current density of 45.9 A/dm^2, the structure ranges from cauliflower- like crystals at 0 and 150 rpm, nucleation of acicular crystals over big nodular crystals at 350 rpm, a mixture of fine and coarse acicular crystals at 500, 1000 and 1500 rpm, and acicular crystals with a slight nucleation of nodular crystals at 2000 rpm.

At a current density of 56.1 A/dm^2, the structure varied from a mixture of large and small nodular crystals at 0 rpm, a nucleation of acicular crystals over nodular crystals at 150 rpm, acicular crystals with 3-D nodular crystals at 350 rpm, acicular crystals at 500 and 1000 rpm, coarse acicular crystals at 1500 rpm and a mixture of a coarse and fine acicular crystals at 2000 rpm.

At 66.3 A/dm^2, the structures varied from cauliflower-like crystals at 0 rpm, coarse nodular crystals at 150 rpm, a mixture of nodular and fine acicular crystals at 350 rpm, fine acicular crystals with a slight nucleation of nodular crystals at 500 rpm, a mixture of fine and coarse acicular crystals at 1000 rpm, nucleation of nodular crystals covered with a coarse acicular crystals at 1500 rpm, and large coarse acicular crystals at 2000 rpm.

At a current density of 76.5, the structure was varied from nodular crystals at 0,150 and 350 rpm, a mixture of acicular and nodular crystals at 500 rpm, acicular crystals with a slight nucleation of nodular crystal covered with acicular crystals at 1000 rpm, coarse acicular crystals at 1500 and 2000 rpm.

At 86.7 A/dm^2, the structures varied from cauliflower-like crystals at 0, 150 and 350 rpm, a mixture of nodular and acicular crystals at 500 and 1000 rpm, large nodular crystals covered with acicular crystals at 1500 rpm, and coarse acicular crystals at 2000 rpm.

At a current density of 96.9 A/dm^2, the structures varied from cauliflower-like crystals at 0, 150 and 350 rpm, a mixture of nodular and acicular crystals at 500 and 1000 rpm, and coarse acicular crystals at 1500 and 2000 rpm.

At 135.9 A/dm^2, the structures varied from sponge-like growth at 0, 150, 350 and 500 rpm, nodular crystals with interlocking porosity at 1000 rpm and fine nodular crystals at 1500 and 2000 rpm.

At a current density of 152.9 A/dm^2, the structure varied from a broken burned structures at 0 rpm, sponge-like growth at 150 and 350 rpm, finer sponge-like growth at 500 rpm and nodular crystals at 1000, 1500 and 2000 rpm.

At a current density of 169.9 A/dm^2, the structures varied from a broken burned structure at 0, 150, 350 and 500 rpm, a fine nodular crystals at 1000 rpm, fine nodular and acicular crystals at 1500 and a smaller but finer morphology at 2000 rpm.

As a general trend it appeared that the microstructure of Zn-Ni electrodeposits was affected to a great extent by the nickel content in the deposit and the rotation speed, the nodular crystal morphology accompanied a high nickel content ($\geq$10%) whilst acicular crystals accompanied a low nickel content ($\leq$ 4%), whilst, a mixture of nodular and acicular crystals structure with medium nickel content values between 4< Ni % <10.

4-2-2-2-2 Corrosion studies

A series of Zn-Ni single layer alloy coatings with a nominal thickness of 8 microns and having a range of 2 to 17% nickel were tested in order to study the corrosion performance and behaviour of these coatings.

The corrosion performance of these coatings were examined using a neutral salt spray test. Whilst the corrosion behaviour was assessed using two methods, method (1) measured the linear polarisation resistance of the coatings and hence the corrosion currents. Method (2) measured the Tafel slopes to determine the corrosion currents of the coatings.

4-2-2-2-2-1 Neutral salt spray studies

The results of the corrosion performance of Zn- 2 to 17% Ni alloy coatings in a neutral salt spray chamber are presented in table (47) which shows the corrosion performances of these coatings in terms of hours to red rust and also in terms

Table (47). Corrosion Data for Different Types of Zn/Ni Alloy Coatings

	C.C.D A dm^{-2}	RPM	LPR Ω cm^2	I_{corr} mA cm^{-2} (LPR)	E_{corr} mV cm^{-2}	I_{corr} mA cm^{-2} (Tafel)	Hours to red rust*	% Red Rust after 300 Hours
Zn-2%Ni	5.1	1500	184.8	0.865×10^{-1}	-950	0.98×10^{-1}	192	80
Zn-3%Ni	2.55	500	399	0.48×10^{-1}	-1145	1.97×10^{-1}	196	80
Zn-4%Ni	15.3	1000	422.4	0.77×10^{-1}	-1070	4.66×10^{-1}	216	90
Zn-5%Ni	35.7	1000	649.4	0.28×10^{-1}	-1120	1.69×10^{-1}	196	85
Zn-6%Ni	66.3	500	207	1.37×10^{-1}	-1100	0.796×10^{-1}	216	60
Zn- 8%Ni	96.6	500	603	0.436×10^{-1}	-1060	3.17×10^{-1}	196	50
Zn-10%Ni	76.5	350	673	0.437×10^{-1}	-1070	0.316×10^{-1}	240	25
Zn-11%Ni	56.1	0	366.5	0.38×10^{-1}	-1070	0.9×10^{-2}	264	25
Zn-12%Ni	45.9	0	710	1.3×10^{-2}	-1105	0.9×10^{-2}	269	25
Zn-13%Ni	86.7	150	296.4	3.8×10^{-2}	-1020	1.3×10^{-2}	240	15
Zn-14%Ni	86.7	1500	484.4	2.49×10^{-2}	-1090	0.73×10^{-2}	288	5
Zn-16%Ni	76.5	150	153.5	1.7×10^{-1}	-1110	1.63×10^{-2}	240	15
Zn-17%Ni	66.3	0	227	1.14×10^{-1}	-1080	1.63×10^{-2}	240	30

* First appearance of red rust

of a red rust percentage on the coatings after 300 hours test. The amount of red rust was judged by naked eye.

It is clear from these results that single layer Zn-Ni alloy coatings with 10-17% nickel content have a relatively higher corrosion resistance than the others. This observation appears to be, to some extent, in a good agreement with reported literature's on zinc-nickel alloys which showed that the best corrosion property is achieved with alloys containing 10-14% of nickel in the coating (21) where the coating is relatively less active than alloys having less than 10% nickel in the deposit and hence tends to have a lower dissolution reaction of zinc and then a lower corrosion rate of the coating.

The results showed that an alloy containing 16-17 % nickel also has a good corrosion performance and this increase of nickel content did not appear to affect the sacrificial nature of the coating. This could be due to the morphology of the coating and also due to other physical properties such as adhesion and the stress properties (such as cracking) which will affect the corrosion performance of the coating.

It was observed that the voluminous white corrosion products, which have been reported by Baldwin et al (92) to be mainly a form of a stable film of zinc hydroxy chloride ($Zn_5(OH)_8Cl_2H_2O$) and a trace of zinc oxide, tend to build up more slowly than with zinc deposits and appeared after about 15 hours. Whilst, in the case of a zinc deposit the white products tended to build up after only 3 hours.

Table (47) also presents the corrosion performance of these coatings after 300 hours, the results indicate that Zn-4%Ni deteriorates faster than Zn-Ni alloys containing 2,3 and 5% nickel. This observation could be due to one or more of the following factors:

1- Surface morphology of the coating adjacent to substrate surface.

2- Thickness of corrosion product film.

3- Dezincification phenomenon on the coating surfaces.

The deterioration of the coated substrates seem to be significantly slower for the Zn-Ni alloy coating containing 10-16 % nickel and the best of them all is the Zn-14%Ni alloy coating which has 5% red rust after 300 hours, which also showed the best corrosion performance of 288 hours to red rust.

4-2-2-2-2-2 Electrochemical corrosion measurements

Table (47) and figures (94) to (96) illustrate the corrosion current and potential data obtained from linear polarisation resistance measurements and Tafel slopes and the cathodic and anodic behaviour of the single layer coated samples.

The corrosion potential for various types of alloy coated samples (table (47)) did not reflect the amount of nickel content in the coatings and they seem to have almost the same corrosion potential. The possible reason for this observation is the possibility of forming some sort of air formed oxide on the surface during the storage period prior to the testing of the samples.

1- Linear polarisation resistance measurements

Linear polarisation results showed a non linear relationship between corrosion current and nickel content in the zinc-nickel alloy coated samples (figure (94)). The fluctuation of corrosion current values versus nickel content could be attributed to the fact that linear polarisation resistance measurements, at potential intervals of ± 20 mV either side of the zero current potential, will give only an indication of the behaviour of an outer alloy coatings surface. Though, only a very thin oxide film on the surface could affect the measurement and hence could give peculiar results. Despite that figures (94) and (95) indicate that Zn-Ni alloy coatings containing 10-14% nickel have almost the lowest corrosion currents and hence probably the best overall corrosion performance.

2- Potentiodynamic polarisation behaviour and Tafel slope measurements (Figures (97-110))

The potentiodynamic behaviour of Zn-2-17%Ni alloy coatings was studied by sweeping the potential in a range of -250 to +250 mV either side of the zero current potential. The cathodic polarisation curves for Zn-Ni alloy coatings containing 2,9,10, 12,13,16 and 17% nickel showed that these coatings have similar cathodic behaviour. When the applied potential increases from E_{corr} to higher negative values, an increase in current density takes place which is an indication of the reactivity of the surface to the predominant cathodic reaction (hydrogen evolution). Further increase in potential, results in a sluggish increase in current density which indicates that the evolution of hydrogen at the coated surface slowed down. Zn-Ni alloy coatings containing 3, 4, 5 and 6% nickel also have two regions, a sharp increase of current density accompanying

Figure (94)
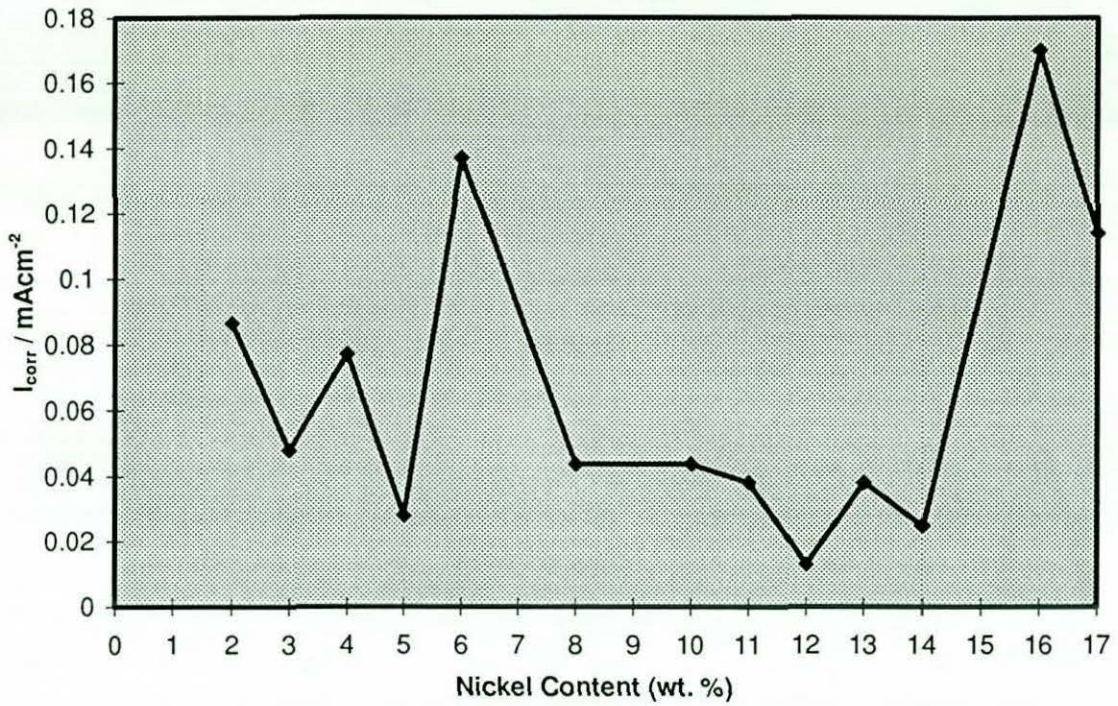**Effect of Nickel Content in the Zn-Ni Alloy Coatings on the Corrosion Current values**

Figure (95)
Linear Polarisation Resistance for Different Types of Zn-Ni Alloy Coatings
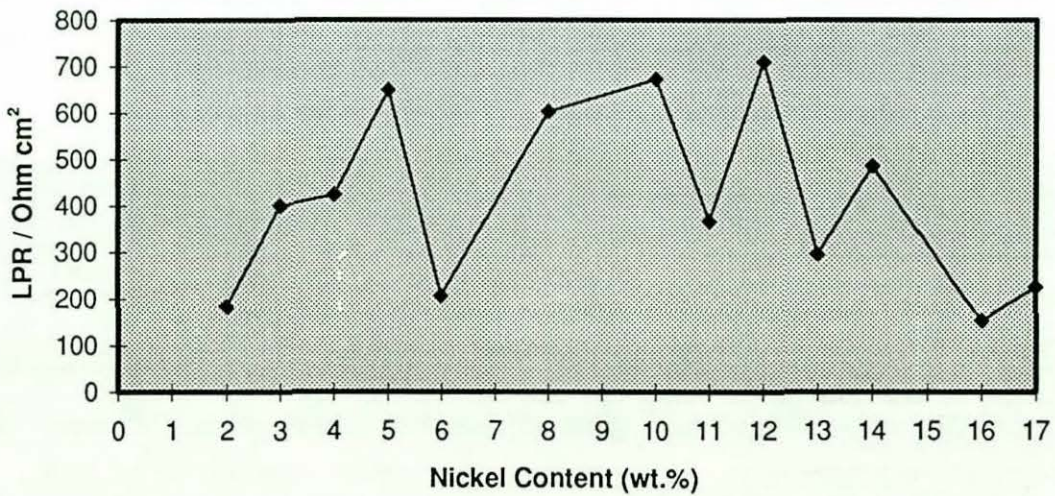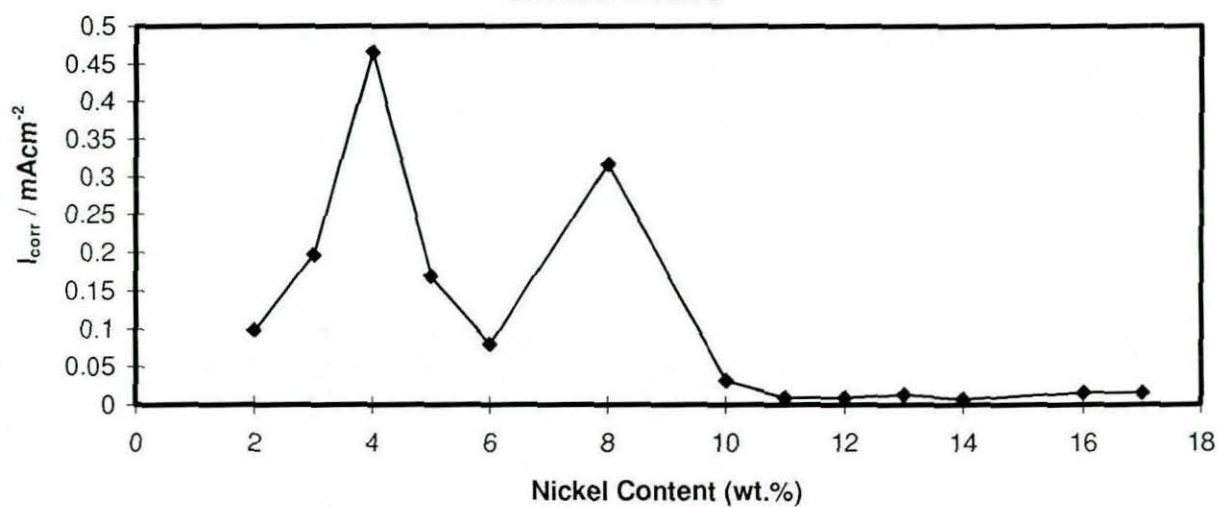
Figure (96)
Effect of Nickel Content in Zn-Ni Alloy Coating on the Corrosion Current values

a small increase in potential (negative). Further increase in potential resulted in a limiting current density region. Zn-Ni alloy coatings containing 8 and 14% nickel have a very small region which consists of a sharp increase of current density as the potential increase followed by a limiting current density region.

As a general rule, the point in terms of current density at which the gradient of the cathodic polarisation curve changes is an indication of the beginning of the reactivity of the surface to the predominant cathodic reaction (hydrogen evolution).

Anodic polarisation behaviour of Zn- 2-17% Ni alloy coatings were also studied. The anodic polarisation curves for Zn-Ni alloys containing 3, 4, 6, 7, 8 and 11 % nickel seem to have the same " S " shape. This interesting trend occurred for the behaviour of Zn-Ni alloys containing 9, 12, 13, 16 and 17 % nickel. Four regions can be identified. The first two regions are relatively small and consist of a very small rapid increase in current density accompanying a slight increase in potential. Further increase in potential produces a small limiting current region. These two regions seem to be as a result of an active cathodic behaviour. It is believed that an active cathodic behaviour associated with the formation of some sort of hydroxides might be responsible for this type of behaviour. The second two regions seem to have a repeated " S " shape with the exception that the limiting current periods seem to have different curve gradients.

The anodic behaviour of the Zn-Ni alloy containing 10% nickel seems to have a slightly different limiting current region which exhibits an actual reduction in current levels. This could be as a result of forming a more effective passive film than the other coating types.

As a general rule, the E / I curves indicate that when the applied potential increases above zero current, an accompanying sharp increase in current was observed. The initial stages of corrosion of this type of coating involve the selective dissolution of zinc, attributed to a dealloying (dezincification) phenomenon. The dissolution of the zinc from the coating surface is believed to increase the surface concentration of the more noble nickel component of the Zn-Ni alloy. The working electrode surface was observed to blacken, this could possibly be a consequence of the dezincification. Further increases in applied potential resulted in the destruction of the black surface, culminating in an approach to a limiting current and the formation of an observed gelatinous corrosion product around the electrode.

Table (47) and figure (96) show the I_{corr} values for different types of Zn-Ni coatings obtained after applying the Tafel extrapolation method. The results appear to be in a good agreement with reported literature (21).

The corrosion data and performance of Zn-Ni alloy coatings seem to be greatly affected by the morphology of the electrodeposited Zn-Ni alloy. This was confirmed when another set of four samples having 2, 4,11 and 13 % nickel in the coating.

Table (48) illustrates the plating conditions at which the samples were prepared and the corrosion data obtained from figures (97), (99), (105), (107) and (108).

From experimental observations it is apparent that electrodeposit morphology has a marked influence on the corrosion resistance of the coatings. Table (48) illustrates pairs of samples of similar compositions but of different morphologies and their salt spray corrosion resistance results. Although these figures are not widely dissimilar, it was apparent that some compositionally similar samples did corrode at different rates, particularly after the onset of red rust. The shapes of cathodic and anodic polarisation curves were also different.

Zn-Ni alloy coatings types	Current density A/dm^2	rotation speed RPM	Hours to red rust (S.S.T)	% red rust after 300 hrs
Zn-2%Ni	2.55	2000	192	80
Zn-2%Ni	5.1	150	200	50
Zn-4%Ni	15.3	350	216	90
Zn-4%Ni	86.7	2000	165	90
Zn-11%Ni	56.1	0	264	25
Zn-11%Ni	86.7	350	240	15
Zn-13%Ni	86.7	150	240	15
Zn-13%Ni	66.3	150	265	5

Table (48) Corrosion performance in N.S.S.T for different types of Zn-Ni alloy coatings at different plating conditions.

The " S " type curve is repeated in almost all the tested samples. The differences between these curves are in the rate of zinc dissolution accompanying the increase in
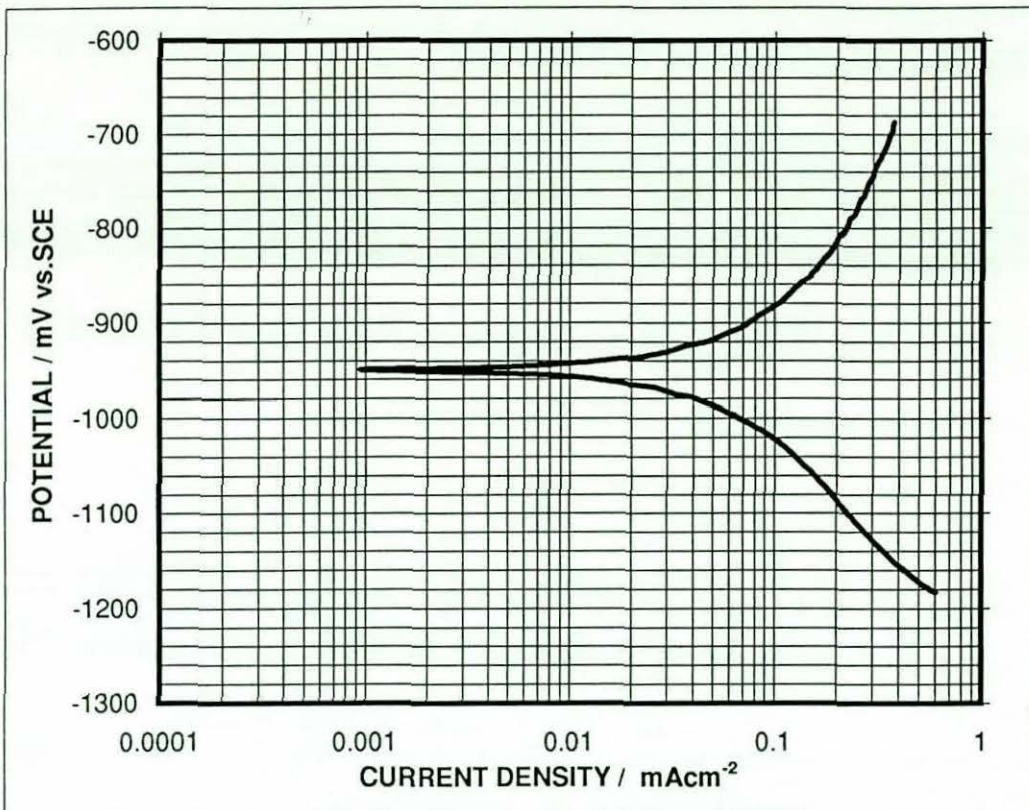
POLARISATION CURVE FOR Zn-2%Ni ALLOY
Figure (97)
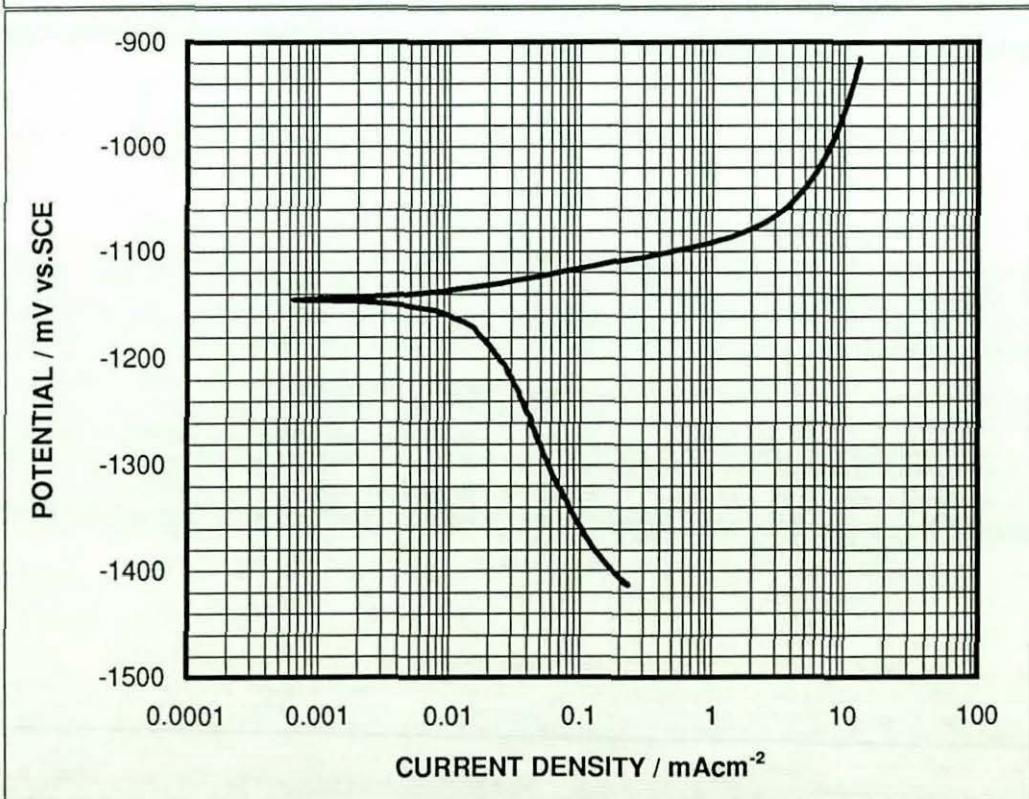
POLARISATION CURVE FOR Zn-3%Ni ALLOY
Figure (98)
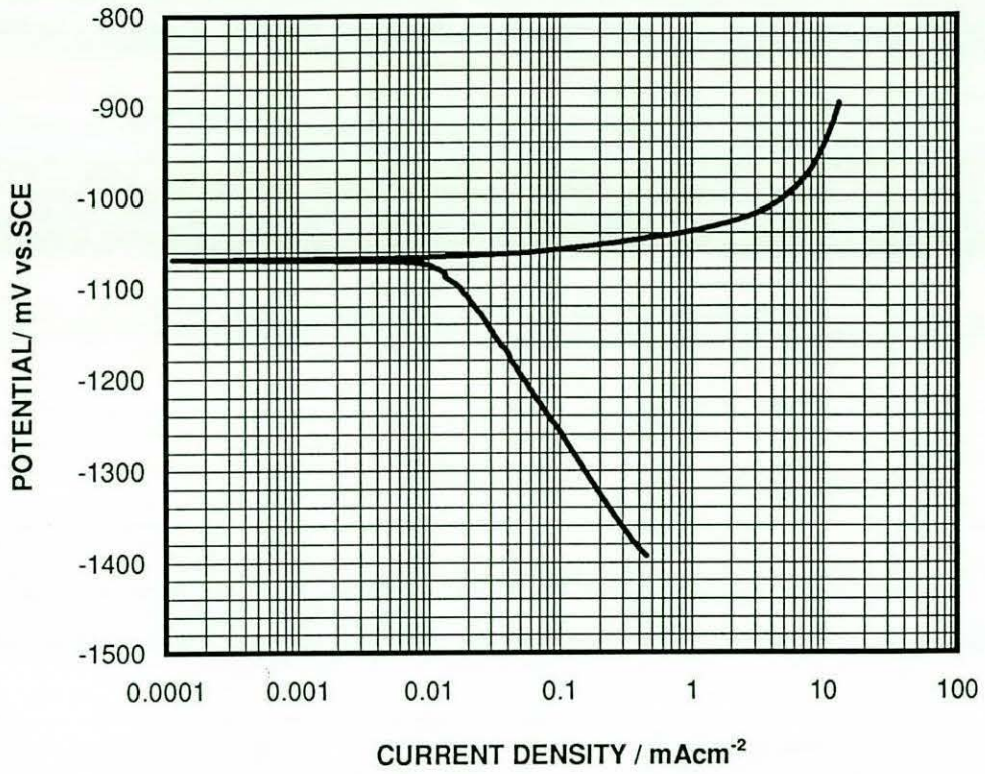
POLARISATION CURVE FOR Zn-4%Ni ALLOY
Figure (99)
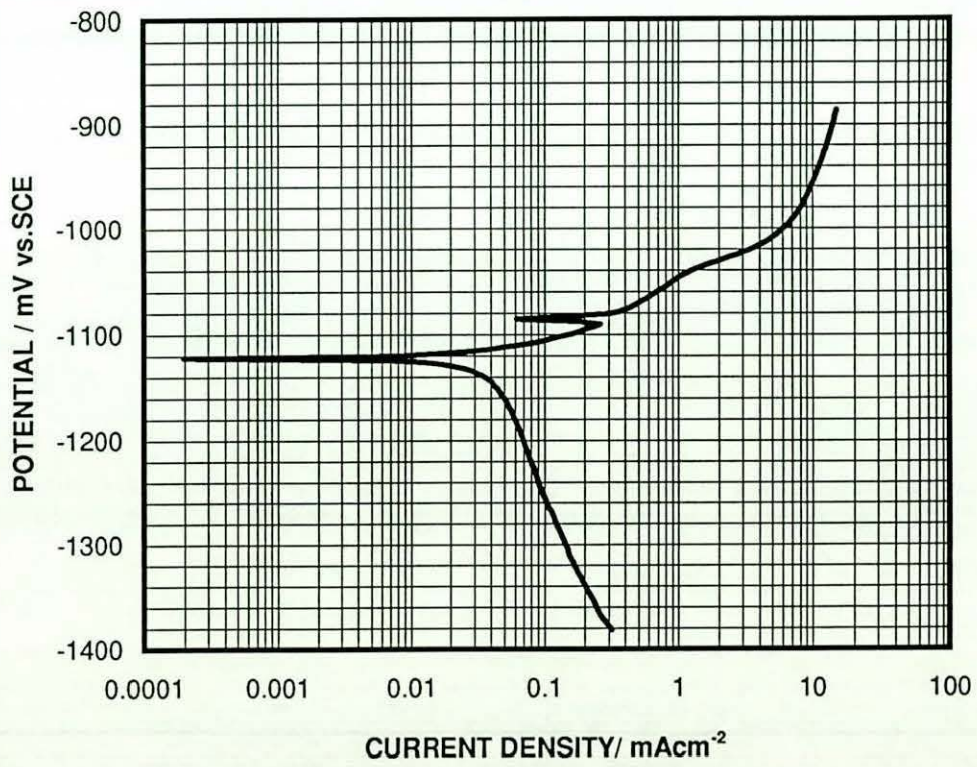
POLARISATION CURVE FOR Zn-5%Ni ALLOY
Figure (100)
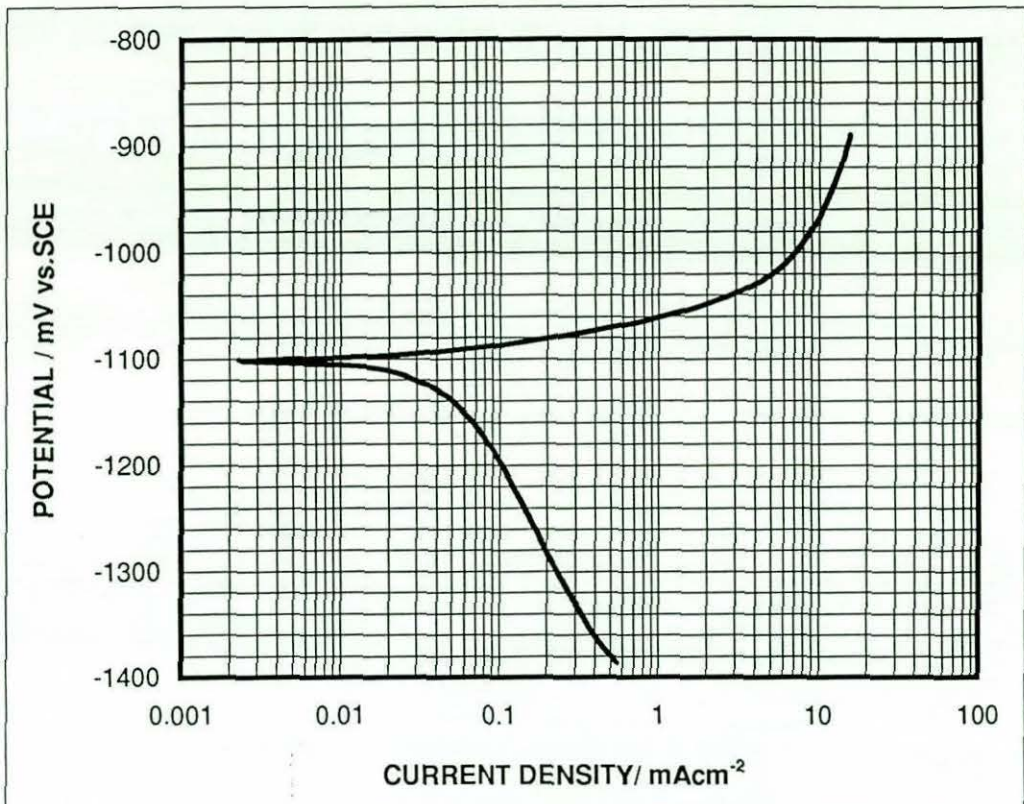
POLARISATION CURVE FOR Zn-6%Ni ALLOY
Figure (101)
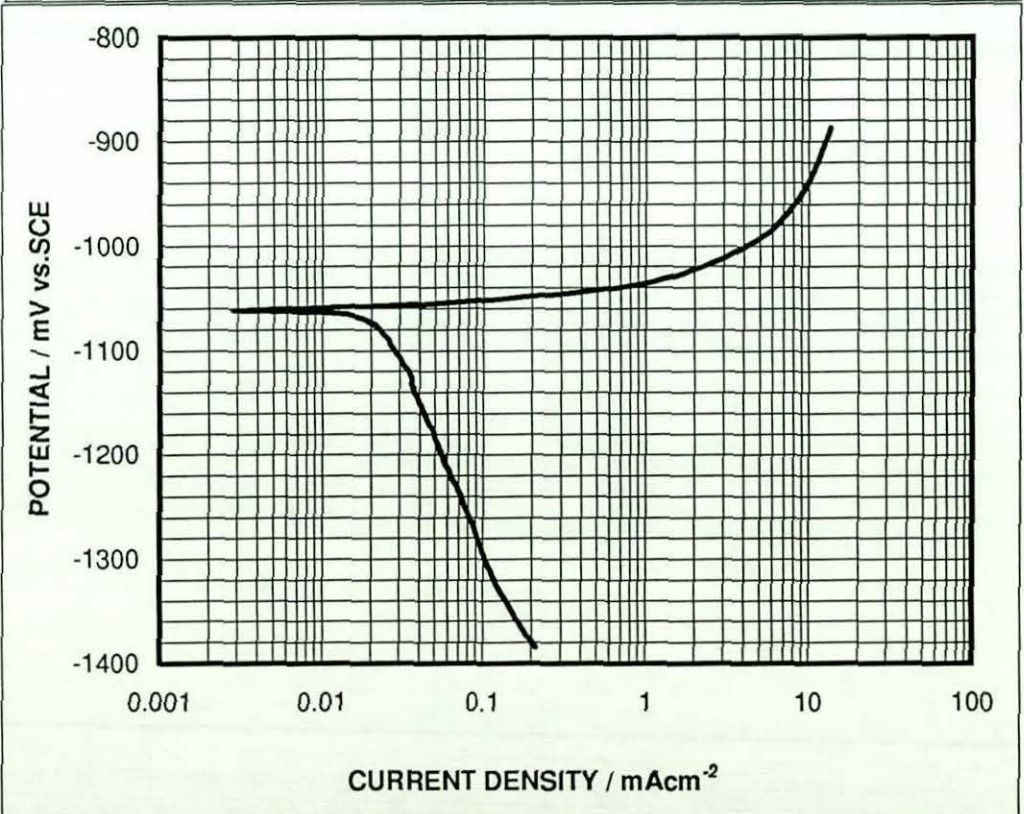
POLARISATION CURVE FOR Zn-8%Ni ALLOY
Figure (102)
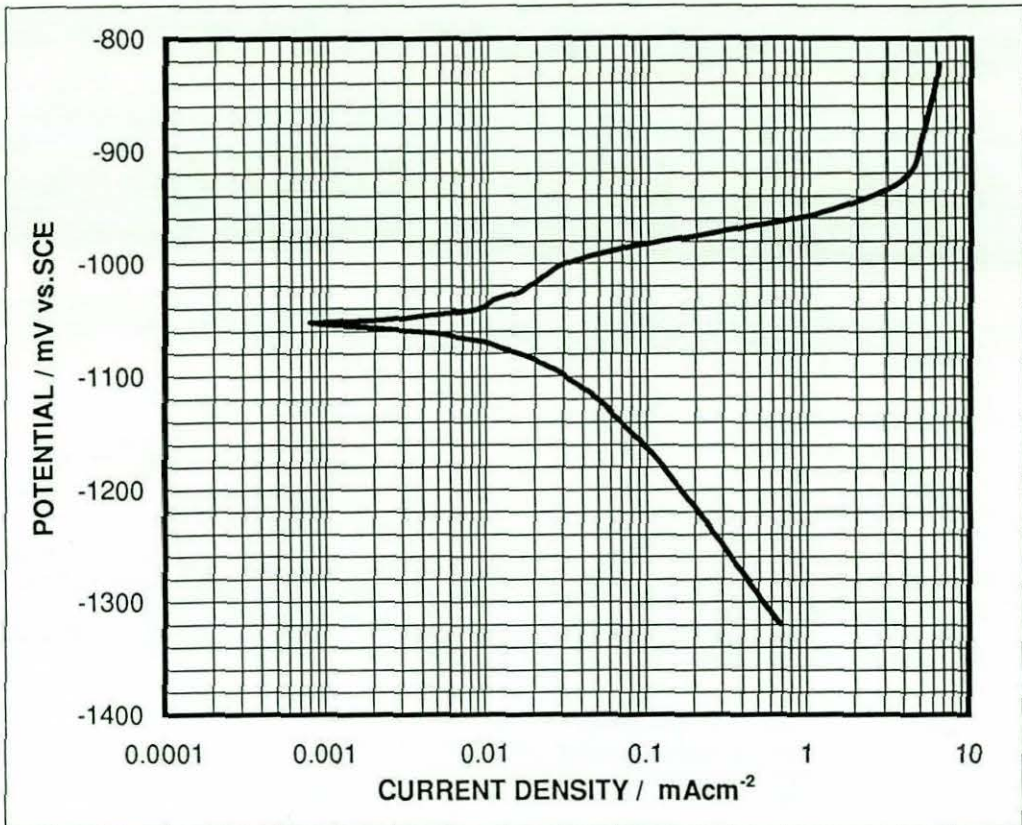
POLARISATION CURVE FOR Zn-9%Ni ALLOY
Figure (103)
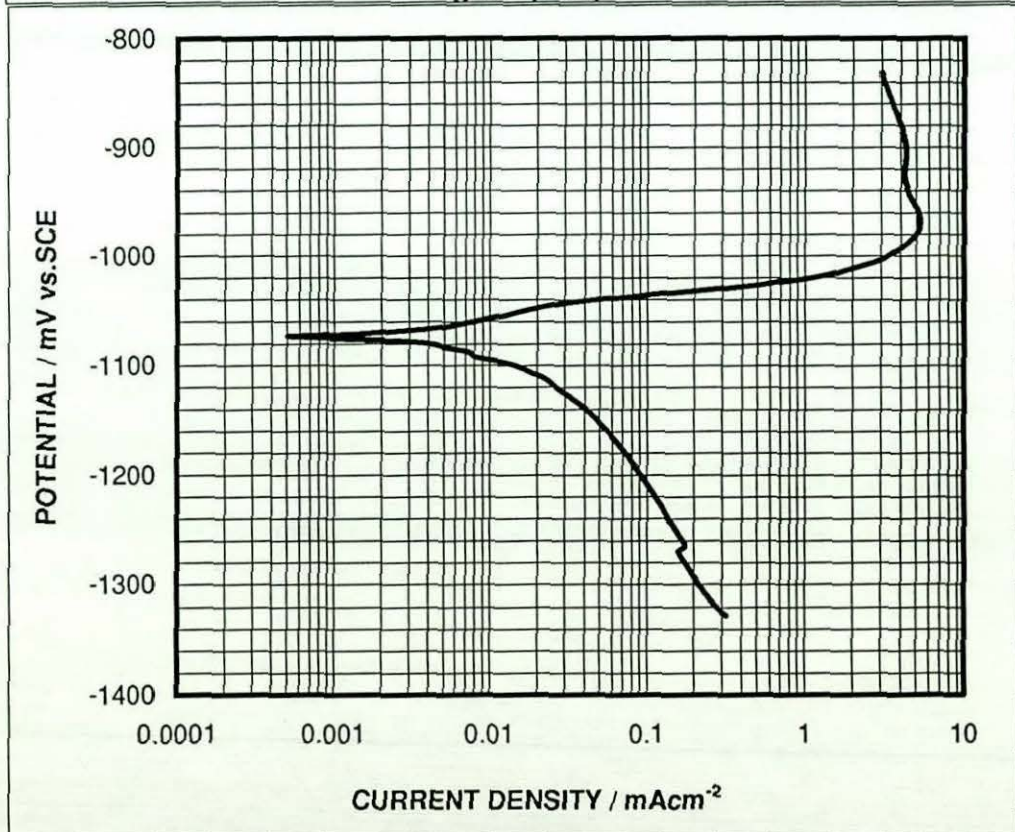
POLARISATION CURVE FOR Zn-10%Ni ALLOY
Figure (104)
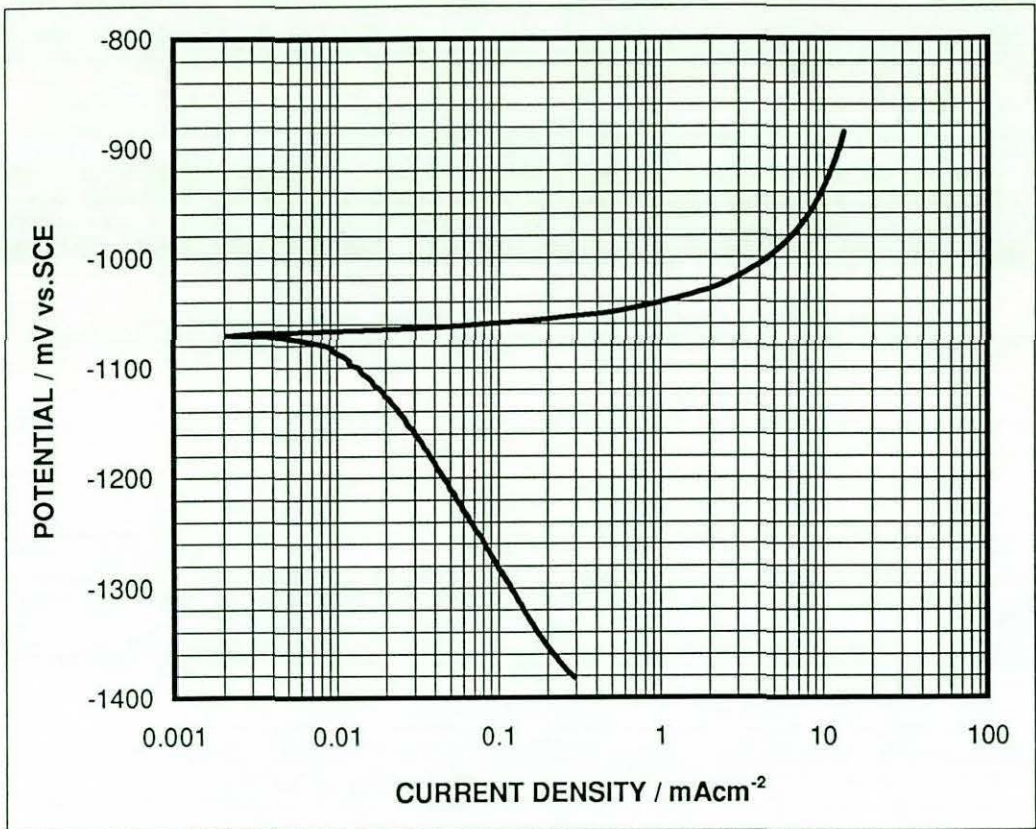
POLARISATION CURVE FOR Zn-11%Ni ALLOY
Figure (105)
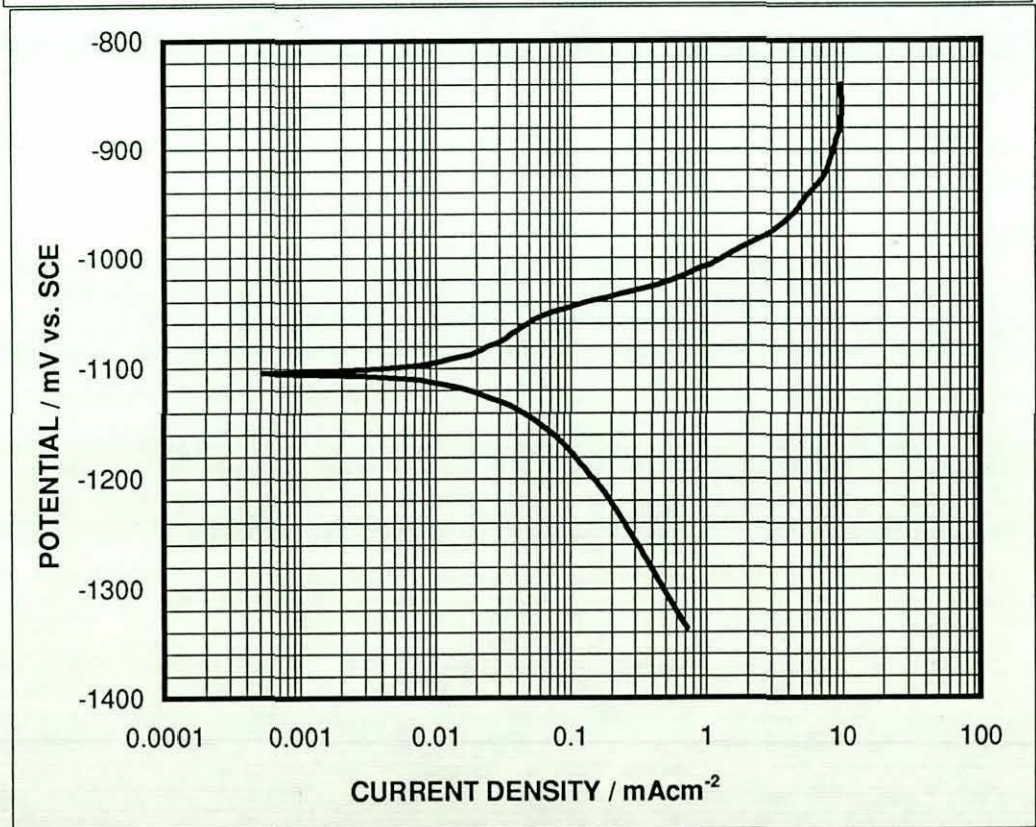
POLARISATION CURVE FOR Zn-12%Ni ALLOY
Figure (106)
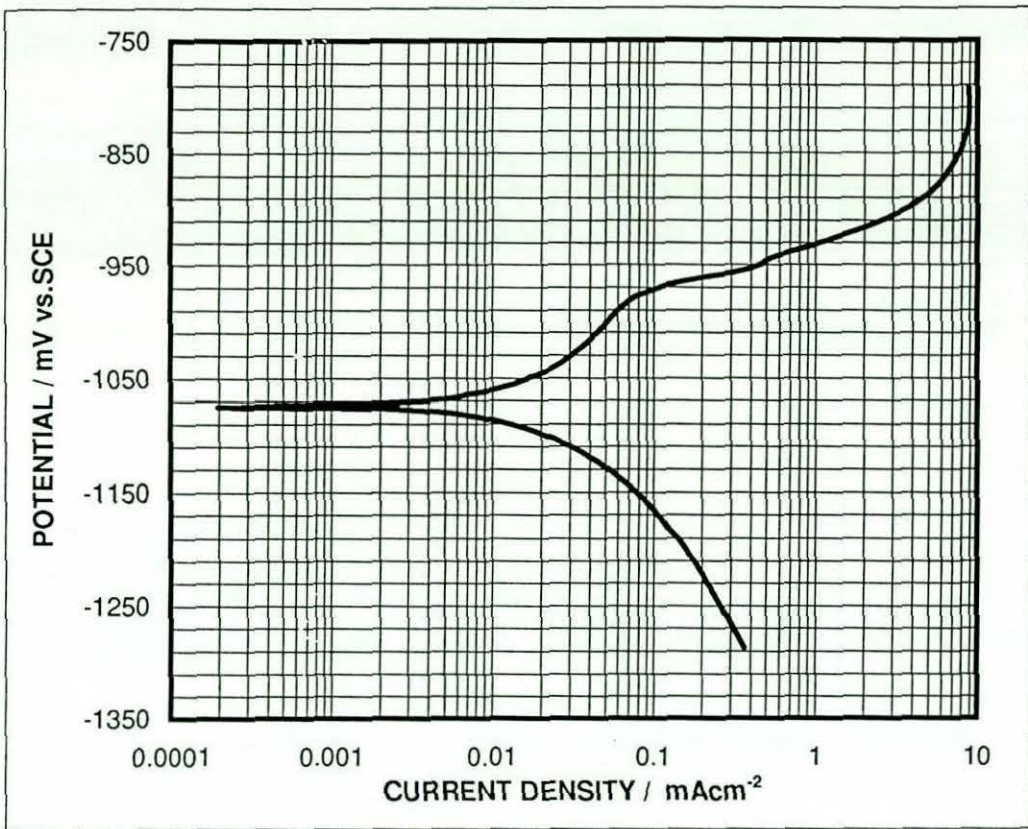
POLARISATION CURVE FOR Zn-13%Ni ALLOY
Figure (107)
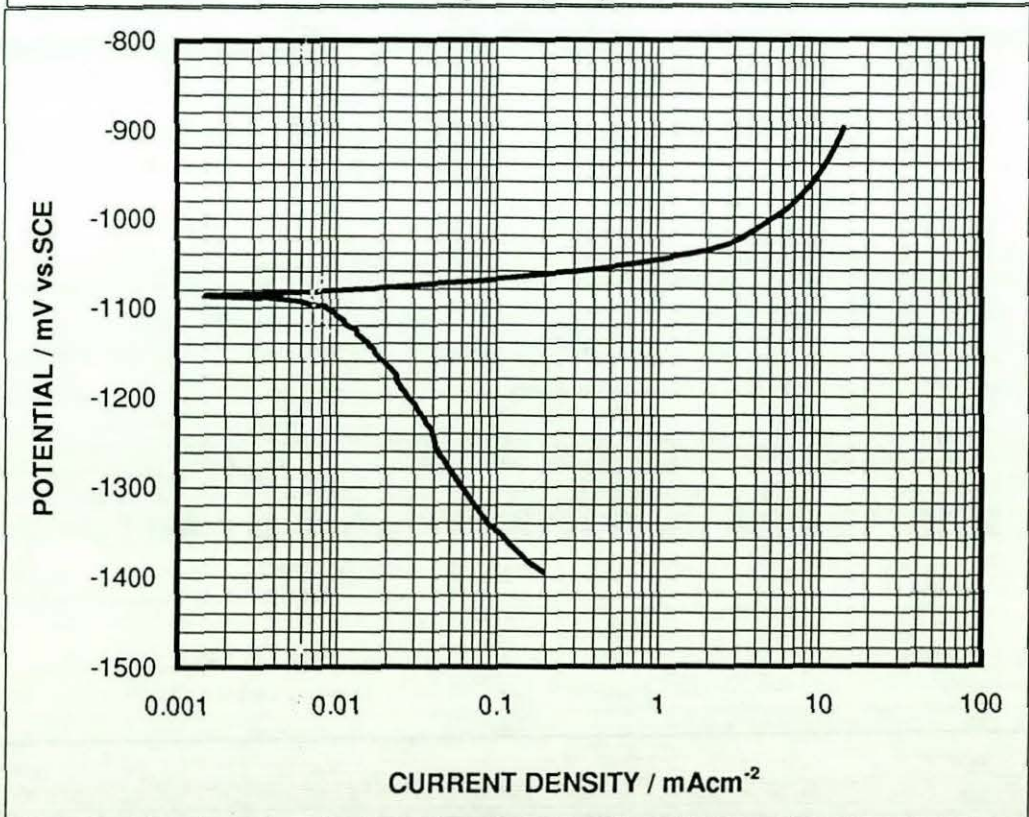
POLARISATION CURVE FOR Zn-14%Ni ALLOY
Figure (108)
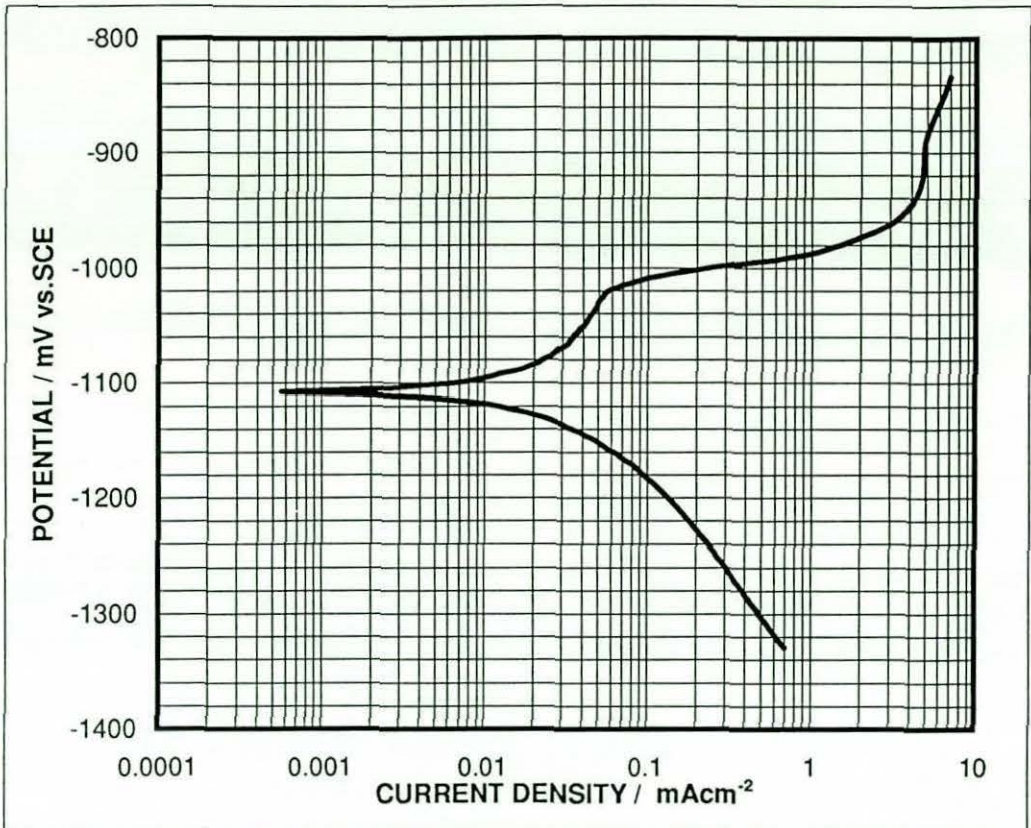
POLARISATION CURVE FOR Zn-16%Ni ALLOY
Figure (109)
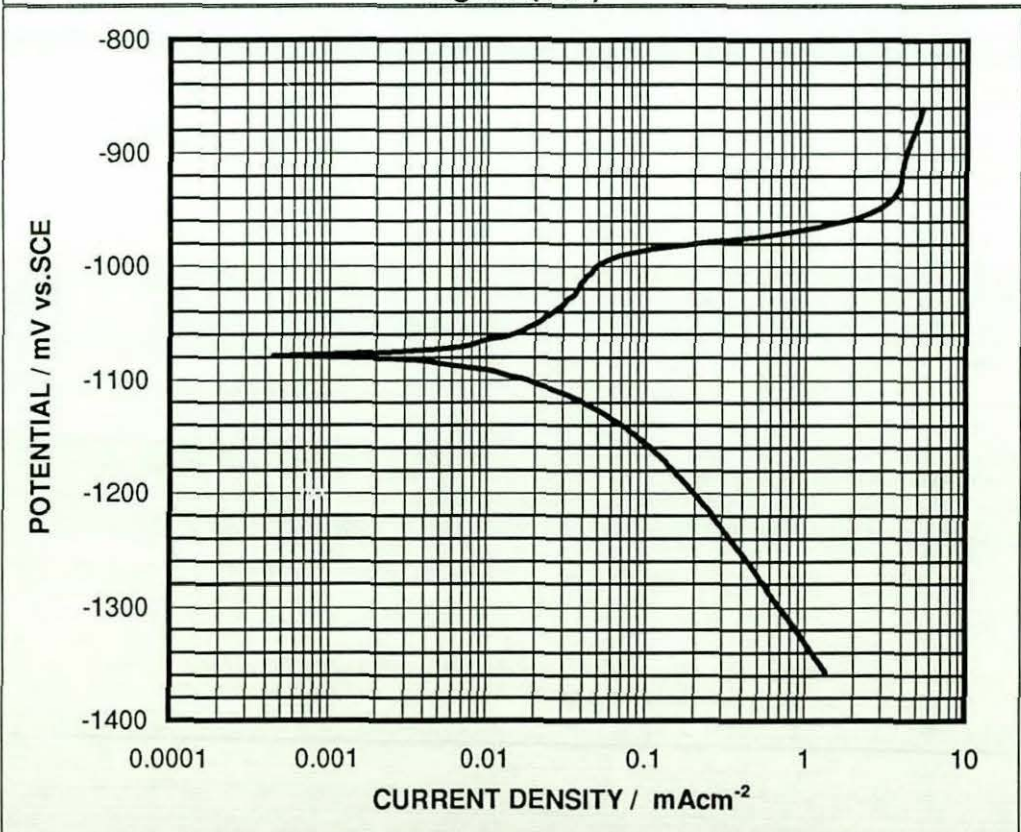
POLARISATION CURVE FOR Zn-17%Ni ALLOY
Figure (110)
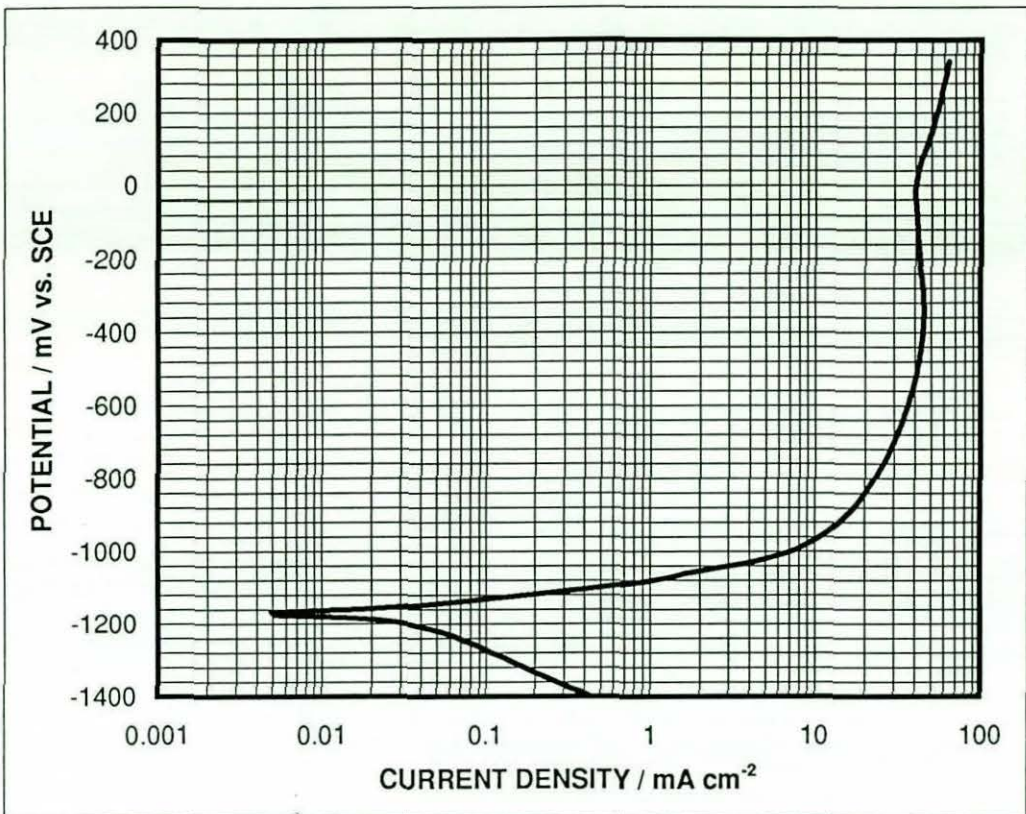
POLARISATION CURVE FOR Zn-2% Ni ALLOY
Figure (111)
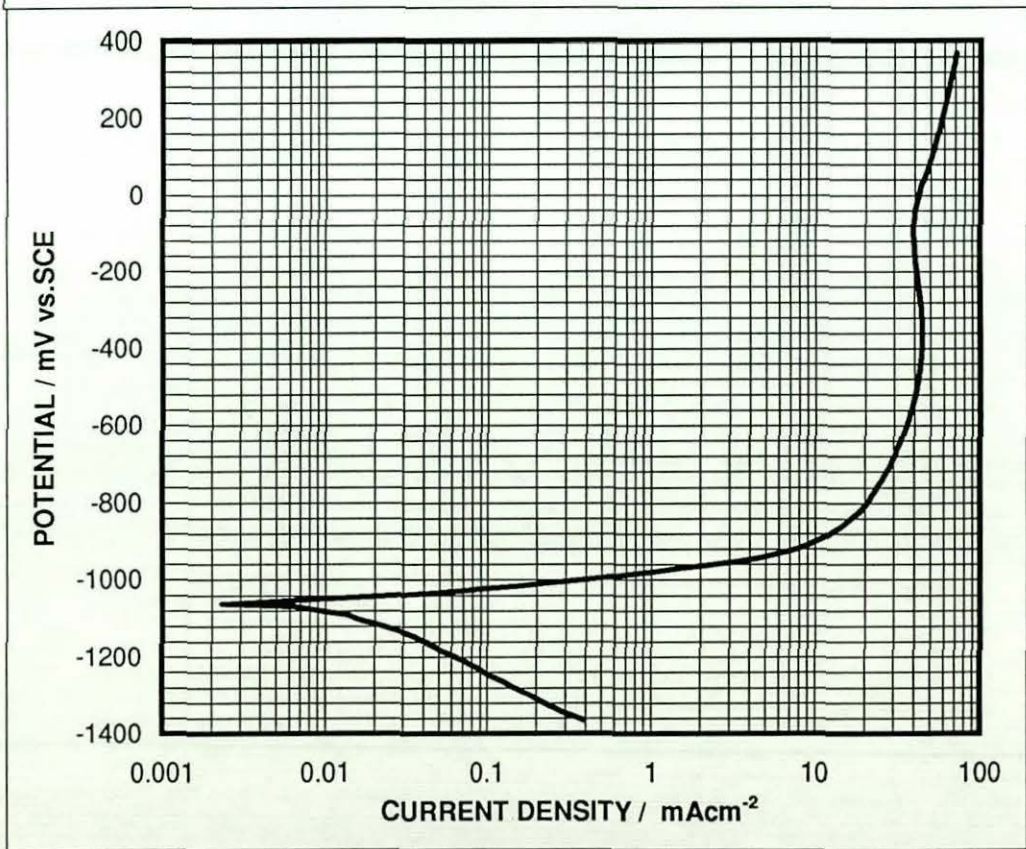
POLARISATION CURVE FOR Zn-4% Ni ALLOY
Figure (112)
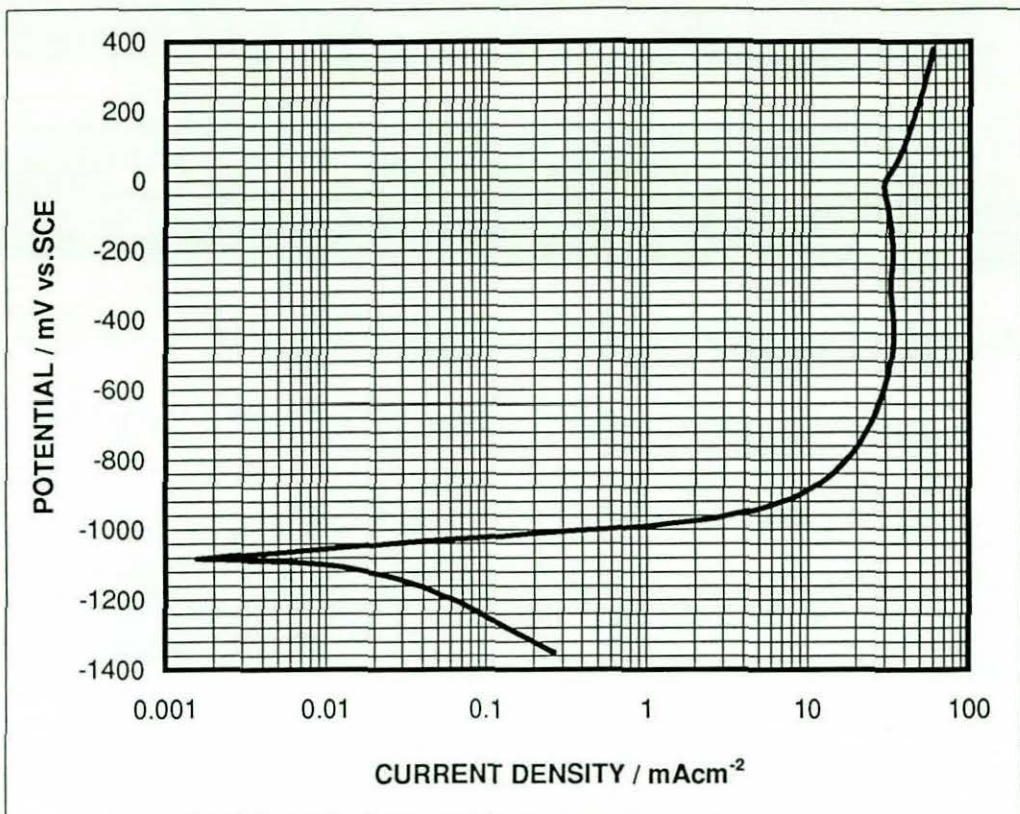
Polarisation Curve For Zn-11% Ni Alloy
Figure (113)
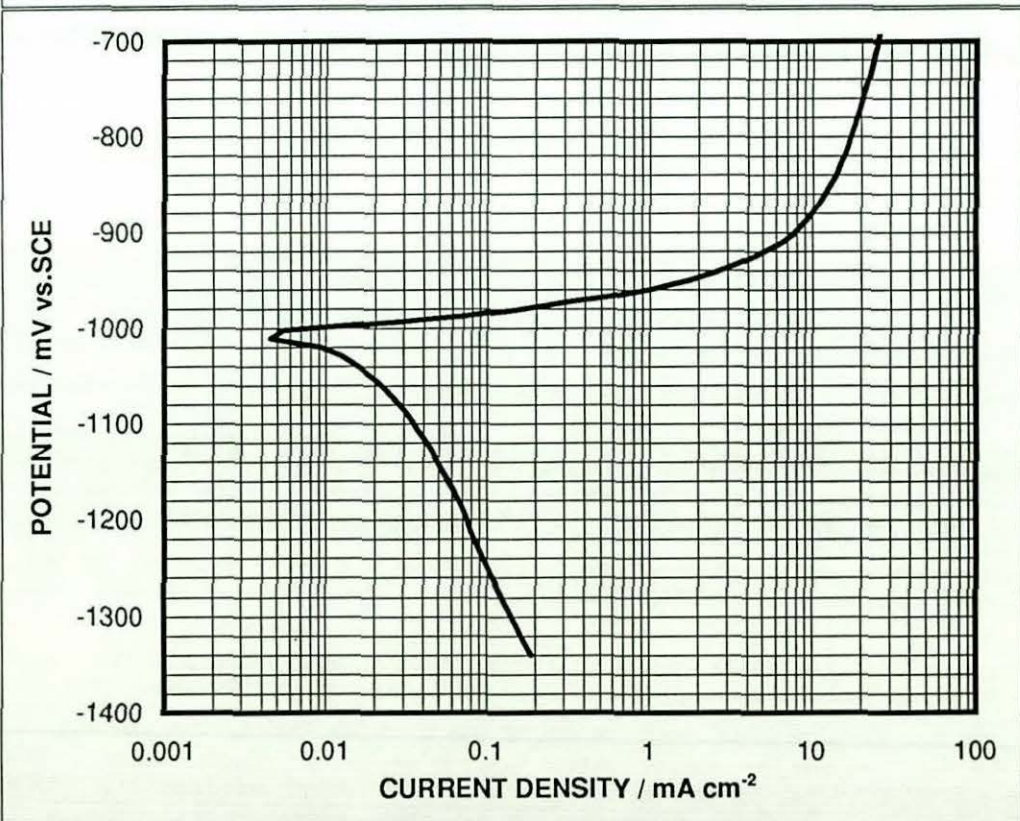
POLARISATION CURVE FOR Zn-13%Ni ALLOY
Figure (114)

potential, and also the length of the limiting current density period. The curves showed that Zn-2%Ni coating produced at 2000 rpm and 2.55 A/dm^2 seems to be more active than Zn-2%Ni coating produced at 150 rpm and 5.1 A/dm^2. The potentiodynamic polarisation curves for Zn-Ni coating samples showed that The Zn-4%Ni and Zn-11%Ni alloy coatings produced at 2000 rpm, 86.7 A/dm^2 and at 350 rpm, 86.7 A/dm^2 respectively have the same anodic polarisation behaviour of that of Zn-4%Ni and Zn-11%Ni alloy coatings produced at 350 rpm, 15.3 A/dm^2 and at 0 rpm, 56.1 A/dm^2 respectively, but different cathodic polarisation behaviour. The Zn-4%Ni and Zn-11%Ni alloy coatings produced at 2000 rpm, 86.7 A/dm^2 and at 0 rpm, 56.1 A/dm^2 respectively seem to be more active towards hydrogen evolution than the other coatings. Furthermore, the Zn-13%Ni coating produced at 150 rpm and 86.7 A/dm^2 has different cathodic and anodic behaviours than that of Zn-13%Ni coating produced at 150 rpm cathodic and anodic behaviours than that of Zn-13% Ni coating produced at 150 rpm and 66.3 A/dm^2. The Zn-13%Ni produced at 150 rpm and 86.7 A/dm^2 coating seems to be relatively less active towards hydrogen evolution, and also seems to be anodically less active during the limiting current region.

4-2-2-3 The investigation of the electrodeposition of layered Zn-Ni CMAM coatings

From the aforementioned results of the high speed alloy electrodeposition, the deposit characteristics of the coatings in terms of surface appearance, coating composition, crystal morphology, corrosion resistance and behaviour of Zn-Ni alloy coatings have been established for a range of current densities and electrode rotation speeds. It is possible to design compositionally modulated alloy multilayer coatings from a single electrolyte.

Using the quadruple pulse current regime (see section 2-3-3-3), two plating conditions were selected to produce compositionally modulated Zn-Ni alloy multilayer coatings with a repetitive layered structure consisting of a layer of Zn-2%Ni and a layer of Zn-13%Ni. The selected operating conditions are presented in table (49).

Two different types of Zn-Ni CMAM coatings were produced, Zn-2%Ni/Zn-13%Ni and Zn-13%Ni/Zn-2%Ni CMAM coatings, each of which consisted of 2, 4, 8 and 12 layers with an overall nominal thickness of 8 microns. These coatings were then tested

in terms of surface appearance and morphology, composition, layered structure and corrosion behaviour and performance.

4-2-2-3-1 Surface appearance and morphology

The surface appearance of the 2, 4, 8 and 12 layers Zn-2%Ni/Zn-13%Ni and Zn-13%Ni/Zn-2%Ni CMAM coated samples seem to reflect, to a great extent, the surface appearance of the Zn-2%Ni and Zn-13%Ni 8 microns single layer coatings respectively. The outer surface morphology of 2, 4, 8 and 12 layers Zn-2%Ni/Zn-13%Ni and Zn-13%Ni/Zn-2%Ni CMAM coated samples also seem to reflect the outer surface morphology of Zn-2%Ni and Zn-13%Ni 8 microns single layer coatings respectively. It can be seen from figures (115) to (119) that the crystal size of the coated layered samples was not affected by layer thickness, this might be attributed to the effect of the morphological structure of the under layer, whilst in the case of Ni/Zn CMMM coatings produced by the dual bath technique, the morphology of the outer surface layers seem to be affected by layer thickness.

4-2-2-3-2 Cross-sectional microstructures

The structures of the electrodeposited layered samples are presented in figures (120) to (123). It can be observed that the layered structure could be identified easily especially in the case of the 2 and 4 layered samples. It could also be seen that relatively clear interfaces between layered structure could be observed. The 8 and 12 layer coating structures seemed to be more difficult to identify. It seems from figure (123) that the layered structure of most coated samples were separated from the steel substrate (the left hand image). But, with a close examination of the secondary scanning electron image on the right hand side of the micrographs it can be observed that the layer separated from the substrate has a layered structure. This might indicate that the etching solution was preferentially attacked the layered adjacent to the substrate surface more than the upper layers (due to compositional differences). In general, it can be concluded that the micrographs confirm the possibility of producing Zn-Ni CMAM coatings from a single bath.

The compositions of Zn-Ni CMAM coatings were examined using energy dispersive x-ray analysis. The modulated alloy compositions were then measured. Table (50) shows the compositional analysis of the repetitive layers for different Zn-Ni CMAM coatings.
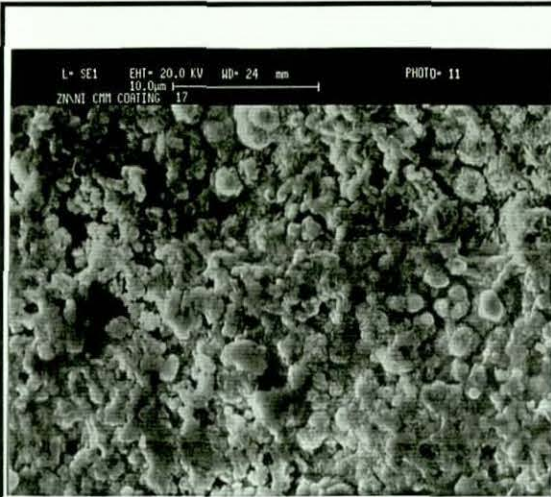
Fig.(115). Surface morphology for 2 layer Zn-2%Ni/ Zn-13% Ni CMAM coating
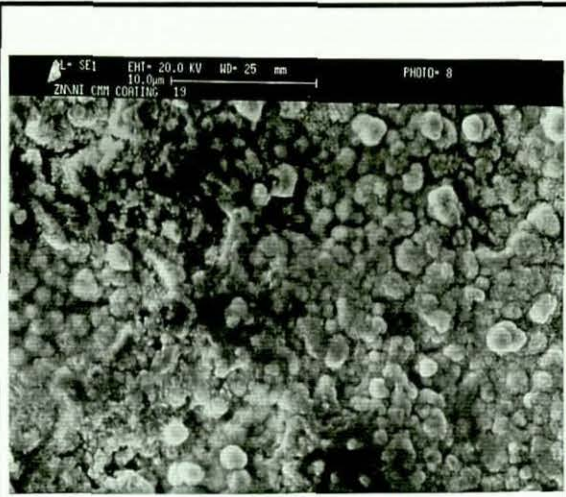
Fig.(116). Surface morphology for 4 layer Zn-13%Ni/Zn-13% Ni CMAM coating
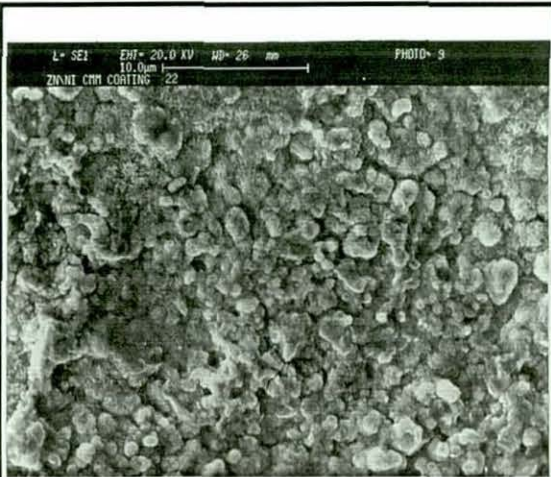
Fig.(117). Surface morphology for 8 layer Zn-2%Ni/Zn-13%Ni CMAM coating
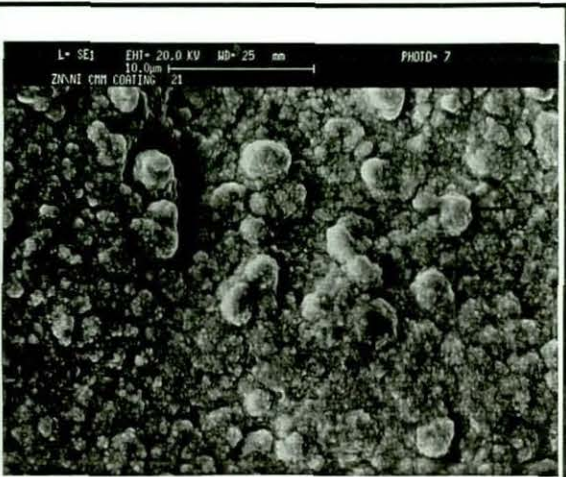
Fig.(118). Surface morphology for 12 layer Zn-2%Ni/Zn-13%Ni CMAM coating

Fig.(119). Surface morphology for 8μ Zn-13%Ni alloy single layer coating
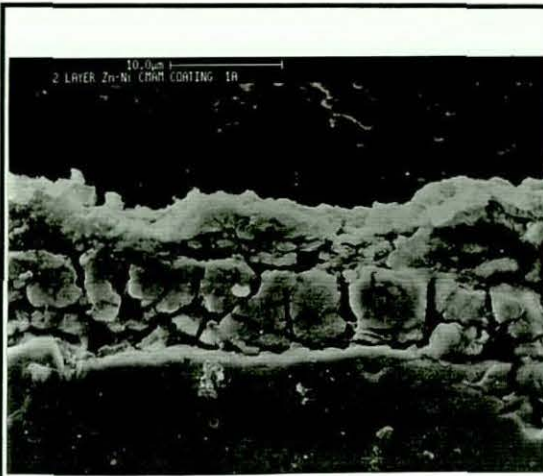
Fig.(120). SEM micrograph for 2 layer Zn-2%Ni/ Zn-13% Ni CMAM coating
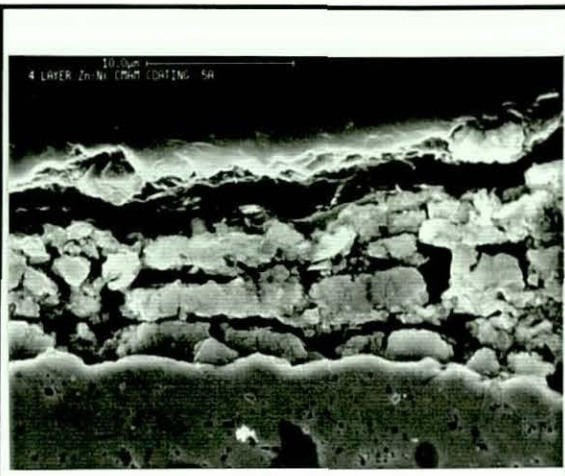
Fig.(121). SEM micrograph for 4 layer Zn-13%Ni/Zn-13% Ni CMAM coating
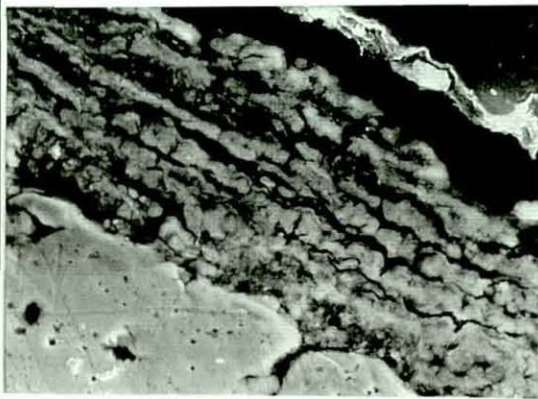
Fig.(122). SEM micrograph for 8 layer Zn-2%Ni/Zn-13%Ni CMAM coating
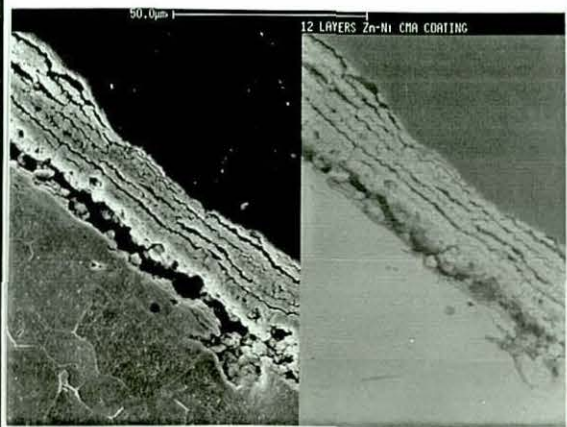
Fig.(123). SEM micrograph for 12 layer Zn-2%Ni/Zn-13%Ni CMAM coating

The results indicate that the outer layer composition of 2, 4, 8 and 12 layers Zn-2%Ni/Zn-13%Ni and Zn-13%Ni/Zn-2%Ni CMAM coated samples seem to reflect the composition of the 8 microns single layer coatings of Zn-2%Ni and Zn-13%Ni. The inter layers composition results do not seem to reflect the composition of single layer coatings. One of the possible causes might be due to an inter-diffusion from the high nickel layer to the low nickel layer during sample mounting where heat was applied during sample curing. Other reasons might be due to the smearing of the layers during polishing or surface zinc hydroxide films forming during the electrodeposition of one layer having a strong influence on the electrodeposition of subsequent layers.

4-2-2-3-3 Corrosion studies

The coated samples were tested in order to study the corrosion behaviours of the layered coatings and also to evaluate their corrosion performances. It was hoped to be able to draw comparisons with the single layer alloy coatings corrosion results.

Table (50) represents the corrosion data obtained from Tafel slopes and Neutral salt spray test.

4-2-2-3-3-1 Electrochemical corrosion studies

The cathodic and anodic behaviours of the coated samples are shown in figures (124) to (131). The cathodic behaviour of the layered coatings seems to be reasonably similar with, an initial sluggish increase in current accompanying the negative increase in potential, except the 2 layer Zn-13%Ni/Zn-2%Ni coating which has a rapid increase in current density as the potential increased. This might be attributed to the activity of this type of coating towards hydrogen evolution.

In order to study the anodic polarisation behaviour of the multilayered coated samples and to be able then to compare their behaviour with the anodic behaviour of the single layer alloy coatings, the anodic polarisation curves were divided into three main regions:

1- Tafel region which represents a rapid increase in current with a small change in potential.

Table (49) EDAX Analysis of outer surface and multilayer cross-section compositions for Zn/Ni CMAM coatings

Type of CMM coatings	Number of layers	Outer surface analysis (Ni%)	Cross sectional composition analysis (Ni%)
Zn-2%Ni/ Zn-13%Ni	2	14.2	4 / 2.8 / 11 / 12.3
Zn-13%Ni/ Zn-2%Ni	2	3.8	11.3 / 12 / 6 / 3.2
Zn-2%Ni/ Zn-13%Ni	4	13.2	3.4 / 12.5 / 6.8 / 13.7
Zn-13%Ni/ Zn-2%Ni	4	2.3	8.9 / 3.5 / 15 / 4
Zn-2%Ni/ Zn-13%Ni	8	13.9	2.3 / 16.2 / 4 / 14 / 3.2 / 13.2
Zn-13%Ni/ Zn-2%Ni	8	4.2	13.8 / 2.7 / 15 / 3.5 / 13.2 / 5.1
Zn-2%Ni/ Zn-13%Ni	12	9.8	6 / 12.2 / 4 / 13.8 / 8 / 13.2 / 5 / 9.3 / 2.2 / 10 / 5 / 10.6
Zn-13%Ni/ Zn-2%Ni	12	2.8	13.5 / 1.5 / 12 / 4 / 15.2 / 3.8 / 8 / 5 / 13.1 / 2 / 18 / 2.8

Table (50) Corrosion data and operating conditions for different types of Zn/Ni multilayer alloy coatings and their comparison with single Zn-Ni alloy layers

Type of CMM Coatings	Number of Layers	Cathode Current Density A/dm^2	RPM	E_{corr} mV vs.SCE	I_{corr} A/dm^2 (Tafel)	Hours to red rust	% Red Rust after 300 Hours
Zn-13%Ni	1	66.3	150	-1075	1.3×10^{-2}	240	15
Zn-2%Ni	1	5.1	150	-1170	0.98×10^{-1}	192	80
Zn-2%Ni/ Zn-13%Ni	2	5.1 / 66.3	150	-1110	1.11×10^{-2}	262	25
Zn-13%Ni/ Zn-2%Ni	2	66.3 / 5.1	150	-1140	0.633×10^{-1}	250	25
Zn-2%Ni/ Zn-13%Ni	4	5.1 / 66.3	150	-1080	0.84×10^{-2}	-	0
Zn-13%Ni/ Zn-2%Ni	4	66.3 / 5.1	150	-1110	1.6×10^{-2}	266	30
Zn-2%Ni/ Zn-13%Ni	8	5.1 / 66.3	150	-1040	0.52×10^{-2}	-	0
Zn-13%Ni/ Zn-2%Ni	8	66.3 / 5.1	150	-1080	0.42×10^{-2}	260	25
Zn-2%Ni/ Zn-13%Ni	12	5.1 / 66.3	150	-1040	0.52×10^{-2}	-	0
Zn-13%Ni/ Zn-2%Ni	12	66.3 / 5.1	150	-1100	0.65×10^{-2}	290	5
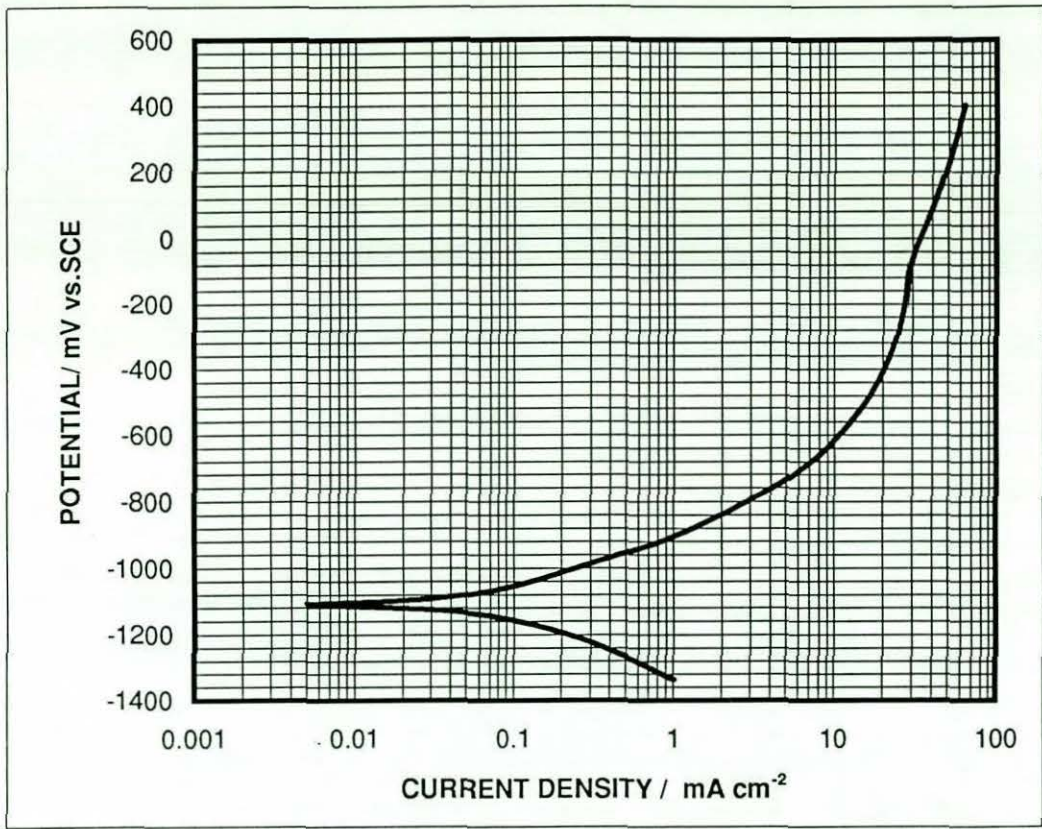
POLARISATION CURVE FOR 2 LAYER Zn-Ni
CMAM COATING / BILAYER 2-13% Ni
Figure (124)
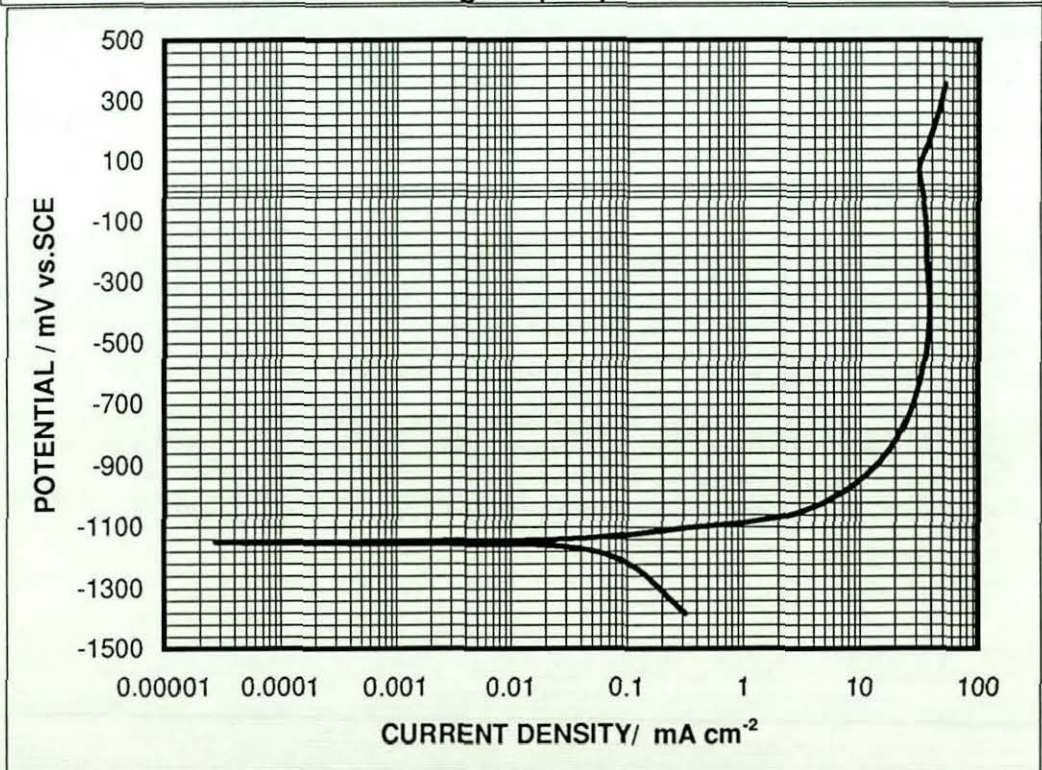
POLARISATION CURVE FOR 2 LAYER Zn-Ni
CMAM COATING / BILAYER 13-2% Ni
Figure (125)
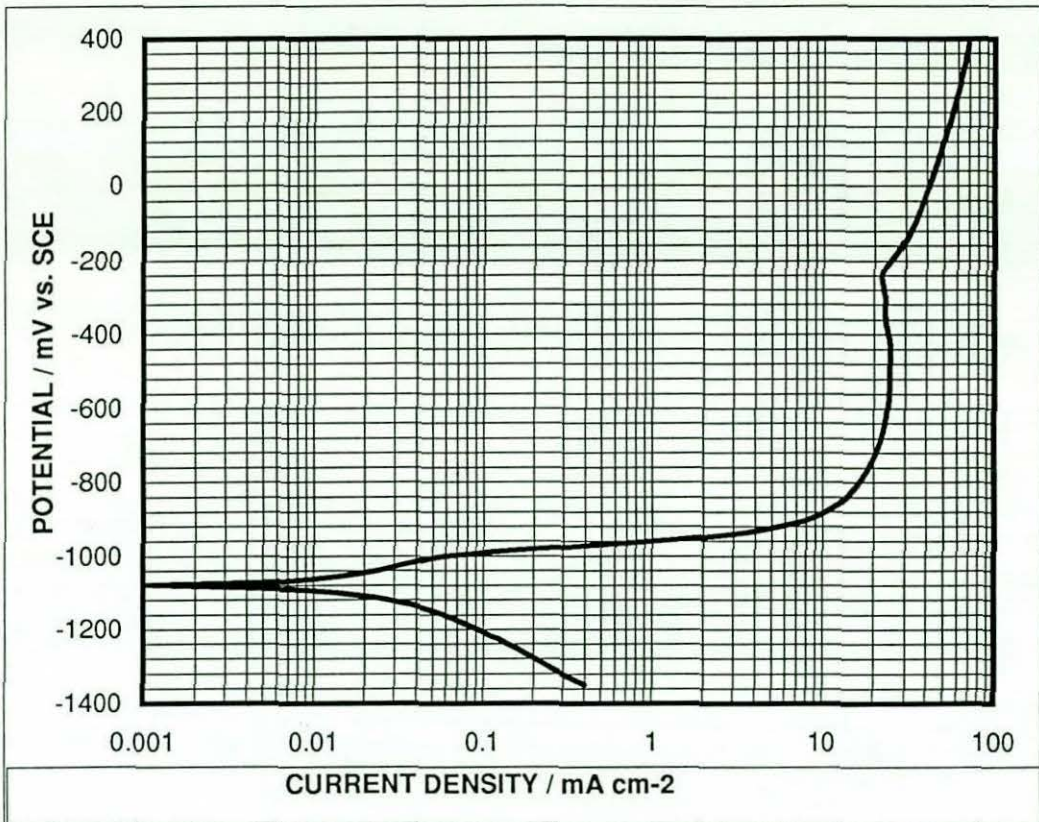
POLARISATION CURVE FOR 4 LAYER Zn-Ni CMAM COATING / BI LAYER 2-13%Ni

Figure (126)
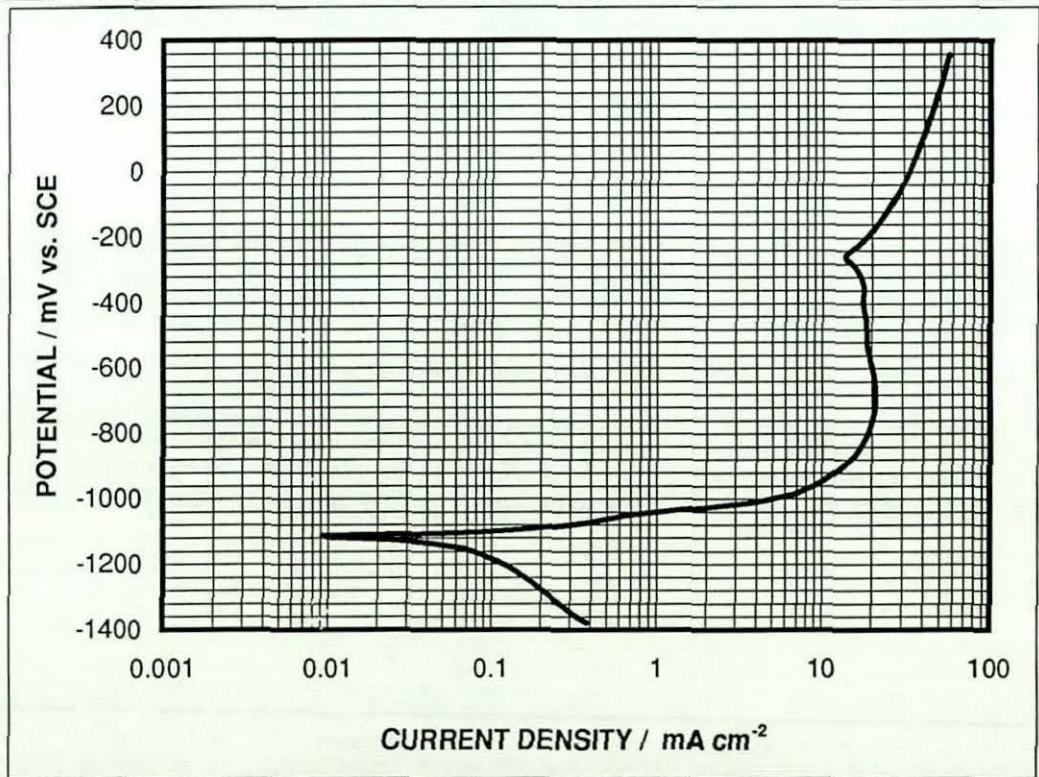
POLARISATION CURVE FOR 4 LAYER CMAM COATING / BI LAYER 13- 2% Ni

Figure (127)
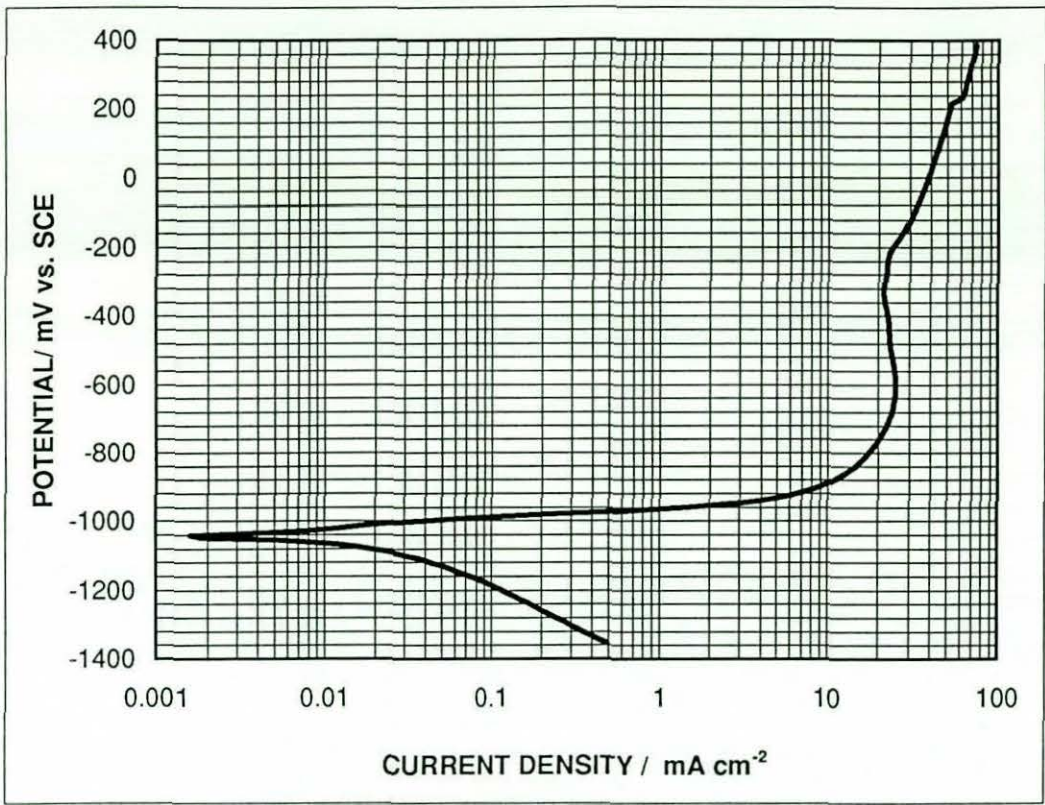
POLARISATION CURVE FOR 8 LAYER Zn-Ni
CMAM COATING/ BI LAYER 2-13%Ni
Figure (128)
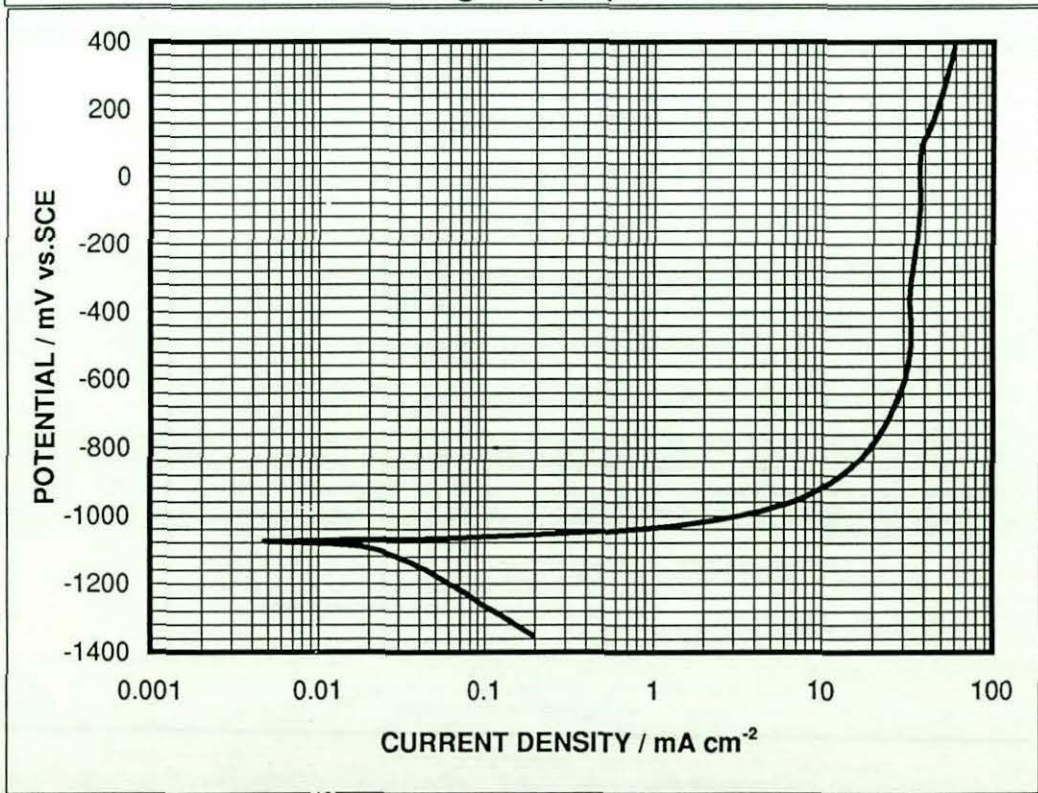
POLARISATION CURVE FOR 8 LAYER Zn-Ni
CMAM COATING / BI LAYER 13-2% Ni
Figure (129)
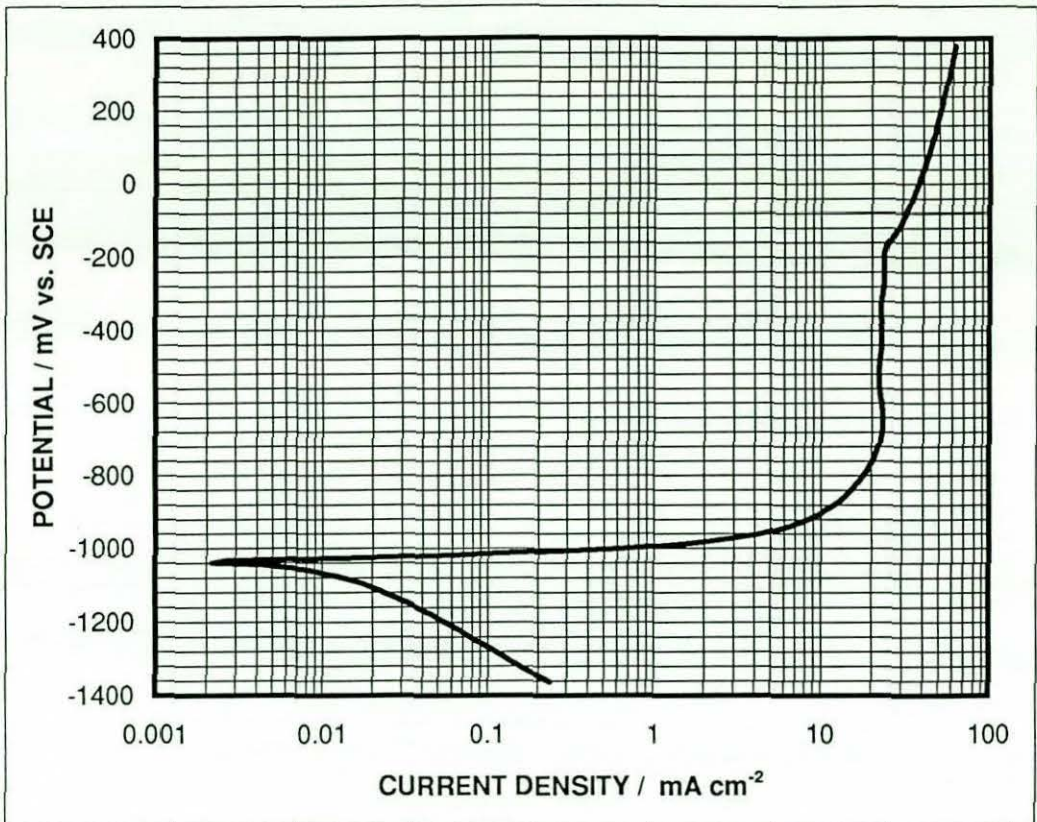
POLARISATION CURVE FOR 12 LAYER Zn-Ni
CMAM COATING / BI LAYER 2-13% Ni
Figure (130)
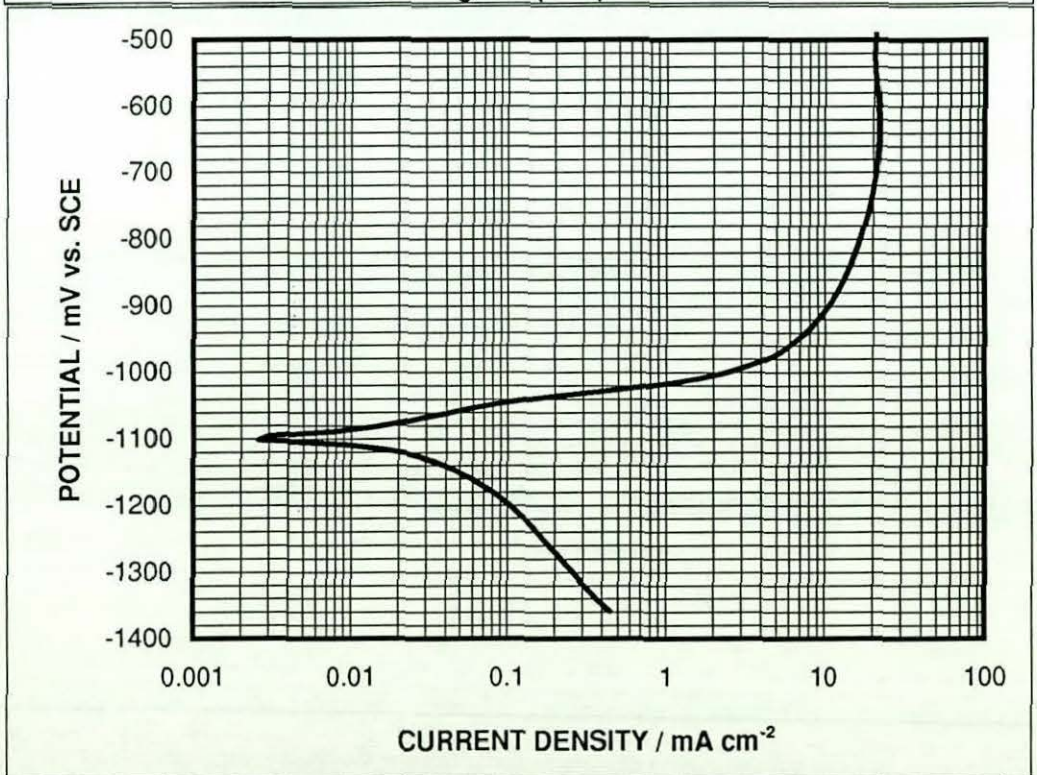
POLARISATION CURVE FOR 12 LAYER Zn-Ni
CMAM COATING / BI LAYER 13-2% Ni
Figure (131)

2- A limiting current (LC) region which represents a small change in current density with a large change in potential.

3- A post LC (PLC) region representing a sluggish increase in current density with a medium increase in potential.

The Tafel region was associated with a zinc dissolution process and hence the formation of a stable zinc corrosion product layer at the end of this period. The limiting current region could be associated with the formation of this stable zinc corrosion product film which lead to only a very small increase in current density. The post-LC region was associated with a break down of this stable film and thus, the current density starts to increase again. Table (51) illustrate the current density and potential values of these three regions for 2, 4, 8 and 12 layer Zn-2%Ni/Zn-13%Ni and Zn-13%Ni/Zn-2%Ni CMAM coatings.

It can be seen from the potential and current density values that the multilayer coatings, have, in general, better electrochemical corrosion behaviour than single layer alloy coatings. The corrosion potential of the upper layer of each type of multilayered coatings seem to have the same value of that for Zn-2%Ni and Zn-13%Ni single layer alloy coatings. The corrosion current of multilayered coatings however, have lower values than that of single layer alloy coatings. Also, it can be seen that I_{LC} for the multilayered coatings seem to have the same value to that of the single layer alloy coatings. Whilst, the I_{PLC} for the multilayered coatings seem to have lower values than those of the single layer alloy coatings which means that the breakdown of the corrosion product film for example happened at 13.5 A/dm^2 for Zn-2%Ni single layer alloy coating, whilst, the breakdown of the corrosion product film happened at 13- 10.5 and 13 A/dm^2 for 2 - 4 and 8 layers Zn-13%Ni/Zn-2%Ni CMAM coatings respectively. This observation could be attributed to the fact that the single layer alloy coatings form a slightly more stable film than the multilayered ones in the limiting current region.

Type of coatings	Number of layers	E_{corr} (A/dm^2)	I_{corr} (mV)	E_{LC} [1] (A/dm^2)	I_{LC} [2] (mV)	E_{PLC} [3] (A/dm^2)	I_{PLC} [4] (mV)
Zn-2%Ni	1	-1170	$0.98e^{-1}$	-760	10.5	+40	13.5
Zn-13%Ni	1	-1075	$1.3e^{-2}$	-840	10.5	-	-
Zn-13%Ni/Zn-2%Ni	2	-1140	$0.63e^{-1}$	-820	11	+100	13
Zn-13%Ni/Zn-2%Ni	4	-1110	$1.6e^{-2}$	-880	10.5	-280	10.5
Zn-13%Ni/Zn-2%Ni	8	-1080	$0.42e^{-2}$	-760	11.3	-100	13
Zn-13%Ni/Zn-2%Ni	12	-1100	$0.65e^{-2}$	-860	10.5	-	-
Zn-2%Ni/Zn-13%Ni	2	-1110	$1.11e^{-2}$	-400	11	-40	12
Zn-2%Ni/Zn-13%Ni	4	-1080	$0.84e^{-2}$	-840	10.5	-820	11.5
Zn-2%Ni/Zn-13%Ni	8	-1040	$0.52e^{-2}$	-800	10.5	-200	11.5
Zn-2%Ni/Zn-13%Ni	12	-1040	$0.52e^{-2}$	-800	10.5	-160	11.5

(1) E_{LC} Limiting current region (potential)

(2) I_{LC} Limiting current region (current density)

(3) E_{PLC} Post limiting current region (potential)

(4) I_{PLC} Post limiting current region (current density)

Table (51). The current density and potential values of these three regions for 2, 4, 8 and 12 layer Zn-2%Ni/Zn-13%Ni and Zn-13%Ni/Zn-2%Ni CMAM coatings

The anodic polarisation behaviour of the 2 layer Zn-2%Ni/Zn-13%Ni CMAM coating seems to have no LC region, and the sluggish start of current density as the potential increase over E_{corr} continues all the way which means that the coating has failed to form a thick stable corrosion product film. Whilst, in the case of 2 layer Zn-13%Ni/Zn-2%Ni CMAM coating, the situation is different. After a rapid increase of current density an obvious limiting current region takes place for a relatively long period.

The anodic polarisation curves for 4, 8 and 12 layers Zn-2%Ni/Zn-13%Ni and Zn-13%Ni/Zn-2%Ni CMAM coatings seem to show similar behaviour to that of 2 layer Zn-13%Ni/Zn-2%Ni CMAM coatings with one exception that the length of the limiting current region is different. The anodic behaviour of the 4 layer Zn-13%Ni/Zn-2%Ni

CMAM coating shows a relatively small region of limiting current which could mean that this type of coating builds up less stable corrosion product film.

4-2-2-3-3-2 Neutral salt spray test studies

The results of corrosion performance testing of 2, 4, 8 and 12 layers Zn-2%Ni/Zn-13%Ni and Zn-13%Ni/Zn-2%Ni CMAM coatings in a neutral salt spray chamber are presented in table (49) which shows the corrosion performances of these coatings in terms of hours to red rust and also in terms of a red rust percentage on the coatings after 300 hours test.

The values indicate that the multilayered coatings have significantly better performance to that of single layer alloy coatings and the corrosion improvement in performance increases with the increase in the number of the layers.

Chapter 5

CONCLUSIONS and FUTURE WORK

5-1 Conclusions

5-1-1 Dual Bath Electrodeposition of Cu/Ni CMMM coatings

5-1-1-1 The dual bath electrodeposition technique offers a simple, relatively easy way to build up compositionally modulated multilayer systems.

5-1-1-2 Cu/Ni CMMM coatings produced by this technique have a reletively pure distinct and continuous sublayer structures in a range of 1micron to 500 nanometres.

5-1-1-3 The Cu/Ni CMMM coatings produced showed sharp interfaces between the adjacent layers.

5-1-1-4 The multilayers produced had a smooth pore-free layers.

5-1-1-5 The dual bath technique can be used as a model system to build up a better understanding of the multilayer electrodeposition techniques.

5-1-1-6 It was found that inregular agitation could strongly affect the smoothness of the layered structure as well as could the preparation process for the substrate surface.

5-1-1-7 The etching method used in sample preparation for SEM observation has a strong effect on the clarity of the layered structures.

5-1-2 Dual Bath Electrodeposition of Zn/Ni CMM coatings

5-1-2-1 The production of Zn/Ni CMMM coatings was effected to a great extent by the operating conditions of the nickel layer electrodeposition.

128

5-1-2-2 The porosity of the nickel layer had a great effect on the corrosion resistance of the systems.

5-1-2-3 The layered system with the zinc layer on top seem to perform remarkably better than the other systems where the nickel or the Zn-Ni alloy layer was on top.

5-1-2-4 The corrosion performance of layered structures consisting of Zn-Ni alloy and Zn layers respectively have the best corrosion performance in neutral salt spray environments.

5-1-2-5 Four layer systems have better corrosion resistance than 8 layer systems. Hence, the lower the number of layers the greater the corrosion resistance.

5-1-3 Single Bath Electrodeposition of Cu/Ni CMAM coatings

5-1-3-1 The single bath electrodeposition technique for Cu/Ni CMAM coatings can be used as a tool to establish a better understanding of high speed electrodeposition techniques needed for the Zn/Ni CMAM coatings.

5-1-3-2 The quadruple pulse-current regime has a strong effect on the smoothness of the layered structure, and the purity of the nickel layers.

5-1-3-3 The Cu/Ni CMAM coatings produced under the optimum conditions have a smooth pore-free continuous layered structure in the range of 1 micron to 25 nanometres layer thicknesses.

5-1-3-4 The single bath technique can be used as a succesful method for producing very thin layers of Cu/Ni CMAM coatings.

5-1-4 Single Bath Electrodeposition of Zn/Ni CMAM coatings

5-1-4-1 High speed electrodeposition techniques can be used as a tool for predicting suitable plating conditions for the production of compositionally modulated alloy multilayer coatings.

5-1-4-2 The composition of the Zn-Ni alloy can be controlled by changing the current density and electrode rotation speed.

5-1-4-3 A zinc rich deposit of up to 98% is possible at low current densities. A deposit with a nickel content of up to 36% is possible at higher current densities and at very low rotation speeds.

5-1-4-4 The investigations of Zn-Ni CMAM coatings proved that there is a great possibility to produce this type of coatings with improved corrosion properties.

5-1-4-5 The surface appearance of the CMAM coatings has been found to be generally similar to that of similar single layer alloy coatings.

5-1-4-6 Under the conditions studied, the CMAM coatings, in general, produced a better corrosion behaviour and performance than single layer alloy coatings.

5-1-4-7 Under the conditions studied, the higher the number of repeated multilayer, the better the corrosion behaviour and performance of the coatings.

5-1-4-8 From the energy dispersive x-ray analysis (EDAX), it was found that the composition of the outer surface layer of the CMAM coated samples approximately corresponded to that of the single layer alloy coatings, which would have been produced under the deposition conditions of the top layer.

5-1-4-9 From the energy dispersive x-ray analysis (EDAX), it was found that the composition of the deposit of each layer of the CMAM coated samples did not correspond to that of the discrete single layer alloy coatings, which would have been produced under those conditions.

5-2 Suggestions for future work

5-2-1 After the successful trials to produce compositionally modulated multilayers with the Zn/Ni system and because of the significant improvements in corrosion behaviour and performance of the layered Zn/Ni CMMM and CMAM coatings over the single layer Zn and Zn-Ni alloy coatings, it would be useful to continue to investigate other coating systems such as Zn/Co, Zn/Cr, and Zn/Mn systems and to evaluate their corrosion behaviours and performances.

5-2-2 This investigation's results showed that the morphology of the coated samples and hence the texture plays an important role in corrosion behaviour and performance of the Zn-Ni CMAM coatings. It is therefore worthwhile to continue this work with the Zn-Ni CMAM coatings and to study in more detail how the texture of Zn-Ni alloy layer coatings change with rotation speed and current density and then it could be possible to enhance the overall corrosion resistance of Zn-Ni CMAM coatings to a higher level and to be able then to transfer the process from a laboratory investigation perhaps a pilot plant study.

5-2-3 According to the results obtained from Zn/Ni dual bath trials, it might be also possible to look at the nickel electrolyte in terms of enhancing its electrodeposit's physical and mechanical properties by the use of appropriate addition agents and then to be able to improve the overall corrosion performance (believed to be greatly affected by porosity for example) of the Zn/Ni CMMM coatings which could give a significant industrial importance to the coating system. It may possible to simply passivate the zinc layer in Ni/Zn CMMM coatings system and to use the Zn/Ni CMMM coatings without a final decorative layer because of the barrier and aesthetic properties of nickel layer on top.

References

1- H. Geduld, Zinc Plating, ASM International Metals Park, OH, Finishing Publications Ltd., Teddington, Middlesex. England, 1988.

2- F. A. Lowenheim, Electroplating: Principles and practice, Finishing Publications, Ltd New York, 1985.

3- Finishing Hand Book and Directory, 1983, Product Finishing Sawell Publications Ltd.

4- K. Boto, Electrop & Surface treatment,. 3, 77, 1975

5- H. G. Greutz and S. Martin, Plating and Surface Finishing, 681, July 1975.

6- R. K. Preiksaite and R. R. Sarmaitis, Corrosion of Electrodeposited Zinc Coatings, Plat& Surf. Finish, Aug. 1981.

7- A. Brenner: Electrodeposition of Alloys, Academic Press, New York and London Vol. 2, 1983.

8- A. P. Shears, Tran. Inst. Metal Finishing, 87, 67, 1989.

9- A.Krohn and C. W. Bohn, Plating. 58, 237, 1971 Electrodeposition and Surface Treatment, 1, 199, 1983.

10- R. G. Baker and C. A. Holden, Zinc-Nickel Alloy Electrodeposits, Rack Plating, Plat & Surf. Finish., 72, 54-57, 1985.

11- G. D. Wilcox and D. R. Gabe, Electrodeposited Zinc Alloy Coatings, Corrosion Science, 35, 1251-1258, Nov, 1993.

12- T. Tsuda and T. Kuremoto, U. S. Patent 4, 249, 999, 1981.

13- R. Albalat, E. Gomez, C. Muller, J. Pregonas, M. Saret and E. Valles. J. Applied Electrochemistry 12, 44-49, 1991.

14- R. Noumi and Alkomoda, Fourth Continuous Strip Plating Symposium, Chicago, Winter Park Flo. 1984, 1-3 May 1984. Pub. Amer. Electroplaters Soc..

15- A. Matsuda, European Patent Application 147, 463. June 1983.

16- K. H. Killian et al., AESF Fifth Continuous Strip Plating Symposium, dearborn, Michigan, 5-7 May 1987.

17- R. G. Baker, C. A. Holden. Plat. & Surf. Finish., 72, 54-57, March 1985.

18- M. R. Kalantary, Zinc Alloy Electrodeposition for Corrosion Protection, Plat &Surf. Finish., **80**, June 1994.

19- N. Zaki, Metal Finishing, **87**, 57-60, 1989.

20- K. Yamato et al, Kawasaki Steel Tech., Report $N^0 12$, July 1985.

21- S. A. Watson, Zinc-Nickel Alloy Electroplated Steel Coil and Other Pre-coated Coil for Use by The Automotive Industry, A review of Literature Published 1983-1987, A nickel Development Review N^0 1300.

22- T. Adaniya et al., AES Fourth Continuous Strip Plating Symposium, 1984.

23- A. Abibsi, J. K. Dennis and N. R. Short, The Effect of Plating Variables on Zinc-Nickel Alloy Electrodeposition, Institute of Metal Finishing Annual Technical Conference, Torquay, 24-26 April 1991.

24- R. Sard, Advances Functional Zinc and Zinc Alloy Coatings, Plat & Surf. Finish., **74**, 30-34, 1987.

25- M. Sagiyama, T. Urakawa, T. Adaniya, T. Hara and Y. Fukuda, Electrodeposition of Zinc Manganese on Steel Strip, Plat. & Surf. Finish., 77-82 Nov. 1987

(26)- David R. Gabe, Protective Layered Electrodeposits, , Electrochimia Acta, Vol 39. No **8/9**, 1115-1121, 1994.

27- L.L. Chang and E.E. Mendze, Synthetic Modulated Structures, (eds) L.L. Chang and B.C. Giessen, Academic Press Inc. **123**, 1985.

28- I. K. Schuller, Mater. Res. Soc. Symp. **103**, 335, 1988.

29- I.K. Schuller, C.M. Falco, Microstructure Sience and Engineering / VLSI, Vol.4 .Norman G. Einspruch, Editor.

30- P. Grunberg, R. Shreiber,Y. Pang, M. B. Brodsky, H. Sowers: Phys. Rev. Letters, **57**, 2442, 1986.

31- P. Boher, Ph. Houdy, R. Barchewitz, J. C. Joud, L.J. Van Ijzendoorn 12 IXCOM Conferrence Cracovie, August 1989.

32- R.C. Cammarata and K. Sieradzki, Phys. Rev. Lett. **62**, 2005, 1989.

33- J.E. Hilliard, W.M.C. Yang and T. Tsakalakos, J. Appl. **48**, 876, 1977.

34- E.M. Iogothetis, R.E. Soltis, R.M. Ager, W. Win, C.J. Mcewan, K. Chang, J. T. Chen, T. Kushida, L.E. Wenger. Physica C, Vol. 153-155, **2**, 1439-40, 1988.

35- T. Morishita, R. Sato, K. Sato and H. Kida Proc. of ICM'88 (J. de physique).

36- D.P. Monaghan, T. Hirst, D. Cross and R.D. Arnell Materials Science Forum Cols **163-165**, 551-556, 1994.

37- A.B. Smith, Private communication.

38- W. Blum, The Structure and Properties of Alternately Electrodeposition Metals. Trans. Am. Electrochem. Chem. Soc. **40**, 307, 1921.

39- W. H. Safranek and G. R. Schaer, Properties of Electrodeposits at Elevated Temperatures, American Electroplaters Society, **43rd**, Annual Technical Pro, 105, 1956.

40- Art O'cone. Alloy, Combination and Layered Coatings, Surf. & Met. Finish., NOV. 1982.

41- T. Honjo, Effect of Iron-Phosphorous Upper Layer Coating Weight on Paintability and Corrosion Resistance of Double-layer Alloy-coated Steel Shafts, Tetsuto Hagane **72(8)**, 976, 1983.

42- J. Gini Dhar and W. J. Van Ooij. Study of Zn-Ni and Zn-Co Alloy Coatings Electrodeposited on Steel Strips, Surface and Coating Technology 53 (1992) 35-47.

43- A. Haseeb, J. P. Celis and J. R. Roos, Synthesis of CMM by Electrodeposition: An Overview, Transactions of The Metal Finishers Association of India, Vol1 **No 3**, 15-16 July-Sep 1992.

44- A. Haseeb, J. P. Celis and J. R. Ross. Dual Bath Electrodeposition of Cu/Ni Compositionally Modulated Multilayers, J. Electrochem. Soc. , Vol 141, **No1**, Jan 1994.

45- M. Kalantary, G. Wilcox and D. Gabe, Compositioally Modulated Alloy Synthesis by Electrochemical Deposition, AESF SUR/FIN '95, Baltimore, Maryland.

46- C. A. Roos, L. M. Goldman, and F. Spaepen. J. Electrochem. Soc. Vol 1, Jan. 1993.

47- T. Pearson and J. K. Dennis, Tran. Inst. Metal Finish, **69(3)**, 75, 1991.

48- Popov, Keca and Viidojkovic, J. Appl. Electrochem. **6**, 365-370, 1976.

49- J. C. Puippe, Pulse Plating Versus DC Plating, AESF 3rd International Pulse Plating Symposium, Washington DC, **28-29** Oct. 1986.

50- Krivstov, Ivanovsk, Khim Tekh Inst **7**, 87, 1958.

51- N. Ibl, J. C. Puippe and H. Angrer, Electrocrystallization in Pulse Electrolysis, Surface Technology **6**, 287-300, 1978.

52- C. L. Faust, G. R. Schaer and D. E. Semones, Plating **48**, 605, 1961.

53- Dolzhenkov, Andreev, Vystrelkove and Batishchev, Chem. Abst, **78**, 37054, 1973.

54- Ozerov, Litvishkoo, Vavilina, Chetvertnov and Zhak J. Appl. Chem USSR, **40.** 1101, 1967.

55- Puippe, Leaman, Theory and Practice of Pulse Plating AESF, Orlando, Florida, 1986.

56- Avila and Brown, Plating, **57**. 1105, 1970.

57- Kleinekathofer, Ruab. Surface Technology 7, 23-24, 1978.

58- Fluhmann, Reid, Mousli and Steinmann, Plating and Surface Finishing **67(6)**, 62-65 1980.

59- A. R. Despic, Electrodeposition of Laminar Structures, Fauculty of Technology and Metallurgy, University of Beograd, Beograd, Yugoslavia.

60- D.S.Lashmore, R.Oberle and M.P.Dariel, Electrodeposition of Artificially Layered Materials, AESF 3rd Int'1 Pulse Plating Symposium, Washington DC, Oct. 28-29 (1986).

61- K.Hosokawa, M.Matsunage and Y.Tsuru, Influences of Pulse Parameters on Electroplating, Proc-Symp. Electroplating Engineering and Waste Recycle New Developments and Trends, Ohio, Aug-Sep. 1982.

62- R. De Docker, J.Vanhumbeeck, Control and Optimisation of Plating Baths by The Use of Rotating Electrodes, Connector'85, Organised by East Midland Branch of IMF, Leicester, 20th March 1985.

63- H. Koeppe, Dissertation, Ciessen, 1923.

64- W. Deubuer, Ann. Phys. Leipzig, 5, 261, 1930.

65- C. Odgen, Plating and Surface Finishing, 5, 130, 1986.

66- G. Barral and S. Maximovitch, Colloque de Phsic, **14 (15)**, C 4- 291, 1991.

67- C. A. Roos, L. M. Goldman, and F. Spaepen. J. Electrochem. Soc. Vol 1. Jan. 1993.

68- A. Brenner, Electrodeposition of Alloys: Principles and Practice, Vol. I&II, Academic Press, New York NY (1963).

69- J. S. Koehler, Phys. Rev. B 2, 547, 1970.

70- U.Cohen, F.B.Koch and R. Sard, Electrochem. Soc. Meeting, Orlando (1981).

71- D. Tench and J. White, Met. Trans., **15**, 2039, 1984.

72- Yahalom and O. Zadoc, J. Mater. Res., **22**, 449, 1987.

73- E. A. Rossett, C. E. Johnson, D. s. Lashmore, Electrodeposition of Ni-Mn Compositionally Modulated Microlayered Alloys (CMA) for Neutron Mirror, Abs. 348, Metallurgy Division, National Institute of Standards and Technology, Gaithersburg, MD 20899.

74- A. W. Ruff and D. S. Lashmore, Wear of Materials (1991) Proc. Int. Conf. Wear of Mate. Orlando, **Vol1**, 137, 1991.

75- A. R. Despic, V. D. Jovic and S. Spaic, Electrochemical Formation of Laminar Deposits of Controlled Structure and Composition, J. Electrochem. Soc., Vol. 136, **No 6**, June 1989.

76- A. R. Celis, J. R. Roos, B. Blanpain, and M. Gilles, Dept. Metallurgy and Materials Engineering (MTM), KU Leuven, B-3030 Leuven, Belgium.

77- M. R. Kalantary, G. D. Wilcox and D. R. Gabe, The Production of Compositionally Modulated Alloys by Simulated High Speed Electrodeposition from A Single Solution, Electrochimia Acta, Vol 40, **No 11**, 1609-1616, 1995.

78- W. H. Safranek, The Properties of Electrodeposited Metals and Alloys, Second Edition, American Electroplaters and Surface Finishers Society, Orlando, Florida, 1986.

79- R. F. Ashton and M. T. Hepworth, Effect of Crystal Orientation on The Anodic Polarisation and Passivity of Zinc, Corrosion Science, **24**, 50, 1968.

80- J. F. Batty, N. Nelson and P. A. Martens, Etching Electrodeposited Copper Foil, PC, **10**, 60, Dec 1987.

81- M. Schlesinger, X. Meng, W. T. Evans, D. A. Saunders and W. P. Kampert, Micromorpholgy and Magnetic Studies of Electroless Cobalt/Phosphorous Thin Films, J. Electrochem. Soc., **137**, 1706, 1990.

82- J. W. Dini, Deposit Structure, Plating and Surface Finishing, **75**, 11, Oct 1988.

83- L. H. Bennette, L. J. Swatzendruber, D. s. Lashmore, R. Oberle, U. Atzmony, M. P. Dariel and R.e. Watson, Phys. Rev.B, **40** (7), 4633, 1989.

84- G. Wouters, J. P. Celis and J. R. Roos, The Electrocrytallisation of Compositionally Modulated Multilayers of Tin and Amorphous Nickel-Phosphorous, J. Electrochem. Soc., Vol 140, **No 12**, Dec 1993.

85- L. H. Bennette, D. s. Lashmore, , M. P. Dariel, M.Rubinstein, W.L.Lechter and M.Z.Harford, J. Appl. Phys., 4067, 1987.

86- S.Menezes and D.P.Anderson, J. Electrochem. Soc., **137** (2), 88, 1990.

87- R. Weil and C. Sheu, Cited in Metals Abstracts, Abs. No. 35-1340, 1991.

88- N. Thon and E. T. Addison, Monthly Rev. Am. Electroplaters Soc., Vol. **34**, 445-722, 1949.

89- H. Yan, J. Downes, P. J. Boden and S. J. Harris, Morphology and Fine Structure of Zinc Deposits, Philosophical Magazine A, Vol 70, **No 2**, 391-404, 1994.

90- M. R. Kalantary, G. D. Wilcox and D. R. Gabe, Unpublished Work.

91- K. Higashi, Y. Higashi, H. Fukushima, T. Akiyama and H. Hagi, A fundamental Study of Corrosion Resistant Zinc-Nickel Electroplating, NiDI Technical Series, No 10036.

92- K. R. Baldwin, M. J. Robinson and C. J. E. Smith, Corrosion Rate Measurements of Electrodeposited Zinc-Nickel Alloy Coatings, Corr. Sci., **7**, 35, 1994

93- R. J. O' Halloran, L. F. G. Williams and C. P. Lioyd, Corrosion- Nace, **40** (7), 344-349, July 1984.

Appendices

1- Polarisation resistance methode

The corrosion current is calculated using the polarisation resistance technique, applying the Stern-Geary equation (93) This is applicable to very small values of polarisation (in the range of ± 20 mV) from corrosion potential, where there is a linear relationship between the applied current (I) and polarisation potential (E). The slope of this straight line, dE/dI (determined experimentaly), is a measure of polarisation resistance (R_p) of the coating (figure (132)). Therefore, $R_p = dE / dI$ and corrosion current (I_{corr}) is obtained from the Stern-Geary equation which is $I_{corr} = \pm b_a b_c / 2.3 (b_a + b_c) R_p$, where ba is the anodic slope and bc is the cathodic slope. The values of ba and bc are determined from the Tafel slopes (figure (133)).

2- Tafel extrapolation method

The corrosion current can also be dertermined directly from the point of intersection of the anodic or cathodic Tafel lines, with a line drawn through E_{corr}.
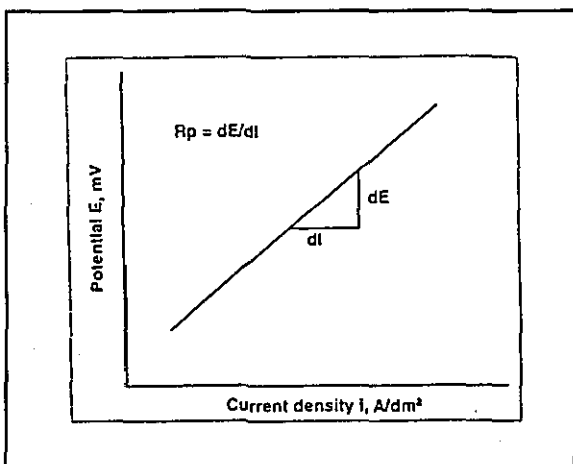

Figure (132). Potential vs. current density for measurement of polarisation resistance.
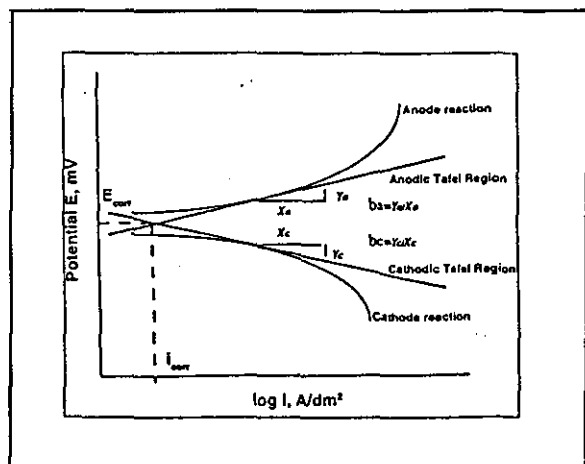
Figure (133). Potential vs. logarithmic current density for oxidation and reduction of a metal for measurement of Tafel slopes and corrosion current

138

3- Calculation of metal removal rate during anodic polarisation

The calculation explained below, assumes that all the available electrons at the electrode surface are being used in the zinc dissolution reaction, and also that the scan rate is 0.5 mV/sec and the electrode area is 9 cm². From figure (56) which represents the anodic polarisation behaviour for the 8 layer Ni/Zn CMMM coating, it is possible to calculate the charge passed in the defined curve area between -1040 and -720 mV vs. SCE.

The potential range traversed = | -1040 - (-720) | = | -320 | mV = 320 mV which is equal to 640 seconds duration. The defined area under the curve is equal to:

The length of rectangle located between 0.3 and 1 mA/cm² is equal to 0.1 mA (which for the whole electrode area is equal to 0.9 mA), and the width of rectangle located between -1040 and -720 mV is equal to 40 mV (80 sec). The number of individual graph paper squares located between 0.3 and 1 mA/cm² and between -1040 and -720 mV are equal to 52.

In the same manner, the length of rectangle located between 1 and 6 mA/cm² is equal to 1 mA/cm² (which for the whole electrode area is equal to 9 mA), and the width is equal to 40 mV (80 sec). The number of rectangle squares located between 1 and 6 mA/cm² and between -1040 and -720 mV is equal to 20. The defined surface area is then equal to:

52(80 x 0.9) + 20(80 x 9) = 18144 mA.sec = **18.144 A.sec**

The charge passed in defined area:

$m = M \, It \, / \, n.F$ where m = Mass deposited (g), M =Molar mass (g mol^{-1}), I = Current (A), T = Time (sec) n = number of electrons involved in reaction and F = Faraday constant (96500 C mol^{-1})

Substituting experimental figures:

$m = 65.4 \times 18.144 \, / \, 96500 \times 2 \cong 6.147. \, 10^{-3}$ g $\Rightarrow$

$\rho = m \, / \, V$ or $\rho = m \, / \, x.A$ where ρ = Density (g cm^{-3}), V Volume (cm^{3}), x = Thickness of deposit (cm) and A = Area (cm^{-2}) $\Rightarrow$ rearranging $x = m \, / \, \rho.A = 6.147.10^{-3} \, / \, 7.17 \times 9 = 9.57.10^{-5}$ cm $\cong 0.96$ μm.

This calculation suggest that the whole zinc layer has essentially been dissolved at point A.